11-26-2014 12:00 AM

The Role of the Ku70 vWA Domain in the Response to DNA Double Strand Breaks

Victoria L. Fell, *The University of Western Ontario*

Supervisor: Dr. Caroline Schild-Poulter, *The University of Western Ontario*

A thesis submitted in partial fulfillment of the requirements for the Doctor of Philosophy degree in Biochemistry

THE ROLE OF THE KU70 VWA DOMAIN IN RESPONSE TO DNA DOUBLE STRAND BREAKS

(Integrated Article)

by

Victoria Fell

Graduate Program in Biochemistry

A thesis submitted in partial fulfillment
of the requirements for the degree of
Doctor of Philosophy

The School of Graduate and Postdoctoral Studies
The University of Western Ontario
London, Ontario, Canada

Abstract

Ku is an abundant, highly conserved DNA binding protein found in both prokaryotes and eukaryotes that plays essential roles in the maintenance of genome integrity. In eukaryotes, Ku is a heterodimer comprised of two subunits, Ku70 and Ku80, that is best characterized for its central role as the initial DNA end binding factor in the "classical" non-homologous end joining (C-NHEJ) pathway, the main DNA double-strand break (DSB) repair pathway in mammals. At the break, Ku directly and indirectly interacts with several C-NHEJ factors and processing enzymes, serving as the scaffold for the entire DNA repair complex. In this work we aim to characterize the role of the Ku70 von Willebrand A-like (vWA) domain, a protein-protein interaction domain, in Ku's role in the response to DSBs.

In this study we identified a requirement for the Ku70 vWA domain in both NHEJ and signaling to the DNA damage response (DDR) pathway to determine cell fate decisions. We demonstrate that mutation of residues D192A/D195R in helix 5 resulted in extremely low survival after ionizing radiation (IR) treatment and decreased DNA repair efficiency, indicating a role for these residues in NHEJ. We also identified a novel phosphorylation event at Ku70 S155 in response to DNA damage. Mutation of this residue to alanine has no impact on DNA repair, however results in increased survival and decreased activation of apoptosis following IR treatment, indicating a defect in the DDR pathway to relay the signal of failed repair to the cell death machinery. The expression of a phosphomimetic S155D substitution had the opposite phenotype, with very low survival after IR, and the constitutive activation of DDR markers and cell cycle arrest even in the absence of any DNA damage. We found Ku70 S155 phosphorylation was required to interact with and inhibit the Aurora Kinase B after IR, a kinase that promotes cell cycle progression, to induce cell cycle arrest.

Overall we propose that the Ku70 vWA domain functions to both facilitate the repair of breaks by NHEJ, and to relay the signal of unsuccessful repair to the DDR in order to activate cell cycle arrest and apoptosis.

Keywords

Ku, Ku70, DNA repair, NHEJ, vWA, DSB, DNA damage response, phosphorylation, apoptosis, cell cycle arrest, Aurora B

Co-Authorship Statement

A portion of Chapter 1 was published in the manuscript: The Ku heterodimer: Function in DNA repair and beyond. Victoria L Fell and Caroline Schild-Poulter. Reviews in Mutation Research (2014). The manuscript was written by VLF and edited by CSP.

The data in Chapter 2 of this thesis is published in: Ku regulates signaling to DNA damage response pathways through the Ku70 von Willebrand A domain. Victoria L Fell and Caroline Schild-Poulter. Molecular and Cellular Biology (2012). All experiments and data analysis in this chapter were performed by VLF. Carl Shen, Michael Widlicki and Samantha Hershenfeld generated the pMSCVpuro-Ku70 S155A, D156A, 155-160A, S155D constructs. Probe preparation and gene chip hybridization for Supplementary Table 2-1 were performed by the London Regional Genomics Centre (LRGC). The manuscript was written and edited by VLF and CSP.

All experiments and data analysis in Chapter 3 were performed by VLF with some exceptions. Stephanie Rogers conducted the experiments for Figures 3-2A and 3-4D, and Amelia Aitken performed the experiments for Figure 3-6B. Probe preparation and gene chip hybridization for Supplementary Table 3-2 were performed by the London Regional Genomics Centre. S155 phosphorylation identification in Supplementary Table 3-1, and the Aurora B protein identification in Supplementary Figure 3-2 were performed at the London Regional Proteomics Centre (LRPC). The manuscript was written and edited by VLF and CSP.

Acknowledgments

The primary acknowledgement for this thesis goes to my supervisor, Dr. Caroline Schild Poulter, for your consistent encouragement and guidance throughout my degree. I am grateful that you welcomed me into your lab and for all the time you have dedicated to my development as a scientist.

I would also like to acknowledge the members of my advisory committee, Drs. Chris Brandl, Greg Gloor and Megan Davey. I appreciate all of your scientific and technical insight during my committee meetings and believe they were an invaluable contribution to the project and this thesis.

Next I would like to thank the past and present members of the CSP lab. As for helping me complete my thesis, I thank all of undergrads for providing much needed man-power to Team Ku, and Xu, for making everyone's life so much easier. Thank you to our lab benefactor Pat, for your many kind donations, and for which in return I grant you ghost authorship on this thesis. To the bulk part of the lab, Elnaz, Louisa, Wesley and Sarah: thank you for bringing a lot of laughs, a healthy amount of fighting, and an unnatural amount of hugging to my life. Lastly, I also give a shout-out to some of the lesser-known members, Christmas Cats, the Narwhals and BagBag (gone too soon), as their contribution to my degree has been immeasurable.

Finally, I need to thank my friends and family for helping me get through the last six years. I especially thank my parents for their unwavering support (emotional and financial!) despite having no idea what I do every day.

Table of Contents

List of Tables

List of Figures

List of Appendices

List of Abbreviations

5'dRP	5' deoxyribosephosphate
53BP1	p53 binding protein 1
A-NHEJ	Alternative Non-homologous end joining
A/Ala	Alanine
ANOVA	Analysis of variance
AP	Apurinic/Apyrimidine
AP-1	Activator protein 1
APLF	Aprataxin and PNKP like factor
ATF	Activating transcription factor
ATM	Ataxia telangiectasia mutated
ATR	Ataxia telangiectasia and Rad3 related
Bax	Bcl-2 associated X
Bcl-2	B cell lymphoma 2
BER	Base excision repair
BH3	Bcl-2 homology domain 3
BRCA1	Breast cancer 1
C-NHEJ	Classical Non-homologous end joining
C(t)	Cycle threshold
CDC25A	Cell division cycle 25
CDK	Cyclin dependent kinase
Chk	Checkpoint kinase
CHOP	C/EBP homologous protein
CPC	Chromosomal passenger complex
CREB	cAMP response element-binding protein
CST	Cdc13-Stn1-Ten1
CTD	C-terminal domain
CtIP	CtBP interacting protein
D/Asp	Aspartate
Da	Dalton
DDR	DNA damage response
DNA-PK	DNA dependent protein kinase
DNA-PKCS	DNA dependent protein kinase catalytic subunit
DSB	Double strand break
DSBR	Double strand break repair
EM	Electron microscopy
ExoI	Exonuclease 1
FA	Fanconi anemia
FACS	Fluorescence activated cell sorter
G1	Gap 1
G2	Gap 2

Gy	Gray
H3S10	Histone H3 Serine 10
HDAC	Histone deacetylase
HR	Homologous recombination
hRT	RNA component of human telomerase
hTERT	Telomerase reverse transcriptase
ICL	Intra-strand crosslinks
Id	Inhibitor of differentiation
IF	Immunofluorescence
Ig	Immunoglobulins
IR	Ionizing radiation
JNK	Jun N-terminal kinase
M	Mitosis
MALDI	Matrix-assisted laser desorption/ionization
MAPK	Mitogen activated protein kinase
MDC1	Mediator of DNA damage checkpoint 1
Mdm2	Mouse double minute 2 homolog
MEF	Mouse embryonic fibroblast
MMEJ	Microhomology mediated end joining
MMR	Mismatch repair
Mre11	Meiotic recombination 11
MRN	Mre11-Rad50-NBS1
MRX	Mre11-Rad50-Xrs2
MS	Mass spectrometry
MSCV	Murine stem cell virus
NBS1	Nibrin
NER	Nucleotide excision repair
PARP-1	Poly (DP-ribose) polymerase 1
PCAF	P300/CBP-associated factor
PFGE	Pulsed-field gel electrophoresis
PIKK	Phosphoinositide 3-kinase-related kinase
PLA	Proximity ligation assay
PNKP	Polynucleotide kinase/phosphatase
POT1	Protection of telomeres 1
PP	Protein phosphatase
PTIP	Pax transactivation domain-interacting protein
Q/Glu	Glutamine
R/Arg	Arginine
Rad	Radiation repair
RAG	Recombination-activating gene
RAP1	Repressor activator protein
Rb	Retinoblastoma protein
RECQ1	ATP-dependent helicase Q1
Rif1	RAP1 interacting factor

RNF8	E3 ubiquitin ligase RING finger protein 8
ROS	Reactive oxygen species
RT-qPCR	Reverse transcriptase quantitative polymerase chain reaction
S	Synthesis
S/Ser	Serine
SAP	SAF-A/B, Acinus and PIAS
SCF	Skp1-Cul1-FbxI12
Sir	Silent information regulator
SIRT	Sirtuin
SSB	Single strand break
T/Thr	Threonine
TDP2	Tyrosyl DNA phosphodiesterase 2
TIN2	TERF1-interacting factor 2
TLC1	Telomerase component 1
TOP2	Topoisomerase II
TPE	Telomere position silencing effect
TRF	Telomere repeat factor
UV	Ultraviolet
vWA	von Willebrand A
WT	Wild type
XAF-1	X-linked inhibitor of apoptosis associated factor 1
XLF	XRCC4 like factor
XRCC4	X-ray cross complementing protein
γ-H2AX	Serine 139 phosphorylated H2AX

Chapter 1

1 Introduction

1.1 General introduction

Structural changes to DNA pose a serious threat to organismal health as the maintenance of genomic integrity is required for proper cellular homeostasis and the faithful transmission of genetic material to progeny. Unfortunately, it is estimated that each cell in the human body is subjected to tens of thousands of genomic insults per day (1). These DNA lesions can arise spontaneously from physiological processes, such as meiosis, DNA replication errors, or byproducts from metabolism and inflammation (1). We are also exposed to numerous environmental damaging agents, including ultraviolet radiation, ionizing radiation and carcinogenic chemical compounds (1). If not repaired properly, these DNA lesions can be cytotoxic, or even more problematic, can cause altered cellular function leading to malignant transformation.

In order to combat the threat of DNA damage, organisms have developed a complex and sophisticated signaling pathway, collectively termed the DNA damage response (DDR). The end goal of this process is DNA repair, coordinated enzymatic processes specific to the type of DNA damage, that restore integrity of the DNA. Simultaneously, numerous signaling cascades are initiated that induce cell cycle arrest, in order to give the cell type to repair the DNA, but also activate cell death if the repair cannot be completed. This thesis will examine the role of Ku, an integral component of

the DNA double strand break (DSB) pathway, non-homologous end joining (NHEJ), in both the execution of DNA repair and coordination of cell fate decisions to the DDR.

1.2 Ku Heterodimer

1.2.1 General introduction

Ku was first identified in the early 80's as an autoantigen targeted by autoantibodies in the serum of patients diagnosed with an autoimmune disease known as scleroderma polymyositis overlap syndrome (2). The name Ku comes from the first two letters of the name of the original patient in whose serum it was identified. Autoantibodies directed against Ku were subsequently found in several other autoimmune diseases, including systemic lupus erythematosus, Sjorgren's syndrome, polymyositis and scleroderma (3-5). Early studies using serum from Ku-positive patients identified Ku as an abundant, mostly nuclear protein (2, 6). Subsequent reports showed that Ku had unusual DNA binding properties, binding avidly to the ends of double-stranded DNA molecules in a sequence-independent manner and to a lesser extent to other forms of DNA discontinuities such as hairpins gaps and nicks (6-8). These unusual end-binding properties made Ku an appealing candidate for a role in DSB repair and V(D)J recombination, which was confirmed when the two Ku subunits (XRCC5, Ku80 and XRCC6, Ku70) were found to complement the DNA repair defect of several IR-sensitive cell lines (9-15). It is now well established that while not essential to individual life in the short term, Ku function is critical to the maintenance of genomic integrity and to the proper cellular and organismal development. A better understanding of Ku's diverse roles at the cellular and organismal level have implications for the study and the treatment of other human diseases, such as immune system disorders, cancer and aging.

1.2.2 Ku Structure

Ku is a highly abundant protein found *in vivo* as a stable heterodimer consisting of two subunits, Ku70 and Ku80 (70 and 80 kDa, respectively). Both Ku70 and Ku80 eukaryotic Ku subunits contain three domains (Figure 1-1A): an N-terminal alpha helix/beta barrel von Willebrand A (vWA) domain; a central core domain required for DNA binding and dimerization; and a helical C-terminal domain.

The Ku70/80 crystal structure (Figure 1-1B) shows that the two subunits dimerize through the central domain to form a ring capable of accommodating two turns of double-stranded DNA (approximately 14 base pairs) (16). This ring, consisting of intertwined strands of both Ku70 and Ku80, is lined with positively charged residues positioned to interact with the sugar phosphate backbone of DNA in a sequence-independent manner. Ku binds double-stranded DNA ends with high affinity (Kd~10^{-9} M), including 5'-3' or 3'-5' overhangs and blunt ends, however has significantly less affinity for circular DNA and single-stranded DNA ends (6, 17, 18). Ku has a preferred orientation when loaded onto the DNA, placing Ku70 proximal to the DNA end, and Ku80 on the distal side, facing away from the end (16).

The N-terminal vWA domain (also called α/β domain) consists of a six-stranded beta-sheet in a Rossman fold. The amino side of the beta-sheet makes contact with the DNA groove, although it contributes little to Ku70/80 dimerization or DNA binding. The carboxyl end of the fold points away from the break, which makes it available as a protein-protein interaction surface (16). This domain, named for its prototype protein, the von Willebrand Factor type A, is present in mostly extracellular matrix proteins but also several intracellular proteins, where it facilitates protein-protein interactions with a wide

Figure 1-1 Representation of Ku structure

(A) Schematic diagram of domain representation of the Ku70 and Ku80 subunits. The subunit domain structure of yeast and human Ku consists of the alpha helix, beta barrel N-terminal vWA domain, a central DNA binding core and a C-terminal helical domain (CTD). The eukaryotic Ku80 CTD contains the region required for binding DNA-PK_{CS} , while the Ku70 CTD is shorter and contains a SAF-A/B, Acinus and PIAS domain (SAP). The location of the nuclear localization signals and post translation modifications (phosphorylation and acetylation) on the human Ku protein is indicated. Yeast Ku is comprised of a similar domain structure to human Ku, except for a truncated C-terminal domain in Ku80. Prokaryotes encode for a single Ku subunit that is homologous to the eukaryotic core DNA binding domain. (B) The crystal structure of human Ku (PDB: IJEY) coloured according to the domain structure. The dimer forms an asymmetrical basket structure with a positively charged ring large enough to accommodate two turns of the DNA. The Ku80 C-terminus is not included in this crystal structure.

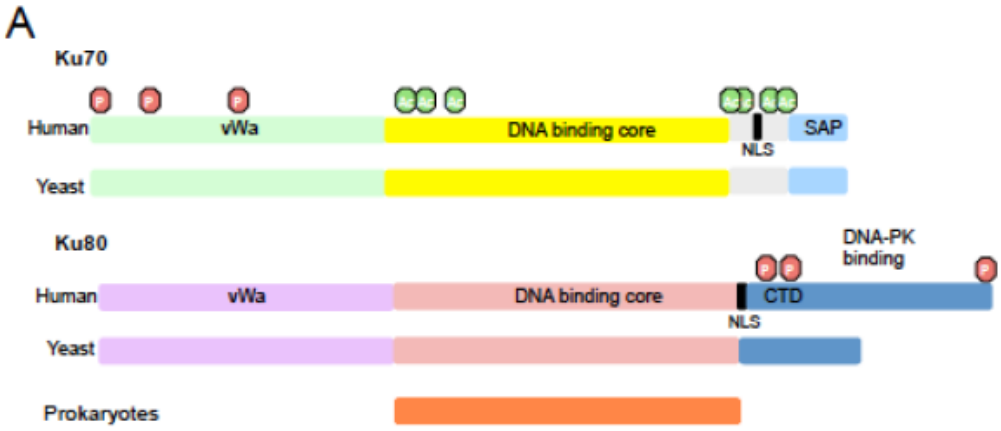
A
Ku70
Human
vWa
DNA binding core
NLS
SAP
Yeast
Ku80
DNA-PK
binding
Human
vWa
DNA binding core
CTD
NLS
Yeast
Prokaryotes

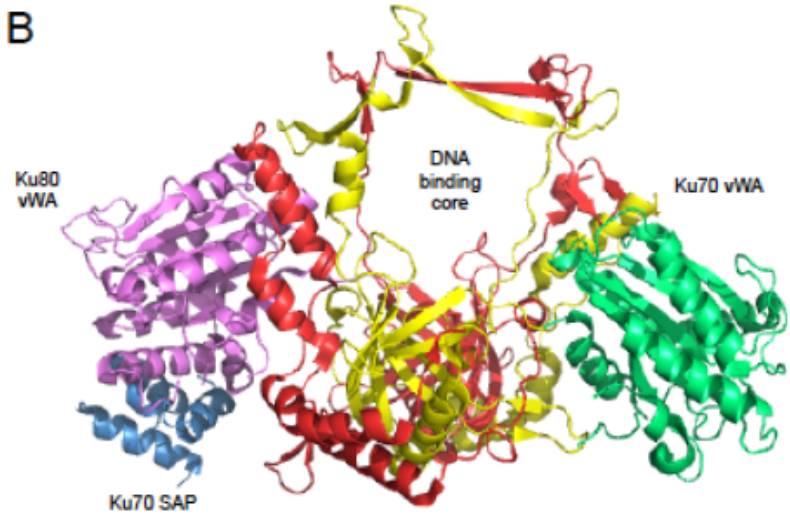
B
Ku80
vWA
DNA
binding
core
Ku70 vWA
Ku70 SAP

variety of ligands (19). Overall, the function of this domain is not well characterized but there is emerging evidence that it has an important role in DSB repair and telomere regulation. In *Saccaromyces cerevisae,* mutations in helix 5 of Ku80 abrogated telomere silencing, while mutations in helix 5 of Ku70 had a negative impact on DSB repair in yeast and mouse cells (20-22). Specific residues in the Ku70 vWA domain were also shown to be critically implicated in conferring abasic site processing by Ku *in vitro* (23, 24). Additionally, another region of the human Ku70 vWA domain in helix 4 was found to regulate DNA damage signaling to apoptosis (22). Consistent with its predicted role as a protein-protein interaction surface, the vWA domain has been shown to mediate an interaction with both the telomere complex component telomere repeat binding factor 2 (TRF2) and NHEJ factor aprataxin and PNKP like factor (APLF) (21, 25).

Both Ku subunits contain a helical C-terminal domain (CTD), however this is the most divergent region of the two proteins. The Ku80 CTD is approximately 15 kDa and contains a helical and a disordered region. In vertebrates, the extreme Ku80 C-terminus is involved in the recruitment of DNA-dependent protein kinase catalytic subunit (DNA-PK_{CS}) to DNA (26, 27). Lower eukaryotes, such as *S. cerevisiae* and *Aradopsis thaliana,* encode for a smaller Ku80 protein, missing this DNA-PK_{CS} binding region, which correlates with the fact that DNA-PK_{CS} is not present in these organisms. The Ku70 CTD is composed of a highly flexible linker region followed by a structured 5 kDa helix-loop-helix region known as the SAP domain (named after SAF-A/B, Acinus and PIAS motifs) (28). The SAP domain has putative DNA binding properties and has been shown to increase the overall DNA binding affinity of the heterodimer (29, 30). This C-terminal region is also subject to post translational modifications. Multiple C-terminal lysine

residues are acetylated to regulate Ku interaction with pro-apoptotic proteins (31, 32). Acetylation and sumoylation of Ku70's C-terminal tail were also implicated in modulating its recruitment to DNA damage sites and Ku's DNA binding affinity, respectively (32, 33). The Ku70 SAP domain was also shown to mediate the recruitment of homeodomain proteins to DNA ends (34). Furthermore, Ku is primarily a nuclear protein, and the CTD in both subunits contains the basic nuclear localization signal motif that regulates the heterodimer's nuclear transport (35).

It is currently unclear whether Ku subunits can exist alone in a monomeric form, but there is strong evidence that Ku is an obligate heterodimer. Cells derived from Ku70 deficient mice show very low expression of Ku80, and similarly, the expression of Ku70 is severely reduced in cells derived from Ku80 deficient mice (15, 36, 37). This phenomenon is also observed in yeast strains null for either Ku subunit, and in fact, these strains are phenotypically identical to the double Ku subunit knockout strain (38). This is likely due to the instability of each subunit in the absence of their interacting partner, as exogenous re-expression of the missing subunit restores the protein levels of its heterodimeric partner (37). Overall, evidence suggests that the individual Ku subunits are unstable and require heterodimerization to function.

The Ku subunits share little primary sequence, but do have a conserved secondary structure, indicating that they may be derived from a common ancestor. Ku is an evolutionarily conserved protein, found in both the prokaryotic and eukaryotic kingdoms, and its overall structure is preserved throughout. As several homologues have been identified in bacterial and archaea species, Ku is thought to have prokaryotic origins (39, 40). For the most part, prokaryotic genomes contain a single copy of a Ku-like protein

which also functions in a bacterial NHEJ pathway, but as a homodimer (41). While having little DNA or protein sequence similarity to its eukaryotic counterparts, prokaryotic Ku homologues display structural homologies to the central core DNA binding domain region of both eukaryotic Ku subunits and form homodimers that bind double-stranded DNA ends (42). Prokaryotic Ku is much smaller however, only approximately 30-40 kDa, lacking both the vWA and C-terminal domains found in eukaryotes (39, 40).

1.3 DNA Repair

1.3.1 Types of DNA damage and repair

DNA is subject to a wide variety of chemical modifications as a result of damage from both extrinsic and intrinsic agents. In order to resolve this diverse collection of modifications, several separate DNA repair pathways have evolved. The simplest DNA damaging agent is hydrolysis, which deletes DNA bases by severing the N-glycosidic bond between the base and the deoxyribose, as well as the deamination of bases that create conversions (eg. uracil to cytosine) (43-45). Other base modifications are produced from endogenous reactive molecules like nitric oxide (NO-) and reactive oxygen species (ROS) (46, 47). These base damages that do not distort DNA structure are generally resolved through the base excision repair (BER) pathway (48). Larger lesions that do distort the DNA structure are repaired by the nucleotide excision repair (NER) pathway (49). Examples of these bulky lesions are the pyrimidine dimers formed by UV radiation, or DNA intra-strand crosslinks created from drugs such as cisplatin (50). The mismatch repair (MMR) pathway is utilized in the correction of DNA polymerase errors like insertions, deletions or incorrect base incorporation (51-53). Finally, there are both single

strand break (SSB) and double strand break repair (DSBR) pathways that are utilized when the DNA damaging agent severs the sugar phosphate backbone of DNA (54).

The DNA DSB is considered to be the most dangerous and lethal form of DNA damage. DSBs can arise from both exogenous sources, such as ionizing radiation (IR), chemotherapeutic drugs and endogenous sources, such as meiosis, immune system gene rearrangements, stalled replication forks and reactive oxygen species (ROS) (1). All organisms are exposed to low levels of environmental IR and to varying amounts throughout our lifetime during medical procedures such as X-rays and cancer treatment (1). IR is a particularly complex DNA damaging agent due to the wide variety of DNA damage it produces. The DNA is initially damaged through the direct deposition of energy, but also, the ionization of surrounding water molecules produces ROS, which themselves damage the DNA (55). As a consequence, 1 Gy of IR produces approximately 40 DSBs per cell, but also 1000 single-strand breaks (SSBs), and 2000 base modifications (56-58). DSBs generated from IR can often be complex, clustered lesions that contain additional single strand overhangs and base damage that require additional processing before repair. There are three main DSB repair pathways in eukaryotes (Figure 1-2): the classical NHEJ (C-NHEJ), alternative NHEJ or microhomology-mediated end joining (A-NHEJ or MMEJ) and homologous recombination (HR) (59-61). C-NHEJ and A-NHEJ have the potential to be active in all stages of the cell cycle, however HR, is only active in the S and G2 phases because it utilizes the complementarity of the sister chromatid to repair the DSB with high accuracy (60, 61). C-NHEJ is capable of ligating any two DNA ends, regardless of sequence. Due to this

Figure 1-2 Schematics of the double-strand break repair pathways in higher eukaryotes.

(A) Homologous Recombination. After the introduction of a DSB, the ends are recognized by the MRN complex (Mre11-Rad50-NBS1), which recruits proteins Sae2, Sgs1, Exo1 and Dna2 to facilitate resection of the break in the 5' direction and leave 3' single-stranded extensions. The 3' single-stranded overhangs are bound by the proteins RPA, Rad51, and Rad54 to form a nucleoprotein filament. The next step, aided by the recruitment of Rad52, is the invasion of this filament strand into the DNA of the homologous chromosome to form a D-loop structure. A polymerase extends the 3' overhang to create a cross structure known as the Holliday junction, which is later cut to resolve the chromosome. (B) Alternative end joining/microhomology-mediated end joining (A-NHEJ/MMEJ). The break is recognized by the MRN complex, PARP1 and XRCC1, which promote the nucleolytic degradation of DNA to reveal 5-25 bp regions of microhomology between the DNA strands. After the alignment of complementary regions, the gaps are filled in by polymerase β, and ligated by either ligase I or ligase III. (C) Non homologous end joining (C-NHEJ). (1) The ends are recognized by the Ku heterodimer which slides directly onto the break via its DNA binding ring. The PIKK member DNA-PK_{CS} binds at the Ku80 C-terminus to create the DNA-PK complex. (2) DNA-PK autophosphorylates to create the catalytically active DNA-PK complex. Artemis is recruited to DNA-PK and phosphorylated. (3) Several enzymes, including polymerases (polymerase μ or λ), nucleases, kinases (polynucleotide kinase) are recruited to the break and remove damaged bases or single-strand overhangs to create compatible ends for ligation. (4) The ligation complex, consisting of Ligase IV, XRCC4, and XLF are recruited by Ku and ligate the two DNA ends. (5) It is unclear how the Ku dimer is removed from the ligated break. Possible mechanisms include degradation of Ku by proteases and the ubiquitin pathway, or physical nicking of the repaired DNA by nucleases to allow Ku to slide off.

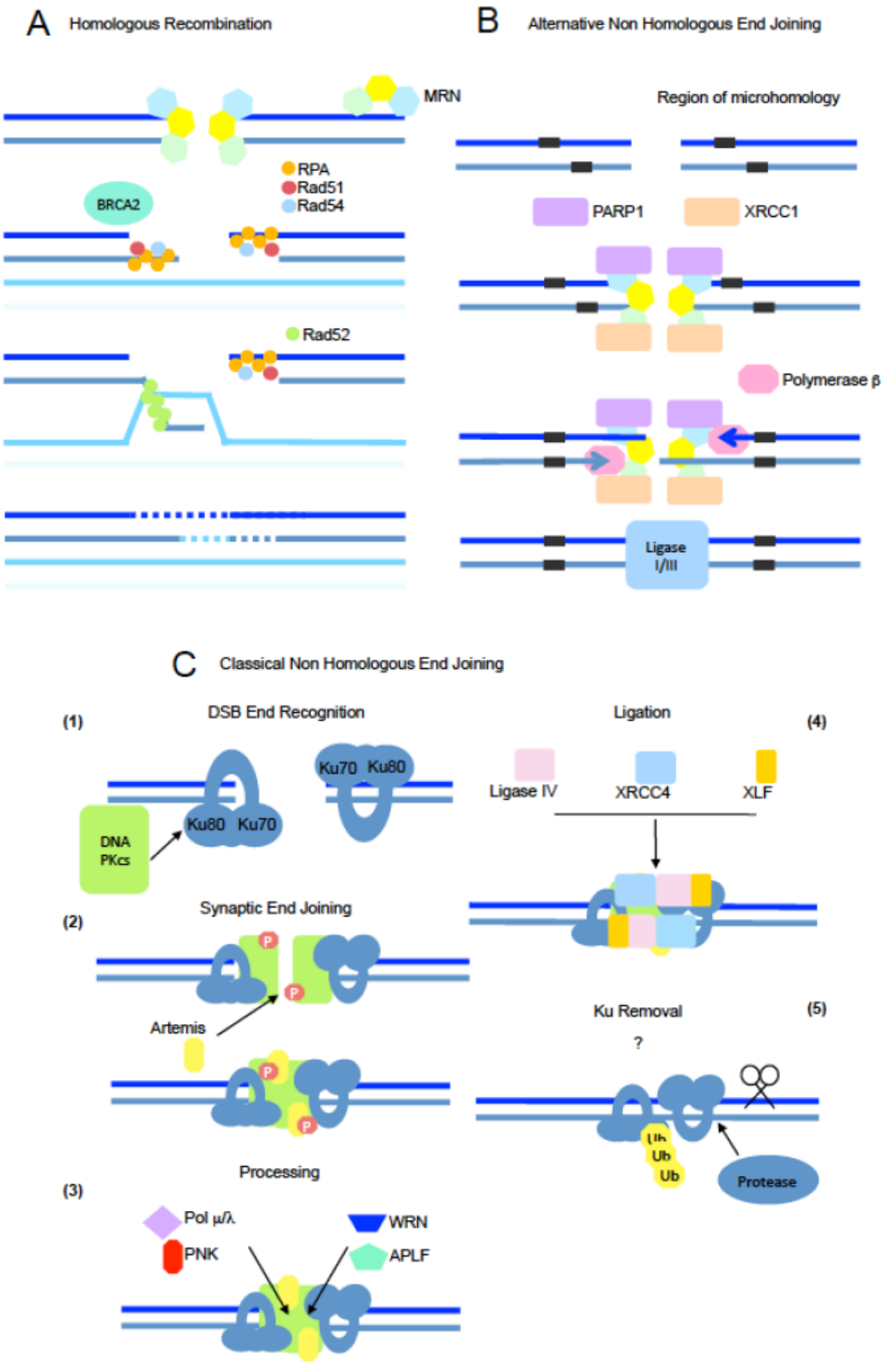
A
Homologous Recombination
MRN
RPA
Rad51
Rad54
BRCA2
Rad52
B
Alternative Non Homologous End Joining
Region of microhomology
PARP1
XRCC1
Polymerase β
Ligase I/III
C
Classical Non Homologous End Joining
(1)
DSB End Recognition
Ku70 Ku80
Ku80 Ku70
DNA PKcs
(2)
Synaptic End Joining
Artemis
(3)
Processing
Pol μ/λ
PNK
WRN
APLF
Ligation
(4)
Ligase IV
XRCC4
XLF
Ku Removal
(5)
?
Ub
Protease

flexibility, C-NHEJ is the predominant DSB repair pathway in humans and other higher eukaryotes (62-64).

1.3.2 Classical Non Homologous End Joining (C-NHEJ)

1.3.2.1 Overview

C-NHEJ can be divided into five main stages: I) recognition of the break by Ku, II) Synaptic end bridging, III) DNA end processing to produce compatible ends, IV) ligation of the break, and finally, V) Ku removal from the restored DNA. The importance of Ku to DSB repair has been well documented with reports of Ku deficient cells displaying inaccurate end-joining, dramatic radiosensitivity, and chromosomal breakage, translocations and aneuploidy (15, 65-69).

1.3.2.2 DNA end recognition

The initial step of C-NHEJ is the rapid recognition of the DSB by Ku. Ku's abundance (in humans, approximately 500,000 molecules per cell (6, 16, 70)) and strong affinity for DNA allows it to associate with DNA ends within 5 seconds of damage (71). Ku binding has a protective role and in Ku-deficient cells, nucleolytic processing occurs at DSB ends (72). Once Ku has encircled the DNA via its central ring domain, it directly and indirectly interacts with several NHEJ factors, serving as the scaffold for the entire NHEJ complex. Some uncertainty remains as to how many Ku molecules are recruited to a DNA break. Many DNA damage response factors form distinct foci easily visible at the site of DNA damage. However there has been difficulty in observing Ku following DNA damage by microscopy, leading to the conclusion that Ku does not accumulate in large numbers at a DSB. Furthermore, an *in vitro* study showed that only one or two Ku molecules were able to load onto a chromatin substrate (73). A recently developed

method for visualizing Ku foci also demonstrated that on average there are only two Ku molecules present at a DSB *in vivo*, presumably one at each end of the DNA break (74).

1.3.2.3 Bridging of the DNA ends

Ku is the DNA binding subunit of the DNA-dependent protein kinase (DNA-PK) complex, which comprises Ku and DNA-PK catalytic subunit (DNA-PK_{CS}), a member of the phosphoinositide 3-kinase-related kinase (PIKK) family (75). DNA-PK_{CS} activity is very important for successful DNA repair, as loss of DNA-PK_{CS} activity through mutations or knockout, strongly diminishes C-NHEJ efficiency and, at the organismal level, results in profound immunodeficiency (11). The low-resolution electron microscopic structure of the DNA-PK complex indicates that Ku70/80 makes several contacts with DNA-PK_{CS}, including the N-terminal and C-terminal regions of DNA-PK_{CS} (76). At DSBs, DNA-PK_{CS} is recruited by Ku to form the active complex, leading to Ku translocation and the eventual activation of DNA-PK_{CS} catalytic activity. This translocation allows DNA-PK_{CS} to be positioned at the tip of the break and mediates the synaptic joining of the two broken ends and the stabilization of the complex (77). Another important consequence of DNA-PK kinase activation are 15 auto-phosphorylation events on DNA-PK_{CS} (78-82). Ku70 and Ku80 were shown to be phosphorylated by DNA-PK *in vitro*, however the importance of these events in C-NHEJ function is unclear, as mutation of these residues does not impact cell survival after ionizing radiation (IR) (83). Similarly, DNA-PK phosphorylates several NHEJ factors *in vitro* such as DNA ligase IV, X-ray cross complementing protein 4 (XRCC4), XLF (XRCC4 like factor, also known as Cernunnos) and Artemis but again many of these were dispensable for NHEJ *in vivo* (80, 84-86).

There is increasing evidence that, along with DNA-PK_{CS}, Ku itself mediates the DNA end bridging and stabilization of the C-NHEJ ligation complex. Several early observations lead to the conclusion that Ku functions to bridge DNA ends, including the *in vitro* joining of two radiolabelled DNA ends by recombinant Ku protein and the visualization of Ku dependent DNA fragment joining by electron and atomic force microscopy (87, 88). More recently, utilizing an experimental system designed to visualize DSBs introduced by restriction endonucleases in mammalian cells, it was observed that the loss of Ku80 resulted in increased distance between DNA ends (89). Despite these observations, there has been little insight into the precise mechanism of Ku end bridging. A mutation in helix 5 of the Ku70 vWA domain, noted for its ability to impair DSB repair in both yeast and mammalian cells, was found to decrease multimerization of Ku proteins, leading to the speculation that this helix mediates DNA end bridging through the binding of two Ku70 molecules (20-22).

1.3.2.4 DNA end processing

Between the initial break recognition by Ku and the final ligation of the break, there is considerable flexibility in the factors involved in repair. For example, IR is known to produce a variety of damage to the DNA, occasionally leaving non-ligatable 3′-phosphate groups, 3′-phosphoglycolates, or 5′-hydroxyl groups. Therefore, a number of kinases/phosphatases (polynucleotide kinase/phosphatase (PNKP), nucleases (Werner, Mre11, Artemis, ExoI), polymerases (DNA polymerases μ and λ), helicases (RECQ1), and phosphodiesterases (tyrosyl-DNA phosphodiesterase 1) may be required to produce compatible DNA ends (90). In the case of DSBs induced by Topoisomerase II (TOP2) poisons, TOP2 remains covalently linked to via a phosphotyrosyl bond to the 5’ terminus

and requires a specific end-processing enzyme, tyrosyl DNA phosphodiesterase 2 (TDP2), that hydrolyses 5'-phosphotyrosyl bonds at TOP2-associated DSBs (91, 92). In many cases, recruitment of these factors to the DNA break is dependent on Ku, with some factors directly interacting with Ku (Table 1-1). Interestingly, Ku itself has been shown to have some enzymatic activity and may also participate in the processing of DNA ends. It was identified as a 5′-dRP/AP lyase that removes abasic sites by nicking DNA 3' of the abasic site via a mechanism involving a Schiff-base covalent intermediate. Several lysine residues in the Ku70 vWA domain catalyze this reaction, notably K160/164, which when mutated to an alanine residues completely inhibit Ku's ability to form a Schiff base (23, 24).

1.3.2.5 Ligation of the break

Following end-processing, the two DNA ends are ligated back together. Ku also has an important role in the recruitment of the ligase complex, which is comprised of DNA ligase IV, XRCC4 and XLF. The complex requires Ku to be recruited to the break through a direct interaction with Ku, with DNA ligase IV and XLF interacting with the whole heterodimer and XRCC4 interacting with Ku70 specifically (71, 93-96). There is still great uncertainty regarding the stepwise recruitment of NHEJ factors following Ku binding, although this is not surprising given that different processing enzymes are required in different situations. Indeed there is also some evidence that high complexity DSBs (containing single-strand overhangs, base oxidation and abasic sites) are repaired with slow kinetics and are dependent on DNA-PK_{CS} activity, while low complexity DSBs (without surrounding DNA damage) do not require DNA-PK_{CS} binding, and are efficiently ligated with only Ku and the ligation complex (97-100).

NHEJ and V(D)J	DNA-PK$_{cs}$(283)	Polymerase μ (284)	Polymerase λ (285)
	XRCC4/Lig4(93)	APLF(25)	
	XLF(95)	TdT (286)	
	WRN(287)	Rag-1 (288)	
DNA repair (other)	γ-H2AX (199)	CAF-1 (289)	Kub5-Hera (290)
	BRCA1 (140)	NBS1 (228)	INHAT (32)
	PARP-1 (291)	ABH2 (145)	MSH6 (292)
	RECQ1 (293)	Mre11 (294)	BARD1 (295)
Telomere	TRF1 (183)	HP1α (296)	
	TRF2 (184)	Rap1 (186)	
	TLC1 (166)		
	TERT (168)		
Apoptosis	BAX (227)	PCAF (31)	
	p18-cyclin E (229)	Clusterin (297)	
	HDAC6 (230)	CBP (31)	
	SIRT1(231)		
Cell Cycle	CDK9 (298)	Cyclin A/CDK1 (133)	
Transcription and Replication	Oct-1 (34)	REF1 (299)	HIV-IN (300)
	HOXC4 (34)	ESE-1(301)	Tat (302)
	dlx2 (34)	Runx2(303)	HSF-1(304)
	TOP2A(305)	Dlx5(303)	NAA15(303)

Table 1 Ku protein-protein interactions.

A list of proteins proposed to directly interact with Ku, classified according to cellular process.

1.3.2.6 Ku removal from the DNA

One of the outstanding questions in NHEJ is how Ku is removed from DNA following ligation of the DSB. Ku is rapidly recruited to the break, but is only found there transiently, as laser micro-irradiation studies found that Ku signal steadily depletes within the few hours following the initial damage, presumably being removed as DNA is repaired (71, 101). Ku differs from many other DNA binding proteins in that it binds DNA ends by encircling them through its ring domain, which would suggest that once the two DNA breaks are ligated, Ku is trapped on the linear repaired DNA. Furthermore, the crystal and electron microscopy (EM) structures do not indicate an obvious escape mechanism given that the vWA and central ring domain conformations of Ku remain unchanged whether or not bound to DNA (16, 76). One possible mechanism is that the removal of Ku from DNA occurs via a protein degradation pathway. Studies in *Xenopus laevis* have shown that poly-ubiquitination of Ku80 Lysine 48 leads to its degradation by the Skp1-Cul1-Fbxl12 (SCF) E3 ubiquitin ligase complex (102). Similarly in human cells, Ku80 ubiquitination was found to be dependent on the E3 ubiquitin ligase RING finger protein 8 (RNF8) (103). The depletion of RNF8 led to increased Ku80 retention at the break and decreased NHEJ efficiency, suggesting that removal of Ku80 by ubiquitin-mediated degradation is an important step in successful DSB repair (103). Another proposed mechanism for Ku removal is the direct nicking of DNA to allow Ku escape. Evidence for this has emerged from yeast systems, with the HR complex MRX (Mre11-Rad50-Xrs2) performing an endonucleolytic incision adjacent to the DNA end, followed by digestion of the DNA to allow Ku removal and then restoration of the DNA by MRX and Dna2 resection (104-106). Overall, protein degradation and direct DNA nicking are

very different possible mechanisms for Ku removal and further work needs to be done to resolve this discrepancy. It should be noted that these results were obtained from different biological systems and could indicate that there is a divergence in Ku removal mechanisms between yeast and higher eukaryotes.

1.3.3 Competition between repair pathways

There is much investigation regarding how organisms regulate the DSB repair pathway choice and increasing evidence suggests that Ku has an inhibitory effect on the other DSB pathways. Ku is one of the first proteins found at DSB regardless of cell cycle stage and cells will first attempt to repair DSBs by C-NHEJ if the ends are compatible (101, 107-109). HR is the preferred pathway in the S and G2 phases, and the initial end binding factors of HR, for example Mre11, antagonize Ku for DNA end binding. The binding of HR factors initiates DNA end resection to produce single-stranded DNA, which Ku does not have a strong affinity for, and promotes the completion of DSB repair by HR (61). In yeast, Ku appears to outcompete HR factors in G1 phase, as the loss of Ku results in increased Mre11 recruitment and Exo1 mediated resection (72, 110-113). Overexpression of Ku is even able to reduce recruitment of Mre11 in G2, when HR is the preferred DSB repair pathway (110). The HR inhibitory effect appears to be specifically dependent upon Ku's DNA end binding function, as deletion of other NHEJ factors, such as ligase IV, were not able to increase HR activity to the same extent (110). Another study has implicated, not only Ku binding, but the kinase activity of DNA-PK_{CS} in the DNA repair pathway choice, as initiated of HR in G2 depended upon DNA-PK_{CS} autophosphorylation events (114). Ku70 also antagonizes HR via the Fanconi Anemia (FA) and break-induced replication (BIR) repair pathways. The FA pathway repairs DNA

interstrand cross-links (ICLs) in cooperation with the HR pathway during replication (115). Cell lines deficient in FA genes display increased sensitivity to DNA damaging agents that specifically create DNA cross-links and show a greater dependence on repair by NHEJ. The simultaneous deletion of Ku70 however, reverses this sensitivity, and repair is completed by HR once again (116). Similarly, BIR is responsible for the repair of breaks that occur in S phase following a replication fork collapse (117). This pathway is also dependent on HR, and yeast cells null for Mre11 activity are sensitive to agents that induce replication stress (118). Several Ku70 mutants were identified that rescue this Mre11 loss, again suggesting a competitive interplay between Ku and Mre11 (118, 119).

A-NHEJ is Ku-independent end joining, and while it is not currently fully characterized, it is considered to be a more mutagenic DSB pathway as it occasionally utilizes microhomologies far from the DSB which results in extended resection and deletions at the repair site (59, 60, 120, 121). Similar to C-NHEJ, this pathway is active in all phases of the cell cycle, however it was only identified after the deletion of essential C-NHEJ components, suggesting that this pathway is secondary to C-NHEJ (57, 120, 122). It is still unclear why A-NHEJ may be selected over the less mutagenic C-NHEJ pathway, however A-NHEJ, similar to HR, often begins with resection to form SSBs, which would inhibit Ku binding and promote the binding of A-NHEJ factors, such as PARP-1(59, 60, 120, 121). Ku outcompetes the DNA binding factor PARP-1, and deletion of Ku results in increased repair by this pathway (123-125). Furthermore the DNA-PK complex has an inhibitory effect on the enzymatic activity of PARP-1 (126). Studies have indicated that human somatic cell lines with Ku80 deletions retain DSB repair capability, but show a shift towards the A-NHEJ pathway (127). However Ku80-

expressing cell lines with individual deletions of the other proteins required for C-NHEJ have a dramatic decrease in all DSB repair pathways (127). These results suggest that the binding of Ku, or the entire DNA-PK complex to DNA has a dominant negative effect on the other DSB repair pathways if C-NHEJ cannot be completed.

The DNA repair pathway choice is largely determined by cell cycle stage, with breaks in G1 phase repaired by end joining, and breaks in G2/S phases largely repaired by HR. Not surprisingly, members of the cell cycle machinery, namely the cyclin-dependent kinases (CDKs), have been implicated in regulating the activity of several DNA repair factors (128, 129). Several studies have shown, in both yeast and mammalian systems, that CDKs phosphorylate the HR factors CtBP-interacting protein (CtIP) and Dna2 in order to initiate the switch to recombination at the G1/S transition (130-132). There is some evidence that Ku could also be regulated by CDK phosphorylation. Cyclin A1/CDK2 was implicated in the regulation of NHEJ following radiation and was proposed to be a binding partner of Ku in vertebrates (133). Furthermore, mass spectrometry studies revealed potential CDK phosphorylation sites on Ku (134, 135). However, the functional significance of Ku phosphorylation by CDKs has yet to be elucidated. While several potential CDK1 phosphorylation sites were identified in *S. cerevisae* Ku, mutation of these sites did not elicit a DNA repair defect (136).

Recent work has also implicated the factors p53 binding protein 1 (53BP1) and breast cancer 1 (BRCA1) as essential regulators in the pathway choice in mammalian cells. 53BP1, along with RAP1 interacting factor (Rif1) and Pax transactivation domain-interacting protein (PTIP), promote NHEJ and negatively regulate resection in G1 phase (137, 138). BRCA1, along with CtBP-interacting protein (CtiP), promotes the removal of

53BP1 during the switch to HR at the G1/S transition (139). It is currently unclear how Ku fits into this mechanism, however there is evidence that Ku associates with BRCA1 and that this interaction is important for successful NHEJ in G1 (140-142). It is possible that this association is essential for the removal of Ku from breaks, with BRCA1 utilizing the exonuclease activity of the MRN (Mre11-Rad50-NBS1) complex in a nicking mechanism analogous to that proposed for yeast Ku removal.

1.3.4 Role of Ku in other DNA repair pathways

In addition to its role in the repair of DSBs by C-NHEJ, Ku has been implicated in a number of other DNA repair pathways. Ku has been implicated in base excision repair (BER), which repairs DNA base damage, apurinic/apyrimidic (AP) sites and single-strand breaks (SSBs) (48). Cells deficient in Ku70 and Ku80 were sensitive to reactive oxygen species (ROS) and alkylation damage producing agents that result in base lesions and SSBs (143). Additionally, *in vitro* experiments demonstrated that Ku subunits bind AP sites and cell extracts from Ku deficient cells have decreased BER activity (143, 144). Furthermore, Ku has been shown to interact with ABH2, an enzyme involved DNA alkylation repair, potentially implicating it in this pathway as well (145).

1.4 Ku at Telomeres

Telomeres are the linear ends of chromosomes and therefore have the potential to be recognized as DSBs and processed by DSB repair pathways. Specific protein complexes, such as the shelterin complex in mammals and the Rap1 or CST (Cdc13–Stn1–Ten1) complexes in yeast have evolved to bind and form protective caps on the DNA ends to prevent access by the DNA repair complexes (Figure 1-4) (146, 147). A

Figure 1-3 General structure of telomeres

In most eukaryotes telomeric DNA consists of extended tracts of G-rich repeat arrays. The G-rich strand forms a short 3' single-strand protrusion called the G-overhang, which mediates the formation of a complex secondary structure called a t-loop. The t-loop structure allows the folding of the end of the chromosome to mask and protect the DNA end from degradation. **A.** Structure of the yeast telomere. The MRX (Mre11/Rad50/Xrs2) and Sir/Rap1 complexes directly bind the telomeric DNA (281). Ku could potentially (a) bind the DNA end via its DNA binding domain or (b) bind via a protein-protein interaction with telomeric complexes (such as Sir/Rap1). Ku has a role in recruiting telomerase, mediated by an interaction with the TLC1 RNA and Ku80. Ku interaction with the telomere may be indirect, requiring the heterotetramerization of two Ku molecules. **B.** Structure of the mammalian telomere. The Shelterin (TRF1/TRF2/Tin1/Pot1/TPP1) and MRN (Mre11/Rad50/Nbs1) complexes coat the telomeric DNA to protect from degradation (282). Again there is controversy whether (a) Ku directly binds the telomeric DNA or (b) is retained through a protein interaction with components of the Shelterin complex (such as TRF1/TRF2).

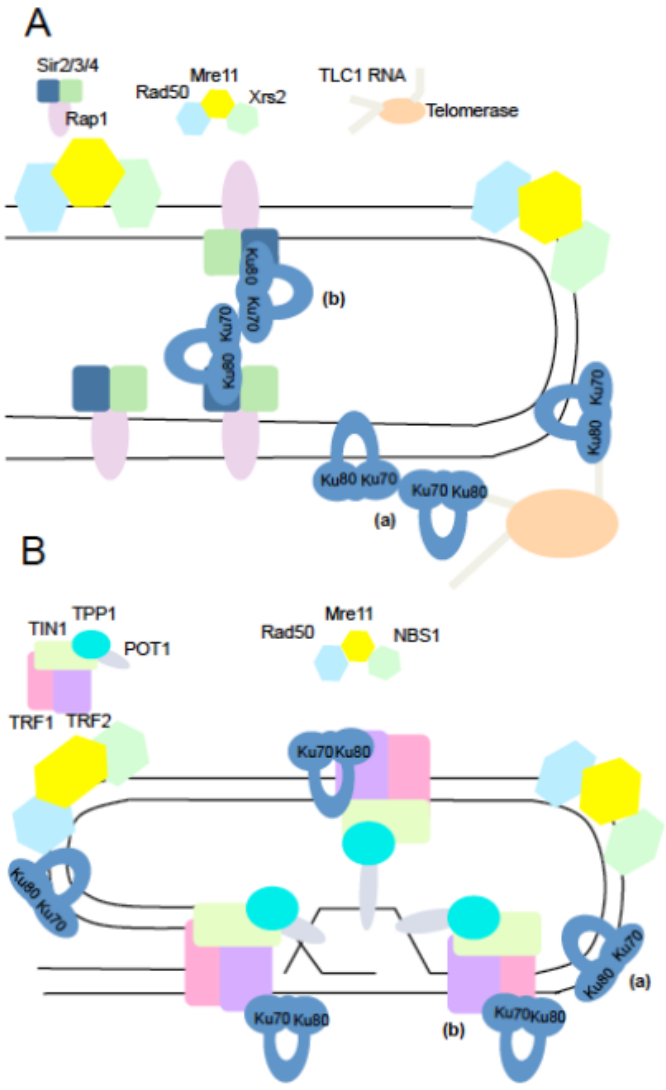
A
Sir2/3/4
Rap1
Mre11
Rad50
Xrs2
TLC1 RNA
Telomerase
Ku80
Ku70
(b)
Ku70
Ku80
Ku80
Ku70
Ku70
Ku80
(a)
B
TIN1
TPP1
POT1
Mre11
Rad50
NBS1
TRF1
TRF2
Ku70Ku80
Ku80
Ku70
Ku70
Ku80
(a)
Ku70 Ku80
(b)
Ku70Ku80

role for Ku in the maintenance of telomeres in yeast has been long established. Foundational to this was the observation that deletion of either Ku subunit in *S. cerevisae* resulted in shortened telomeres and long G-tails compared to wildtype (148-150). The requirement of Ku for proper telomere structure and maintenance appears to be separate from C-NHEJ, as DNA Ligase IV deficient strains, the ligase essential for completion of C-NHEJ, do not show any telomere defects (151). Analysis of telomeres in Ku-deficient mice has produced conflicting results regarding telomere length, with reports of telomere shortening as well as lengthening (152-154). Despite this, the same mice exhibit increased telomere end-to-end fusions and chromosomal aberrations (153, 154). Similarly, human cells with deleted Ku80 show telomere loss and abnormal telomere structure, overall indicating a clear role for Ku in proper telomere structure maintenance in mammals (155).

Similar to its role in protecting the DNA ends of DSBs in NHEJ, Ku protects telomere ends from recombination and degradation events (148-150, 152-154). Paradoxically, although Ku promotes the fusion of dysfunctional, or uncapped, telomere ends, it has an inhibitory effect on the HR and A-NHEJ pathways and on the recombination of normal telomeres. Mouse embryonic fibroblasts (MEFs) deficient in Ku70 have normal telomere structure, however they exhibit increased sister telomere exchanges mediated by HR and chromosome fusions by the A-NHEJ pathway (156, 157). Additionally, Ku deficient *S. cerevisiae* display increased RAD52 dependent recombination of the subtelomeric DNA elements, consistent with its general HR inhibitory function (158, 159). While wildtype cells only exhibit long G-tails during late S phase, yeast Ku deficient strains possess long G-tails throughout the cell cycle. This

defect is almost completely suppressed by the deletion of the 5' to 3' exonuclease Exo1, suggesting that Ku acts to inhibit inappropriate nucleolytic degradation of the C strand by nucleases (160).

Ku also positively regulates telomere length through telomere addition by aiding in the recruitment of telomerase. In yeast, Ku has been shown to interact with telomerase component 1 (TLC1), the telomerase RNA subunit, via binding of TLC1's 48nt stem-loop region (161, 162). Deletion of the binding interface from either the Ku80 vWA domain or the TLC1 stem-loop results in decreased telomere length and decreased *de novo* telomere addition, perhaps due to the decreased levels of TLC1 RNA or altered localization of the telomerase holoenzyme (161, 163-166). There is no sequence conservation between TLC1 and the human telomerase RNA counterpart, hRT, however there is evidence that the interaction between the RNA component of human telomerase (hRT) and Ku in humans is conserved (167). Another study detected an interaction with Ku and telomerase in human cells, however this interaction was reported to occur through the catalytic reverse transcriptase protein subunit hTERT (168).

The phenomenon of the telomere position silencing effect (TPE), observed in many eukaryotic species, is the process by which organisms transcriptionally silence genes located near the telomere (reviewed in (169, 170)). In *S. cerevisiae*, Ku, along with the silent information regulator (Sir) complex, are essential for TPE, as deletion of either Ku subunit results in complete loss of telomeric silencing (171-174). As a consequence of this role, Ku is also involved in the nuclear organization of telomeres. Telomeres and TPE proteins in *S. cerevisiae* are found distinctly clustered in foci around the nuclear periphery, and the loss of Ku function often results in the random distribution of

telomeres throughout the nucleus (174-176). Ku participates in these processes as part of multi-protein complexes with various proteins (such as the Sir proteins, Rap1 and Mps3) and Ku is particularly essential for their formation in the G1 phase of the cell cycle (176-178).

It is still currently unknown how Ku is associated with the telomere *in vivo*, whether it is through direct DNA binding of the end, or is mediated through a protein-protein interaction with another telomere bound factor. Ku has the ability to directly bind telomere DNA *in vitro,* in both mammals and yeast (179, 180). Furthermore, mutations in yeast Ku's DNA binding domain reduces association with telomeric chromatin and renders it unable to protect the telomere end, suggesting that this region is key for telomere binding (181). Despite this evidence, there is still some question whether it truly slides onto the telomere end via its DNA binding ring. Telomeres in many species form higher order loop structures designed to conceal the end from attack by Ku and the DSB repair pathways, so further research needs to be done to understand how and when Ku would be allowed access to the telomere end.

Another possibility is that Ku is retained at the telomere through protein-protein interaction with other telomere bound factor(s). Ku has been shown to interact with TRF1, TRF2 and Rap1 (21, 182-186). These components of the shelterin complex bind DNA directly and then mediate the recruitment of other shelterin factors, such as TERF1-interacting nuclear factor 2 (TIN2) to the TRF proteins in humans and Sir3/4 to Rap1 in *S. cerevisiae*, and therefore could also be involved to recruit Ku at the telomeres (187, 188). A longstanding model for telomerase recruitment by Ku in yeast, suggested that Ku bound to the telomere end through its DNA binding ring and then bound the TLC1 RNA

via the yeast Ku80 vWA domain (161). However there is evidence that Ku requires the DNA binding domain for both DNA and RNA binding and cannot bind both simultaneously (189). These observations suggest that Ku does not recruit telomerase to the telomere by binding the telomere directly, and instead favours a model where Ku must bind another telomere bound factor to be retained. A combination of DNA binding and protein interaction is also possible and has been reported for the shelterin component protection of telomeres 1 (POT1), which was shown to bind the G-strand of telomeres, as well as form multiple protein interactions (190, 191). Given that Ku has been shown to multimerize, it is possible that one Ku molecule interacts with the telomere end then multimerizes with another Ku molecule that is bound to telomerase. Although it appears that there are similarities in Ku telomere binding between yeast and mammalian systems, these organisms have different telomere structure and protein complexes present, so it is possible that Ku has different mechanisms for telomere binding and protection. Advances in high-resolution microscopy techniques have allowed for direct visualization of telomere structures, such as mammalian t-loop formation by TRF2, and could help in understanding Ku's role at the telomere (192).

1.5 DNA Damage Response

1.5.1 Overview

The DNA damage response (DDR) (Figure 1-4) is a carefully orchestrated signaling cascade that senses DNA damage and promotes DNA repair to salvage the cell, but also carries out cell fate decisions to protect the overall health of the organism (193). The early stages of the DDR involve the building of a large multi-protein complex at the site of damage, followed by numerous post-translational modifications (including

Figure 1-4 Overview of DNA double-strand break (DSB) recognition and DNA Damage Response (DDR).

After the introduction of a double-strand break (DSB), the broken DNA end is rapidly recognized by the Ku heterodimer and the MRN complex (Mre11/Rad50/NBS1). Next is the recruitment of the PIKK family members DNA-PKcs, bound to Ku, and ATM, which both phosphorylate the histone variant H2AX on its C-terminal residue Ser139 (to yield γ-H2AX). The MRN complex promotes the activation of ATM molecules, which in turn further amplify H2AX phosphorylation and spread the γ-H2AX signal far from the initial damage site. Several other factors are phosphorylated by ATM and recruited to the damaged site in large numbers, including MDC1, 53BP1, Rif1 and BRCA1. ATM also initiates a signaling cascade through the phosphorylation of p53 and Chk1/2 that results in broad transcriptional changes to induce cell cycle arrest or activate apoptosis if the damage is unable to be repaired (193).

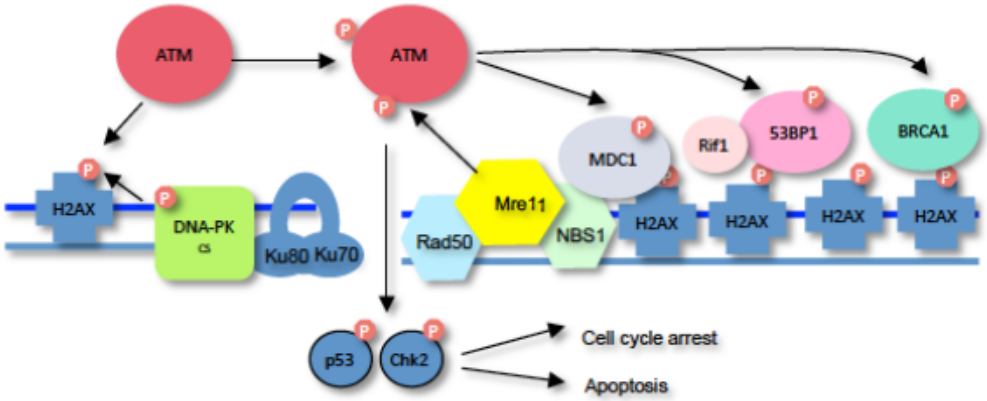
ATM
ATM
MDC1
Rif1
53BP1
BRCA1
H2AX
DNA-PK
cs
Ku80 Ku70
Mre11
Rad50
NBS1
H2AX
H2AX
H2AX
H2AX
p53
Chk2
Cell cycle arrest
Apoptosis

phosphorylation, ubiquitination, acetylation, sumolyation, methylation and ribosylation) to the proteins and surrounding histones. The resulting chromatin modification and reorganization allows access to the DNA for processing and repair to occur (194). Simultaneously, the activation of transducer proteins, mainly kinases, activates numerous downstream effector molecules to induce broad transcriptional changes throughout the cell. This cascade is required to initiate cell cycle checkpoints, and if necessary, programmed cell death and senescence, two mechanisms that eliminate cells damaged beyond repair. The failure to properly execute the DDR can have devastating consequences to the health of an organism, as it can allow DNA damage to persist, resulting in genomic instability and perhaps cellular transformation and cancer.

1.5.2 ATM

The serine/threonine kinase ATM of the PIKK family of kinases is the chief regulator of the DDR (195, 196). ATM has an impressive list of cellular targets including proteins involved in DNA repair, cell cycle regulation, and cell death pathways (197). One of the critical events in ATM signaling is the phosphorylation of p53, a transcription factor that has broad transcriptional control over many cell survival and cell death effector proteins (198). Another well-characterized target is the histone H2A variant, H2AX, which is phosphorylated on its C-terminal tail at residue serine-139. Phosphorylated H2AX (commonly known as ϒ-H2AX) serves as a docking site nearby the DSB for repair factors to accumulate and form large foci (199, 200). H2AX phosphorylation often propagates kilo- to megabases from the initial damage site, making it easily observable by fluorescent microscopy, and is therefore commonly used as a marker for DSBs (199, 200).

The activation of ATM is dependent on both post-translational modifications and protein-protein interactions. Several proteins are recruited to the DSB foci that are required for full ATM activation. Some of the first proteins recruited to the DSB are the Mre11-NBS1-Rad50 proteins (forming the MRN complex), which create a bridge spanning the DSB and play roles in both repair through HR and DDR signaling. The MRN complex activates ATM through an interaction with the NBS1 subunit, and this interaction is further stabilized through the activities of neighboring foci proteins, namely 53BP1 and BRCA1 (195, 196). ATM activation is also mediated by the scaffolding protein, MDC1, which binds ϒ-H2AX and ATM, tethering ATM to the chromatin (195, 196). ATM directs its own positive feedback loop by phosphorylating MDC1 and the MRN complex to recruit and activate further ATM molecules, greatly amplifying the signaling cascade. Additionally, ATM undergoes several phosphorylation and acetylation modifications, including the autophosphorylation of particular residues (most notably, serine 1981) that is essential for retention of ATM at DNA and prolonged DDR signaling (195, 196).

1.5.3 Cell cycle checkpoints

The eukaryotic cell cycle is divided into four phases: gap (G1), synthesis (S), G2 and mitosis (M). During the G1 phase, the cell increases in size and begins synthesizing RNA and proteins. During the S phase, genomic DNA undergoes replication to produce an exact copy for the daughter cell. In G2, the cell continues to grow and produce enough energy for division into two. Finally, during mitosis, the cell divides chromosomes, separates into two daughter cells, and the cell cycle resumes. Cells that are not actively cycling through these four phases are said to be in G0, a state that they may remain in

transiently, or until their death. Cell cycle progression is largely controlled by the activity of cyclins and cyclin dependent kinases (CDKs). Cyclins, small proteins that are expressed and degraded in a coordinated matter as the cells transition between phases, bind and activate the CDKs to induce phosphorylation of a number of cell cycle regulatory proteins. The transition between each phase is tightly regulated and the cell must ensure that the integrity of its DNA is not compromised prior to moving onto the next phase, termed the G1/S, intra-S, G2/M or mitotic DNA damage checkpoints.

The G1/S transition (Figure 1-5A) is mediated by the CyclinD/CDK4/6 complex, which phosphorylates a number of targets, including the Retinoblastoma protein (Rb), to ultimately relieve inhibition on cell cycle promoting E2F transcription factors (201). These factors create a positive feedback loop by promoting the activation of the CyclinE/CDK2 complex, which phosphorylates more Rb, to activate more E2Fs and drives transcription of genes required for the transition (201). The G1/S checkpoint is essential for preventing cells from initiating DNA synthesis with damaged DNA. It is initiated by the ATM-mediated phosphorylation of p53, the p53 inhibitor Mdm2, and the kinase Chk2. Activated p53 upregulates the CDK inhibitor p21, which binds and inhibits both the CyclinD/CDK4/6 and CyclinE/CDK2 complexes (201). In parallel, Chk2 induces the degradation of the phosphatase CDC25a, thereby preventing the removal of inhibitory phosphates and maintaining an inactive CDK2 (201). This checkpoint is extremely sensitive and can be initiated by a single DSB (202-204). At low doses it functions to provide the cell with sufficient time for repair, which is estimated to be about 6 hours for a 1 Gy dose, as measured by the kinetics of H2AX phosphorylation (202-204).

Figure 1-5 DNA damage checkpoints.

(A) The transition from the G1 to S phase (boxed) is initiated by Cyclin D/CDK4/6 complex phosphorylation of the retinoblastoma protein (Rb), allowing the release of the bound E2F transcription factors. The E2Fs stimulate a positive feedback loop by initiating expression of the CyclinE/CDK2 complex, which phosphorylates more Rb, to increase the pool of E2Fs and induce expression of genes necessary for S phase. The G1/S DNA damage checkpoint is accomplished by two parallel mechanisms. (i) ATM phosphorylates Mdm2 to allow the release of the transcription factor p53, and also phosphorylates p53 to stimulate its transcriptional activity (activator phosphates in green). p53 induces the expression of the cell cycle inhibitor p21 which binds and inactivates both the CyclinD/CDK4/6 and CyclinE/CDK2 complexes. (ii) ATM phosphorylates to activate the kinase Chk2, which subsequently phosphorylates the phosphatase Cdc25a to trigger its degradation (inhibitory phosphates in red). Cdc25a is required to remove inhibitory phosphates from the CyclinE/CDK2 complex, and so its degradation keeps CyclinE/CDK2 in its inactive form. (B) The transition from the G2 to M phase (boxed) is triggerered by the activity of the CyclinB/CDK1 complex. Wee1 and Myt1 kinase dependent inhibitory phosphorylation keep this complex inactive, but activity of the Cdc25a phosphatase removes this inhibition to induce G2/M transition. The G2/M DNA damage checkpoint is achieved through two mechanisms similar to that of the G1/S checkpoint. (i) ATM dependent upregulation of p21 to directly bind and inhibit the CyclinB/CDK1 complex. (ii) ATM and Chk2 dependent degradation of the cdc25a phosphatase to prevent removal of inhibitory phosphates from the CyclinB/CDK1 complex.

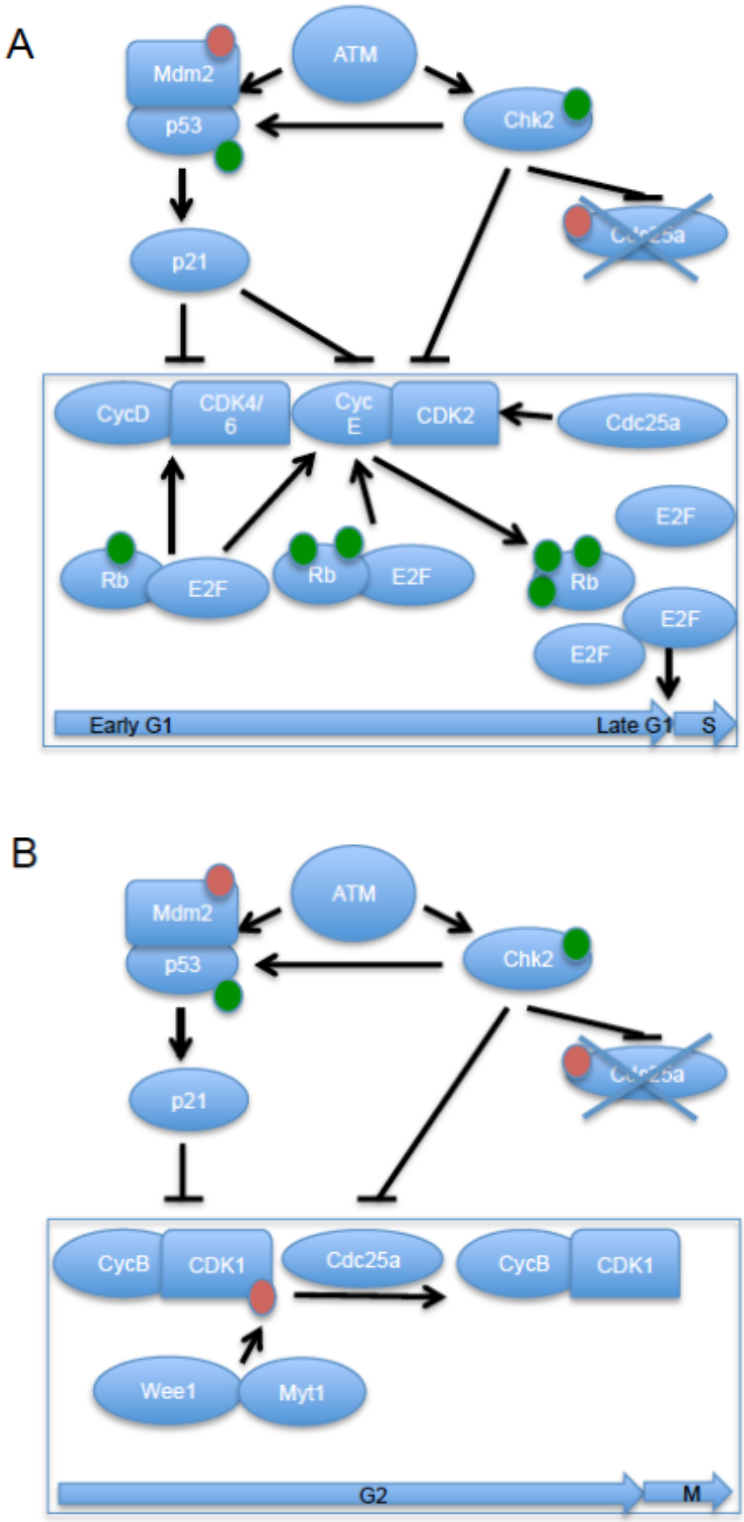
A
Mdm2
ATM
p53
Chk2
p21
CycD
CDK4/
6
Cyc
E
CDK2
Cdc25a
E2F
Rb
E2F
Rb
E2F
Rb
E2F
E2F
Early G1
Late G1
S
B
Mdm2
ATM
p53
Chk2
p21
CycB
CDK1
Cdc25a
CycB
CDK1
Wee1
Myt1
G2
M

Mitotic entry at the G2/M transition (Figure 1-5B) is driven by the activities of the CyclinB/CDK1 complex. Prior to entry, the CyclinB/CDK1 complex is kept inactive by Wee1 and Myt1 kinase mediated phosphorylation, but this inhibition is relieved by the activities of the Cdc25 phosphatase. The G2/M checkpoint is initiated again through the ATM dependent activation of p53 and Chk kinases. Similar to the G1/S transition, p21 is upregulated to bind and inhibit the CyclinB/CDK1 complex, while Chk2 inactivates Cdc25 to prevent the removal of inhibitory phosphates (205, 206). This checkpoint is required to transiently arrest the cells to repair breaks occurring in G2 phase and prevent the entry into mitosis with DNA damage. This process occurs rapidly, however, it does not completely block progression, as there are several reports of cells still entering mitosis in the presense of 10-20 DSBs (207-209).

Once the damage is repaired, cell cycle checkpoints are terminated and normal cycling can resume. Although the mechanisms governing the resolution of damage checkpoints are less well understood, it is known that the action of phosphatases play a large role (210, 211). Examples of phosphatases demonstrated to counteract the DDR activator kinases include Wip1, PP1, PP2A, PP4 and PP6, which remove the phosphates on substrates such as ATM, checkpoint kinases, H2AX and DNA repair proteins, rendering them inactive (212-216). The signaling pathways that drive the shift in balance towards phosphatase over kinase activity remain to be established.

1.5.4 Senescence

Senescence can be defined as irreversible growth arrest to prevent the proliferation of damaged cells (217). Senescent cells can be distinguished from other non-dividing cells, such as quiescent and terminally differentiated cells, by

morphological changes and the expression of several biomarkers. These include the expression of cell cycle inhibitors, the absence of proliferation markers, constitutive heterochromatin foci, and upregulation of the β-galactosidase enzyme (217). Initiation is marked by the activation of p53, leading to the upregulation of several CDK inhibitors, namely p16 (also known as INK4A), p15 (INK4B), p21 (WAF1) and p27, and promoting the hypophosphorylation of the tumor suppressor Rb (198, 217, 218).

It is unclear what mechanisms induce senescence as opposed to transient cell cycle arrest, as they are initiated by the same mechanisms, such as the p53-p21 and p16-Rb pathways (217, 218). It is possible that the quick repair of DNA damage shuts down signaling, whereas slow or incomplete repair results in prolonged signaling and an eventual senescence phenotype. There is evidence that fibroblasts that have fully activated the p16-Rb pathway are unable to resume growth, even after the inactivation of p16, Rb and p53, indicating there is a point of no return in senescence activation, however this point remains to be elucidated (219).

1.5.5 Apoptosis

The most drastic response to overwhelming DNA damage is the initiation of programmed cell death, termed apoptosis. Apoptosis is a tightly regulated cascade, triggered by either external (extrinsic pathway) or internal (intrinsic pathway) stimuli, that converges upon a family of cysteine proteases (caspases) to cleave a broad range of intracellular proteins and induce cell death (218, 220). Morphologically, this process results in cellular shrinkage, chromatin condensation and fragmentation, membrane blebbing and the formation of apoptotic bodies (220).

The intrinsic apoptotic pathway mediates cell death in response to cellular stresses, including DNA damage. The transcription factor p53 is a main regulator of this process, and is activated following damage to transcriptionally upregulate genes encoding apoptotic effectors (198, 220). Main targets of p53 in include the Bcl-2 family of proteins, comprised of multidomain and BH3 domain-only members that regulate the mitochondrial membrane permeability. Upon stimulus of the intrinsic pathway, p53 upregulates the pro-apoptotic Bcl-2 member, Bax, which induces mitochondrial membrane permeability and allows the release of cytochrome c. This triggers the activation of the intiator caspase, caspase 3, that in turn, cleaves to activate the effector caspase, caspase 9, which is responsible for cleaving proteins involved in cell growth and maintenance and ultimately causing cell death (218, 220).

There are additional p53-independent signaling cascades that are activated by DNA damage and contribute to apoptosis. The JNK kinases (JNK1 and JNK2) are stress-induced kinases that execute its pro-apoptotic functions primarily through the activation of the c-Jun, AP-1, and activating transcription factor 2 (ATF2) transcription factors (221). Similarly, the mitogen activated protein kinase (MAPK) family member p38 is often induced after DNA damage and upregulates the activities of ATF2, ATF3, cAMP response element-binding protein (CREB) and C/EBP homologous protein (CHOP) transcription factors (222). These transcription factors will subsequently regulate the expression of vast array of proteins, including those of the Bcl-2 family, to promote cell death (221, 222).

1.5.6 Ku in the DDR

There is some evidence that Ku is involved in the modulation of ATM activity

following DNA damage. Ku appears to prevent ATM-dependent ATR activation, perhaps acting as a signaling block to the HR pathway (223). Furthermore, Ku80 null cells were shown to have increased S phase inhibition after DNA damage due to increased ATM activity (224). We identified a specific residue in Ku70's vWA domain, serine 155, that when mutated to alanine results in decreased DNA damage signaling and apoptotic activation after IR, despite having no impact on Ku's ability to function in C-NHEJ (22). These results suggest that in addition to its essential role in DNA repair, modification of Ku also signals to the ATM dependent DDR cascade to regulate cell fate after DNA damage. This is not entirely surprising as several other DNA repair factors (ex. Mre11), have functions in both DNA repair as well as the DNA damage signaling cascade (225). It is possible that Ku also has a dual role in the DNA damage response, first promoting the repair by NHEJ, as well as relaying signals as to the completion, or lack thereof, of DNA repair.

In addition to its impact on upstream DDR signaling, a number of studies have implicated Ku70 as a direct inhibitor of apoptosis, through the binding and inhibition of the pro-apoptotic factor Bax (226, 227). This interaction is proposed to be modulated by various mechanisms, including protein-protein interactions and post-translational modification of Ku. Some examples of protein interactions include the binding of Ku70 to NBS1 and a cleavage product of cyclin E, both of which were suggested to inhibit the binding of Ku70 to Bax and promote apoptosis (228, 229). The acetylation of Ku70 is also suggested to negatively regulate the Ku70-Bax interaction. Ku70 is acetylated in the C-terminal linker domain on eight lysine residues between K539 and K556 and alanine substitution of these residues decreased Bax-dependent apoptotic activation (31). This

acetylation is mediated by CREB-binding protein (CBP) and P300/CBP-associated factor (PCAF) while deacetylation is controlled by histone deacetylase (HDAC) and sirtuin (SIRT) deacetylase enzymes (31, 230, 231). There is some evidence that Ku may have deubiquitination activity, as it has been proposed to promote the deubuquitination of Bax, and another anti-apoptotic regulator of Bax, Mcl-1 (226, 232). Overall, there are several unanswered questions regarding the interaction with Ku70 and Bax. Many studies have suggested that this interaction occurs in the absence of Ku80, despite the fact that there is little evidence that the Ku subunits exist as monomers. Furthermore, Ku is predominantly a nuclear protein but Bax is largely cytoplasmic in its inactive form and then translocates to the mitochondria during apoptotic activation (233). The regulatory mechanisms that would allow a subset of Ku70 monomers to remain in the cytoplasm bound to Bax remain to be elucidated.

1.5.7 Aurora Kinases

The Aurora kinases are a family of serine/threonine kinases with a well-established role in promoting cell cycle progression (234). Mammalian genomes encode for three members, Aurora A, B and C, which differ in their size, function and subcellular localization. All members can be divided into three general domains: a well conserved central catalytic domain, C-terminal region containing a D-box motif required for degradation, and a diverse N-terminal region largely utilized as a regulatory domain (234). Aurora A and B are most similar in their structure and ubiquitous expression pattern, however their cellular roles vary due to their differing localization. Aurora A promotes mitotic entry and spindle assembly, while Aurora B is involved in the spindle assembly checkpoint, kinetochore attachment, chromatin modification and cytokinesis

(234). Although their roles in mitosis are well described, increasing evidence suggests that the both Aurora A and B also participate in the G1/S and G2/M transitions (235, 236). These proteins are often found upregulated in cancers and have subsequently become the target of several small molecule inhibitors to utilize in cancer treatment (237, 238).

The regulation of aurora kinases is tightly controlled by a number of different mechanisms. Ultimately, the activation is achieved through the autophosphorylation of a threonine residue in the activation loop of the catalytic domain. However, many activating cofactors are involved that bind either the catalytic domain or the N-terminal regulatory region and allow for the specific activation of kinase activity at the correct cell cycle phase and subcellular localization (239). Aurora B is the catalytic member of the mitotic chromosomal passenger complex (CPC) and requires the binding of the other regulatory complex members (INCENP, Survivin and Borealin/Dasra B) for full activation and localization to the centromere (240). Protein binding either induces conformational changes in Aurora to promote catalytic activation, or the regulatory subunits promote Aurora B clustering and subsequent autoactivation. Cofactors also bind and inhibit Aurora activity, such as the PP1 and PP2A phosphatases, that remove activating phosphatases to render it inactive (241, 242).

Not surprisingly, as kinases that promote cell cycle progression, Aurora kinases are found inhibited after the introduction of DNA damage (243, 244). Emerging evidence suggests that this regulation is due to interactions with DDR and DNA repair factors. Aurora B has been shown to interact with, and be inhibited by, the A-NHEJ factor PARP-1, while the HR factor BRCA2 has been demonstrated to promote Aurora B degradation

(244, 245). There are also indications of a reciprocal regulation of DDR factors by Aurora kinases. Aurora B has been shown to phosphorylate ATM, while Aurora A regulates BRCA1 and p53. Overall, given the strong interest in targeting Aurora kinases for cancer treatment, a clearer understanding of how Aurora kinases are regulated after DNA damage is required.

1.6 Ku in Disease

1.6.1 Immune system disorders

The vertebrate immune system utilizes Ku and C-NHEJ to repair physiological DSBs generated to create immune system genetic diversity. Recombination of the V, D, and J segments of immunoglobulins (Ig) in lymphoid cells and class switch recombination of the T-cell receptor genes in mature T cells allows for the recognition of a wide variety antigens, which results in an adaptive immune response (246). The exons of the Ig genes are flanked by recombination-signal sequences that are recognized by the recombination-activating gene (RAG) complex to produce a blunt ended DSB at the signal sequence and a closed hairpin at the coding sequence. This structure is then processed and resolved by the C-NHEJ machinery (246).

Ku70 and Ku80 knockout mice display many immune system abnormalities including B cell developmental arrest, T cell arrest, and failed lymphocyte differentiation following γ-irradiation (67, 247-249). Humans and mice suffering from genetic defects in V(D)J recombination present with a severe combined immunodeficiency (SCID) phenotype resulting in severe infections and poor prognosis. There are several characterized human disorders with various degree of SCID phenotype that have been

linked to mutations in NHEJ factors, such as DNA Ligase IV, Artemis, and XLF, as well as the other DSB repair pathway and DDR factors (250-253). Interestingly, only a few individuals have been reported to have genetic defects in the DNA-PK complex, however, all presented mutations occurred in the DNA-PK_{CS} subunit, and thus far, no disorder linked to Ku mutations has been identified (254, 255). It is currently unknown whether mutations in Ku are better tolerated in humans, or in the contrary, whether deleterious Ku mutations are lethal in humans.

1.6.2 Aging

Aging is the progressive degeneration that occurs at the cellular and organismal level. One of the observed phenotypes of Ku deficient mice is increased aging and senescence (249, 256-258). Mice deficient in one Ku subunit have one-third the lifespan of their wildtype counterparts, partially in due to an early onset of the phenotypic symptoms of aging (259). There is evidence that C-NHEJ declines during the aging process, with lower efficiency observed in aging rodents, and in Alzheimer's patients, so the loss of NHEJ in Ku deficient mice could be contributing to the aging process (260-262). Furthermore, as previously described, Ku deficient mice and cells exhibit shortened telomeres as well as other telomere abnormalities. Shortened telomeres have been linked to increased aging and senescence, due to increased genomic instability leading to cell cycle arrest, so this could also be contributing to the aging phenotype observed in Ku-deficient mice (263, 264).

1.6.3 Cancer

A common characteristic amongst human tumors is genomic instability (265). Cells defective in DSB repair are predisposed to chromosome translocations and gene

amplifications, potentially leading to the activation of oncogenes and tumourigenesis. Through its role in C-NHEJ, Ku functions as a cancer caretaker gene, promoting genomic integrity and preventing tumourigenesis. Ku knockout mice show increased chromosomal breakage, translocations and aneuploidy (249, 256, 258, 259). These mice display slightly increased cancer incidence as compared to controls, however this is mostly restricted to lymphomas (249, 256, 258, 259). Together with a p53 deficiency that impairs control of proliferation, Ku80 deficient mice show early onset tumour formation and further increased incidence of T and B cell lymphomas (68). This suggests that Ku mutations can be oncogenic when accompanied by a mutation in a tumor suppressor gene.

The expression of Ku has been frequently found deregulated in tumour samples and its expression level has been proposed as a marker of predicting patient response to radiation therapy and survival (266-271). The exploitation of genetic defects in DNA repair and DDR factors have long been employed in cancer treatment (272). As previously mentioned, Ku and DNA-PK_{CS} deficient cell lines are sensitive to radiation and chemotherapeutic drugs, and therefore would make them potential druggable targets in cancer treatment. There are a few examples of strategies to target Ku specifically, including a subunit dimerization interference using a peptide, downregulation by RNAi and small molecule inhibition (273-276). The therapeutic potential of targeting the Ku70/Bax interaction to activate apoptosis in cancer has been explored through creation of Bax inhibiting peptides derived from the Ku70 sequence and promoting Ku70 acetylation *in vivo* through deacetylase inhibitors (277-279). A more commonly employed strategy to target the DNA-PK complex however, is to modulate the kinase activity of DNA-PK_{CS} with small molecular inhibitors, as DNA-PK_{CS} expression is

frequently found upregulated in tumours (280).

1.7 Scope of thesis

The cellular response to DSBs is a tightly controlled process with the ultimate goal of repairing the DNA damage, but also protecting the overall health of the organism. Amongst proteins involved in the DDR, there are several examples of DNA repair proteins performing dual roles in both repair and maintaining the signaling cascade. For example, the MRN complex has a mechanistic role in the HR DSB repair pathway, but also is integral for the activation and propagation of ATM signaling. We have identified a similar role Ku, which has a well-established role as the DNA binding component of the NHEJ repair pathway, and for which we now propose a novel role for Ku in the signaling to DDR in the case of unsuccessful DNA repair.

The focus of this work is the Ku70 vWA domain, a conserved protein-protein interaction domain, for which the function in DNA repair has remained uncertain. We begin by investigating the requirement for different regions of the Ku70 vWA domain in response to IR (Chapter 2). We show that helix 5, particularly the residues D192/D195, are integral for Ku's DNA repair function. Mutation of these residues severely compromises cell survival in response to IR and dramatically decreases DNA repair efficiency. In contrast, the loop region between helix 4 and 5, particularly the residue S155, is required for activation of the DDR after IR. Substitution of this residue to alanine surprisingly increased survival in response to IR. Further analysis indicated that mutation of this residue conferred decreased activation of DDR signaling markers and apoptosis, indicating that mutation of this residue was preventing the DDR from signaling to the apoptotic machinery. Overall, this chapter established an important role

for the Ku70 vWA domain in the response to DSBs.

Next, we went on to further characterize the role of S155 in the DDR (Chapter 3). We hypothesized that this residue was a phosphorylation site and used mass spectrometry analyses to observe phosphorylation after IR. Expression of a phosphomimetic substitution at this site, S155D, induced constitutive activation of DDR and cell cycle arrest at both the G1/S and G2/M checkpoints. Through a general screen of interacting factors, we identified the region surrounding S155 as contributing to the binding and inhibition of the cell cycle kinase Aurora B. In wild type cells, we determined that Ku does not bind Aurora B constitutively, but after IR, they complex to inhibit Aurora B activity and induce cell cycle arrest. Altogether, we have characterized a novel phosphorylation event in the Ku70 vWA domain that relays DNA repair signals to the DDR to carry out cell fate decisions.

1.8 References

1. Lindahl T & Barnes DE (2000) Repair of endogenous DNA damage. *Cold Spring Harbor symposia on quantitative biology* 65:127-133.
2. Mimori T*, et al.* (1981) Characterization of a high molecular weight acidic nuclear protein recognized by autoantibodies in sera from patients with polymyositis-scleroderma overlap. *J Clin Invest* 68(3):611-620.
3. Mimori T (2002) Clinical significance of anti-Ku autoantibodies--a serologic marker of overlap syndrome? *Internal medicine* 41(12):1096-1098.
4. Cooley HM, Melny BJ, Gleeson R, Greco T, & Kay TW (1999) Clinical and serological associations of anti-Ku antibody. *The Journal of rheumatology* 26(3):563-567.
5. Takeda Y & Dynan WS (2001) Autoantibodies against DNA double-strand break repair proteins. *Frontiers in bioscience : a journal and virtual library* 6:D1412-1422.
6. Mimori T, Hardin JA, & Steitz JA (1986) Characterization of the DNA-binding protein antigen Ku recognized by autoantibodies from patients with rheumatic disorders. *J Biol Chem* 261(5):2274-2278.
7. de Vries E, van Driel W, Bergsma WG, Arnberg AC, & van der Vliet PC (1989) HeLa nuclear protein recognizing DNA termini and translocating on DNA forming a regular DNA-multimeric protein complex. *Journal of molecular biology* 208(1):65-78.
8. Griffith AJ, Blier PR, Mimori T, & Hardin JA (1992) Ku polypeptides synthesized in vitro assemble into complexes which recognize ends of double-stranded DNA. *J Biol Chem* 267(1):331-338.
9. Getts RC & Stamato TD (1994) Absence of a Ku-like DNA end binding activity in the xrs double-strand DNA repair-deficient mutant. *J Biol Chem* 269(23):15981-15984.
10. Verhaegh GW*, et al.* (1995) A novel type of X-ray-sensitive Chinese hamster cell mutant with radioresistant DNA synthesis and hampered DNA double-strand break repair. *Mutation research* 337(2):119-129.
11. Taccioli GE*, et al.* (1998) Targeted disruption of the catalytic subunit of the DNA-PK gene in mice confers severe combined immunodeficiency and radiosensitivity. *Immunity* 9(3):355-366.
12. Rathmell WK & Chu G (1994) Involvement of the Ku autoantigen in the cellular response to DNA double-strand breaks. *Proc Natl Acad Sci U S A* 91(16):7623-7627.
13. Rathmell WK & Chu G (1994) A DNA end-binding factor involved in double-strand break repair and V(D)J recombination. *Mol Cell Biol* 14(7):4741-4748.
14. Smider V, Rathmell WK, Lieber MR, & Chu G (1994) Restoration of X-ray resistance and V(D)J recombination in mutant cells by Ku cDNA. *Science* 266(5183):288-291.
15. Gu Y, Jin S, Gao Y, Weaver DT, & Alt FW (1997) Ku70-deficient embryonic stem cells have increased ionizing radiosensitivity, defective DNA end-binding activity, and inability to support V(D)J recombination. *Proc Natl Acad Sci U S A* 94(15):8076-8081.

16. Walker JR, Corpina RA, & Goldberg J (2001) Structure of the Ku heterodimer bound to DNA and its implications for double-strand break repair. *Nature* 412(6847):607-614.
17. Paillard S & Strauss F (1991) Analysis of the mechanism of interaction of simian Ku protein with DNA. *Nucleic Acids Res* 19(20):5619-5624.
18. Ono M, Tucker PW, & Capra JD (1994) Production and characterization of recombinant human Ku antigen. *Nucleic Acids Res* 22(19):3918-3924.
19. Whittaker CA & Hynes RO (2002) Distribution and evolution of von Willebrand/integrin A domains: widely dispersed domains with roles in cell adhesion and elsewhere. *Molecular biology of the cell* 13(10):3369-3387.
20. Ribes-Zamora A, Mihalek I, Lichtarge O, & Bertuch AA (2007) Distinct faces of the Ku heterodimer mediate DNA repair and telomeric functions. *Nat Struct Mol Biol* 14(4):301-307.
21. Ribes-Zamora A, Indiviglio SM, Mihalek I, Williams CL, & Bertuch AA (2013) TRF2 Interaction with Ku Heterotetramerization Interface Gives Insight into c-NHEJ Prevention at Human Telomeres. *Cell Rep*.
22. Fell VL & Schild-Poulter C (2012) Ku regulates signaling to DNA damage response pathways through the Ku70 von Willebrand A domain. *Mol Cell Biol* 32(1):76-87.
23. Strande N, Roberts SA, Oh S, Hendrickson EA, & Ramsden DA (2012) Specificity of the dRP/AP lyase of Ku promotes nonhomologous end joining (NHEJ) fidelity at damaged ends. *J Biol Chem* 287(17):13686-13693.
24. Roberts SA*, et al.* (2010) Ku is a 5'-dRP/AP lyase that excises nucleotide damage near broken ends. *Nature* 464(7292):1214-1217.
25. Shirodkar P, Fenton AL, Meng L, & Koch CA (2013) Identification and functional characterization of a Ku-binding motif in aprataxin polynucleotide kinase/phosphatase-like factor (APLF). *J Biol Chem* 288(27):19604-19613.
26. Gell D & Jackson SP (1999) Mapping of protein-protein interactions within the DNA-dependent protein kinase complex. *Nucleic Acids Res* 27(17):3494-3502.
27. Singleton BK, Torres-Arzayus MI, Rottinghaus ST, Taccioli GE, & Jeggo PA (1999) The C terminus of Ku80 activates the DNA-dependent protein kinase catalytic subunit. *Mol Cell Biol* 19(5):3267-3277.
28. Aravind L & Koonin EV (2000) SAP - a putative DNA-binding motif involved in chromosomal organization. *Trends Biochem Sci* 25(3):112-114.
29. Hu S, Pluth JM, & Cucinotta FA (2012) Putative binding modes of Ku70-SAP domain with double strand DNA: a molecular modeling study. *J Mol Model* 18(5):2163-2174.
30. Wang J, Dong X, & Reeves WH (1998) A model for Ku heterodimer assembly and interaction with DNA. Implications for the function of Ku antigen. *J Biol Chem* 273(47):31068-31074.
31. Cohen HY*, et al.* (2004) Acetylation of the C terminus of Ku70 by CBP and PCAF controls Bax-mediated apoptosis. *Mol Cell* 13(5):627-638.
32. Kim KB*, et al.* (2013) Inhibition of Ku70 acetylation by INHAT subunit SET/TAF-Ibeta regulates Ku70-mediated DNA damage response. *Cellular and molecular life sciences : CMLS*.

33. Hang LE*, et al.* (2014) Regulation of Ku-DNA association by Yku70 C-terminal tail and SUMO modification. *J Biol Chem* 289(15):10308-10317.
34. Schild-Poulter C*, et al.* (2001) The binding of Ku antigen to homeodomain proteins promotes their phosphorylation by DNA-dependent protein kinase. *J Biol Chem* 276(20):16848-16856.
35. Bertinato J, Schild-Poulter C, & Hache RJ (2001) Nuclear localization of Ku antigen is promoted independently by basic motifs in the Ku70 and Ku80 subunits. *J Cell Sci* 114(Pt 1):89-99.
36. Singleton BK*, et al.* (1997) Molecular and biochemical characterization of xrs mutants defective in Ku80. *Mol Cell Biol* 17(3):1264-1273.
37. Errami A*, et al.* (1996) Ku86 defines the genetic defect and restores X-ray resistance and V(D)J recombination to complementation group 5 hamster cell mutants. *Mol Cell Biol* 16(4):1519-1526.
38. Downs JA & Jackson SP (2004) A means to a DNA end: the many roles of Ku. *Nature reviews. Molecular cell biology* 5(5):367-378.
39. Doherty AJ, Jackson SP, & Weller GR (2001) Identification of bacterial homologues of the Ku DNA repair proteins. *FEBS Lett* 500(3):186-188.
40. Aravind L & Koonin EV (2001) Prokaryotic homologs of the eukaryotic DNA-end-binding protein Ku, novel domains in the Ku protein and prediction of a prokaryotic double-strand break repair system. *Genome research* 11(8):1365-1374.
41. Bowater R & Doherty AJ (2006) Making ends meet: repairing breaks in bacterial DNA by non-homologous end-joining. *PLoS Genet* 2(2):e8.
42. Weller GR*, et al.* (2002) Identification of a DNA nonhomologous end-joining complex in bacteria. *Science* 297(5587):1686-1689.
43. Lindahl T (1993) Instability and decay of the primary structure of DNA. *Nature* 362(6422):709-715.
44. Yonekura S, Nakamura N, Yonei S, & Zhang-Akiyama QM (2009) Generation, biological consequences and repair mechanisms of cytosine deamination in DNA. *Journal of radiation research* 50(1):19-26.
45. Frederico LA, Kunkel TA, & Shaw BR (1990) A sensitive genetic assay for the detection of cytosine deamination: determination of rate constants and the activation energy. *Biochemistry* 29(10):2532-2537.
46. Apel K & Hirt H (2004) Reactive oxygen species: metabolism, oxidative stress, and signal transduction. *Annual review of plant biology* 55:373-399.
47. Burney S, Caulfield JL, Niles JC, Wishnok JS, & Tannenbaum SR (1999) The chemistry of DNA damage from nitric oxide and peroxynitrite. *Mutation research* 424(1-2):37-49.
48. Krokan HE & Bjoras M (2013) Base excision repair. *Cold Spring Harbor perspectives in biology* 5(4):a012583.
49. Marteijn JA, Lans H, Vermeulen W, & Hoeijmakers JH (2014) Understanding nucleotide excision repair and its roles in cancer and ageing. *Nature reviews. Molecular cell biology* 15(7):465-481.
50. Ravanat JL, Douki T, & Cadet J (2001) Direct and indirect effects of UV radiation on DNA and its components. *Journal of photochemistry and photobiology. B, Biology* 63(1-3):88-102.

51. Pena-Diaz J & Jiricny J (2012) Mammalian mismatch repair: error-free or error-prone? *Trends Biochem Sci* 37(5):206-214.
52. McCulloch SD & Kunkel TA (2008) The fidelity of DNA synthesis by eukaryotic replicative and translesion synthesis polymerases. *Cell research* 18(1):148-161.
53. Noll DM, Mason TM, & Miller PS (2006) Formation and repair of interstrand cross-links in DNA. *Chemical reviews* 106(2):277-301.
54. Caldecott KW (2014) DNA single-strand break repair. *Experimental cell research*.
55. Cadet J*, et al.* (1999) Hydroxyl radicals and DNA base damage. *Mutation research* 424(1-2):9-21.
56. Goodhead DT (1994) Initial events in the cellular effects of ionizing radiations: clustered damage in DNA. *International journal of radiation biology* 65(1):7-17.
57. Rothkamm K, Kruger I, Thompson LH, & Lobrich M (2003) Pathways of DNA double-strand break repair during the mammalian cell cycle. *Mol Cell Biol* 23(16):5706-5715.
58. Nikjoo H, Uehara S, Wilson WE, Hoshi M, & Goodhead DT (1998) Track structure in radiation biology: theory and applications. *International journal of radiation biology* 73(4):355-364.
59. Frit P, Barboule N, Yuan Y, Gomez D, & Calsou P (2014) Alternative end-joining pathway(s): Bricolage at DNA breaks. *DNA Repair (Amst)* 17:81-97.
60. Deriano L & Roth DB (2013) Modernizing the nonhomologous end-joining repertoire: alternative and classical NHEJ share the stage. *Annual review of genetics* 47:433-455.
61. Krejci L, Altmannova V, Spirek M, & Zhao X (2012) Homologous recombination and its regulation. *Nucleic Acids Res* 40(13):5795-5818.
62. Williams GJ*, et al.* (2014) Structural insights into NHEJ: Building up an integrated picture of the dynamic DSB repair super complex, one component and interaction at a time. *DNA Repair (Amst)* 17:110-120.
63. Ochi T, Wu Q, & Blundell TL (2014) The spatial organization of non-homologous end joining: From bridging to end joining. *DNA Repair (Amst)* 17:98-109.
64. Grundy GJ, Moulding HA, Caldecott KW, & Rulten SL (2014) One ring to bring them all-The role of Ku in mammalian non-homologous end joining. *DNA Repair (Amst)* 17:30-38.
65. Boulton SJ & Jackson SP (1996) Saccharomyces cerevisiae Ku70 potentiates illegitimate DNA double-strand break repair and serves as a barrier to error-prone DNA repair pathways. *EMBO J* 15(18):5093-5103.
66. Chen S*, et al.* (2001) Accurate in vitro end joining of a DNA double strand break with partially cohesive 3'-overhangs and 3'-phosphoglycolate termini: effect of Ku on repair fidelity. *J Biol Chem* 276(26):24323-24330.
67. Nussenzweig A, Sokol K, Burgman P, Li L, & Li GC (1997) Hypersensitivity of Ku80-deficient cell lines and mice to DNA damage: the effects of ionizing radiation on growth, survival, and development. *Proc Natl Acad Sci U S A* 94(25):13588-13593.

68. Difilippantonio MJ*, et al.* (2000) DNA repair protein Ku80 suppresses chromosomal aberrations and malignant transformation. *Nature* 404(6777):510-514.
69. Ferguson DO*, et al.* (2000) The nonhomologous end-joining pathway of DNA repair is required for genomic stability and the suppression of translocations. *Proc Natl Acad Sci U S A* 97(12):6630-6633.
70. Blier PR, Griffith AJ, Craft J, & Hardin JA (1993) Binding of Ku protein to DNA. Measurement of affinity for ends and demonstration of binding to nicks. *J Biol Chem* 268(10):7594-7601.
71. Mari PO*, et al.* (2006) Dynamic assembly of end-joining complexes requires interaction between Ku70/80 and XRCC4. *Proc Natl Acad Sci U S A* 103(49):18597-18602.
72. Mimitou EP & Symington LS (2010) Ku prevents Exo1 and Sgs1-dependent resection of DNA ends in the absence of a functional MRX complex or Sae2. *EMBO J* 29(19):3358-3369.
73. Roberts SA & Ramsden DA (2007) Loading of the nonhomologous end joining factor, Ku, on protein-occluded DNA ends. *J Biol Chem* 282(14):10605-10613.
74. Britton S, Coates J, & Jackson SP (2013) A new method for high-resolution imaging of Ku foci to decipher mechanisms of DNA double-strand break repair. *J Cell Biol* 202(3):579-595.
75. Lovejoy CA & Cortez D (2009) Common mechanisms of PIKK regulation. *DNA Repair (Amst)* 8(9):1004-1008.
76. Rivera-Calzada A, Spagnolo L, Pearl LH, & Llorca O (2007) Structural model of full-length human Ku70-Ku80 heterodimer and its recognition of DNA and DNA-PKcs. *EMBO Rep* 8(1):56-62.
77. Hammel M*, et al.* (2010) Ku and DNA-dependent protein kinase dynamic conformations and assembly regulate DNA binding and the initial non-homologous end joining complex. *J Biol Chem* 285(2):1414-1423.
78. Douglas P*, et al.* (2002) Identification of in vitro and in vivo phosphorylation sites in the catalytic subunit of the DNA-dependent protein kinase. *The Biochemical journal* 368(Pt 1):243-251.
79. Chan DW*, et al.* (2002) Autophosphorylation of the DNA-dependent protein kinase catalytic subunit is required for rejoining of DNA double-strand breaks. *Genes Dev* 16(18):2333-2338.
80. Yu Y*, et al.* (2003) DNA-PK phosphorylation sites in XRCC4 are not required for survival after radiation or for V(D)J recombination. *DNA Repair (Amst)* 2(11):1239-1252.
81. Chen BP*, et al.* (2005) Cell cycle dependence of DNA-dependent protein kinase phosphorylation in response to DNA double strand breaks. *J Biol Chem* 280(15):14709-14715.
82. Douglas P*, et al.* (2007) The DNA-dependent protein kinase catalytic subunit is phosphorylated in vivo on threonine 3950, a highly conserved amino acid in the protein kinase domain. *Mol Cell Biol* 27(5):1581-1591.
83. Douglas P, Gupta S, Morrice N, Meek K, & Lees-Miller SP (2005) DNA-PK-dependent phosphorylation of Ku70/80 is not required for non-homologous end joining. *DNA Repair (Amst)* 4(9):1006-1018.

84. Yu Y, *et al.* (2008) DNA-PK and ATM phosphorylation sites in XLF/Cernunnos are not required for repair of DNA double strand breaks. *DNA Repair (Amst)* 7(10):1680-1692.
85. Goodarzi AA, *et al.* (2006) DNA-PK autophosphorylation facilitates Artemis endonuclease activity. *EMBO J* 25(16):3880-3889.
86. Wang YG, Nnakwe C, Lane WS, Modesti M, & Frank KM (2004) Phosphorylation and regulation of DNA ligase IV stability by DNA-dependent protein kinase. *J Biol Chem* 279(36):37282-37290.
87. Ramsden DA & Gellert M (1998) Ku protein stimulates DNA end joining by mammalian DNA ligases: a direct role for Ku in repair of DNA double-strand breaks. *EMBO J* 17(2):609-614.
88. Cary RB, *et al.* (1997) DNA looping by Ku and the DNA-dependent protein kinase. *Proc Natl Acad Sci U S A* 94(9):4267-4272.
89. Soutoglou E, *et al.* (2007) Positional stability of single double-strand breaks in mammalian cells. *Nat Cell Biol* 9(6):675-682.
90. Mahaney BL, Meek K, & Lees-Miller SP (2009) Repair of ionizing radiation-induced DNA double-strand breaks by non-homologous end-joining. *The Biochemical journal* 417(3):639-650.
91. Zeng Z, Cortes-Ledesma F, El Khamisy SF, & Caldecott KW (2011) TDP2/TTRAP is the major 5'-tyrosyl DNA phosphodiesterase activity in vertebrate cells and is critical for cellular resistance to topoisomerase II-induced DNA damage. *J Biol Chem* 286(1):403-409.
92. Gomez-Herreros F, *et al.* (2013) TDP2-dependent non-homologous end-joining protects against topoisomerase II-induced DNA breaks and genome instability in cells and in vivo. *PLoS Genet* 9(3):e1003226.
93. Costantini S, Woodbine L, Andreoli L, Jeggo PA, & Vindigni A (2007) Interaction of the Ku heterodimer with the DNA ligase IV/Xrcc4 complex and its regulation by DNA-PK. *DNA Repair (Amst)* 6(6):712-722.
94. Hsu HL, Yannone SM, & Chen DJ (2002) Defining interactions between DNA-PK and ligase IV/XRCC4. *DNA Repair (Amst)* 1(3):225-235.
95. Yano K, *et al.* (2008) Ku recruits XLF to DNA double-strand breaks. *EMBO Rep* 9(1):91-96.
96. Yano K, Morotomi-Yano K, Lee KJ, & Chen DJ (2011) Functional significance of the interaction with Ku in DNA double-strand break recognition of XLF. *FEBS Lett* 585(6):841-846.
97. Reynolds P, *et al.* (2012) The dynamics of Ku70/80 and DNA-PKcs at DSBs induced by ionizing radiation is dependent on the complexity of damage. *Nucleic Acids Res* 40(21):10821-10831.
98. Datta K, Jaruga P, Dizdaroglu M, Neumann RD, & Winters TA (2006) Molecular analysis of base damage clustering associated with a site-specific radiation-induced DNA double-strand break. *Radiat Res* 166(5):767-781.
99. Datta K, Neumann RD, & Winters TA (2005) Characterization of complex apurinic/apyrimidinic-site clustering associated with an authentic site-specific radiation-induced DNA double-strand break. *Proc Natl Acad Sci U S A* 102(30):10569-10574.

100. Datta K, Neumann RD, & Winters TA (2005) Characterization of a complex 125I-induced DNA double-strand break: implications for repair. *International journal of radiation biology* 81(1):13-21.
101. Kim JS*, et al.* (2005) Independent and sequential recruitment of NHEJ and HR factors to DNA damage sites in mammalian cells. *J Cell Biol* 170(3):341-347.
102. Postow L*, et al.* (2008) Ku80 removal from DNA through double strand break-induced ubiquitylation. *J Cell Biol* 182(3):467-479.
103. Feng L & Chen J (2012) The E3 ligase RNF8 regulates KU80 removal and NHEJ repair. *Nat Struct Mol Biol* 19(2):201-206.
104. Langerak P, Mejia-Ramirez E, Limbo O, & Russell P (2011) Release of Ku and MRN from DNA ends by Mre11 nuclease activity and Ctp1 is required for homologous recombination repair of double-strand breaks. *PLoS Genet* 7(9):e1002271.
105. Neale MJ, Pan J, & Keeney S (2005) Endonucleolytic processing of covalent protein-linked DNA double-strand breaks. *Nature* 436(7053):1053-1057.
106. Wu D, Topper LM, & Wilson TE (2008) Recruitment and dissociation of nonhomologous end joining proteins at a DNA double-strand break in Saccharomyces cerevisiae. *Genetics* 178(3):1237-1249.
107. Pierce AJ, Hu P, Han M, Ellis N, & Jasin M (2001) Ku DNA end-binding protein modulates homologous repair of double-strand breaks in mammalian cells. *Genes Dev* 15(24):3237-3242.
108. Frank-Vaillant M & Marcand S (2002) Transient stability of DNA ends allows nonhomologous end joining to precede homologous recombination. *Mol Cell* 10(5):1189-1199.
109. Allen C, Kurimasa A, Brenneman MA, Chen DJ, & Nickoloff JA (2002) DNA-dependent protein kinase suppresses double-strand break-induced and spontaneous homologous recombination. *Proc Natl Acad Sci U S A* 99(6):3758-3763.
110. Clerici M, Mantiero D, Guerini I, Lucchini G, & Longhese MP (2008) The Yku70-Yku80 complex contributes to regulate double-strand break processing and checkpoint activation during the cell cycle. *EMBO Rep* 9(8):810-818.
111. Barlow JH, Lisby M, & Rothstein R (2008) Differential regulation of the cellular response to DNA double-strand breaks in G1. *Mol Cell* 30(1):73-85.
112. Tomita K*, et al.* (2003) Competition between the Rad50 complex and the Ku heterodimer reveals a role for Exo1 in processing double-strand breaks but not telomeres. *Mol Cell Biol* 23(15):5186-5197.
113. Shim EY*, et al.* (2010) Saccharomyces cerevisiae Mre11/Rad50/Xrs2 and Ku proteins regulate association of Exo1 and Dna2 with DNA breaks. *EMBO J* 29(19):3370-3380.
114. Shibata A*, et al.* (2011) Factors determining DNA double-strand break repair pathway choice in G2 phase. *EMBO J* 30(6):1079-1092.
115. Walden H & Deans AJ (2014) The Fanconi Anemia DNA Repair Pathway: Structural and Functional Insights into a Complex Disorder. *Annual review of biophysics* 43:257-278.
116. Pace P*, et al.* (2010) Ku70 corrupts DNA repair in the absence of the Fanconi anemia pathway. *Science* 329(5988):219-223.

117. Carr AM & Lambert S (2013) Replication stress-induced genome instability: the dark side of replication maintenance by homologous recombination. *Journal of molecular biology* 425(23):4733-4744.
118. Foster SS, Balestrini A, & Petrini JH (2011) Functional interplay of the Mre11 nuclease and Ku in the response to replication-associated DNA damage. *Mol Cell Biol* 31(21):4379-4389.
119. Balestrini A*, et al.* (2013) The Ku heterodimer and the metabolism of single-ended DNA double-strand breaks. *Cell Rep* 3(6):2033-2045.
120. Wang H*, et al.* (2003) Biochemical evidence for Ku-independent backup pathways of NHEJ. *Nucleic Acids Res* 31(18):5377-5388.
121. Betermier M, Bertrand P, & Lopez BS (2014) Is non-homologous end-joining really an inherently error-prone process? *PLoS Genet* 10(1):e1004086.
122. Guirouilh-Barbat J, Huck S, & Lopez BS (2008) S-phase progression stimulates both the mutagenic KU-independent pathway and mutagenic processing of KU-dependent intermediates, for nonhomologous end joining. *Oncogene* 27(12):1726-1736.
123. Wang M*, et al.* (2006) PARP-1 and Ku compete for repair of DNA double strand breaks by distinct NHEJ pathways. *Nucleic Acids Res* 34(21):6170-6182.
124. Mansour WY, Borgmann K, Petersen C, Dikomey E, & Dahm-Daphi J (2013) The absence of Ku but not defects in classical non-homologous end-joining is required to trigger PARP1-dependent end-joining. *DNA Repair (Amst)* 12(12):1134-1142.
125. Cheng Q*, et al.* (2011) Ku counteracts mobilization of PARP1 and MRN in chromatin damaged with DNA double-strand breaks. *Nucleic Acids Res* 39(22):9605-9619.
126. Ariumi Y*, et al.* (1999) Suppression of the poly(ADP-ribose) polymerase activity by DNA-dependent protein kinase in vitro. *Oncogene* 18(32):4616-4625.
127. Fattah F*, et al.* (2010) Ku regulates the non-homologous end joining pathway choice of DNA double-strand break repair in human somatic cells. *PLoS Genet* 6(2):e1000855.
128. Enserink JM & Kolodner RD (2010) An overview of Cdk1-controlled targets and processes. *Cell division* 5:11.
129. Trovesi C, Manfrini N, Falcettoni M, & Longhese MP (2013) Regulation of the DNA damage response by cyclin-dependent kinases. *Journal of molecular biology* 425(23):4756-4766.
130. Yun MH & Hiom K (2009) CtIP-BRCA1 modulates the choice of DNA double-strand-break repair pathway throughout the cell cycle. *Nature* 459(7245):460-463.
131. Huertas P & Jackson SP (2009) Human CtIP mediates cell cycle control of DNA end resection and double strand break repair. *J Biol Chem* 284(14):9558-9565.
132. Chen X*, et al.* (2011) Cell cycle regulation of DNA double-strand break end resection by Cdk1-dependent Dna2 phosphorylation. *Nat Struct Mol Biol* 18(9):1015-1019.
133. Muller-Tidow C*, et al.* (2004) The cyclin A1-CDK2 complex regulates DNA double-strand break repair. *Mol Cell Biol* 24(20):8917-8928.
134. Chi Y*, et al.* (2008) Identification of CDK2 substrates in human cell lysates. *Genome Biol* 9(10):R149.

135. Olsen JV, *et al.* (2010) Quantitative phosphoproteomics reveals widespread full phosphorylation site occupancy during mitosis. *Sci Signal* 3(104):ra3.
136. Zhang Y, Shim EY, Davis M, & Lee SE (2009) Regulation of repair choice: Cdk1 suppresses recruitment of end joining factors at DNA breaks. *DNA Repair (Amst)* 8(10):1235-1241.
137. Bothmer A, *et al.* (2010) 53BP1 regulates DNA resection and the choice between classical and alternative end joining during class switch recombination. *J Exp Med* 207(4):855-865.
138. Bunting SF, *et al.* (2010) 53BP1 inhibits homologous recombination in Brca1-deficient cells by blocking resection of DNA breaks. *Cell* 141(2):243-254.
139. Escribano-Diaz C, *et al.* (2013) A cell cycle-dependent regulatory circuit composed of 53BP1-RIF1 and BRCA1-CtIP controls DNA repair pathway choice. *Mol Cell* 49(5):872-883.
140. Wei L, *et al.* (2008) Rapid recruitment of BRCA1 to DNA double-strand breaks is dependent on its association with Ku80. *Mol Cell Biol* 28(24):7380-7393.
141. Jiang G, *et al.* (2013) BRCA1-Ku80 protein interaction enhances end-joining fidelity of chromosomal double-strand breaks in the G1 phase of the cell cycle. *J Biol Chem* 288(13):8966-8976.
142. Lin WY, Wilson JH, & Lin Y (2013) Repair of chromosomal double-strand breaks by precise ligation in human cells. *DNA Repair (Amst)* 12(7):480-487.
143. Li H, Marple T, & Hasty P (2013) Ku80-deleted cells are defective at base excision repair. *Mutation research* 745-746:16-25.
144. Choi YJ, *et al.* (2014) Deletion of individual Ku subunits in mice causes an NHEJ-independent phenotype potentially by altering apurinic/apyrimidinic site repair. *PloS one* 9(1):e86358.
145. Li P, *et al.* (2013) ABH2 couples regulation of ribosomal DNA transcription with DNA alkylation repair. *Cell Rep* 4(4):817-829.
146. Longhese MP, Anbalagan S, Martina M, & Bonetti D (2012) The role of shelterin in maintaining telomere integrity. *Frontiers in bioscience* 17:1715-1728.
147. Price CM, *et al.* (2010) Evolution of CST function in telomere maintenance. *Cell Cycle* 9(16):3157-3165.
148. Porter SE, Greenwell PW, Ritchie KB, & Petes TD (1996) The DNA-binding protein Hdf1p (a putative Ku homologue) is required for maintaining normal telomere length in Saccharomyces cerevisiae. *Nucleic Acids Res* 24(4):582-585.
149. Boulton SJ & Jackson SP (1996) Identification of a Saccharomyces cerevisiae Ku80 homologue: roles in DNA double strand break rejoining and in telomeric maintenance. *Nucleic Acids Res* 24(23):4639-4648.
150. Gravel S, Larrivee M, Labrecque P, & Wellinger RJ (1998) Yeast Ku as a regulator of chromosomal DNA end structure. *Science* 280(5364):741-744.
151. Teo SH & Jackson SP (1997) Identification of Saccharomyces cerevisiae DNA ligase IV: involvement in DNA double-strand break repair. *EMBO J* 16(15):4788-4795.
152. d'Adda di Fagagna F, *et al.* (2001) Effects of DNA nonhomologous end-joining factors on telomere length and chromosomal stability in mammalian cells. *Curr Biol* 11(15):1192-1196.

153. Samper E, Goytisolo FA, Slijepcevic P, van Buul PP, & Blasco MA (2000) Mammalian Ku86 protein prevents telomeric fusions independently of the length of TTAGGG repeats and the G-strand overhang. *EMBO Rep* 1(3):244-252.
154. Espejel S*, et al.* (2002) Mammalian Ku86 mediates chromosomal fusions and apoptosis caused by critically short telomeres. *EMBO J* 21(9):2207-2219.
155. Wang Y, Ghosh G, & Hendrickson EA (2009) Ku86 represses lethal telomere deletion events in human somatic cells. *Proc Natl Acad Sci U S A* 106(30):12430-12435.
156. Celli GB, Denchi EL, & de Lange T (2006) Ku70 stimulates fusion of dysfunctional telomeres yet protects chromosome ends from homologous recombination. *Nat Cell Biol* 8(8):885-890.
157. Sfeir A & de Lange T (2012) Removal of shelterin reveals the telomere end-protection problem. *Science* 336(6081):593-597.
158. Fellerhoff B, Eckardt-Schupp F, & Friedl AA (2000) Subtelomeric repeat amplification is associated with growth at elevated temperature in yku70 mutants of Saccharomyces cerevisiae. *Genetics* 154(3):1039-1051.
159. Lundblad V & Blackburn EH (1993) An alternative pathway for yeast telomere maintenance rescues est1- senescence. *Cell* 73(2):347-360.
160. Maringele L & Lydall D (2002) EXO1-dependent single-stranded DNA at telomeres activates subsets of DNA damage and spindle checkpoint pathways in budding yeast yku70Delta mutants. *Genes Dev* 16(15):1919-1933.
161. Stellwagen AE, Haimberger ZW, Veatch JR, & Gottschling DE (2003) Ku interacts with telomerase RNA to promote telomere addition at native and broken chromosome ends. *Genes Dev* 17(19):2384-2395.
162. Fisher TS, Taggart AK, & Zakian VA (2004) Cell cycle-dependent regulation of yeast telomerase by Ku. *Nat Struct Mol Biol* 11(12):1198-1205.
163. Peterson SE*, et al.* (2001) The function of a stem-loop in telomerase RNA is linked to the DNA repair protein Ku. *Nat Genet* 27(1):64-67.
164. Mozdy AD, Podell ER, & Cech TR (2008) Multiple yeast genes, including Paf1 complex genes, affect telomere length via telomerase RNA abundance. *Mol Cell Biol* 28(12):4152-4161.
165. Zappulla DC*, et al.* (2011) Ku can contribute to telomere lengthening in yeast at multiple positions in the telomerase RNP. *RNA* 17(2):298-311.
166. Gallardo F, Olivier C, Dandjinou AT, Wellinger RJ, & Chartrand P (2008) TLC1 RNA nucleo-cytoplasmic trafficking links telomerase biogenesis to its recruitment to telomeres. *EMBO J* 27(5):748-757.
167. Ting NS, Yu Y, Pohorelic B, Lees-Miller SP, & Beattie TL (2005) Human Ku70/80 interacts directly with hTR, the RNA component of human telomerase. *Nucleic Acids Res* 33(7):2090-2098.
168. Chai W, Ford LP, Lenertz L, Wright WE, & Shay JW (2002) Human Ku70/80 associates physically with telomerase through interaction with hTERT. *J Biol Chem* 277(49):47242-47247.
169. Mekhail K & Moazed D (2010) The nuclear envelope in genome organization, expression and stability. *Nature reviews. Molecular cell biology* 11(5):317-328.
170. Kueng S, Oppikofer M, & Gasser SM (2013) SIR proteins and the assembly of silent chromatin in budding yeast. *Annual review of genetics* 47:275-306.

171. Aparicio OM, Billington BL, & Gottschling DE (1991) Modifiers of position effect are shared between telomeric and silent mating-type loci in S. cerevisiae. *Cell* 66(6):1279-1287.
172. Boulton SJ & Jackson SP (1998) Components of the Ku-dependent non-homologous end-joining pathway are involved in telomeric length maintenance and telomeric silencing. *EMBO J* 17(6):1819-1828.
173. Nugent CI*, et al.* (1998) Telomere maintenance is dependent on activities required for end repair of double-strand breaks. *Curr Biol* 8(11):657-660.
174. Laroche T*, et al.* (1998) Mutation of yeast Ku genes disrupts the subnuclear organization of telomeres. *Curr Biol* 8(11):653-656.
175. Gotta M*, et al.* (1996) The clustering of telomeres and colocalization with Rap1, Sir3, and Sir4 proteins in wild-type Saccharomyces cerevisiae. *J Cell Biol* 134(6):1349-1363.
176. Taddei A, Hediger F, Neumann FR, Bauer C, & Gasser SM (2004) Separation of silencing from perinuclear anchoring functions in yeast Ku80, Sir4 and Esc1 proteins. *EMBO J* 23(6):1301-1312.
177. Schober H, Ferreira H, Kalck V, Gehlen LR, & Gasser SM (2009) Yeast telomerase and the SUN domain protein Mps3 anchor telomeres and repress subtelomeric recombination. *Genes Dev* 23(8):928-938.
178. Hediger F, Neumann FR, Van Houwe G, Dubrana K, & Gasser SM (2002) Live imaging of telomeres: yKu and Sir proteins define redundant telomere-anchoring pathways in yeast. *Curr Biol* 12(24):2076-2089.
179. Hsu HL, Gilley D, Blackburn EH, & Chen DJ (1999) Ku is associated with the telomere in mammals. *Proc Natl Acad Sci U S A* 96(22):12454-12458.
180. Wu TJ*, et al.* (2009) Sequential loading of Saccharomyces cerevisiae Ku and Cdc13p to telomeres. *J Biol Chem* 284(19):12801-12808.
181. Lopez CR*, et al.* (2011) Ku must load directly onto the chromosome end in order to mediate its telomeric functions. *PLoS Genet* 7(8):e1002233.
182. Bianchi A & de Lange T (1999) Ku binds telomeric DNA in vitro. *J Biol Chem* 274(30):21223-21227.
183. Hsu HL*, et al.* (2000) Ku acts in a unique way at the mammalian telomere to prevent end joining. *Genes Dev* 14(22):2807-2812.
184. Song K, Jung D, Jung Y, Lee SG, & Lee I (2000) Interaction of human Ku70 with TRF2. *FEBS Lett* 481(1):81-85.
185. Fink LS, Lerner CA, Torres PF, & Sell C (2010) Ku80 facilitates chromatin binding of the telomere binding protein, TRF2. *Cell Cycle* 9(18):3798-3806.
186. O'Connor MS, Safari A, Liu D, Qin J, & Songyang Z (2004) The human Rap1 protein complex and modulation of telomere length. *J Biol Chem* 279(27):28585-28591.
187. Ye JZ*, et al.* (2004) TIN2 binds TRF1 and TRF2 simultaneously and stabilizes the TRF2 complex on telomeres. *J Biol Chem* 279(45):47264-47271.
188. Cockell M*, et al.* (1995) The carboxy termini of Sir4 and Rap1 affect Sir3 localization: evidence for a multicomponent complex required for yeast telomeric silencing. *J Cell Biol* 129(4):909-924.
189. Pfingsten JS*, et al.* (2012) Mutually exclusive binding of telomerase RNA and DNA by Ku alters telomerase recruitment model. *Cell* 148(5):922-932.

190. Lei M, Podell ER, & Cech TR (2004) Structure of human POT1 bound to telomeric single-stranded DNA provides a model for chromosome end-protection. *Nat Struct Mol Biol* 11(12):1223-1229.
191. Liu D*, et al.* (2004) PTOP interacts with POT1 and regulates its localization to telomeres. *Nat Cell Biol* 6(7):673-680.
192. Doksani Y, Wu JY, de Lange T, & Zhuang X (2013) Super-resolution fluorescence imaging of telomeres reveals TRF2-dependent T-loop formation. *Cell* 155(2):345-356.
193. Giglia-Mari G, Zotter A, & Vermeulen W (2011) DNA damage response. *Cold Spring Harbor perspectives in biology* 3(1):a000745.
194. Gospodinov A & Herceg Z (2013) Chromatin structure in double strand break repair. *DNA Repair (Amst)* 12(10):800-810.
195. Shiloh Y & Ziv Y (2013) The ATM protein kinase: regulating the cellular response to genotoxic stress, and more. *Nature reviews. Molecular cell biology* 14(4):197-210.
196. Marechal A & Zou L (2013) DNA damage sensing by the ATM and ATR kinases. *Cold Spring Harbor perspectives in biology* 5(9).
197. Matsuoka S*, et al.* (2007) ATM and ATR substrate analysis reveals extensive protein networks responsive to DNA damage. *Science* 316(5828):1160-1166.
198. Carvajal LA & Manfredi JJ (2013) Another fork in the road--life or death decisions by the tumour suppressor p53. *EMBO Rep* 14(5):414-421.
199. Kinner A, Wu W, Staudt C, & Iliakis G (2008) Gamma-H2AX in recognition and signaling of DNA double-strand breaks in the context of chromatin. *Nucleic Acids Res* 36(17):5678-5694.
200. Podhorecka M, Skladanowski A, & Bozko P (2010) H2AX Phosphorylation: Its Role in DNA Damage Response and Cancer Therapy. *J Nucleic Acids* 2010.
201. Bartek J & Lukas J (2001) Pathways governing G1/S transition and their response to DNA damage. *FEBS Lett* 490(3):117-122.
202. Di Leonardo A, Linke SP, Clarkin K, & Wahl GM (1994) DNA damage triggers a prolonged p53-dependent G1 arrest and long-term induction of Cip1 in normal human fibroblasts. *Genes Dev* 8(21):2540-2551.
203. Wahl GM, Linke SP, Paulson TG, & Huang LC (1997) Maintaining genetic stability through TP53 mediated checkpoint control. *Cancer surveys* 29:183-219.
204. Yamauchi M*, et al.* (2008) Growth of persistent foci of DNA damage checkpoint factors is essential for amplification of G1 checkpoint signaling. *DNA Repair (Amst)* 7(3):405-417.
205. Taylor WR & Stark GR (2001) Regulation of the G2/M transition by p53. *Oncogene* 20(15):1803-1815.
206. Rieder CL (2011) Mitosis in vertebrates: the G2/M and M/A transitions and their associated checkpoints. *Chromosome research : an international journal on the molecular, supramolecular and evolutionary aspects of chromosome biology* 19(3):291-306.
207. Deckbar D*, et al.* (2007) Chromosome breakage after G2 checkpoint release. *J Cell Biol* 176(6):749-755.
208. Lobrich M & Jeggo PA (2007) The impact of a negligent G2/M checkpoint on genomic instability and cancer induction. *Nature reviews. Cancer* 7(11):861-869.

209. Syljuasen RG, Jensen S, Bartek J, & Lukas J (2006) Adaptation to the ionizing radiation-induced G2 checkpoint occurs in human cells and depends on checkpoint kinase 1 and Polo-like kinase 1 kinases. *Cancer Res* 66(21):10253-10257.
210. Heideker J, Lis ET, & Romesberg FE (2007) Phosphatases, DNA damage checkpoints and checkpoint deactivation. *Cell Cycle* 6(24):3058-3064.
211. Lee DH & Chowdhury D (2011) What goes on must come off: phosphatases gate-crash the DNA damage response. *Trends Biochem Sci* 36(11):569-577.
212. den Elzen NR & O'Connell MJ (2004) Recovery from DNA damage checkpoint arrest by PP1-mediated inhibition of Chk1. *EMBO J* 23(4):908-918.
213. Lu X*, et al.* (2008) The type 2C phosphatase Wip1: an oncogenic regulator of tumor suppressor and DNA damage response pathways. *Cancer metastasis reviews* 27(2):123-135.
214. Chowdhury D*, et al.* (2005) gamma-H2AX dephosphorylation by protein phosphatase 2A facilitates DNA double-strand break repair. *Mol Cell* 20(5):801-809.
215. Nakada S, Chen GI, Gingras AC, & Durocher D (2008) PP4 is a gamma H2AX phosphatase required for recovery from the DNA damage checkpoint. *EMBO Rep* 9(10):1019-1026.
216. Douglas P*, et al.* (2010) Protein phosphatase 6 interacts with the DNA-dependent protein kinase catalytic subunit and dephosphorylates gamma-H2AX. *Mol Cell Biol* 30(6):1368-1381.
217. Munoz-Espin D & Serrano M (2014) Cellular senescence: from physiology to pathology. *Nature reviews. Molecular cell biology* 15(7):482-496.
218. Surova O & Zhivotovsky B (2013) Various modes of cell death induced by DNA damage. *Oncogene* 32(33):3789-3797.
219. Beausejour CM*, et al.* (2003) Reversal of human cellular senescence: roles of the p53 and p16 pathways. *EMBO J* 22(16):4212-4222.
220. Norbury CJ & Zhivotovsky B (2004) DNA damage-induced apoptosis. *Oncogene* 23(16):2797-2808.
221. Chen F (2012) JNK-induced apoptosis, compensatory growth, and cancer stem cells. *Cancer Res* 72(2):379-386.
222. Cuadrado A & Nebreda AR (2010) Mechanisms and functions of p38 MAPK signalling. *The Biochemical journal* 429(3):403-417.
223. Tomimatsu N*, et al.* (2007) Ku70/80 modulates ATM and ATR signaling pathways in response to DNA double strand breaks. *J Biol Chem* 282(14):10138-10145.
224. Zhou XY*, et al.* (2002) Ku affects the ATM-dependent S phase checkpoint following ionizing radiation. *Oncogene* 21(41):6377-6381.
225. Stracker TH & Petrini JH (2011) The MRE11 complex: starting from the ends. *Nature reviews. Molecular cell biology* 12(2):90-103.
226. Amsel AD, Rathaus M, Kronman N, & Cohen HY (2008) Regulation of the proapoptotic factor Bax by Ku70-dependent deubiquitylation. *Proc Natl Acad Sci U S A* 105(13):5117-5122.
227. Sawada M*, et al.* (2003) Ku70 suppresses the apoptotic translocation of Bax to mitochondria. *Nat Cell Biol* 5(4):320-329.

228. Iijima K*, et al.* (2008) NBS1 regulates a novel apoptotic pathway through Bax activation. *DNA Repair (Amst)* 7(10):1705-1716.
229. Mazumder S, Plesca D, Kinter M, & Almasan A (2007) Interaction of a cyclin E fragment with Ku70 regulates Bax-mediated apoptosis. *Mol Cell Biol* 27(9):3511-3520.
230. Subramanian C, Jarzembowski JA, Opipari AW, Jr., Castle VP, & Kwok RP (2011) HDAC6 deacetylates Ku70 and regulates Ku70-Bax binding in neuroblastoma. *Neoplasia* 13(8):726-734.
231. Yuan Z & Seto E (2007) A functional link between SIRT1 deacetylase and NBS1 in DNA damage response. *Cell Cycle* 6(23):2869-2871.
232. Wang B*, et al.* (2014) Role of Ku70 in deubiquitination of Mcl-1 and suppression of apoptosis. *Cell death and differentiation*.
233. Martinou JC & Youle RJ (2011) Mitochondria in apoptosis: Bcl-2 family members and mitochondrial dynamics. *Developmental cell* 21(1):92-101.
234. Fu J, Bian M, Jiang Q, & Zhang C (2007) Roles of Aurora kinases in mitosis and tumorigenesis. *Mol Cancer Res* 5(1):1-10.
235. Dutertre S*, et al.* (2004) Phosphorylation of CDC25B by Aurora-A at the centrosome contributes to the G2-M transition. *J Cell Sci* 117(Pt 12):2523-2531.
236. Song J, Salek-Ardakani S, So T, & Croft M (2007) The kinases aurora B and mTOR regulate the G1-S cell cycle progression of T lymphocytes. *Nature immunology* 8(1):64-73.
237. Kitzen JJ, de Jonge MJ, & Verweij J (2010) Aurora kinase inhibitors. *Critical reviews in oncology/hematology* 73(2):99-110.
238. Mountzios G, Terpos E, & Dimopoulos MA (2008) Aurora kinases as targets for cancer therapy. *Cancer Treat Rev* 34(2):175-182.
239. Carmena M, Ruchaud S, & Earnshaw WC (2009) Making the Auroras glow: regulation of Aurora A and B kinase function by interacting proteins. *Current opinion in cell biology* 21(6):796-805.
240. Vader G, Medema RH, & Lens SM (2006) The chromosomal passenger complex: guiding Aurora-B through mitosis. *J Cell Biol* 173(6):833-837.
241. Murnion ME*, et al.* (2001) Chromatin-associated protein phosphatase 1 regulates aurora-B and histone H3 phosphorylation. *J Biol Chem* 276(28):26656-26665.
242. Sun L*, et al.* (2008) EB1 promotes Aurora-B kinase activity through blocking its inactivation by protein phosphatase 2A. *Proc Natl Acad Sci U S A* 105(20):7153-7158.
243. Krystyniak A, Garcia-Echeverria C, Prigent C, & Ferrari S (2006) Inhibition of Aurora A in response to DNA damage. *Oncogene* 25(3):338-348.
244. Monaco L*, et al.* (2005) Inhibition of Aurora-B kinase activity by poly(ADP-ribosyl)ation in response to DNA damage. *Proc Natl Acad Sci U S A* 102(40):14244-14248.
245. Ryser S*, et al.* (2009) Distinct roles of BARD1 isoforms in mitosis: full-length BARD1 mediates Aurora B degradation, cancer-associated BARD1beta scaffolds Aurora B and BRCA2. *Cancer Res* 69(3):1125-1134.
246. Malu S, Malshetty V, Francis D, & Cortes P (2012) Role of non-homologous end joining in V(D)J recombination. *Immunologic research* 54(1-3):233-246.

247. Ouyang H*, et al.* (1997) Ku70 is required for DNA repair but not for T cell antigen receptor gene recombination In vivo. *J Exp Med* 186(6):921-929.
248. Manis JP*, et al.* (1998) Ku70 is required for late B cell development and immunoglobulin heavy chain class switching. *J Exp Med* 187(12):2081-2089.
249. Gu Y*, et al.* (1997) Growth retardation and leaky SCID phenotype of Ku70-deficient mice. *Immunity* 7(5):653-665.
250. Slatter MA & Gennery AR (2010) Primary immunodeficiency syndromes. *Advances in experimental medicine and biology* 685:146-165.
251. Moshous D*, et al.* (2001) Artemis, a novel DNA double-strand break repair/V(D)J recombination protein, is mutated in human severe combined immune deficiency. *Cell* 105(2):177-186.
252. O'Driscoll M*, et al.* (2001) DNA ligase IV mutations identified in patients exhibiting developmental delay and immunodeficiency. *Mol Cell* 8(6):1175-1185.
253. Buck D*, et al.* (2006) Cernunnos, a novel nonhomologous end-joining factor, is mutated in human immunodeficiency with microcephaly. *Cell* 124(2):287-299.
254. Woodbine L*, et al.* (2013) PRKDC mutations in a SCID patient with profound neurological abnormalities. *J Clin Invest* 123(7):2969-2980.
255. van der Burg M, van Dongen JJ, & van Gent DC (2009) DNA-PKcs deficiency in human: long predicted, finally found. *Curr Opin Allergy Clin Immunol* 9(6):503-509.
256. Li GC*, et al.* (1998) Ku70: a candidate tumor suppressor gene for murine T cell lymphoma. *Mol Cell* 2(1):1-8.
257. Vogel H, Lim DS, Karsenty G, Finegold M, & Hasty P (1999) Deletion of Ku86 causes early onset of senescence in mice. *Proc Natl Acad Sci U S A* 96(19):10770-10775.
258. Nussenzweig A*, et al.* (1996) Requirement for Ku80 in growth and immunoglobulin V(D)J recombination. *Nature* 382(6591):551-555.
259. Li H, Vogel H, Holcomb VB, Gu Y, & Hasty P (2007) Deletion of Ku70, Ku80, or both causes early aging without substantially increased cancer. *Mol Cell Biol* 27(23):8205-8214.
260. Ren K & Pena de Ortiz S (2002) Non-homologous DNA end joining in the mature rat brain. *J Neurochem* 80(6):949-959.
261. Vyjayanti VN & Rao KS (2006) DNA double strand break repair in brain: reduced NHEJ activity in aging rat neurons. *Neurosci Lett* 393(1):18-22.
262. Shackelford DA (2006) DNA end joining activity is reduced in Alzheimer's disease. *Neurobiol Aging* 27(4):596-605.
263. Reaper PM, di Fagagna F, & Jackson SP (2004) Activation of the DNA damage response by telomere attrition: a passage to cellular senescence. *Cell Cycle* 3(5):543-546.
264. Shammas MA (2011) Telomeres, lifestyle, cancer, and aging. *Current opinion in clinical nutrition and metabolic care* 14(1):28-34.
265. Hanahan D & Weinberg RA (2011) Hallmarks of cancer: the next generation. *Cell* 144(5):646-674.
266. Luk JM*, et al.* (2005) Proteomic identification of Ku70/Ku80 autoantigen recognized by monoclonal antibody against hepatocellular carcinoma. *Proteomics* 5(7):1980-1986.

267. Korabiowska M*, et al.* (2006) Altered expression of DNA double-strand repair genes Ku70 and Ku80 in carcinomas of the oral cavity. *Anticancer research* 26(3A):2101-2105.
268. Mazzarelli P*, et al.* (2005) DNA end binding activity and Ku70/80 heterodimer expression in human colorectal tumor. *World journal of gastroenterology : WJG* 11(42):6694-6700.
269. Parrella P*, et al.* (2006) Expression and heterodimer-binding activity of Ku70 and Ku80 in human non-melanoma skin cancer. *Journal of clinical pathology* 59(11):1181-1185.
270. Abdelbaqi K, Di Paola D, Rampakakis E, & Zannis-Hadjopoulos M (2013) Ku protein levels, localization and association to replication origins in different stages of breast tumor progression. *Journal of Cancer* 4(5):358-370.
271. Komuro Y*, et al.* (2002) The expression pattern of Ku correlates with tumor radiosensitivity and disease free survival in patients with rectal carcinoma. *Cancer* 95(6):1199-1205.
272. Lord CJ & Ashworth A (2012) The DNA damage response and cancer therapy. *Nature* 481(7381):287-294.
273. Kim CH, Park SJ, & Lee SH (2002) A targeted inhibition of DNA-dependent protein kinase sensitizes breast cancer cells following ionizing radiation. *J Pharmacol Exp Ther* 303(2):753-759.
274. Bertolini LR*, et al.* (2007) Transient depletion of Ku70 and Xrcc4 by RNAi as a means to manipulate the non-homologous end-joining pathway. *J Biotechnol* 128(2):246-257.
275. Ayene IS, Ford LP, & Koch CJ (2005) Ku protein targeting by Ku70 small interfering RNA enhances human cancer cell response to topoisomerase II inhibitor and gamma radiation. *Mol Cancer Ther* 4(4):529-536.
276. Zhu P*, et al.* (2006) Granzyme A, which causes single-stranded DNA damage, targets the double-strand break repair protein Ku70. *EMBO Rep* 7(4):431-437.
277. Yoshida T*, et al.* (2004) Bax-inhibiting peptide derived from mouse and rat Ku70. *Biochem Biophys Res Commun* 321(4):961-966.
278. Sawada M, Hayes P, & Matsuyama S (2003) Cytoprotective membrane-permeable peptides designed from the Bax-binding domain of Ku70. *Nat Cell Biol* 5(4):352-357.
279. Subramanian C, Opipari AW, Jr., Bian X, Castle VP, & Kwok RP (2005) Ku70 acetylation mediates neuroblastoma cell death induced by histone deacetylase inhibitors. *Proc Natl Acad Sci U S A* 102(13):4842-4847.
280. Hsu FM, Zhang S, & Chen BP (2012) Role of DNA-dependent protein kinase catalytic subunit in cancer development and treatment. *Translational cancer research* 1(1):22-34.
281. Wellinger RJ & Zakian VA (2012) Everything you ever wanted to know about Saccharomyces cerevisiae telomeres: beginning to end. *Genetics* 191(4):1073-1105.
282. O'Sullivan RJ & Karlseder J (2010) Telomeres: protecting chromosomes against genome instability. *Nature reviews. Molecular cell biology* 11(3):171-181.

283. West RB, Yaneva M, & Lieber MR (1998) Productive and nonproductive complexes of Ku and DNA-dependent protein kinase at DNA termini. *Mol Cell Biol* 18(10):5908-5920.
284. Mahajan KN, Nick McElhinny SA, Mitchell BS, & Ramsden DA (2002) Association of DNA polymerase mu (pol mu) with Ku and ligase IV: role for pol mu in end-joining double-strand break repair. *Mol Cell Biol* 22(14):5194-5202.
285. Ma Y*, et al.* (2004) A biochemically defined system for mammalian nonhomologous DNA end joining. *Mol Cell* 16(5):701-713.
286. Purugganan MM, Shah S, Kearney JF, & Roth DB (2001) Ku80 is required for addition of N nucleotides to V(D)J recombination junctions by terminal deoxynucleotidyl transferase. *Nucleic Acids Res* 29(7):1638-1646.
287. Karmakar P, Snowden CM, Ramsden DA, & Bohr VA (2002) Ku heterodimer binds to both ends of the Werner protein and functional interaction occurs at the Werner N-terminus. *Nucleic Acids Res* 30(16):3583-3591.
288. Raval P, Kriatchko AN, Kumar S, & Swanson PC (2008) Evidence for Ku70/Ku80 association with full-length RAG1. *Nucleic Acids Res* 36(6):2060-2072.
289. Hoek M, Myers MP, & Stillman B (2011) An analysis of CAF-1-interacting proteins reveals dynamic and direct interactions with the KU complex and 14-3-3 proteins. *J Biol Chem* 286(12):10876-10887.
290. Morales JC*, et al.* (2014) Kub5-Hera, the human Rtt103 homolog, plays dual functional roles in transcription termination and DNA repair. *Nucleic Acids Res*.
291. Galande S & Kohwi-Shigematsu T (1999) Poly(ADP-ribose) polymerase and Ku autoantigen form a complex and synergistically bind to matrix attachment sequences. *J Biol Chem* 274(29):20521-20528.
292. Shahi A*, et al.* (2011) Mismatch-repair protein MSH6 is associated with Ku70 and regulates DNA double-strand break repair. *Nucleic Acids Res* 39(6):2130-2143.
293. Parvathaneni S, Stortchevoi A, Sommers JA, Brosh RM, Jr., & Sharma S (2013) Human RECQ1 interacts with Ku70/80 and modulates DNA end-joining of double-strand breaks. *PloS one* 8(5):e62481.
294. Goedecke W, Eijpe M, Offenberg HH, van Aalderen M, & Heyting C (1999) Mre11 and Ku70 interact in somatic cells, but are differentially expressed in early meiosis. *Nat Genet* 23(2):194-198.
295. Feki A*, et al.* (2005) BARD1 induces apoptosis by catalysing phosphorylation of p53 by DNA-damage response kinase. *Oncogene* 24(23):3726-3736.
296. Song K, Jung Y, Jung D, & Lee I (2001) Human Ku70 interacts with heterochromatin protein 1alpha. *J Biol Chem* 276(11):8321-8327.
297. Leskov KS, Klokov DY, Li J, Kinsella TJ, & Boothman DA (2003) Synthesis and functional analyses of nuclear clusterin, a cell death protein. *J Biol Chem* 278(13):11590-11600.
298. Liu H*, et al.* (2010) 55K isoform of CDK9 associates with Ku70 and is involved in DNA repair. *Biochem Biophys Res Commun* 397(2):245-250.
299. Chung U*, et al.* (1996) The interaction between Ku antigen and REF1 protein mediates negative gene regulation by extracellular calcium. *J Biol Chem* 271(15):8593-8598.

300. Zheng Y, Ao Z, Wang B, Jayappa KD, & Yao X (2011) Host protein Ku70 binds and protects HIV-1 integrase from proteasomal degradation and is required for HIV replication. *J Biol Chem* 286(20):17722-17735.
301. Wang H, Fang R, Cho JY, Libermann TA, & Oettgen P (2004) Positive and negative modulation of the transcriptional activity of the ETS factor ESE-1 through interaction with p300, CREB-binding protein, and Ku 70/86. *J Biol Chem* 279(24):25241-25250.
302. Kaczmarski W & Khan SA (1993) Lupus autoantigen Ku protein binds HIV-1 TAR RNA in vitro. *Biochem Biophys Res Commun* 196(2):935-942.
303. Willis DM*, et al.* (2002) Regulation of osteocalcin gene expression by a novel Ku antigen transcription factor complex. *J Biol Chem* 277(40):37280-37291.
304. Huang J, Nueda A, Yoo S, & Dynan WS (1997) Heat shock transcription factor 1 binds selectively in vitro to Ku protein and the catalytic subunit of the DNA-dependent protein kinase. *J Biol Chem* 272(41):26009-26016.
305. Matheos D, Ruiz MT, Price GB, & Zannis-Hadjopoulos M (2002) Ku antigen, an origin-specific binding protein that associates with replication proteins, is required for mammalian DNA replication. *Biochimica et biophysica acta* 1578(1-3):59-72.

Chapter 2

2 Ku regulates DNA repair and the DNA damage response through the Ku70 vWA domain

2.1 Introduction

One of the most dangerous forms of DNA damage is the DNA double-strand break (DSB), which can lead to aberrant genomic rearrangement if not repaired properly (1, 2). In eukaryotic cells, DSBs trigger signaling pathways that induce cell cycle checkpoints and alter gene transcription allowing DNA integrity to be re-established through the action of repair complexes (3-6).

The DNA damage response (DDR) pathway is initiated by a phosphorylation cascade that triggers chromatin modifications which enhance accessibility of the broken DNA to repair factors and promote the subsequent accumulation of DDR factors into foci at the site of damage (4, 7). The Mre11-Rad50-NBS1 (MRN) complex immediately binds the DSB, independently of other factors (8), functioning to recruit the serine/threonine (S/T) phosphoinositide-3-kinase (PI3K) family member ATM (Ataxia Telangiectasia Mutated), an essential regulator of the DNA damage response that is responsible for many phosphorylation events at the site of DNA damage (9, 10). An important signal amplification step involves the ATM phosphorylation of the histone variant H2AX to create a platform to which other DDR proteins are able to bind (11). ATM activates signaling cascades that trigger the activation of cell cycle checkpoints leading to cell

cycle arrest through phosphorylation of several substrates including p53, MDC1, BRCA1, Chk1 and Chk2. ATM also contributes to the establishment of apoptotic pathways (9).

Two main pathways function to repair DSBs, homologous recombination (HR) which uses a homologous chromosome or sister chromatid as template to repair the broken DNA, and non-homologous end-joining (NHEJ), which simply re-ligates the two broken ends together (2). In mammals, NHEJ is the predominant DSB repair pathway, functioning throughout the cell cycle, and exclusive to the G_1 and S phases (12, 13). NHEJ also mediates the rejoining of programmed breaks generated in V(D)J recombination during B and T cell maturation (12, 13). NHEJ can be subdivided into two sub-pathways, the core or "classical" NHEJ pathway (C-NHEJ) which represents the main end-joining activity in the cell, and "alternative" NHEJ activities (A-NHEJ) consisting of microhomology-mediated repair that function as backup pathway(s) to join DSBs (2, 12, 14).

The C-NHEJ complex in higher eukaryotic cells consists of DNA-dependent protein kinase (DNA-PK), composed of the Ku heterodimer and DNA-PK catalytic subunit (DNA-PKcs), Artemis, a DNA processing enzyme, a DNA ligase complex, XRCC4/DNA ligase IV and a recently identified factor called Cernunnos-XLF (12, 13, 15). Other accessory factors, including polynucleotide kinase (PNK) and DNA polymerases μ and λ have been implicated in some aspects of C-NHEJ (12, 13).

Ku is the DNA-binding component of the C-NHEJ repair machinery. Upon recognition and binding to the broken DNA end Ku recruits DNA-PKcs to form the active protein kinase complex DNA-PK (12, 13). DNA-PKcs is a large (p450) S/T kinase

that is a member of the PI3K kinase group that includes ATM, ATM-related (ATR) and mammalian target of rapamycin (mTOR) (16-18). The importance of DNA-PK in maintaining genomic integrity is underscored by the profound immunodeficiency, radiosensitivity and prevalence of tumours in mice lacking any of the 3 subunits (19-22). However, DNA-PKcs knockout mice display milder defects than $Ku^{-/-}$ mice, suggesting that Ku has additional functions independent of DNA-PKcs (22, 23). Besides DNA end recognition, Ku appears to protect broken DNA from aberrant nucleolytic processing (24). Ku has also been shown to bind to telomeres and to function in telomere maintenance, notably by anchoring telomeres to the nuclear periphery, contributing to telomeric silencing and preventing telomere shortening (24, 25) .

In addition to its main function in DNA repair, several reports have suggested that DNA-PK may also be involved in signaling to regulate specific aspects of the DDR. DNA-PK participates in replication protein-A2 (RP-A2) and nuclear factor-κB (NF-κB) phosphorylation in response to DNA damage and also contributes to the modification of histone H2AX (reviewed in (17, 26)). Roles for Ku in signaling to the apoptotic machinery have also been documented (17).

Aside from a recently identified end-processing activity (27), much of Ku's function appears to be mediated by protein-protein interactions with other factors. A number of proteins interact with Ku, including C-NHEJ core proteins and factors implicated in the DDR, in telomere maintenance, transcription and replication (26, 28). Within the mammalian C-NHEJ complex, interaction of Ku with XRCC4/DNA ligase IV is required to recruit the complex to DNA and to stimulate the ligase activity (29, 30). Yeast Ku also interacts with factors of the RSC complex that mediates ATP-dependent chromatin

remodelling in yeast (31). Interaction with DNA repair and damage-response factors Mre11, Werner and PARP have also been documented (26, 28).

Ku is a heterodimer of two proteins, Ku70 and Ku80 that form a complex that is conserved throughout evolution both structurally and functionally (24, 28, 32, 33). Ku homologs are found from bacteria to man (33). The two subunits of Ku in eukaryotes feature three structurally similar domains: an amino-terminal α/β domain, a central β-barrel domain and a α-helical carboxy-terminal arm that come together in the heterodimer to form a quasi-symmetrical ring structure that envelopes up to two helical turns of DNA end as seen in the crystal structure (32). The Ku70 carboxy-terminal domain sequence shows similarities with SAP domains that are involved in DNA binding (32, 34), whereas the Ku80 C-terminal domain, forms a globular structure with similarity to protein domains involved in protein-protein interactions (35, 36). The amino-terminal domains of Ku70 and Ku80 (α/β domains (32)) share similarity with von Willebrand factor A (vWA), a domain that mediates protein-protein interactions (32, 33, 37). The vWA domains of Ku fall into the "ancient conserved vWA proteins" that comprises a group of evolutionarily conserved intracellular proteins (37). However, while Ku interacts with many proteins, few have been mapped to the vWA domains (13, 24, 26, 28). Site directed mutagenesis of the Saccharomyces cerevisiae *YKU80* and *YKU70* genes identified that α-helices on the surface of the vWA domain confer different Ku functions (38). The Yku80 α-helix 5 is critical for telomeric functions, while Yku70 α-helix 5 is required for C-NHEJ. This likely results from differences in the orientation of the two vWA domains, the Ku70 vWA domain facing outwards in close proximity to the DNA

end, whereas the Ku80 vWA domain faces inwards, thus facilitating telomeric functions (32, 38).

In mammals, very little is known about the precise function of the Ku70/Ku80 N-terminal vWA domains. In this study, we introduced point mutations in various regions of the Ku70 vWA domain with the intent of identifying structural determinants that direct Ku function in response to DNA damage (Fig. 1). Mutation of Ku70 vWA α-helix 5 residues (D192A/D195R) resulted in a sharp decrease in survival. These substitutions, previously shown to confer a DNA repair defect in yeast (38), markedly impaired the DNA repair function of Ku in mouse embryonic fibroblasts (MEFs), suggesting that the function of these residues is conserved between yeast and mammals. Unexpectedly, the mutagenesis of residues adjacent to α-helix 4 (S155A/D156A) resulted in increased survival following ionizing radiation (IR) treatment. C-NHEJ appeared unaffected, but a marked decrease in the activation of apoptosis and alterations in the DNA damage signaling response as well as in the transcriptional profile of gene expression following DNA damage were identified. In particular, this mutation affected an activating transcription factor 2 (ATF2)-dependent transcriptional pathway that modulates several genes implicated in the activation of apoptosis. The D192A/D195R survival defect was rescued by introducing the S155A/D156A substitution, inferring that separate regions of the Ku70 vWA domain confer two different Ku functions in response to DNA damage. Further, S155 was identified as the critical residue regulating cell survival. Thus, importantly, the defects resulting from these mutations suggest that the N-terminal vWA domain of Ku70 is implicated in the activation of apoptotic pathways by linking signals

of DNA repair completion (or lack thereof) to the signaling machinery that controls the activation of cell death pathways.

2.2 Material and Methods

2.2.1 Plasmid expression constructs

Ku70 human cDNA was cloned from the BamHI site in pEGFP Ku70 (39) into the HpaI site of pMSCVpuro retroviral vector (Clontech). Ku70 point mutations were introduced by site directed mutagenesis using Pfu polymerase (Stratagene) with primers bearing the targeted point mutations (primers are listed in Table S3 in the supplemental material). All mutations were confirmed by sequencing. pGL3-Promoter and pRL-SV40 plasmids are from Promega.

2.2.2 Cell culture treatments

$Ku70^{-/-}$ MEFs were obtained from S. Matsuyama (Case Western, Cleveland (40)). All cells were cultured in high glucose Dulbecco's modified Eagle's medium (DMEM) supplemented with 10% fetal bovine serum (FBS) at 37°C in 5% CO2.

pMSCV vectors containing wild-type and mutant Ku70, as well as the empty pMSCVpuro vector were transfected via calcium phosphate into the Phoenix Ampho retroviral packaging cell line. The media-containing virus was collected 48 hours later and used to infect $Ku70^{-/-}$ MEFs. Twenty-four hours post infection the media was replaced with 2.5μg/ml puromycin containing media to select and maintain cells infected with the pMSCV vector. Cells were maintained as a pool for all subsequent experiments.

For irradiation experiments, cells were plated the night before at 50-70% confluency. Irradiations were performed with a Faxitron RX-650 at a dose rate of 1.42 Gy/min.

2.2.3 Extracts and western blot analyses

Whole cell extracts were prepared as described (41). Nuclear Extracts were prepared as described (42). For Western blot analysis, extracts were resolved by SDS PAGE (either 8% or 10%), transferred onto a PVDF membrane and hybridized with the following antibodies:, Ku70 (N3H10, Neomarkers), Ku80 (M-20, Santa Cruz), β-actin (I-19, Santa Cruz), GADD153/CHOP (F-168, Santa Cruz), ATF3 (C-19, Santa Cruz), PCNA (clone PC-10, Millipore), 69/71 phospho ATF2 (Cell Signaling), ATF2 (N-96, Santa Cruz).

2.2.4 Clonogenic survival assays

Cells were plated in triplicate at single cell density, irradiated 6 hours later at various doses of IR and then incubated for 7 days. The plates were washed with PBS and stained with 0.5% crystal violet in 20% methanol. Colonies were counted and survival was assessed by calculating the ratio of colony number on the irradiated plates over the unirradiated controls.

2.2.5 Caspase assays

Cell extracts were prepared in Lysis buffer (1mM KCl, 10mM HEPES (pH 7.4), 1.5mM $MgCl_2$, 1mM DTT, 1mM PMSF, 5μg/ml leupeptin, 2μg/ml aprotinin, and 10% glycerol). Caspase activity was measured in caspase assay buffer (25 mM HEPES, pH 7.4, 10 mM DTT, 10% sucrose, 0.1% CHAPS containing 10 μM caspase-3 substrate, *N*-acetyl-Asp-Glu-Val-Asp-(7-amino-4trifluoromethyl-coumarin) (DEVD-AFC, BIOMOL

International)). The fluorescence produced by DEVD-AFC cleavage was measured on a SpectraMax M5 fluorimeter (excitation 400 nm, emission 505 nm) over a 2 h interval. Caspase activity was calculated as the ratio of the fluorescence output in treated samples relative to corresponding untreated controls.

2.2.6 Pulsed-field gel electrophoresis

One day prior to irradiation, 3.5 million cells were seeded onto a 10 cm plate. Following 40 Gy of IR or mock treatment, cells were harvested into agarose plugs using the Bio-Rad CHEF Genomic DNA Plug Kit. Agarose plugs were run on a 0.8% gel using the Bio-Rad CHEF-DR II system (200-500s switch time, 120° angle, 3V/cm, 48 hours). The gels were stained with ethidium bromide, images captured using a BioRad ChemiDoc and ImageLab software and staining was quantified using ImageJ. The fraction released (fraction of activity released, FAR) corresponding to unrepaired DNA was calculated by calculating the ratio of the DNA migrating below the plug over the total DNA loaded (DNA remaining in the plug and fraction entering the gel).

2.2.7 Plasmid repair luciferase assays

The pGL3-Promoter luciferase reporter plasmid was digested with Bgl II, which cuts between the promoter and the luciferase coding region. pMSCV infected MEFs were transfected with 750 ng of linearized PGL3-Promoter and 5 ng of pRL-SV40 in 12 well plates using Fugene6 (Roche) following the manufacturer's instructions. Forty-eight hours post transfection the cells were harvested in 0.3 ml 1x passive lysis buffer (Promega) and luciferase assays were performed with 30 μl of extract with the Promega

Dual-Luciferase Reporter Assay System (50 μl of both LAR II and Stop & Glo® reagents) using an Orion II luminometer (Titertek-Berthold).

2.2.8 Immunofluorescence

One day prior to irradiation, cells were seeded at 60-80% confluence on 10 mm glass coverslips. At the given time points post irradiation, cells were washed in cold PBS and fixed in 3% paraformaldehyde. Cells were permeabilized in 0.5% Triton-X and blocked in 5% FBS, followed by incubation with the primary antibodies, either phospho-serine 139 H2AX antibody (20E3, Cell Signaling) or ATF2 (C-19, Santa Cruz), or 69/71 phospho ATF2 (Cell Signaling). Slides were then incubated with an anti-rabbit Alexa 497 secondary antibody (Invitrogen). Coverslips were mounted onto glass slides using ProLong Gold containing DAPI (Invitrogen). Cell pictures were taken with an Olympus BX51 microscope at 40x magnification and the Image-Pro Plus software (Media Cybernetics, Inc.). For g-H2AX and phospho-ATF2, pixel density was measured with ImageJ software and used as a measure of foci content per picture. DAPI nuclei staining were used for cell counting and the pixel density was averaged per cell for approximately 500 cells. For quantification of ATF2 foci, all pictures were set to an equal contrast threshold on ImageJ and cells were scored positive if containing at least one focus.

2.2.9 Reverse transcriptase (RT-qPCR)

Total RNA was isolated using the Qiagen RNeasy RNA Extraction kit. RNA (2 μg) was reverse transcribed with the Superscript II cDNA kit (Invitrogen). Quantitative PCR was performed using Bio-Rad MyiQ single-colour real-time PCR detection and Bio-Rad IQ SYBR green mix. Primers are listed in Table S3 in the supplemental material. Relative

quantification of specific gene expression was determined by the ΔΔC(t) method, with the target gene C(t) values normalized to that of the beta-2-microglobulin control. Change of gene expression in irradiated samples was calculated relative to the unirradiated controls.

2.2.10 Sequence alignments

Sequences were obtained from the NCBI database and aligned using MUSCLE software (43). Percent identity calculations were performed using Jalview software.

2.2.11 Statistical analyses

Differences between two groups were compared using an unpaired two-tailed *t*-test and analysis of variance (ANOVA) was used when comparing multiple groups. Results were considered significant when $P<0.05$.

2.3 Results

2.3.1 Identification of Ku70 mutations that impair survival in response to IR

In order to investigate the contribution of the Ku70 vWA domain in Ku70's function in the response to DSBs, several point mutations were produced in the human Ku70 vWA domain. These mutations targeted residues located on the solvent exposed surface of the protein and showing various degrees of conservation across Ku70 homologs (Figure 2-1). For instance, residues in Ku70 α-helix 5 previously involved in DNA repair in yeast are fairly well conserved (Figure 2-1A) (38). In contrast, α-helix 3 is much less conserved (Figure 2-1A). We produced five different Ku70 mutations: two mutations in α-helix 3,

Figure 2-1 Generation of Ku70 vWA domain mutants

(A) Sequence alignment of the Ku70 N-terminal vWA domain (α-helices 3 to 5) from a selection of Ku70 eukaryotic homologs. The position of the vWA domain α-helices is indicated at the top. Conservation between species of the residues within α-helices 3 to 5 is highlighted according to percent identity (PID) (light grey >40%, dark grey >60%, and black >80% PID). The residues mutated in this study are boxed and the substitutions introduced are indicated below the alignments. (B) Space-filling representations of the human Ku dimer structure bound to DNA (32) (PDB ID: IJEY depicted in PyMol). Top, front view of the Ku dimer (facing the DNA end). The Ku70 vWA domain E145/W148, S155/D156 and D192/D195 residues are highlighted in black and their position is indicated. DNA is represented as a black helix. Below, side view of the Ku dimer (DNA end to the left). The position of the Ku70 vWa domain K114/L117 and K129/D133 residues is shown.

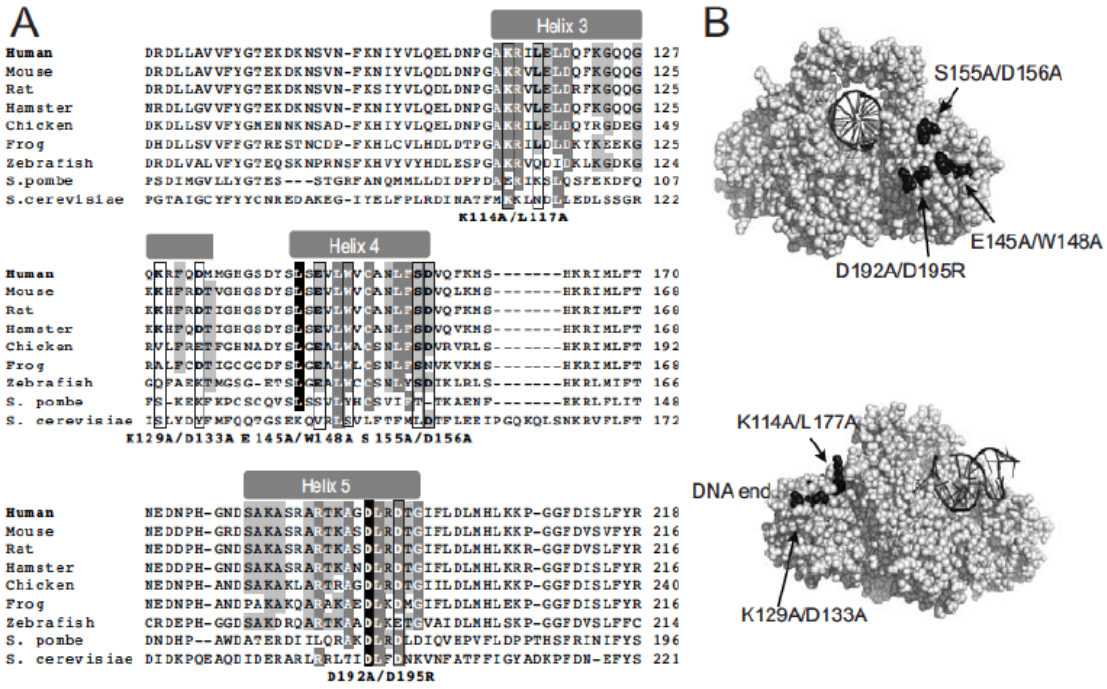
A
Helix 3
Human DRDLLAVVFYGTEKDKNSVN-FKNIYVLQELDNPGAKRILELDQFKGQQG 127
Mouse DRDLLAVVFYGTEKDKNSVN-FKNIYVLQDLDNPGAKRVLELDQFKGQQG 125
Rat DRDLLAVVFYGTEKDKNSVN-FKSIYVLQDLDNPGAKRVLELDRFKGQQG 125
Hamster NRDLLGVVFYGTEKDKNSVN-FKNIYVLQELDNPGAKRVLELDQFKGQQG 125
Chicken DKDLLSVVFYGMENNKNSAD-FKHIYVLQELDNPGAKRILELDQYRGDEG 149
Frog DHDLLSVVFFGTRESTNCDP-FKHLCVLHDLDTPGAKRILDLDKYKEEKG 125
Zebrafish DRDLVALVFYGTEQSKNPRNSFKHVYVYHDLESPGAKRVQDIDKLKGDKG 124
S.pombe FSDIMGVLLYGTES---STGRFANQMMLLDIDPFDAEKIKSLQSFEKDFQ 107
S.cerevisiae PGTAIGCYFYYCNREDAKEG-IYELFPLRDINATFMLKLNDLLEDLSSGR 122
K114A/L117A
Helix 4
Human QKRFQDMMGHGSDYSLSEVLWVCANLESDVQFKMS-------HKRIMLFT 170
Mouse EKHFRDTVGHGSDYSLSEVLWVCANLESDVQLKMS-------HKRIMLFT 168
Rat EKHFRDTIGHGSDYSLSEVLWVCANLESDVQFKMS-------HKRIMLFT 168
Hamster EKHFQDTIGHGSDYSLSEVLWVCANLESDVQVKMS-------HKRIMLFT 168
Chicken RVLFRETFGHNADYSLCEALWACSNLESDVRVRLS-------HKRIMLFT 192
Frog RALFCDTICCCGDFSLCEALWLCSNLESNVKVKMS-------HKRIMLFT 168
Zebrafish GQFAEKTMGSG-ETSLCEALWCCSNLYSDIKLRLS-------HKRLMIFT 166
S. pombe FS-KEKFKPCSCQVSLSSVLWHCSVIIT-TKAENF-------EKRLFLIT 148
S. cerevisiae ISLYDVFMFQQTGSEKQVPLSVLFTFMLDTFLERIPGQKQLSNKRVFLFT 172
K129A/D133A E145A/W148A S155A/D156A
Helix 5
Human NEDNPH-GNDSAKASRARTKAGDLRDTGIFLDLMHLKKP-GGFDISLFYR 218
Mouse NEDDPH-GRDSAKASRARTKASDLRDTGIFLDLMHLKKP-GGFDVSVFYR 216
Rat NEDDPH-GNDSAKASRARTKASDLRDTGIFLDLMHLKKR-GGFDVSLFYR 216
Hamster NEDDPH-GNDSAKASRARTKANDLRDTGIFLDLMHLKRR-GGFDISLFYR 216
Chicken NEDNPH-ANDSAKAKLARTRAGDLRDTGIILDLMHLKKP-GGFDISLFYR 240
Frog NEDNPH-ANDPAKAKQARAKAEDLKDMGIFLDLMHLEKP-GGFDISLFYR 216
Zebrafish CRDEPH-GGDSAKDRQARTKAADLKETGVAIDLMHLSKP-GGFDVSLFFC 214
S. pombe DNDHP--AWDATERDIILQRLKDLRDLDIQVEPVFLDPPTHSFRINIFYS 196
S. cerevisiae DIDKPQEAQDIDERARLARLTIDEFDNKVNFATFFIGYADKPFDN-EFYS 221
D192A/D195R
B
S155A/D156A
E145A/W148A
D192A/D195R
K114A/L177A
DNA end
K129A/D133A

one in α-helix 4, one in α-helix 5, and one in a loop region bordering α-helix 4 (S155A/D156A) (Figure 2-1B). At each location, we substituted 2 amino acids to maximize the likelihood of disrupting a protein interacting surface. Wild-type human Ku70 as well as the various mutant human Ku70 cDNAs were stably introduced into $Ku70^{-/-}$ immortalized MEFs via a murine stem cell virus construct. To determine whether the mutations interfered with Ku's function in response to IR, we measured the radiosensitivity of MEFs expressing wild-type or mutant Ku70 at various doses of IR (between 2 and 10 Gy) using a clonogenic assay. Cells lacking Ku70 are severely deficient in DSB repair and therefore have very low survival following treatment with IR (44). Consistent with previous reports (44, 45), the re-expression of human Ku70 in the $Ku70^{-/-}$ MEFs restored wild-type MEF survival in response to IR (Figure 2-2A). Western blot analyses indicated that the level of Ku70 restored was similar to that in wild-type cells (Supplementary Figure 2-1). Also, we verified that the expression of Ku80, which is reduced to undetectable levels in the absence of the Ku70 subunit was re-established upon expression of the human Ku70 construct (Figure 2-2D and 2-3D).

MEFs expressing α-helix 3 and α-helix 4 Ku70 mutant constructs produced survival curves not significantly different from wild-type, therefore suggesting that these substitutions do not interfere with Ku's role in response to IR (Supplementary Figure 2-2). An α-helix 5 mutation (D192A/D195R) was designed based on the previously identified DNA repair defect associated with the mutation of the corresponding residues in yeast Ku70 (38). The Ku70 D192A/D195R expressing cells showed a dramatic decrease in survival following IR treatment, displaying a survival curve that more closely

Figure 2-2 Analysis of cell survival properties of Ku70−/− MEFs expressing Ku70 bearing substitutions in the N-terminal vWA domain.

(A) Re-expression of human wild-type Ku70 via retroviral infection restores wild-type survival levels of MEFs following ionizing radiation. Clonogenic survival of MEFs wild-type ($Ku70^{+/+}$), Ku70-deficient ($Ku70^{-/-}$) or $Ku70^{-/-}$ expressing empty vector (pMSCV) or Ku70 cDNA (Ku70 pMSCV) was tested at the IR doses indicated. Results are the means of three separate experiments performed in triplicate with error bars representing the standard deviation (SD). Error bars are included for all data points but may not be visible when smaller than symbol size. (B) $Ku70^{-/-}$ MEFs expressing Ku70 mutant bearing substitutions D192A/D195R exhibit radiation sensitivity. Clonogenic assay was done as in A with $Ku70^{-/-}$ MEFs expressing Ku70 wild-type (WT), Ku70 with substitutions (D192A/D195R) or empty vector (pMSCV). (C) MEFs expressing Ku70 with S155A/D156A substitutions show increased survival following IR. Clonogenic assay results are presented as in A. Error bars represent the SD. (D) Representative western blot analysis of $Ku70^{-/-}$ MEFs or $Ku70^{-/-}$ MEFs expressing wild-type Ku70 (WT) and Ku70 S155A/D156A. The blot was analyzed with antibodies to Ku80, Ku70 and PCNA, as indicated. The star (*) indicates the position of a non-specific band migrating above Ku80.

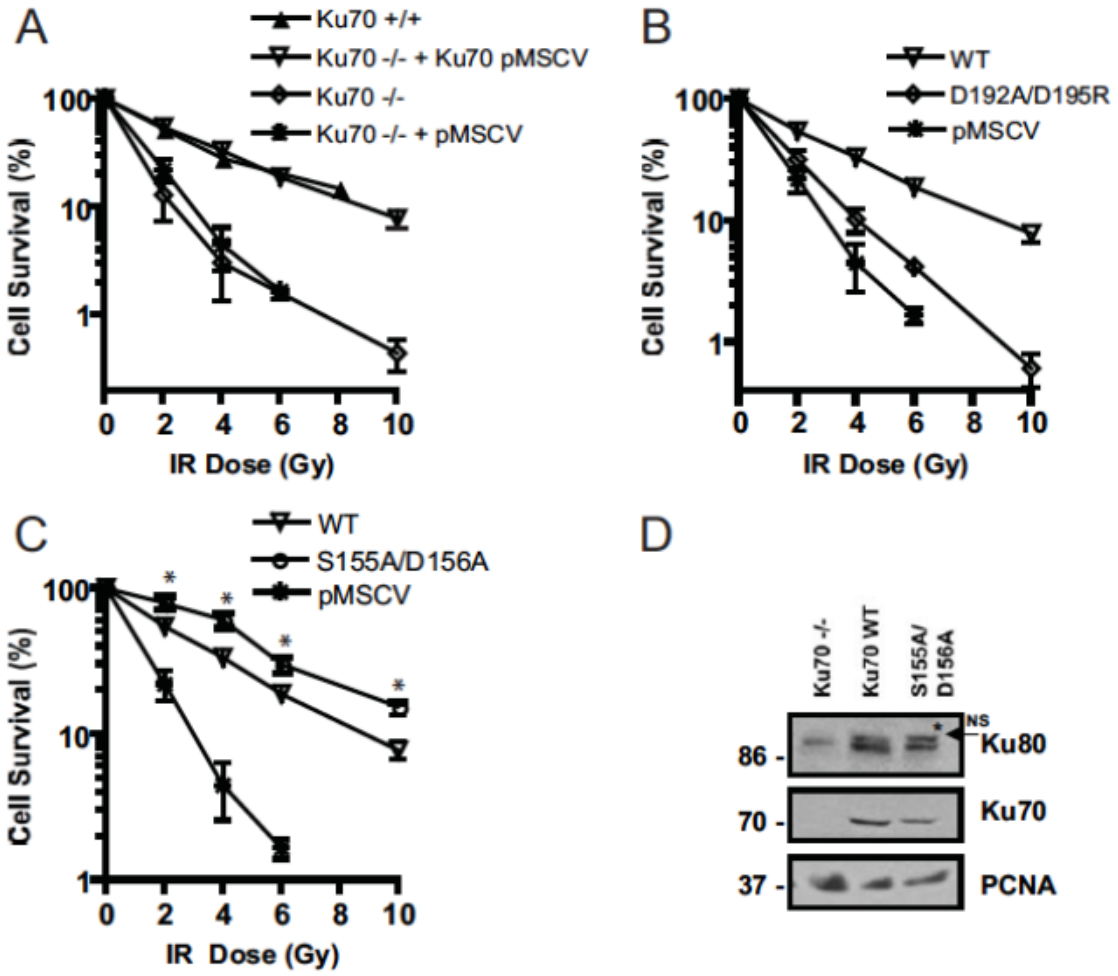
A
Ku70 +/+
Ku70 -/- + Ku70 pMSCV
Ku70 -/-
Ku70 -/- + pMSCV
Cell Survival (%)
100
10
1
0 2 4 6 8 10
IR Dose (Gy)
B
WT
D192A/D195R
pMSCV
Cell Survival (%)
100
10
1
0 2 4 6 8 10
IR Dose (Gy)
C
WT
S155A/D156A
pMSCV
Cell Survival (%)
100
10
1
0 2 4 6 8 10
IR Dose (Gy)
D
Ku70 -/-
Ku70 WT
S155A/ D156A
NS
86 -
Ku80
70 -
Ku70
37 -
PCNA

matched that of the Ku70$^{-/-}$ cells than that of wild-type (Figure 2-2B). For example at 4 Gy, 34% of Ku70 wild-type expressing MEFs formed colonies, versus 4.5% of cells expressing empty vector and 10% of Ku70 D192A/D195. At 6 Gy, 20% of wild-type cells survived versus 4% in Ku70 D192A/D195R and 1.5% in cells expressing empty vector. This suggests that these residues may be functionally conserved between yeast and human. Intriguingly, a Ku70 mutant bearing alanine substitutions of residues S155 and D156 located in a loop region between α-helices 4 and 5 consistently conferred a 40-50% increase in survival compared to wild-type (at 4 Gy, 60% versus 33% and at 6 Gy, 30% versus 19%, Figure 2-2C). This was unexpected, and as the expression of this mutant was similar to that of Ku70 wild-type (Figure 2-2D), suggested that the mutation enhanced viability in response to IR.

2.3.2 S155A/D156A does not affect DNA repair efficiency

Since Ku's prominent documented function is to recruit DNA repair factors to DSBs and promote C-NHEJ, we first considered the possibility that the increase in survival conferred by the Ku S155A/D156A mutant was due to an improved capacity for DNA repair. To test this possibility, we employed pulsed-field gel electrophoresis (PFGE) to analyze DNA repair. The analysis was performed with samples processed immediately following IR, to measure the total amount of genomic DNA breakage, 2 hours later, when DNA repair is on-going and then 6 hours after IR treatment, at which time most DNA breaks are already repaired (46, 47). Comparison of Ku70 wild-type and Ku70 S155A/D156A mutant cells revealed no significant differences in their abilities to repair genomic DNA damaged by IR (Figure 2-3A). To confirm this result, an *in vivo* plasmid repair assay was employed, which measures the cell's ability to recircularize a transfected

Figure 2-3 The Ku70 S155A/D156A mutation does not affect DNA repair.

(A) The S155A/D156A mutation does not interfere with the repair of IR induced genomic DNA damage. PFGE analysis of genomic DNA from $Ku70^{-/-}$ MEFs expressing Ku70 wild-type (WT), Ku70 S155A/D156A or empty pMSCV either untreated (control) or immediately after IR (0h), 2h or 6h following IR treatment. For all samples, FAR (fraction of activity released) was averaged from 3 independent experiments with error bar representing SEM. (B) The Ku S155A/D156A mutation does not interfere with the repair of extrachromosomal DNA breaks. $Ku70^{-/-}$ MEFs expressing Ku70 wild-type (WT) mutant S155A/D156A or empty vector (pMSCV) were transfected with a linearized pGL3-Promoter plasmid and control pRL-SV40 plasmid and assayed for luciferase activity 48 hours later. Data represents the average firefly luciferase values normalized to the renilla luciferase for 3 separate experiments with error bars representing SD (*P <0.01). (C) Ku70 S155A/D156A mutation rescues the IR sensitivity conferred by the D192A/D195R substitution. Clonogenic survival assay of $Ku70^{-/-}$ MEFs expressing Ku70 wild-type (WT), Ku70 bearing the substitutions D192A/D195R or the double mutant D192A/D195R, S155A/D156A. Results are averaged from 3 experiments and the error bars represent the SD. (D) Western blot analysis of $Ku70^{-/-}$ MEFs with empty vector (pMSCV) or $Ku70^{-/-}$ MEFs expressing wild-type Ku70 (WT) and Ku70 mutants as indicated. The blot was analyzed with antibodies to Ku80, Ku70 and actin. (E) Ku70 S155A/D156A substitutions do not rescue the DNA repair defect conferred by the Ku70 D192A/D195R mutation. PFGE analysis was done as in A with genomic DNA from $Ku70^{-/-}$ MEFs expressing Ku70 wild-type (WT), D192A/D195R, the double mutant D192A/D195R, S155A/D156A or empty pMSCV either untreated (control) or immediately after IR (0h), and 6h following IR treatment. FAR was averaged from 3 independent experiments with error bar representing SEM (*P <0.05).

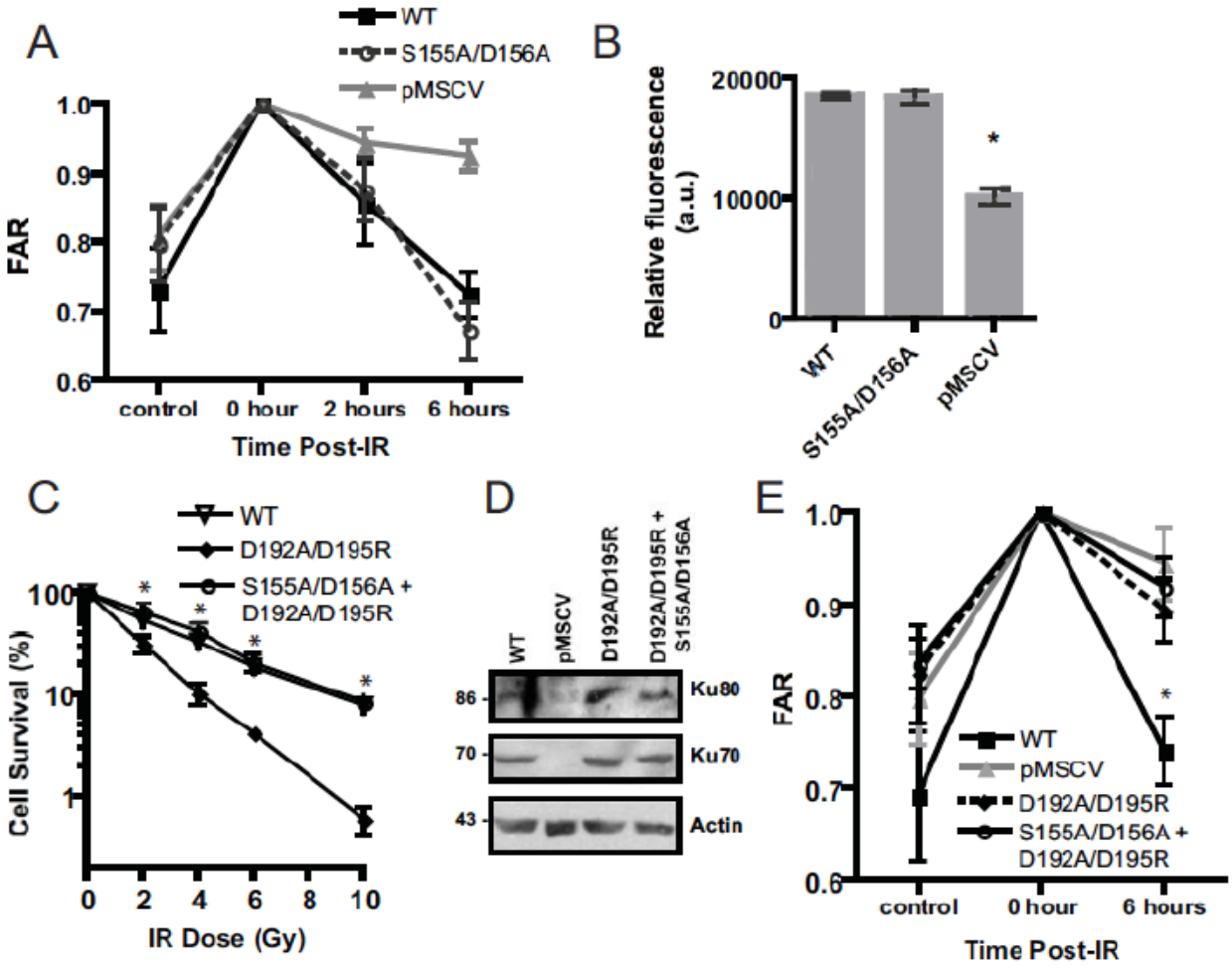
A
WT
S155A/D156A
pMSCV
FAR
1.0
0.9
0.8
0.7
0.6
control
0 hour
2 hours
6 hours
Time Post-IR
B
Relative fluorescence (a.u.)
20000
10000
0
*
WT
S155A/D156A
pMSCV
C
WT
D192A/D195R
S155A/D156A + D192A/D195R
Cell Survival (%)
100
10
1
*
0
2
4
6
8
10
IR Dose (Gy)
D
WT
pMSCV
D192A/D195R
D192A/D195R + S155A/D156A
86
Ku80
70
Ku70
43
Actin
E
FAR
1.0
0.9
0.8
0.7
0.6
WT
pMSCV
D192A/D195R
S155A/D156A + D192A/D195R
*
control
0 hour
6 hours
Time Post-IR

linearized luciferase expression plasmid by measuring luciferase activity. Ku wild-typeand Ku70 S155A/D156A cells showed no significant difference in their ability to repair restriction enzyme cut extra-chromosomal plasmid DNA (Figure 2-3B), suggesting that the mutated residues did not enhance the DNA repair function of Ku. To substantiate the potential for the Ku S155A/D156A mutation to increase survival independent of DNA repair, we tested whether this mutation could rescue the survival defect conferred by a Ku repair mutation. To this end, we introduced the D192A/D195R substitution in α-helix 5 in the Ku70 S155A/D156A construct. The survival of cells expressing the double mutant Ku70 S155A/D156A, D192A/D195R was completely rescued (Figure 2-3C), suggesting that mutation of the S155/D156 residues can compensate for the defects imparted by a DNA repair deficiency. To confirm this result, we analyzed DNA repair in cells expressing Ku70 D192A/D195R versus the double mutant Ku70 S155A/D156A, D192A/D195R using PFGE (Figure 2-3E). As expected, Ku70 D192A/D195R expressing cells displayed a marked repair defect not statistically different than that of the Ku70-deficient cells. A similar repair defect was observed in cells expressing the Ku70 S155A/D156A, D192A/D195R substitutions, providing evidence that S155A/D156A substitutions do not affect Ku's function in DNA end-joining and confer a survival advantage that is independent of DNA repair.

2.3.3 Ku70 S155A/D156 mutant cells display decreased activation of apoptosis

Since the S155A/D156A mutation did not affect DNA repair, it suggested the possibility that it may interfere with DNA damage response pathways and prevent the execution of apoptosis. To determine whether apoptosis was affected in Ku70

S155A/D156A expressing cells, we tested the endpoint of apoptosis, using a caspase-3 assay. While wild-type Ku70 MEFs showed a strong caspase-3 activity at 48 and 72 hours post-IR, the mutant cells displayed significantly lower caspase-3 activity, and therefore decreased apoptotic activation (Figure 2-4A). We then compared the ability of Ku70 wild-type and Ku70 S155A/D156A expressing cells to form γ-H2AX foci, an early marker of the DNA damage response (46). Ku70 S155A/D156A cells showed no significant difference in basal foci levels in absence of IR treatment, whereas, $Ku70^{-/-}$ cells had increased γ-H2AX foci levels indicative of unrepaired endogenous DSBs. Early foci formation 1 hour following IR treatment was again similar in Ku70 wild-type and S155A/D156A-expressing cells, suggesting that the mutation did not interfere with the initial phosphorylation events. However Ku70 S155A/D156A cells displayed persistent foci 24 hours following IR compared to Ku70 wild-type cells (Figure 2-4B) suggesting an abnormally prolonged DNA damage response. Altogether, these results suggested that the mutation interfered with the activation of apoptosis and resulted in a persistent DNA damage response.

2.3.4 Ku70 S155A/D156A mutant cells display altered transcriptional regulation in response to DNA damage

DNA damage-induced apoptosis is largely regulated at the transcriptional level (48, 49), so we thought to investigate whether Ku S155A/D156A could interfere with the transcriptional regulation of genes involved in the IR-induced apoptotic response. In order to examine global gene expression differences between S155A/D156A and wild-type Ku70 expressing MEFs following IR, Affymetrix GeneChip analysis was performed using RNA prepared from unirradiated control cells and from cells at 8 hours and 24

Figure 2-4 Ku70 S155A/D156A expressing cells exhibit DNA damage signaling defects.

(A) Analysis of IR-induced apoptosis in Ku70 S155A/D156A expressing cells. Irradiated or mock-treated $Ku70^{-/-}$ MEFs expressing Ku70 wild-type (WT) or Ku70 S155A/D156A were assayed for caspase-3 activity at the times indicated. Fold activation of caspase-3 activity is shown relative to the unirradiated control, averaged over 4 experiments with error bars representing the SEM (**P <0.01, * P <0.05). (B) S155A/D156A Ku70 mutant cells display prolonged H2AX serine 139 phosphorylation (γ-H2AX) 24 hours post-IR. Cells as in A were irradiated with 4 Gy of IR or mock treated, fixed at the time points indicated, and subjected to analysis with a γ-H2AX antibody and DAPI. Foci were quantified based on pixel intensity and averaged over the number of cells present (a.u., arbitrary units). Data represents the average of 4 separate experiments, each assessing approximately 500 cells, and error bars represent SEM (*P <0.05).

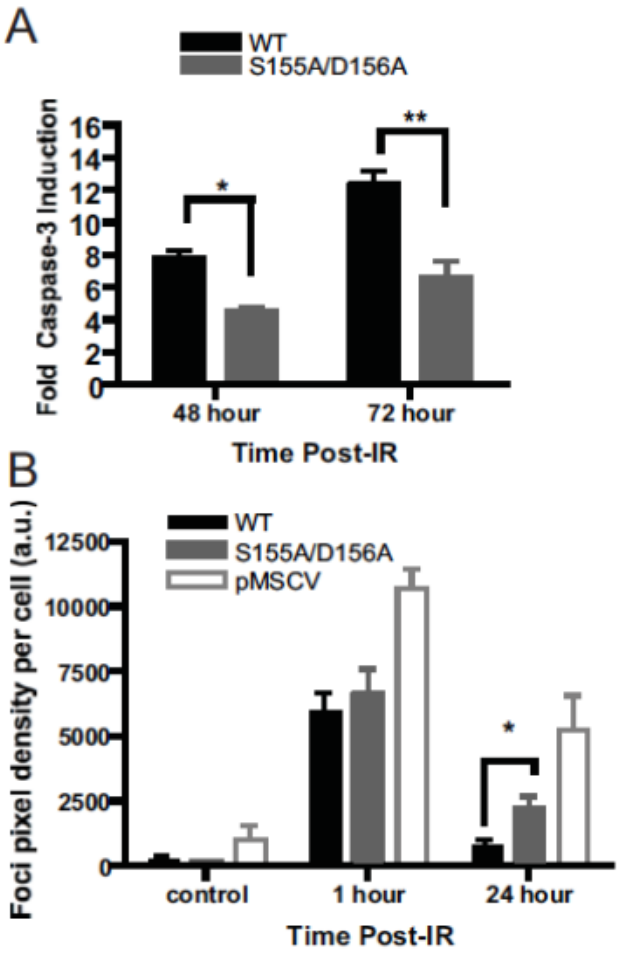
A
WT
S155A/D156A
Fold Caspase-3 Induction
16
14
12
10
8
6
4
2
0
*
**
48 hour
72 hour
Time Post-IR
B
WT
S155A/D156A
pMSCV
Foci pixel density per cell (a.u.)
12500
10000
7500
5000
2500
0
*
control
1 hour
24 hour
Time Post-IR

hours post-IR treatment. We noticed that the change of expression of several genes induced or repressed by IR was reduced in Ku S155A/D156A expressing cells (Supplementary Table 2-1). Genes found differentially regulated in WT and S155A/D156A cells included the Inhibitor of differentiation (Id) genes (Id1, Id2, Id3), Activating Transcription Factor 3 (ATF3) and Growth arrest and DNA damage-inducible gene 153 (GADD153), also known as DNA-damage-inducible transcript 3 (Ddit3) and C/EBP-homologous protein (CHOP), which have previously been characterized as participating in the regulation of apoptosis (50-53). Id1 was shown to be downregulated by ATF3 during stress (53, 54), whereas GADD153/CHOP was found to be upregulated by ATF3 to induce cell death programs in response to stress (55, 56). Change of expression of these genes was confirmed using quantitative RT-PCR analysis. Downregulation of Id1 and Id2 expression in response to IR was found severely inhibited in Ku70 S155A/D156A cells while Id3 also showed a decreased inhibition, albeit less pronounced (Figure 2-5A). The induction of GADD153/CHOP was also affected 24 hours post-IR in cells expressing Ku70 S155A/D156A (Figure 2-5B). Western blot analysis further confirmed the reduction in GADD153/CHOP protein expression in Ku70 S155A/D156A mutant cells compared to wild-type (Figure 2-5C). Since ATF3 activation would be expected to precede that of its target genes Id1 and GADD153/CHOP, we tested ATF3 protein levels in Ku70 wild-type and S155A/D156A mutant cells by western blot at earlier time points following IR treatment. A marked decrease in ATF3 induction in cells expressing Ku70 S155A/D156A was detected 2 and 8 hours after IR treatment and was still noticeable at 16 hours post-IR, confirming that Ku70 S155A/D156A interferes with and/or delays ATF3 activation (Figure 2-5D). Altogether, these results

Figure 2-5 S155A/D156A Ku70 expressing cells show altered expression of ATF3, GADD153/CHOP and Id1, Id2, and Id3 in response to IR.

(A) RT-PCR analysis of Id family genes Id1, Id2, and Id3. RNA samples from Ku70 S155A/D156A (Mt) and Ku70 wild-type (WT) expressing MEFs, 24 hours following 6 Gy of irradiation or unirradiated control cells were analyzed by RT-qPCR with primers for the indicated Id genes (Id1, Id2, Id3). Fold change of gene expression relative to that of unirradiated control samples is shown with error bars indicating SEM. For all samples, $P < 0.05$ between WT and Mt. **(**B) RT-PCR analysis of pro-apoptotic GADD153/CHOP expression. RNA samples were processed as in A and RT-qPCR was performed using primers specific for GADD153/CHOP ($P < 0.05$). (C) Western blot analysis of GADD153/CHOP protein levels in Ku70 S155A/D156A (Mt) and Ku70 wild-type (WT) MEFs following IR. Representative western blot analysis of cells irradiated at 6 Gy or mock treated (control) and extracts taken at the time points indicated**.** The membrane was hybridized with the indicated antibodies. (D) Western blot analysis of ATF3 expression. Cells were treated and harvested as in C at the times indicated and the blot was hybridized with ATF3 and actin antibodies. Both panels are from the same blot, but a longer exposure is shown for ATF3 in the left panel (no IR, 2h) due to weaker ATF3 signal intensity.

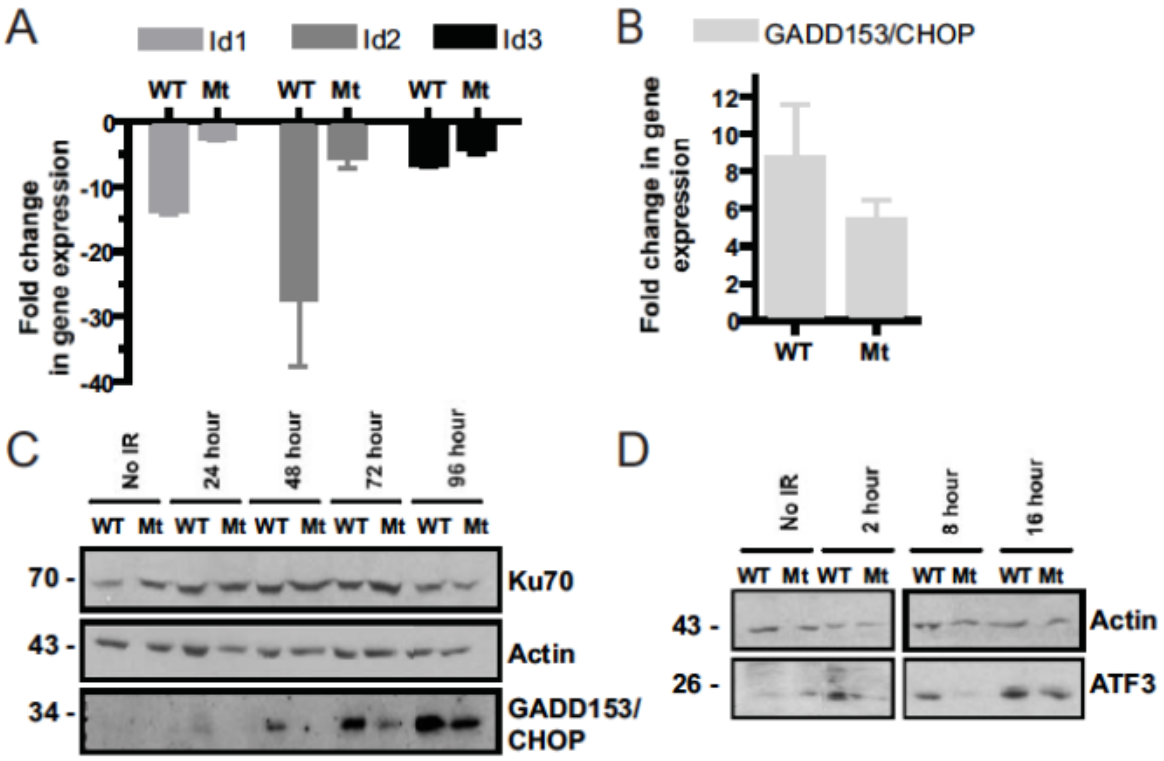
A
Id1
Id2
Id3
WT Mt WT Mt WT Mt
Fold change in gene expression
0
-10
-20
-30
-40
B
GADD153/CHOP
Fold change in gene expression
12
10
8
6
4
2
0
WT
Mt
C
No IR
24 hour
48 hour
72 hour
96 hour
WT Mt WT Mt WT Mt WT Mt WT Mt
70 -
Ku70
43 -
Actin
34 -
GADD153/
CHOP
D
No IR
2 hour
8 hour
16 hour
WT Mt WT Mt WT Mt WT Mt
43 -
Actin
26 -
ATF3

suggest that the Ku70 S155A/D156A mutation impairs a signaling pathway that affects ATF3 and its target genes in response to IR. ATF3 itself is regulated by ATF2, a transcription factor of the same family (57, 58). Interestingly, we identified additional genes known to be regulated by ATF2 and whose expression is altered by stress or DNA damage that were differentially expressed in Ku wild-type and S155A/D156A cells in response to IR (Supplementary Table 2-2). This suggested that the Ku70 S155/D156 residues could function to modulate the activation of an ATF2-dependent pathway in response to IR.

2.3.5 Ku70 S155A/D156A inhibits ATF2 phosphorylation and foci formation

ATF2 expression is not altered in response to IR, but ATF2 is rapidly recruited to IR-induced foci that co-localize with γ-H2AX (59). Foci formation by ATF2 is dependent on phosphorylation of C-terminal residues (490, 498) (59). In addition, the activation of ATF2 transcriptional activity in response to DNA damage and other forms of stress is dependent on the phosphorylation of two residues in the N-terminal region (Thr69/71) (57). Thus, to determine whether the Ku70 S155A/D156A mutation interfered with ATF2 activation in response to IR, we first analyzed ATF2 foci formation in $Ku70^{-/-}$ pMSCV MEFs and cells re-expressing Ku70 wild-type and the Ku70 S155A/D156A mutant. While all 3 cell lines displayed equivalent background level of ATF2 foci in untreated cells, IR-induced ATF2 foci formation was much stronger in Ku deficient cells than in cells re-expressing Ku70 wild-type (Figure 2-6A). Foci formation was reduced in cells expressing Ku70 S155A/D156A compared to wild-type at both 1 and 4 hours after IR treatment. Next, to determine whether Ku also modulated ATF2 phosphorylation at the

Figure 2-6 Deficient ATF2 activation in response to DNA damage in Ku70 S155/D156 expressing cells.

(A) Representative images of ATF2 foci formation in response to IR in $Ku70^{-/-}$ MEFs expressing wild-type Ku70 (WT), Ku70 S155A/D156A and empty vector (pMSCV). Cells fixed either untreated (no IR) or 1h after IR (6 Gy) were stained with an ATF2 antibody and DAPI. Below, quantification of foci formation was done for unirradiated cells (control) or cells processed 1h or 4h after IR treatment as described in Materials and Methods and the results were averaged from 4 experiments (about 250 cells/experiments), with error bars representing SEM (*P<0.05). (B) Cells were analyzed as in A with a phospho-ATF2 (69/71) antibody. Representative images are shown at the top, with quantification of phospho-ATF2 staining intensity from 3 separate experiments shown below (a.u., arbitrary units of signal intensity). (C) Western blot analysis of phospho-ATF2 (69/71) in $Ku70^{-/-}$ MEFs expressing wild-type Ku70 (WT) and Ku70 S155A/D156A (Mt). Cells were left untreated (no IR) or subjected to 10 Gy and collected at the time points indicated to prepare nuclear extracts. Western blot analysis was done with a phospho-ATF2 69/71 antibody (p69/71) or with an ATF2 antibody to determine total ATF2 protein expression and actin as indicated.

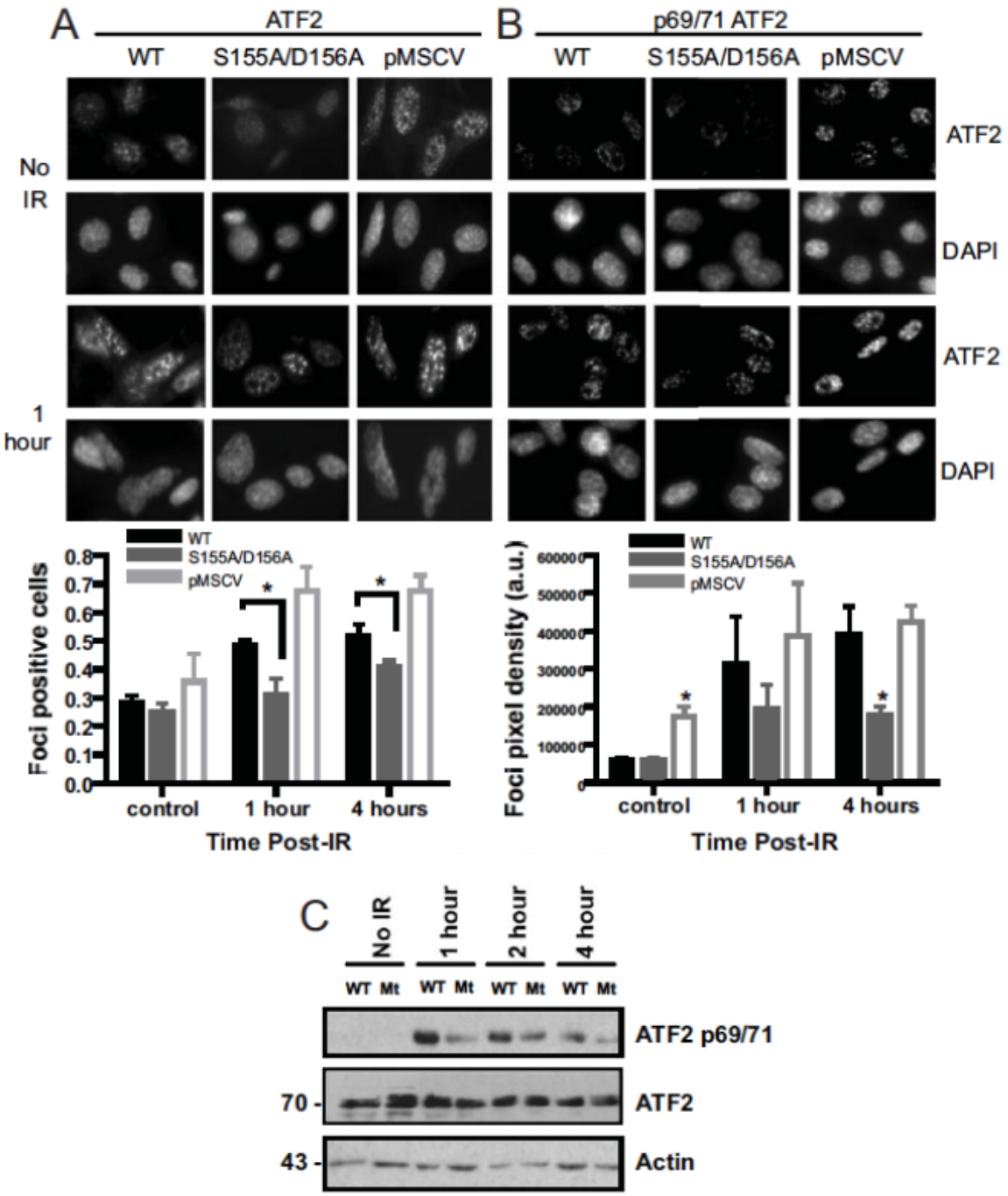
A
ATF2
WT
S155A/D156A
pMSCV
B
p69/71 ATF2
WT
S155A/D156A
pMSCV
No IR
1 hour
ATF2
DAPI
ATF2
DAPI
Foci positive cells
WT
S155A/D156A
pMSCV
control
1 hour
4 hours
Time Post-IR
Foci pixel density (a.u.)
WT
S155A/D156A
pMSCV
control
1 hour
4 hours
Time Post-IR
C
No IR
1 hour
2 hour
4 hour
WT Mt WT Mt WT Mt WT Mt
ATF2 p69/71
70 -
ATF2
43 -
Actin

N-terminal sites (Thr69/71) that activate ATF2 transcriptional function, we analyzed phospho-ATF2 at the 69/71 residues using immunocytochemistry. IR-induced phospho-69/71 ATF2 staining appeared mostly diffuse, but exhibited small foci (Figure 2-6B). Similar to ATF2 foci formation, phospho 69/71 was enhanced in $Ku^{-/-}$ cells compared to Ku70 wild-type MEFs, and reduced in Ku70 S155A/D156A at both time points tested. To confirm the difference in phosphorylation at the ATF2 69/71 site between Ku70 wild-type and S155A/D156A mutant MEFs, we analyzed phospho-ATF2 by western blotting. Consistent with the immunofluorescence result, a noticeable reduction in ATF2 phosphorylation was observed at all times points between 1 and 4 hours post-IR in Ku70 S155A/D156A MEFs compared to wild-type, suggesting that substitutions at S155/D156 impaired ATF2 69/71 phosphorylation (Figure 2-6C). Together, these results suggest that Ku functions to repress ATF2 activation in response to DNA damage and that the S155A/D156A mutation further enhances this repression.

2.3.6 Increased survival in response to IR is dependent on the mutation of S155

The Ku70 S155/D156 residues are present in a loop region between α-helix 4 and α-helix 5 of the Ku70 vWA domain (32). The effect of the mutation could be due either to the disruption of a key phosphorylation event on Ser155, or could simply be disrupting a protein-protein interaction surface. To address the latter possibility, we produced a Ku70 mutant containing alanine substitutions across the entire loop (aa 155 to 160), reasoning that extending the mutated surface could amplify the effect observed with the S155A/D156A mutation. Analysis of IR survival curves revealed no significant difference in survival between MEFs expressing the Ku70 155-160A mutant and those

expressing the S155A/D156A mutant, suggesting that S155A/D156A alone conferred maximal increased resistance to IR (Figure 2-7A). We next tested the effect of the single S155A and D156A substitutions on cell survival in response to IR. Ku70 D156A expression resulted in a survival profile not significantly different than wild-type Ku70. The Ku70 S155A however, conferred enhanced survival that was similar to that of the 155-160 mutant and the double S155/6 mutation (Figure 2-7B). This suggests that the DNA damage signaling events that modulate cell survival in response to IR are solely dependent on Ku70 S155.

As this residues is a serine, it suggested the possibility that S155 might be targeted for phosphorylation to modulate DNA damage signaling, and that the S to A substitution prevented this crucial modification. To test this possibility, we generated an aspartic acid mutant, S155D, to assess the effect of a phosphomimetic substitution on cell survival in response to IR. Cells expressing Ku70 S155D appeared fragile and susceptible to cell death. Also, while we confirmed expression of Ku70 S155D (Figure 2-7D), the protein levels appeared to decline quickly in the first few passages following drug selection, and only about 65% of MEFs were found expressing this mutant, versus over 90% for Ku70 WT and other mutants (Supplementary Table 2-2). Clonogenic assays revealed that the Ku70 S155D mutation conferred a pronounced hypersensitivity to IR, as cells expressing Ku70 S155D displayed even greater radiosensitivity than the Ku-deficient cells (Figure 2-7C). To determine the effect of the S155D substitution on ATF2 phosphorylation, we compared ATF2 69/71 phosphorylation in cells expressing Ku70 S155D, Ku70 S155A, wild-type Ku70 and Ku70$^{-/-}$ pMSCV MEFs. In control unirradiated cells, both Ku70-deficient MEFs and S155D showed strong background levels of phospho-ATF2 in

Figure 2-7 Ku70 S155A substitution is required and sufficient to confer increased survival following IR.

(A) Clonogenic assay of Ku70$^{-/-}$ MEFs expressing Ku70 with 155-160 alanine substitutions (155-160A) and S155A/D156A in comparison Ku70$^{-/-}$ expressing wild-type Ku70 (WT). Survival is expressed as the number of colonies present at each IR dose relative to the unirradiated control, averaged over 3 experiments and with error bars representing the SD (**P<0.01, *P<0.05). (B) Clonogenic assay comparing survival of MEFs expressing Ku70 wild-type (WT) and Ku70 D156A and S155A substitutions. Survival is expressed as in A. (*P<0.01). (C) Clonogenic assay of MEFs expressing Ku70 wild-type (WT), Ku70 S155A and empty pMSCV vector (KO) in comparison to Ku70 bearing the phosphomimetic S155D substitution. Survival is expressed as in A. WT, S155A and pMSCV are significantly different from each other at all time points (P<0.05), but the stars indicating significance are omitted for clarity. Significance is indicated for S155D compared to pMSCV (*P<0.001). (D) Western blot analysis of Ku subunits expression in Ku70$^{-/-}$ MEFs expressing empty vector (pMSCV), wild-type Ku70 (WT), or Ku70 mutants as indicated. (E) Western blot analysis of phospho-ATF2 (69/71) in Ku70$^{-/-}$ MEFs expressing wild-type Ku70 (WT), Ku70 S155A and Ku70 S155D or empty vector (pMSCV). Cells were either left untreated (no IR) or subjected to 10 Gy and collected 2 hours later. Western blot analysis was done with a phospho-ATF2 69/71 antibody (p69/71), an ATF2 antibody to determine total ATF2 protein expression and actin as indicated.

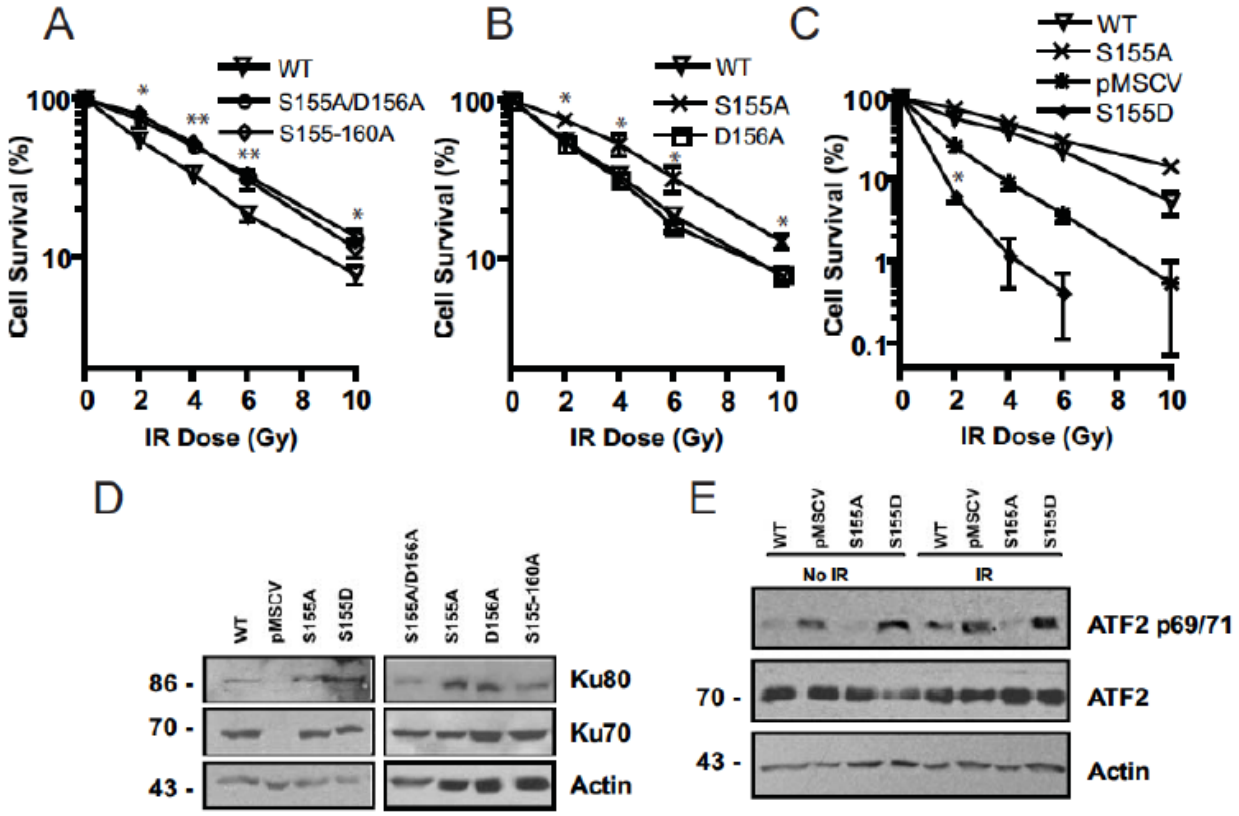
A
B
C
WT
S155A/D156A
S155-160A
S155A
D156A
pMSCV
S155D
Cell Survival (%)
IR Dose (Gy)
D
E
WT
pMSCV
S155A
S155D
S155A/D156A
D156A
S155-160A
No IR
IR
86 -
70 -
43 -
Ku80
Ku70
Actin
ATF2 p69/71
ATF2

comparison to Ku70 wild-type and S155A (Figure 2-7E). In response to IR, as expected, phospho-ATF2 was enhanced in Ku-deficient cells and reduced in Ku70 S155A compared to Ku70 wild-type. As well, Ku70 S155D expressing cells displayed increased levels of phospho-ATF2 in comparison to Ku70 wild-type. Thus, these results are consistent with a phosphomimetic effect of the Asp substitution and support the notion that Ku70 S155 phosphorylation in response to IR is an important event that activates apoptotic pathways in response to DNA damage.

2.4 Discussion

This study identifies a novel function for Ku in regulating signaling pathways leading to apoptosis in response to DNA damage. This regulation occurs through a previously uncharacterized region near α-helix 4 in the Ku70 vWA domain. Amino acid substitutions in this region, while not affecting DNA repair, compromise the activation of apoptosis, and alter the transcriptional profile of genes regulated by an ATF2/ATF3 pathway.

Previous studies have shown the involvement of the Ku70 vWA domain in C-NHEJ. A recent study demonstrated that Ku has a 5' lyase activity that is conferred by specific residues in the Ku70 vWA, supporting a direct role for Ku in end-processing (27). This activity was found to be dependent on an N-terminal "active site" (aa 4-34) and on three lysine residues within the Ku70 N-terminal domain. In yeast, Ku70 α-helix 5 was found to convey crucial C-NHEJ functions (38). We show here that substitutions in the corresponding human Ku70 α-helix 5 residues (D192A/D195R) caused a survival defect in MEFs, consistent with an C-NHEJ defect. α-helix 5 is an exposed α-helix facing

towards the DNA terminus that is well conserved from yeast to man (Figure 1)(38). While the underlying cause of this DNA repair defect is still unknown, this implies that the function of this Ku region is evolutionarily conserved. Mutations in α-helices 3 and 4 did not cause any obvious defects. Our results are consistent with previous findings in yeast showing that α-helix 4 mutations do not affect C-NHEJ (38). Additionally, it should be pointed out that α-helix 3 is positioned away from the DNA and therefore may be less likely to function in DNA repair process (32, 38).

In contrast to the aforementioned involvement of vWA regions in C-NHEJ, the Ku70 S155A/D156A mutation is fully functional for DNA repair, suggesting that these residues are not involved in the interaction of Ku with C-NHEJ factors. In particular, it also indicates that these substitutions do not interfere with the overall DNA-PK kinase activity which is known to be required for C-NHEJ and defects in which result in IR sensitivity (13, 60). Since the DNA-PKcs region of interaction with Ku lies in the Ku80 C-terminal domain, it is unlikely to be affected by a Ku70 N-terminal substitution. However, the possibility remains that S155A/D156A could interfere with phosphorylation of specific targets by DNA-PK.

The increased survival of the MEFs expressing Ku70 S155A/D156A correlated with a marked decrease in apoptosis as measured by caspase-3 activation. In contrast to wild-type cells, persistent γ-H2AX foci were present 24h following IR, suggestive of the presence of residual unrepaired DNA breaks. Since Ku70 S155A/D156A does not confer any repair defects, the persistence of γ-H2AX foci suggests defects in DNA damage signaling. γ-H2AX foci present at 24 hours may indicate DSBs that were unable to be

repaired and would normally trigger apoptotic pathway activation to eliminate the damaged cells. We postulate that in Ku wild-type cells, the activation of apoptotic pathways allows the return of γ-H2AX foci to background levels, whereas defects in signaling to apoptosis in Ku70 S155A/D156A delays or impedes foci disappearance in these cells.

Since Ku70 S155A/D156A resulted in apoptotic defects, we first investigated whether it could affect p53, since this factor is a major regulator of apoptotic pathways in response to DNA damage (49). Analysis of p53 response to IR revealed that p53 expression is not induced in either Ku wild-type or Ku70 S155A/D156A cells (Supplementary Figure 2-3), suggesting that the immortalization of the Ku $Ku70^{-/-}$ MEFs disrupted p53 regulation, an event that frequently occurs in the process of MEFs immortalization (61). However, p53 was efficiently phosphorylated at Ser 15 (Ser 18 in mouse) in response to IR, suggesting that the ATM-dependent signaling which is responsible for p53 phosphorylation at this site is intact in these cells (62). Importantly, no difference in the efficiency of phosphorylation was observed between wild-type and Ku70 S155A/D156A cells, suggesting that the effect of Ku on signaling to apoptosis does not affect p53 response nor appears to be p53 dependent (Supplementary Figure 2-3).

The altered expression of several genes involved in an ATF2/ATF3 signaling pathway in Ku70 S155A/D156A cells led us to speculate that Ku functions to regulate this signaling pathway in response to IR. ATF3 is a basic-region leucine zipper (bZIP) transcription factor member of the ATF/CREB superfamily that is rapidly upregulated by a variety of stress signals including DNA damage (51, 58, 63, 64). ATF3 can function both to activate and repress transcription, depending on its dimerization partner and the

promoter context. Several studies have demonstrated a crucial role for ATF3 activity in inducing apoptosis and the suppression of tumorigenesis (51, 65, 66). Furthermore, ATF3 is directly involved in down-regulating Id1 expression, while contributing to GADD153/CHOP transcriptional activation (53, 55). While Id1 has been shown to be directly regulated by ATF3, Id2 and Id3 expression is not well characterized but there is evidence that they are regulated coordinately (52, 67). Id proteins function as dominant-negative antagonists of the basic helix-loop-helix (bHLH) family of transcription factors and play roles in development, tumorigenesis and cell cycle by promoting cell survival and proliferation (52, 67). Overexpression of Id proteins correlates with tumorigenesis and downregulation of Id1 expression sensitizes cells to apoptotic agents (52, 67-69). Finally, previous studies have shown that Id1 is downregulated in response to stress and DNA damage in an ATF3-dependent manner (53, 54). Consistent with these studies, our RT-PCR analyses showed a strong downregulation of Id1 following IR treatment, concurrent with that of Id2 and Id3. In Ku70 S155A/D156A cells, this repression was substantially lessened, correlating with reduced activation of ATF3. Thus, the combined IR-induced regulation of these transcription factors converge towards the regulation of apoptosis and their dysregulation in Ku70 S155A/D156A cells is consistent with the reduced activation of apoptosis observed in response to DNA damage.

ATF3 activation is mediated by several factors and pathways depending on the activating stimulus (51, 56). DNA damage activation of ATF3 has been suggested to depend on an ATM-NBS1 pathway, and ATF2 (58). Recent studies have implicated ATF2 in the DDR (59, 70). In response to DNA damage, ATF2 transcriptional activity is activated by phosphorylation at N-terminal residues T69/71 by p38 and Jun-N-terminal

Kinase (JNK) in an ATM-dependent manner (58, 71, 72). In addition, ATF2 is phosphorylated at C-terminal S490/498 by ATM, resulting in its accumulation at IR-induced foci that co-localize with γ-H2AX and the MRN complex (59). Mutation of these residues results in loss of ATF2 foci formation, defective DNA damage response and confer increased sensitivity to IR and tumour susceptibility in mice (59, 70).

Analysis of ATF2 IR-induced foci formation and T69/71 phosphorylation showed that both were affected by Ku expression and Ku70 S155A/D156A mutation. Previously, it was determined that while mutation of ATF2 S490/498 prevented foci formation, T69/71 phosphorylation was dispensable for ATF2 localization into foci, and phosphorylation at both sites were suggested to be independent events (59, 71). The relationship between these two phosphorylation events is still unclear as ATM is required for ATF2 T69/71 phosphorylation (58), but whether T69/71 phosphorylation is an independent event, or is contingent on S490/498 modification has not been determined. We found that phospho T69/71-ATF2 is localized into IR-induced foci. This infers the existence of an ATF2 population that is phosphorylated at both N-terminal and C-terminal motifs suggesting that phosphorylation at both sites is not exclusive and that transcriptionally active ATF2 is present at DNA breaks. Thus, our results suggest that Ku functions to modulate both events whether or not they are independent of one another.

The deregulation of several genes directly or indirectly dependent on ATF2 transcriptional activity in Ku70 S155A/D156A cells suggests that this mutation can interfere with the transcriptional activity of ATF2 mediated by T69/71 phosphorylation. Phosphorylation of T69/71 is induced in $Ku70^{-/-}$ cells compared to wild-type, suggesting that Ku plays an inhibitory role on ATF2 transcriptional activation in response to IR.

Since ATF2 T69/71 phosphorylation initiates signaling cascades leading to the activation of apoptosis, one potential explanation is that Ku-mediated inhibition of ATF2 activation is linked to Ku's ability to activate DNA repair. Ku-mediated assembly of a functional C-NHEJ complex and/or completion of DNA repair could prevent ATF2 activation. In the case of overwhelming DSBs, Ku may be present at the break, however, may not be able to assemble a functional repair complex because of the limiting availability of other C-NHEJ factors, thus allowing ATF2 phosphorylation and the establishment of a signaling pathway leading to the activation of apoptosis. The increased repression of ATF2 phosphorylation by Ku70 S155A suggests that this mutation disrupts an event that normally allows ATF2 activation when DNA repair is not completed. As ATF2 phosphorylation and activation in response to DNA damage is ATM dependent (58, 59), the Ku70 vWA region may function to link Ku to ATM signaling and modulate an ATM-dependent pathway.

We demonstrated that S155 is the essential residue implicated in this regulation of cell survival. As serine/threonine kinases are an integral part of the DNA damage response signaling pathway, the S155A mutation could be preventing an important post-translational signaling event in the regulation of apoptosis. However, S155 has not been previously identified as a DNA-PK phosphorylation site on Ku70 (73), nor is it located in any canonical kinase phosphorylation motif (as determined using NetworKIN) (74). Interestingly, a recent proteomics study analyzing site-specific phosphorylation after IR treatment identified a new DNA damage-related phosphorylation motif, S*XX*Q, which was overrepresented amongst phospho-sites regulated within 1 hour following IR treatment (75). Peptides with this motif were found to follow a profile of phosphorylation

similar to that of SQ motifs, suggesting that this site could be targeted by ATM or DNA-PK. S155 is located in a S*XX*Q motif (SDVQ – Figure 2-1), thus making these two kinases prime candidates for a phosphorylation event at this site. Future experiments will have to determine whether ATM or DNA-PK can phosphorylate this site and whether phosphorylation of S155 is indeed responsible for the modulation of cell survival through regulation of ATF2-dependent pathway.

The idea that S155 is a phosphorylation site is supported by our experimental results showing that that the survival advantage conferred by the S155A substitution is completely overturned by the S155D mutation. This suggests that this phosphomimetic substitution provides for a constitutive activation of apoptosis irrespective of DNA repair. Somewhat surprisingly, cells expressing Ku70 S155D displayed an even more pronounced hypersensitivity to IR than cells lacking Ku. ATF2 phosphorylation appeared similar in Ku-deficient and S155D within the limit of sensitivity of the western blot analysis. Thus, it is possible that Ku70 phosphorylation at S155 not only potentiates ATF2 phosphorylation but also has additional effects that contribute to further activation of downstream apoptotic pathways.

The apoptotic pathway regulated by Ku identified in this study seems independent from the control of Bax by Ku70 described in previous studies (76). First, the Bax-Ku70 interaction that has been described relies on the acetylation of several residues in the Ku70 C-terminal domain, thus in a region that is quite distinct from S155 in the N-terminal domain (77). Second, Bax regulation by Ku70 hinges on the modulation of an interaction between Bax and Ku that has been suggested to occur in the cytoplasm (40), while the regulation that we have uncovered here involves the interplay between proteins

that form DNA-induced foci at DNA breaks. However, further investigations will be needed to determine whether Ku70 S155 modulates the activation of apoptosis through other pathways and in particular, whether Ku-Bax interaction is affected by this regulation.

Finally, it is interesting to consider the positioning of the α-helix 5 residues (D192, D195) which mutation confers a DNA repair defect in yeast and that we have confirmed here severely impair viability, and the loop region adjacent to α-helix 4 where the S155 is located. Both are facing outwards, towards the DNA break (Figure 2-1B), in proximity to one another, suggesting the potential for interactions or cross-talk between the two regions. Because of its presence at the DNA break and its primary function in C-NHEJ, Ku is well positioned to act as a "sensor" of DNA repair. Therefore, the proximity of α-helix 5, which appears essential for DNA repair, to the S155 residues suggests that Ku could function to relay signals from the repair machinery to nearby regulators of signaling pathways that control apoptosis.

2.5 References

1. Helleday T, Lo J, van Gent DC, & Engelward BP (2007) DNA double-strand break repair: From mechanistic understanding to cancer treatment. *DNA Repair (Amst)* 6(7):923-935.
2. Hartlerode AJ & Scully R (2009) Mechanisms of double-strand break repair in somatic mammalian cells. *Biochem. J.* 423(2):157-168.
3. Cann KL & Hicks GG (2007) Regulation of the cellular DNA double-strand break response. *Biochem. Cell. Biol.* 85(6):663-674.
4. Su TT (2006) Cellular responses to DNA damage: one signal, multiple choices. *Annu. Rev. Genet.* 40:187-208.
5. Karagiannis TC & El-Osta A (2004) Double-strand breaks: signaling pathways and repair mechanisms. *Cell. Mol. Life Sci.* 61(17):2137-2147.
6. Valerie K & Povirk LF (2003) Regulation and mechanisms of mammalian double-strand break repair. *Oncogene* 22(37):5792-5812.
7. Riches LC, Lynch AM, & Gooderham NJ (2008) Early events in the mammalian response to DNA double-strand breaks. *Mutagenesis* 23(5):331-339.
8. Kim J-S*, et al.* (2005) Independent and sequential recruitment of NHEJ and HR factors to DNA damage sites in mammalian cells. *J.Cell Biol.* 170(3):341-347.
9. Lavin MF & Kozlov S (2007) ATM activation and DNA damage response. *Cell Cycle* 6(8):931-942.
10. Lee JH & Paull TT (2007) Activation and regulation of ATM kinase activity in response to DNA double-strand breaks. *Oncogene* 26(56):7741-7748.
11. Fernandez-Capetillo O, Lee A, Nussenzweig M, & Nussenzweig A (2004) H2AX: the histone guardian of the genome. *DNA Repair (Amst)* 3(8-9):959-967.
12. Lieber MR (2010) The mechanism of double-strand DNA break repair by the nonhomologous DNA end-joining pathway. *Annu. Rev. Biochem.* 79:181-211.
13. Mahaney BL, Meek K, & Lees-miller SP (2009) Repair of ionizing radiation-induced DNA double-strand breaks by non-homologous end-joining. *Biochem. J.* 417(3):639-650.
14. Nussenzweig A & Nussenzweig MC (2007) A Backup DNA Repair Pathway Moves to the Forefront. *Cell* 131(2):223-225.
15. Sekiguchi JM & Ferguson DO (2006) DNA double-strand break repair: a relentless hunt uncovers new prey. *Cell* 124(2):260-262.
16. Abraham RT (2004) PI 3-kinase related kinases: 'big' players in stress-induced signaling pathways. *DNA Repair (Amst)* 3(8-9):883-887.
17. Hill R & Lee PW (2010) The DNA-dependent protein kinase (DNA-PK): More than just a case of making ends meet? *Cell Cycle* 9(17):3460-3469.
18. Meek K, Dang V, & Lees-Miller SP (2008) Chapter 2 DNA-PK: The Means to Justify the Ends? *Advances in Immunology*, ed Frederick WA (Academic Press), Vol Volume 99, pp 33-58.
19. Fulop GM & Phillips RA (1990) The scid mutation in mice causes a general defect in DNA repair. *Nature* 347(6292):479-482.
20. Li GC*, et al.* (1998) Ku70: a candidate tumor suppressor gene for murine T cell lymphoma. *Mol. Cell* 2:1-8.

21. Nussenzweig A, Sokol K, Burgman P, Li L, & Li GC (1997) Hypersensitivity of Ku80-deficient cell lines and mice to DNA damage: the effects of ionizing radiation on growth, survival, and development. *Proc. Natl. Acad. Sci. U. S. A.* 94(25):13588-13593.
22. Smith GC & Jackson SP (1999) The DNA-dependent protein kinase. *Genes Dev.* 13:916-934.
23. Lieber MR, Ma Y, Pannicke U, & Schwarz K (2003) Mechanism and regulation of human non-homologous DNA end-joining. *Nat. Rev. Mol. Cell. Biol.* 4(9):712-720.
24. Downs JA & Jackson SP (2004) A means to a DNA end: the many roles of Ku. *Nat. Rev. Mol. Cell Biol.* 5(5):367-378.
25. Riha K, Heacock ML, & Shippen DE (2006) The Role of the Nonhomologous End-Joining DNA Double-Strand Break Repair Pathway in Telomere Biology. *Annu. Rev. of Genet.* 40(1):237-277.
26. Collis SJ, Deweese TL, Jeggo PA, & Parker AR (2005) The life and death of DNA-PK. *Oncogene* 24(6):949-961.
27. Roberts SA*, et al.* (2010) Ku is a 5'-dRP/AP lyase that excises nucleotide damage near broken ends. *Nature* 464(7292):1214-1217.
28. Schild-Poulter C, Haché R.J.G., & Soubeyrand S (2004) Ku antigen: a versatile DNA binding protein with multiple cellular functions. *Recent Research Developments in Dynamical Genetics, Ed, V. Parisi, V. De Fonzo and F. Aluffi-Pentini,*, (Research Signpost, Transworld Research Network), pp 257-284.
29. Costantini S, Woodbine L, Andreoli L, Jeggo PA, & Vindigni A (2007) Interaction of the Ku heterodimer with the DNA ligase IV/Xrcc4 complex and its regulation by DNA-PK. *DNA Repair (Amst)* 6(6):712-722.
30. Lieber MR, Yu K, & Raghavan SC (2006) Roles of nonhomologous DNA end joining, V(D)J recombination, and class switch recombination in chromosomal translocations. *DNA Repair (Amst)* 5(9-10):1234-1245.
31. Shim EY, Ma J-L, Oum J-H, Yanez Y, & Lee SE (2005) The Yeast Chromatin Remodeler RSC Complex Facilitates End Joining Repair of DNA Double-Strand Breaks. *Mol. Cell. Biol.* 25(10):3934-3944.
32. Walker JR, Corpina RA, & Goldberg J (2001) Structure of the Ku heterodimer bound to DNA and its implications for double-strand break repair. *Nature* 412:607-614.
33. Aravind L & Koonin EV (2001) Prokaryotic homologs of the eukaryotic DNA-end-binding protein Ku, novel domains in the Ku protein and prediction of a prokaryotic double-strand break repair system. *Genome Res.* 11:1365-1374.
34. Aravind L & Koonin EV (2000) SAP - a putative DNA-binding motif involved in chromosomal organization. *Trends Biochem. Sci.* 25(3):112-114.
35. Harris R*, et al.* (2004) The 3D Solution Structure of the C-terminal Region of Ku86 (Ku86CTR). *J. Mol. Biol.* 335(2):573-582.
36. Zhang Z*, et al.* (2004) Solution structure of the C-terminal domain of Ku80 suggests important sites for protein-protein interactions. *Structure (Camb)* 12(3):495-502.

37. Whittaker CA & Hynes RO (2002) Distribution and Evolution of von Willebrand/Integrin A Domains: Widely Dispersed Domains with Roles in Cell Adhesion and Elsewhere. *Mol. Biol. Cell* 13(10):3369-3387.
38. Ribes-Zamora A, Mihalek I, Lichtarge O, & Bertuch AA (2007) Distinct faces of the Ku heterodimer mediate DNA repair and telomeric functions. *Nat. Struct. Mol. Biol.* 14(4):301-307.
39. Bertinato J, Schild-Poulter C, & Hache RJ (2001) Nuclear localization of Ku antigen is promoted independently by basic motifs in the Ku70 and Ku80 subunits. *J. Cell Sci.* 114(Pt 1):89-99.
40. Gama V*, et al.* (2009) Hdm2 is a ubiquitin ligase of Ku70-Akt promotes cell survival by inhibiting Hdm2-dependent Ku70 destabilization. *Cell Death Differ.* 16(5):758-769.
41. Schild-Poulter C*, et al.* (2007) DNA-PK phosphorylation sites on Oct-1 promote cell survival following DNA damage. *Oncogene* 26(27):3980-3988.
42. Andrews NC & Faller DV (1991) A rapid micropreparation technique for extraction of DNA-binding proteins from limiting numbers of mammalian cells. *Nucleic Acids Res.* 19(9):2499.
43. Edgar RC (2004) MUSCLE: multiple sequence alignment with high accuracy and high throughput. *Nucleic Acids Res.* 32(5):1792-1797.
44. Gu Y, Jin S, Gao Y, Weaver DT, & Alt FW (1997) Ku70-deficient embryonic stem cells have increased ionizing radiosensitivity, defective DNA end-binding activity, and inability to support V(D)J recombination. *Proc. Natl. Acad. Sci. U. S. A.* 94:8076-8081.
45. Gu Y*, et al.* (1997) Growth retardation and leaky SCID phenotype of Ku70-deficient mice. *Immunity* 7:653-665.
46. Kinner A, Wu W, Staudt C, & Iliakis G (2008) γ-H2AX in recognition and signaling of DNA double-strand breaks in the context of chromatin. *Nucleic Acids Res.* 36(17):5678-5694.
47. Rothkamm K, Kruger I, Thompson LH, & Lobrich M (2003) Pathways of DNA double-strand break repair during the mammalian cell cycle. *Mol. Cell. Biol.* 23(16):5706-5715.
48. Norbury CJ & Zhivotovsky B (2004) DNA damage-induced apoptosis. *Oncogene* 23(16):2797-2808.
49. Roos WP & Kaina B (2006) DNA damage-induced cell death by apoptosis. *Trends Mol. Med.* 12(9):440-450.
50. Maytin EV, Ubeda M, Lin JC, & Habener JF (2001) Stress-inducible transcription factor CHOP/gadd153 induces apoptosis in mammalian cells via p38 kinase-dependent and -independent mechanisms. *Exp. Cell Res.* 267(2):193-204.
51. Thompson M, Xu D, & Williams B (2009) ATF3 transcription factor and its emerging roles in immunity and cancer. *J. Mol. Med.* 87(11):1053-1060.
52. Ruzinova MB & Benezra R (2003) Id proteins in development, cell cycle and cancer. *Trends Cell Biol.* 13(8):410-418.
53. Kashiwakura Y*, et al.* (2008) Down-regulation of Inhibition of Differentiation-1 via Activation of Activating Transcription Factor 3 and Smad Regulates REIC/Dickkopf-3–Induced Apoptosis. *Cancer Res.* 68(20):8333-8341.

54. Kang Y, Chen C-R, & Massagué J (2003) A Self-Enabling TGF[beta] Response Coupled to Stress Signaling: Smad Engages Stress Response Factor ATF3 for Id1 Repression in Epithelial Cells. *Mol. Cell* 11(4):915-926.
55. Jiang H-Y*, et al.* (2004) Activating Transcription Factor 3 Is Integral to the Eukaryotic Initiation Factor 2 Kinase Stress Response. *Mol. Cell. Biol.* 24(3):1365-1377.
56. Wek RC, Jiang HY, & Anthony TG (2006) Coping with stress: eIF2 kinases and translational control. *Biochem. Soc. Trans.* 34(Pt 1):7-11.
57. Lopez-Bergami P, Lau E, & Ronai Z (2010) Emerging roles of ATF2 and the dynamic AP1 network in cancer. *Nat. Rev. Cancer* 10(1):65-76.
58. Kool J*, et al.* (2003) Induction of ATF3 by ionizing radiation is mediated via a signaling pathway that includes ATM, Nibrin1, stress-induced MAPkinases and ATF-2. *Oncogene* 22(27):4235-4242.
59. Bhoumik A*, et al.* (2005) ATM-dependent phosphorylation of ATF2 is required for the DNA damage response. *Mol. Cell* 18(5):577-587.
60. Dobbs TA, Tainer JA, & Lees-Miller SP (2010) A structural model for regulation of NHEJ by DNA-PKcs autophosphorylation. *DNA Repair* 9(12):1307-1314.
61. Hahn WC & Weinberg RA (2002) Modelling the molecular circuitry of cancer. *Nat. Rev. Cancer* 2(5):331-341.
62. Kurz EU & Lees-Miller SP (2004) DNA damage-induced activation of ATM and ATM-dependent signaling pathways. *DNA Repair* 3(8-9):889-900.
63. Hai T & Hartman MG (2001) The molecular biology and nomenclature of the activating transcription factor/cAMP responsive element binding family of transcription factors: activating transcription factor proteins and homeostasis. *Gene* 273(1):1-11.
64. Turchi L*, et al.* (2008) Hif-2alpha mediates UV-induced apoptosis through a novel ATF3-dependent death pathway. *Cell Death Differ.* 15(9):1472-1480.
65. Lu D, Wolfgang CD, & Hai T (2006) Activating Transcription Factor 3, a Stress-inducible Gene, Suppresses Ras-stimulated Tumorigenesis. *J. Biol. Chem.* 281(15):10473-10481.
66. Lee SH, Bahn JH, Whitlock NC, & Baek SJ (2010) Activating transcription factor 2 (ATF2) controls tolfenamic acid-induced ATF3 expression via MAP kinase pathways. *Oncogene* 29(37):5182-5192.
67. Perk J, Iavarone A, & Benezra R (2005) Id family of helix-loop-helix proteins in cancer. *Nat. Rev. Cancer* 5(8):603-614.
68. Mern DS, Hasskarl J, & Burwinkel B (2010) Inhibition of Id proteins by a peptide aptamer induces cell-cycle arrest and apoptosis in ovarian cancer cells. *Br. J. Cancer* 103(8):1237-1244.
69. Zhang X, Ling MT, Wong YC, & Wang X (2007) Evidence of a novel antiapoptotic factor: role of inhibitor of differentiation or DNA binding (Id-1) in anticancer drug-induced apoptosis. *Cancer Sci.* 98:308-314.
70. Li S*, et al.* (2010) Radiation Sensitivity and Tumor Susceptibility in ATM Phospho-Mutant ATF2 Mice. *Genes Cancer* 1(4):316-330.
71. Bhoumik A, Lopez-Bergami P, & Ronai Z (2007) ATF2 on the double - activating transcription factor and DNA damage response protein. *Pigment Cell Res.* 20(6):498-506.

72. Xia Y, Ongusaha P, Lee SW, & Liou Y-C (2009) Loss of Wip1 Sensitizes Cells to Stress- and DNA Damage-induced Apoptosis. *J. Biol. Chem.* 284(26):17428-17437.
73. Chan DW, Ye R, Veillette CJ, & Lees-Miller SP (1999) DNA-dependent protein kinase phosphorylation sites in Ku 70/80 heterodimer. *Biochemistry* 38(6):1819-1828.
74. Linding R*, et al.* (2008) NetworKIN: a resource for exploring cellular phosphorylation networks. *Nucleic Acids Res.* 36(suppl 1):D695-D699.
75. Bennetzen MV*, et al.* (2010) Site-specific Phosphorylation Dynamics of the Nuclear Proteome during the DNA Damage Response. *Mol. Cell. Proteomics* 9(6):1314-1323.
76. Rathaus M, Lerrer B, & Cohen HY (2009) DeubiKuitylation: a novel DUB enzymatic activity for the DNA repair protein, Ku70. *Cell Cycle* 8(12):1843-1852.
77. Cohen HY*, et al.* (2004) Acetylation of the C Terminus of Ku70 by CBP and PCAF Controls Bax-Mediated Apoptosis. *Mol. Cell* 13(5):627-638.

2.6 Supplementary materials

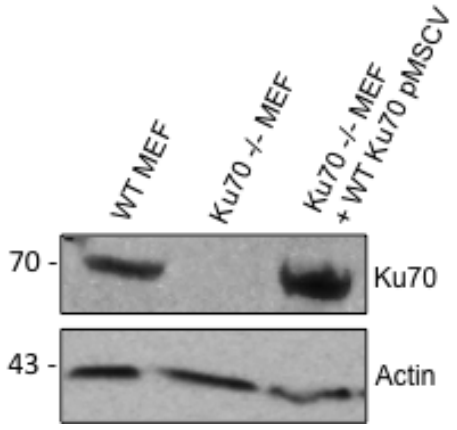

Supplementary Figure 2-1 Retroviral mediated re-expression of Ku70 in Ku70 deficient MEFs restores WT protein level

Western blot analysis of Ku70 protein level in normal WT MEFs, Ku70 -/- MEFs or Ku70 -/- MEFs that have stable integration of human Ku70 cDNA mediated through the pMSCV retroviral system.

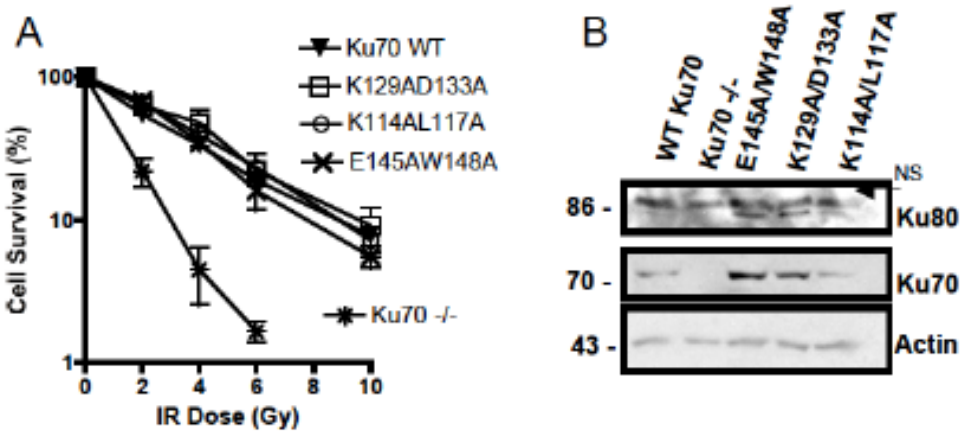

Supplementary Figure 2-2 Ku70 vWA mutations that do not alter survival after IR

(A) Several vWa alanine mutations have no effect on Ku70's function in response to IR. MEFs expressing Ku70 wild-type or Ku70 with the Ku70 mutants bearing substitutions at the amino acids indicated were irradiated and processed by clonogenic assay. Survival is expressed as the number of colonies present at each IR dose relative to the unirradiated control, averaged over 3 experiments and with error bars representing the SD. (B) Western blot analysis of Ku70 and Ku80 expression in Ku70-/- MEFs re-expressing Ku70 with the indicated substitutions.

Supplementary Table 2-1 List of genes differentially regulated after IR in S155A/D156A Ku70 expressing MEFs relative to WT Ku70.

Samples from control and IR-treated (8h and 24h) MEFs were subjected to microarray analysis using a GeneChip Mouse Gene 1.0 ST Array (Affymetrics, Santa Clara, CA). Gene Chips were processed at the London Regional Genomics Centre (Robarts Research Institute, London, ON; http://www.lrgc.ca). Fold induction/repression of expression with respect to unirradiated controls was calculated for each gene and cell line. The fold difference in gene expression change between Ku70 wild-type relative to S155A/D156A expressing MEFs is shown for those genes with a 1.4 fold or greater difference at either the 8h or 24h time point. The data shown for the 8h time point is an average of two replicates, while the data shown for the 24h time point is the result of a single experiment.

Gene	8h WT:MUT	24h WT:MUT	Gene	8h WT:MUT	24h WT:MUT	Gene	8h WT:MUT	24h WT:MUT
Car6	35.351798	7.55326236	Pcyt1b	2.5696825	1.73751955	Prss12	2.1549232	1.54156154
Mamdc2	12.474216	3.82403871	Inhba	2.5668592		Podnl1	2.1413956	1.47195299
Ppef1	7.7329359	2.96272219	Jhdm1d	2.566711	1.42608525	Igfbp4	2.1219461	1.46489793
Avil	6.877643	2.29618039	Renbp	2.5370486	1.48377333	Gla	2.1217462	1.50776768
P2rx3	5.4589804	3.01286586	Tubb2b	2.5306381	-1.8844585	Hes1	2.1155286	1.49951441
Thbs1	5.074487	2.21182421	Abca3	2.5267533	1.79230157	Idi1	2.1118744	1.91164025
Cxcl12	4.7572001	2.19052063	Klhl24	2.5215927	1.43085452	Mmp19	2.111035	
Csn3	4.7000408	2.63036226	Creb3l1	2.5093071	1.934425	Wfs1	2.1071946	
Paqr3	4.4760916	2.37121975	Myd116	2.5062049	1.80617833	Lcorl	2.104408	1.46146333
S1pr3	4.4359344	2.58393851	Gpr141	2.4973126	2.74675181	Gpnmb	2.0961174	
F2rl1	4.3232932	-1.7452819	Ern1	2.4917397	1.61018257	Txndc16	2.0844516	1.53372609
Soat2	4.284611	3.10346186	Cxcr7	2.4810491	1.50099509	Ptk2b	2.0842997	1.50812772
Gjb3	4.2585271	3.06775249	Ero1l	2.4694795	1.73056807	Chka	2.0834662	1.46853448
Cdsn	4.0486767	1.93773168	Gja1	2.4597317	1.75018346	Dgkh	2.0769273	1.5898247
Fam171b	3.9569889	1.85789773	Klhdc8a	2.4291506		Cyb5r1	2.0732754	1.45526524
Ostn	3.9187995	2.16337963	Kcnip1	2.4275086	1.43365474	Slc7a3	2.0712235	
Tubb2b	3.8577384	-2.0159257	Atp6ap2	2.4241723		Tgoln1	2.0704914	1.47157816
Cox6a2	3.8113957	2.44722654	Ddit3	2.403586	1.58111022	Osbpl2	2.0701792	1.65101697
Pcdh18	3.7962805	2.16260556	Acox2	2.3946513	1.48126956	Mapre2	2.0650343	1.42625121
Peg10	3.7852163	2.18948459	Tubb2c	2.3869952	1.68216363	Itih2	2.0568804	1.43315215
Fgf7	3.7832067	1.68920371	Gadd45g	2.3798713	1.63135202	Sdpr	2.0551082	
V1ra5	3.7532925	1.96344995	Hmgcr	2.3639928	1.55086849	Rpl31	2.0534317	1.47313069
Acot2	3.6706816	2.28496503	Hectd2	2.3618995	1.97680948	Gnpda1	2.051554	1.55414491
Mospd1	3.4633221		Ablim1	2.3613355	-1.4090042	Cdc42ep3	2.0473104	1.62744867
Arsj	3.4420464	1.70186583	Cth	2.3498195	1.67671702	Tigd2	2.0427765	1.40254449
Id2	3.3702794	2.54762558	Idi1	2.3448046	1.91487885	Fosl2	2.0410395	1.54167379
Serpine1	3.3500708	1.6039716	Leprotl1	2.3229104	1.70251588	Dgat2	2.0379489	1.43704731
B4galnt2	3.2104774	2.39308075	Slc25a33	2.310234	1.77069003	Angptl6	2.0354801	
Ccnd1	3.1906572	1.65937166	Slc38a1	2.3093627	1.77701029	Syt11	2.0323914	1.51205279
Tubb2a	3.1768128	-2.2023027	Them4	2.2833888	1.47613338	Pfn2	2.0071903	1.44926833
Nrn1	3.158247	1.67886004	Pspc1	2.2805638	1.48177071	Atp6v1c1	2.0067536	1.4895575
Cd74	3.1062047	1.53022763	Gadd45a	2.2801223		Ghitm	1.9957273	1.45625149
Elmo1	3.049313	2.2656137	Fibin	2.2740412	2.08350092	Zfp238	1.9910703	1.56519416
Hhipl1	3.0370542	1.94038549	Atp6v1d	2.2691459		Glce	1.9900029	1.54746887
Hsd17b7	3.0348747	1.63036869	Steap1	2.2677334		Tgfb1i1	1.9856515	
Tnfsf18	2.9884692	1.7994522	Slc43a3	2.2595724	1.49224239	Pik3r3	1.9849525	
Odz4	2.9823326	1.68125629	Klf10	2.257088	1.86687	Sec24d	1.9841955	1.50648072
Mfap3l	2.9156403	1.53044397	Cd200	2.2562819	1.49617621	Rbmx	1.9781283	
Acta2	2.8969319	1.53748545	Jhdm1d	2.2355789	1.71611106	Tbpl1	1.9756808	1.4226742
Lsp1	2.8927436	1.67312346	Stard5	2.2242475	1.7506519	Cpox	1.9711308	1.43009643
Lfng	2.8836716	1.67646723	Mfsd2	2.2191745		Ppm1k	1.962641	2.02098394
Trem3	2.8718446	1.77538141	Gtpbp2	2.2173979	1.42786823	Cyp51	1.9574936	-1.76730086
Ctns	2.8363293	1.65227412	Ccdc111	2.2071975	1.61127971	Ascc2	1.9564803	1.40430249
Cgref1	2.8082616	1.65626848	Cd53	2.2010035	2.42259926	Ndrg1	1.9536886	
Kctd4	2.7690659	2.18630657	Tifa	2.1956707	1.68756289	Lhfpl2	1.9514818	
Rasgef1a	2.7523793	2.15343268	Gcnt1	2.192682	1.59664707	Atf3	1.9481539	1.91225943
Prss23	2.7366833		Tuba1a	2.1909731	-1.6784365	H19	1.9443981	
Erlin1	2.7366517		Aldh1l2	2.1859951	1.77086937	Shisa4	1.9424779	1.52080648
Casp4	2.6996524	1.55142668	Atp2a3	2.1796749	1.82418977	Sgk1	1.9406403	
Socs2	2.6933765	1.87246977	Rasgef1b	2.177259	1.62781624	Atf6	1.9400345	1.46625368
Cx3cl1	2.6824395	1.64403133	Cxadr	2.1763515	1.52335953	Got1	1.9396567	
Tubb2c	2.6320276	1.60725104	Akna	2.1722718	1.74517362	Abhd1	1.9389709	1.45983447
Phlda1	2.6266753		Rap2b	2.1700115		Arhgef9	1.9291732	
Nuak1	2.6201672	1.6314884	Atp6v0b	2.1690362		Mfsd1	1.9278966	1.4688081
Cdc42ep2	2.6008806	2.32034111	Txnip	2.1657658		Tmem126b	1.925992	1.47609362
Gjb4	2.5961248	2.08740349	Scpep1	2.157303		Nr1d2	1.9248572	1.41269609

Hsph1	1.9201601		Cyp4f40	1.7517139	1.90172375	Pqlc3	1.612958	
Slc38a7	1.9172381		Gramd1b	1.7501591		Slc17a5	1.6125943	1.42473953
Tlr4	1.9146646		Hexb	1.7454734		Rnf185	1.6101383	
Rhbdd1	1.9082634	1.65098897	Cyb5	1.7450522	1.70241229	Iah1	1.6101325	
Zyg11b	1.9071919	1.4318617	Prrx2	1.7423045	1.68804388	Ccdc28a	1.6082784	
Mtm1	1.9011158	1.45468866	Ror1	1.7412096		Spag7	1.6075526	
Stard13	1.9004154		Gjb2	1.7401819	1.48240281	Map3k2	1.6048082	
Hexa	1.8975173		Fzd4	1.7321927	1.68345095	D14Ertd436e	1.6029689	1.53144538
Zscan4c	1.8939079		Chchd10	1.727917	1.47141192	Sox2	1.600814	1.4139656
Lin52	1.8911624	1.48136664	Ampd3	1.7253922		Fnip2	1.6007837	
Maged1	1.8856593	-1.8983005	Mknk1	1.7250074		Gnb4	1.5982597	
Kcnt2	1.8766199	1.65473887	Gap43	1.7227924		LOC100043377	1.5974348	
Mycbp	1.8723637		Mfsd11	1.7219822	1.42178657	Sel1l	1.5945581	1.43661194
Npc1	1.8673431		Loxl1	1.7181514		Intu	1.5922669	
Micall2	1.8656155		Fnip1	1.7170835		Agap1	1.590925	
Zscan4c	1.8597088		Ostm1	1.7160801		Hdac4	1.5874177	1.49667647
Ankrd12	1.8597043		Fam178a	1.7154287		Neu1	1.5849638	
Serac1	1.8575405	1.42197637	Ccl25	1.7118254		Sars2	1.5816334	
Gtf2h1	1.8563811	1.51269976	Fgd6	1.7116953	1.47156095	Rad9	1.580551	
Clcn3	1.8541753	1.46698769	Cacna2d1	1.7103442		Pvr	1.5801369	
Emp2	1.851322		Syk	1.7073638	1.40014645	Pawr	1.5773272	1.63090913
Zfp187	1.8503534		Ndel1	1.7070799		Snhg1	1.5773082	1.45918755
Naga	1.84989	1.41164796	Lonp1	1.7012834	1.48595993	Nipa1	1.5759317	1.63132614
Ppa1	1.8475762		Ubn1	1.6973613		Trappc1	1.5755968	1.56915774
Rmnd5a	1.8267631	1.44535087	Chpf2	1.6949752		Eprs	1.57551	
Snx16	1.8259933		Id1	1.6866234		Letm2	1.5754116	
Atp6v0d1	1.8247174		Enpp5	1.6864841		Slc38a1	1.5750848	
Zfand2a	1.8243079		Tpp1	1.6857916	1.4067943	Eif4g3	1.574932	
Sord	1.8241724	1.4153378	Ccnf	1.6839586		Zfp655	1.5734067	1.4052844
Lck	1.822613		Ifrg15	1.6830456		Prkar2b	1.5696642	1.45887399
Rragc	1.8219247	1.54459317	Hspa8	1.6806551	1.45188925	Slc26a11	1.5672707	1.52206363
Cln8	1.8217202		Hspa8	1.6763219	1.44682077	Eea1	1.5632144	1.48788782
Crebl2	1.8204641	1.48618771	Gabre	1.6663143	1.60901173	Ccdc15	1.5594109	
Slc7a11	1.8201073		Socs1	1.659868	1.4231927	Tollip	1.5592433	
Fbxo48	1.8159801	1.40688498	Echdc1	1.6581147		Slc35b4	1.5585174	
Abca8b	1.8091591	1.77865379	Ucp2	1.6553069	-1.4602673	Gnpda1	1.5567131	
Manea	1.8089528	1.48560589	Chic1	1.6534133		Tbcel	1.555061	
Jmy	1.8053534		Chmp2b	1.653137		Snx32	1.552689	
N4bp2l1	1.8049026		Herpud2	1.6523057		Ahcyl2	1.5525451	
Adam12	1.8001194		Id3	1.6511606	1.46457371	Trib1	1.5384128	
Chd2	1.7937267		Mtrr	1.6466074	1.59264985	Ier5l	1.5316894	1.50676698
Flcn	1.7909338		Mapkapk3	1.6461378	1.46947343	Kdsr	1.5315071	
Ltbp2	1.7905111		Atad5	1.6448174		Nbr1	1.5310058	
Pdzrn3	1.7881917	1.46929767	Cxx1c	1.6401412	1.43671172	Tnrc6c	1.5282717	
Gaa	1.778258		Zc3h6	1.6348365	1.49781831	Armcx1	1.5270307	
Snx30	1.7745176	1.40473952	Zmym6	1.6345893	1.42376192	Slc23a3	1.5265664	1.48729289
Ank2	1.7739278	1.74855875	Hbp1	1.6327409		Pon2	1.5231683	
Ptgs2	1.7718354		Srrt	1.6303987		Adh7	1.5224364	
Plk2	1.7701335	1.52447539	Wbp1	1.6298901	-1.415566	Mfap1a	1.5217243	
Fhod1	1.7696444		Usp53	1.6286135		Atad2b	1.5206588	1.43555531
Recql4	1.7689527	1.48256428	Lmbrd1	1.6279505		Fam178a	1.5192538	
Pycr1	1.7682591	1.48911203	Pip4k2c	1.6273531		Trpm7	1.5180277	
Hpcal1	1.7678159	1.46282945	Mcoln1	1.6230606		Diap2	1.5152733	1.42091663
Sft2d2	1.762365	1.45749417	Stx3	1.6196043	1.59749504	Gem	1.5141896	
Fyn	1.7564347	1.5736287	Gga2	1.6180539	1.40142053	Clcn7	1.5132979	
Dnm3os	1.7560198	1.63043417	Tmem140	1.6180375		Rab39b	1.5109985	1.48356497
Xpot	1.753066	1.51032446	Prnp	1.6175543		Phf3	1.5099878	
Fam50a	1.7525657		Npy1r	1.6164847		Rab11fip1	1.5097985	

Kctd17	1.5084522		Cfp	1.4139547		Tom1l2	-1.6045891	1.44938259
Rnaset2a	1.5076496		Hspa1a	1.4134225		Elovl3	-1.6252544	1.99057739
Pex1	1.5053057	1.52917586	Tom1	1.4121067		Atp6v1h	-1.6356868	1.5266622
Gpr174	1.5044154	1.54601296	Prkg2	1.4080633		Mgst3	-1.6517545	
Gtf2a1	1.5036435		Chaf1b	1.4064953		Marcks	-1.6628105	1.84515731
Atp6v1b2	1.4988765		Stambpl1	1.4064801		Col1a1	-1.6640281	1.62336255
Kctd11	1.4966708		Pfkfb2	1.4049028	1.48405674	Gnpda2	-1.6650639	
Adamtsl4	1.4964988	1.45204123	Zfyve1	1.4039952		Idua	-1.6676651	1.48600963
Zc3h6	1.4939777	-1.9389697	Wwtr1	1.4005728		Dab2	-1.6834219	1.57361035
Itpr2	1.493064	1.5963841	Zfyve26	1.4001212		Ypel2	-1.6915289	1.54727112
Arl5b	1.4862402		Gtlf3b	-1.407985		Phospho2	-1.699858	
Phf20l1	1.4826609		Zbtb34	-1.408413		Vaultrc5	-1.7089014	
Ccl9	1.4802112		Fuca2	-1.410325	1.66129296	Slc25a44	-1.7254237	1.73818215
Cebpg	1.4800289	1.4554497	Fdft1	-1.41511	1.71930121	F3	-1.7347191	1.44880528
Tmem194	1.4796213		Nsl1	-1.423584	1.56897416	Helq	-1.7572803	1.56087793
Wdr7	1.4764016	1.40290202	Bag4	-1.432748	1.53878605	Nhlrc3	-1.7578207	1.62414217
Mfap1a	1.4748779		Cd59a	-1.434654		Cd248	-1.7607058	1.90026662
Zbtb24	1.4743597	1.41659601	Sh3bgrl2	-1.44526	1.47207129	St3gal5	-1.7623064	1.49131409
Rnf214	1.4739105		Zxdc	-1.45311		Lcn2	-1.765672	1.41532747
Extl1	1.4732526	1.5735995	Fam33a	-1.462599	1.40060564	Cp	-1.7675866	
Strbp	1.4684626	1.48605154	Fam171a2	-1.467632		Galc	-1.7676586	1.43521665
Ankle1	1.4670578		Fam175b	-1.468052		Tmem68	-1.7800826	1.70021597
Mafg	1.4624167		Ahi1	-1.471704	1.62662905	Acss2	-1.7874627	
Vcpip1	1.4617343		Mxd3	-1.47245		Rragb	-1.7878325	1.86651919
Samd8	1.4610175	1.40378536	Klhdc1	-1.480162	1.47968148	Napb	-1.791784	2.10983143
Adamts9	1.4583605	1.47489082	Taf4b	-1.481357	1.49090007	Soat1	-1.7977704	
Slc3a1	1.4579581	1.40230701	Dbt	-1.489391	1.47642871	Lss	-1.8280634	1.46001437
Rnf145	1.4548605	1.40823223	H2-Q6	-1.490049		Tceal1	-1.8488098	
Cdt1	1.4503372		Lpar1	-1.49507	1.56514538	Elovl4	-1.8545102	1.58677832
Nfx1	1.4493831		Zfp30	-1.497653	1.44982344	Pla2g12a	-1.8695517	1.44630792
Psmd3	1.4487677		Thap6	-1.499752	1.42272694	Slc25a1	-1.8788746	1.56032003
Epc2	1.4485547		Cd274	-1.500081	1.63709957	Cpeb4	-1.8811509	1.57718606
Cdh11	1.4463381		Necab3	-1.503617		Nfxl1	-1.8818451	
Lrrc15	1.4455486	1.73231704	Osbpl8	-1.507525	1.50306935	Zscan4c	-1.8838396	
Cmklr1	1.4453161		Sema3a	-1.510492	-1.4169811	Pcyt2	-1.8851732	1.5336036
Gclm	1.4428535		Snrpd2	-1.511373		Abcc4	-1.8871846	1.51993276
Zfyve27	1.4425209		Aldh3b1	-1.515173		Sqle	-1.9184307	-1.67106105
Lrpprc	1.4394058		Dhtkd1	-1.517589	1.43467441	Pde5a	-1.9254491	1.47501292
Slc25a36	1.4363899		Dmxl2	-1.519363		Vcl	-1.9363655	-1.43402451
Tom1	1.4354822		Samd9l	-1.521593		Slc38a4	-1.9444142	1.49623692
Wdr76	1.4348115		Plec1	-1.532722		Mvk	-1.9457642	1.58697369
Plekhm3	1.4347774		Dap	-1.534666	-1.477496	Zbtb10	-1.9583813	1.80621337
Sos2	1.4338364		Sirt1	-1.542143		Acat2	-1.973115	1.46131124
Mafg	1.4305492		Wnt10b	-1.547559	-1.4413662	Nxn	-1.9754234	1.47388768
Hsdl1	1.4300619		Zc3h8	-1.548371		Pgr15l	-1.9896853	2.03752985
Tmem206	1.429989		Neto2	-1.555185		Fads2	-1.989967	-1.60581872
Adh1	1.4272128		Lin54	-1.567111		Prkca	-2.0061759	-1.46089205
Avl9	1.4261379		Atp6v1a	-1.570635		Utp14a	-2.0133472	1.76271345
Zfp422-rs1	1.4246906		Psca	-1.570887		Tubb6	-2.0219033	
Ssfa2	1.4237975		Wnt10a	-1.575599		Pgd	-2.0287838	1.50664876
Rragd	1.4199409	1.48761848	Impact	-1.578538	1.40814151	Nqo1	-2.0444974	-1.66362682
Parvg	1.4191975		Aoc2	-1.5795	1.54009213	Col1a2	-2.1126376	1.93115753
Mid2	1.4184922		Atg12	-1.581043		Mvd	-2.1305326	
Qsox2	1.4169895		Rnf146	-1.582225		Aspn	-2.1322411	4.32184981
Kif21b	1.4163825		Zfp346	-1.585801		Csprs	-2.1352281	
Zfc3h1	1.4163468		Tpm1	-1.58908	-1.5677594	Mtap1a	-2.1716436	-1.57415996
Fam13b	1.4144871		Tcn2	-1.589205	1.45227314	Gnpnat1	-2.1853354	1.53632549
Brca2	1.4142639		Hsd17b1	-1.601239		Fam135a	-2.1886646	1.44703985

Ehd2	-2.198438	-1.4310684	Thbd		1.57758372	Mfsd7c		1.59639171
Gnpnat1	-2.2427114	1.59901817	Fam59b		1.5577031	Sfmbt1		1.46812573
Nsdhl	-2.2681434	1.85714563	V1rb4		1.55313017	Errfi1		1.46644845
Cdkn2b	-2.3181381	1.72873896	Zfp772		1.54561075	Taf1b		1.46061889
Figf	-2.3378437	-2.2676749	Gas5		1.53413439	Armcx3		1.45633319
Cnn2	-2.406833	-1.6980701	Gm5081		1.53201016	Ccl25		1.45094145
Hmgcs1	-2.4936242	2.01395713	Pim3		1.53006309	Zbtb26		1.44200967
Elovl6	-2.5645781	2.13365248	Cftr		1.50134217	Zfp52		1.43849797
Kirrel3	-2.7847759	2.00441949	Zfp715		1.4848643	Zfp113		1.43517177
Phyhd1	-2.8151805	1.86917757	Acvr2a		1.47278634	Lrrc8d		1.43182828
Mrgprf	-2.8627782	-2.436233	Akap10		1.47200656	H2-gs10		1.4310383
Fabp5	-2.8785812	2.34144448	Tmem56		1.87443102	Marcksl1		1.42322118
Lonrf3	-2.9056867	2.56711674	Dnajc28		1.79032135	C2cd2l		1.41497937
Fabp5	-2.9136574	2.31190941	Slc7a3		1.761308	Creg1		1.4138431
Arap2	-2.930112	2.36875016	Plb1		1.73891601	Cldn12		1.4045209
Ldlr	-2.9911491	1.75481201	Tmem144		1.66376254	Zfp84		1.40376018
Dhcr24	-3.0019595	-2.2866797	Dusp4		1.64606874	Pmvk		-1.40292587
Mest	-3.5311891	2.06437933	Mknk1		1.61237653	Ranbp6		-1.48558738
Ccl2	-4.2690591		Bbs4		1.60533845	Kctd13		-1.59967382
Gm10661		1.99061696	Prr5l		1.6002238			

Supplementary Table 2-2 List of ATF2 dependent genes differentially regulated after IR in S155A/D156A Ku70 expressing MEFs relative to WT Ku70.

Samples from control and IR-treated (8h and 24h) MEFs were subjected to microarray analysis using a GeneChip Mouse Gene 1.0 ST Array (Affymetrics, Santa Clara, CA). Gene Chips were processed at the London Regional Genomics Centre (Robarts Research Institute, London, ON; http://www.lrgc.ca). Shown is the list of genes previously identified as regulated by either ATF3 or ATF2 that were found differentially expressed in Ku70 wild-type and Ku70 S155A/D156A cells following IR exposure. Fold induction/repression of expression with respect to unirradiated controls is shown for each gene and the difference in gene expression between Ku70 wild-type and S155A/D156A mutants is shown in brackets.

	Gene		8 hr WT/MUT (fold difference)	24 hr WT/MUT (fold difference)
ATF2 Dependent	ATF3	Activating transcription factor 3	2.8/1.4 (2)	4.1/2.1 (2)
	Gadd45a	Growth arrest and DNA-damage-inducible protein alpha	5.8/2.5 (2.3)	3.8/2.7 (1.4)
	Pdgfra	Alpha-type platelet-derived growth factor receptor	-2.2/1.4 (3.1)	-1.9/1.1 (2.1)
	Rb1	Retinoblastoma protein	1.4/-1.2 (1.7)	1.3/1.1 (1.2)
	Ccnd1	Cyclin D	-3.4/-1.1 (3.1)	-1.8/-1.1 (1.6)
ATF3 Dependent	Id1	Inhibitors of differentiation family	-2.6/-1.5 (1.7)	-2/-1.6 (1.3)
	Id2		-6.1/-1.8 (3.4)	-5.1/-2 (2.6)
	Id3		-3.1/-1.9 (1.6)	-2.9/-2 (1.5)
	Ddit3	CHOP - CCAAT/enhancer binding protein homologous protein	4.8/2.2 (2.2)	4/2.5 (1.6)

Cell Line	Ku70 positive	Total	%
WT	170	182	**93.4**
S155A/D156A	172	184	**93.5**
D192A/D195R	161	208	**77.4**
S155A/D156A + D192A/D195R	223	249	**89.6**
S155D	153	234	**65.4**
S155A	173	190	**91.1**

Supplementary Table 2-2 Ku70 vWA mutant expression

Immunofluorescence analysis of Ku70 expression in untreated Ku70-/- MEFs expressing either the WT or mutant Ku70 constructs. Cells were marked positive if showing a Ku70 expression level above that seen in Ku70-/- + pMSCV cells (Ku70 positive) and were also stained with DAPI for total cell count numbers (Total). Expression level is calculated as a percent of Ku70 positive cells relative to the total cell count (%).

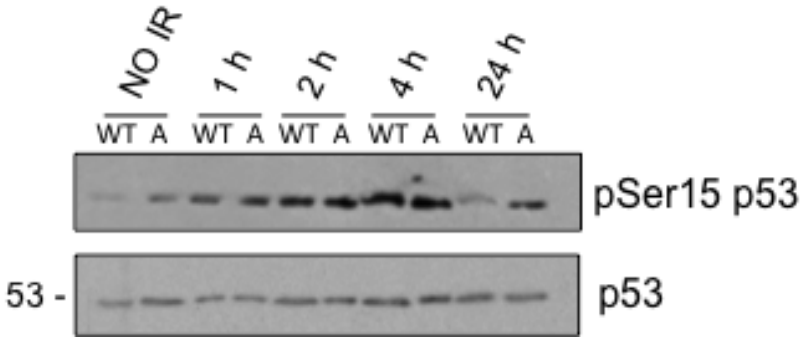

Supplementary Figure 2-3 S155A/D156A Ku70 expression does not inhibit phosphorylation of p53 at serine 15.

Western blot analysis of total p53 and p53 phosphorylated at residue serine 15 (pSer15) in wild type (WT) or S155A/D156A (A) Ku70 expressing MEFs that were either mock treated or exposed to 4 Gy of IR and collected after the indicated time points.

Supplementary Table 2-4 Primers used in this study

(A) Primers used for site-directed mutagenesis of Ku70. (B) Primers used for RT-PCR analyses.

		Mutation	Sequence 5'-3'
A	Plasmid construction	S155AD156A	GTCTGTGCCAACCTCTTTGCTGCTGTCCAATTCAAGATGAG CTCATCTTGAATTGGACAGCAGCAAAGAGGTTGGCACAGAC
		K114AL117A	GCTGGATAATCCAGGTGCAGCACGAATTGCAGAGCTTGACCAG CTGGTCAAGCTCTGCAATTCGTGCTGCACCTGGATTATCCAGC
		K129AD133A	CAGCAGGGACAAGCACGTTTCCAAGCCATGATGGGCCAC GTGGCCCATCATGGCTTGGAAACGTGCTTGTCCCTGCTG
		D192AD195R	CCAAAGCCGGTGCTCTCCGACGTACAGGCATCTTCC GGAAGATGCCTGTACGTCGGAGAGCACCGGCTTTGG
		E145AW148A	CTCACTCAGTGCAGTGCTGGCCGTCTGTGCCAACC GGTTGGCACAGACGGCCAGCACTGCACTGAGTGAG
		155-160A	GCCAACCTCTTTGCTGCTGCCGCAGCCGCGATGAGTCATAAGAGG CCTCTTATGACTCATCGCGGCTGCGGCAGCAGCAAAGAGGTTGGC
		D156A	GTCTGTGCCAACCTCTTTAGTGCTGTCCAATTCAAGATGAG CTCATCTTGAATTGGACAGCACTAAAGAGGTTGGCACAGAC
		S155A	GTCTGTGCCAACCTCTTTGCTGATGTCCAATTCAAGATGAG CTCATCTTGAATTGGACATCAGCAAAGAGGTTGGCACAGAC
B	RT-PCR	Id1	CCTGCAGCTGGAGCTGAACTCG TGGAACACATGCCGCCTCGG
		Id2	GCCCTGGACTCGCATCCCAC CAGATGCCTGCAAGGACAGGATGC
		Id3	CCTCCCGAACGCAGGTGCTG CATGCCCTCAGGCTTCCGGC
		Gadd153/ CHOP	ACAGAGGTCACACGCACATC GGGCACTGACCACTCTGTTT
		Beta-2-microglobulin	CCATTCTCCGGTGGGTGGCG TCGTCAGCATGGCTCGCTCG

Chapter 3

3 Ku70 phosphorylation mediates Aurora B inhibition and activation of the DNA damage response

3.1 Introduction

Double-strand breaks (DSBs) are the most dangerous form of DNA damage, as improperly repaired, they can result in genetic alterations, leading to genomic instability, a hallmark of cancer. Eukaryotic cells employ DNA damage checkpoint surveillance mechanisms to allow the damaged cell time to repair its DNA, or eliminate cells damaged beyond repair through apoptosis and senescence (1, 2).

The DNA damage response (DDR) pathway is initiated by sensor proteins that accumulate in foci at the site of damage (1, 3). This accumulation of DDR proteins activates a phosphorylation cascade as well as modifies surrounding chromatin to allow access of the DNA repair factors. The initial sensors include the Mre11-Rad50-NBS1 (MRN) complex, 53BP1, as well as the serine/threonine (S/T) phosphoinositide-3-kinase (PI3K) family members ATM (Ataxia Telangiectasia Mutated), and ATR (Ataxia Telangiectasia and Rad3-related). The PI3K-like kinases are the main regulators of the DDR and orchestrate many phosphorylation events at the site of DNA damage that promote DNA repair (3). The consequences of DNA damage involve temporary cell cycle arrest to allow for DNA repair and activation of senescence or apoptotic pathways if repair cannot be completed (2, 4). Cellular senescence, although not cytotoxic, is the irreversible exit from the cell cycle, while apoptosis is a form of programmed cell death. Both prevent the proliferation of potentially genomically unstable cells, thereby eliminating the chance of neoplastic transformation (2, 4).

Aurora kinases (Aurora-A, -B and -C) are a family of serine/threonine kinases that play essential roles in cell cycle progression (5). Aurora B coordinates the mitotic process, functioning to regulate many aspects of mitosis including chromosome-microtubule interactions, spindle assembly, sister chromatid and centromeric cohesion and cytokinesis (5). Aurora B's activities, however, are not restricted to mitosis, as it is expressed throughout the cell cycle and there is evidence that it also contributes to G1/S and G2/M checkpoint regulation (6, 7). As a mitotic kinase, Aurora B kinase activity is tightly regulated during cell cycle checkpoints and deregulation of its activity can have devastating consequences. Ectopic expression of both Aurora A and B results in chromosomal abnormalities and cellular transformation, and overexpression of Aurora kinases is observed in a number of different cancers (5, 8-10). Consequently Aurora kinases were identified as possible druggable targets and a number of Aurora kinases inhibitors have been developed for anti-cancer therapy (8, 11). Aurora B inhibitors were shown to prevent cytokinesis and cause cell growth inhibition and cell cycle arrest (12-14). While Aurora B has been implicated in the cellular response to DNA damaging agents (15, 16), a thorough understanding of the regulation of Aurora kinase activity following genotoxic stress is lacking.

DSBs are repaired by one of three pathways: homologous recombination (HR), which occurs primarily in the G2 and M phases, micro-homology mediated end joining (MMEJ), a backup pathway, and non-homologous end joining (NHEJ), the predominant repair pathway in higher eukaryotes, which occurs in the G1 and S phases (17, 18). Ku has a well-characterized role as the DNA binding component of NHEJ (19). Ku is a heterodimer composed of subunits Ku70 and Ku80 (70 and 86 kDa, respectively) which

share structural similarity and are conserved from bacteria to man. Each subunit contains an N terminal α/ß von Willebrand A (vWA) like domain, central ß-barrel domain and a divergent C terminal helical region (20). The Ku dimer forms an asymmetrical ring lined with positively charged and hydrophobic residues that can accommodate the double-stranded DNA backbone independent of sequence (21). Following the introduction of a DSB, Ku rapidly binds the broken end and forms a complex with the PI3K-like kinase DNA-PKcs to recruit other NHEJ repair factors and facilitate repair of the break (22). Ku also has important functions in telomere maintenance and protection, and Ku-deficiency leads to telomere defects (23, 24).

There is increasing evidence that the Ku N-terminal regions play important roles in NHEJ as well as in telomere maintenance and apoptotic signaling. Ku70 residues D192/D195 in Helix 5 of the vWA domain are essential for NHEJ and cell survival following DNA damage (25-27). Other lysine residues nearby, K160 and K164, have been shown to confer lyase activity and are involved in DNA processing during NHEJ (28, 29). The Ku70 and Ku80 N-terminal domains have structural similarities with the von Willebrand A (vWA) domain, an ancient, evolutionarily conserved domain that is found in several extracellular and intracellular proteins, where it mediates protein-protein interactions (30). Indeed Ku forms numerous protein interactions during NHEJ and other processes, and some of these map to the vWA domain (19). Examples include the NHEJ factor Aprataxin and PNKP-like Factor (APLF), which binds to the Ku80 vWA domain, and the Telomere Repeat Binding Factor 2 (TRF2), which interacts with the Ku70 vWA domain (26, 31).

Our previous investigation focused on identifying key residues in the Ku70 vWA

domain involved in the cellular response to DNA damage (25). We demonstrated that mutation of Ku70 serine 155 to alanine increased survival and decreased apoptotic activation following DNA damage, relative to wild-type (WT) Ku70 despite having no impact on DNA repair efficiency. Furthermore, this mutation prevented the activation of a DDR, dependent upon Activating Transcription Factor 2 (ATF2). Since this residue was a serine, a common site for phosphorylation in the DDR, we hypothesized that this mutation was preventing a phosphorylation event. Indeed, a phosphomimetic substitution of S155 to aspartic acid (S155D) constitutively activated ATF2 and conferred a severe hypersensitivity to IR.

In the present study, we demonstrate that Ku70 S155 is indeed phosphorylated after IR, and show that constitutive expression of the phosphomimetic mutant Ku70 S155D induces a DDR marked by a constitutive activation of ATM and cell cycle arrest at both the G1/S and G2/M checkpoints. Additionally, we show that Ku70 S155D interacts with the Aurora B kinase and mediates the inhibition of its kinase activity. The interaction of WT Ku70 and Aurora B was detected following IR treatment, but not in absence of DNA damage. We therefore propose that Ku70 is phosphorylated after IR at serine 155 and this mediates the interaction and inhibition of Aurora B, resulting in activation of the DDR and cell cycle arrest.

3.2 Materials and methods

3.2.1 Plasmid Expression Constructs

Ku70 WT, S155D and S155A pMSCVpuro constructs were previously described (25). Ku70 WT, S155D vWA-FLAG pMSCVpuro constructs were produced by

subcloning the XhoI and EcoRV fragment (aa 1-250) of full length Ku70 into the pMSCVpuro vector, and then inserting a FLAG tag by oligonucleotide annealing (Sigma-Aldrich, Oakville, ON).

3.2.2 Cell Culture and Treatments

Immortalized Ku70$^{-/-}$ MEFs were obtained from S. Matsuyama (Case Western, Cleveland). IMR-90 cells were obtained from ATCC. All cells were cultured in high glucose Dulbecco's modified Eagle's medium (DMEM) supplemented with 10% fetal bovine serum (FBS) at 37°C in 5% CO2. Ku70$^{-/-}$ MEFs stably re-expressing Ku70 WT and mutants were generated as previously described (25). To assess proliferation rates, the Ku expressing MEFs were seeded in triplicate in 6-well dishes. At each time point cells were trypsinized, counted using a hemocytometer, and the mean number of cells was determined. Percent growth was obtained by dividing the number of cells at each time point by the number of cells at day 1. For irradiation experiments, cells were plated the night before at 50-70% confluency. Irradiations were performed with a Faxitron RX-650 at a dose rate of 1.42 Gy/min. For ATM inhibitor treatments, MEFs were incubated with 10 μM of KU-55933 (Selleck Chemicals, Houston, TX) for 1 hour prior to 4 Gy of irradiation. For Aurora B inhibitor treatments, MEFs were incubated with 20 μM of AZD-1152 (Sigma-Aldrich) for 48 hours.

3.2.3 Extracts, Immunoprecipitation, and Western blot analyses

Nuclear Extracts were prepared as described previously (70). For co-immunopreciptation experiments, extracts were adjusted to 0.15% NP-40 and 100 mM KCl, and incubated overnight at 4°C with Ku70 antibody (N3H10, Santa Cruz, Santa

Cruz, CA). Immunoprecipitates were isolated with Pierce Protein G magnetic beads (ThermoFisher Scientific, Rockford, IL). For Western blot analysis, extracts were resolved by SDS-PAGE, transferred onto a PVDF (Polyvinylidene fluoride) membrane and hybridized with the following antibodies: β-actin (I-19, Santa Cruz), Ku70 (N3H10, Santa Cruz), p21 (C-19, Santa Cruz), phospho-serine 1981 ATM (Pierce, ThermoFisher Scientific), ATM (Pierce, ThermoFisher Scientific), phospho-serine 10 Histone H3 (Cell Signaling, Danvers, MA), Aurora B (H-75, Santa Cruz), FLAG (Sigma-Aldrich). The blots were developed using the Clarity Western ECL substrate (Bio-rad, Hercules, CA) and imaged on the Molecular Imager® ChemiDocTM XRS system (Bio-Rad). Quantifications were performed using Image Lab software (Bio-Rad).

3.2.4 Aurora B Kinase Assay

Immunoprecipitation was performed as described above with the Aurora B antibody (H-75, Santa Cruz). Immunoprecipitates were resuspended in kinase buffer (20 mM Tris-HCl, 20 mM KCl, 20 mM MgCl2, 0.4 μM ATP, 0.4 mM DTT) and incubated with 1 μg of purified Histone H3.1 (Cell Signaling) for 1 hour at 37°C. Phosphorylation was detected by western blot with a phospho-H3S10 antibody (Cell Signaling).

3.2.5 β-Galactosidase Senescence Assay

IMR-90 Cells were plated on 35mm dishes or on glass coverslips in 24-well dishes. Cells were washed three times with Phosphate Buffer Saline (PBS) and fixed with 4% paraformaldehyde for 15min at 4°C. The staining solution (40mM citric acid/Na phosphate buffer, 5mM K4[Fe(CN)6] 3H2O, 5mM K3[Fe(CN)6], 150mM NaCl, 2mM MgCl2, 1mg ml-1 X-Gal (Bioshop Canada Inc, Burlington, ON) in DMSO, pH 6.0) was added to each dish and incubated for 12-16h at 37°C. Cells were viewed by bright field

microscopy. Pictures were taken and blue cells cells were counted as a percentage of total cells.

3.2.6 Reverse Transcriptase PCR (RT-qPCR)

Total RNA was isolated using the Qiagen RNeasy RNA extraction kit. RNA (2 μg) was reverse transcribed with the Superscript II cDNA kit (Invitrogen, ThermoFisher Scientific). Quantitative PCR was performed using Bio-Rad MyiQ single-color real-time PCR detection and the Bio-Rad IQ SYBR green mix. The relative quantification of specific gene expression was determined by the ΔΔCT method, with the target gene threshold cycle (CT) values normalized to that of the beta-2-microglobulin control. Primers are listed in Figure E4.

3.2.7 Cell Cycle Analysis by Fluorescence Activated Cell Sorter (FACS)

Cells were incubated with 10 μM EdU for 1 hour then collected by trypsinization at a final concentration of 1×10^7 cells/ml. The samples were processed using the EdU Click-It Alexa 647 Flow cytometry kit (Invitrogen) then stained in 0.1% Triton X-100 (Sigma-Aldrich), 0.2 mg/mL DNase-RNase A (Sigma-Aldrich), and 20 ug/mL of propidium iodide (Sigma-Aldrich). Cell cycle FACS was performed on a Calibur II (BD Biosciences, Mississauga, ON) and 50,000 gated events were measured per sample. Cell cycle modeling and statistics were performed on FlowJo software. All procedures were performed at the London Regional Flow Cytometry Facility.

3.2.8 Immunofluorescence

Cells were seeded at 60-80% confluence on 10 mm glass coverslips, washed in cold PBS and fixed in 3% paraformaldehyde. Cells were permeabilized in 0.5% Triton-X and blocked in 5% FBS, followed by incubation with primary antibodies: phospho-serine 139 H2AX antibody (Abcam, Cambridge, UK), phospho-serine 1981 ATM (Pierce), Histone H3 phospho-serine 10 (Cell Signaling), 53BP1 (Pierce) and then with AlexaFluor 488/555/647 secondary antibodies (Invitrogen). All coverslips were mounted onto glass slides using ProLong Gold containing DAPI (Invitrogen). Cell pictures were taken with an Olympus BX51 microscope at 40x magnification using the Image-Pro Plus software (Media Cybernetics, Inc., Bethesda, MD). For γ-H2AX, 53BP1 and phospho-H3S10 analyses, cells were scored for the presence of foci, with DAPI nuclei staining used for total cell count. Foci-containing cells were quantified as a percentage of total cells, and approximately 500 cells were counted for each experimental condition per experiment.

The *in situ* proximity ligation assay (PLA) was performed with the Duolink (Olink Biosciences, Uppsala, Sweden) kit as per manufacturer instructions with minor modifications. MEFs were plated at 50-70% confluency onto 10 mM glass coverslips containing a hydrophobic wax boundary. Coverslips were fixed and permeabilized as described above and incubated overnight with Ku70 (Santa Cruz) and Aurora B (Santa Cruz) primary antibodies. Immunofluorescence images were obtained as described above. DAPI nuclei staining was used for total cell count and PLA signal was quantified by pixel density measurement in Image J software. The pixel density of the PLA was normalized to total cell count to obtain a mean PLA signal per cell. These measurements

were then normalized to the background signal obtained in Ku70$^{-/-}$ MEFs control samples.

3.2.9 Mass spectrometry and Protein Identification

For phosphorylation identification, 70% confluent MEFs were mock-treated or treated with 40 Gy of IR and incubated for 30 minutes. 10 mg of nuclear extracts were adjusted to 100 mM KCl, 2% NP-40 and immunoprecipitated as described above with a Ku70 antibody (Santa Cruz). Immunoprecipitates were boiled in 1X SDS loading buffer (2% SDS, 2mM DTT, 5% Glycerol, 40 mM Tris-HCl, 0.01% bromophenol blue), run on an SDS-PAGE gel and stained with Coomasssie Blue G-250 (Protea Biosciences, Morgantown, WV).

For peptide pull-down and protein identification, 4 mg of untreated or 10 Gy-treated MEF extracts were incubated for 2 hours with one of the following N-terminal biotin-conjugated peptides (Genscript, Piscataway, NJ): biotin-EVLWVCANLFADVQFKMSH, biotin-EVLWVCANLFDDVQFKMSH. 10 µg of peptide was pre-coupled to 40 µl of Steptavidin beads (Invitrogen) for 30 min at room temperature. Pre-coupled beads and extracts were incubated for 2 hours at 4°C. Beads were washed in (Tris buffer saline, 0.1% Tween20), boiled in 1X SDS loading buffer and run on SDS-PAGE gel. Gels were stained with the Silver Stain Plus Kit (Bio-Rad) as per manufacturer instruction.

In-gel digestion was performed using a MassPREP automated digester station (PerkinElmer, Waltham, MA). Gel pieces were Coomassie de-stained using 50 mM ammonium bicarbonate and 50% acetonitrile or silver de-stained using a 50 mM sodium

thiosulphate 5 hydrate and 15 mM potassium ferricyanide solution, which was followed by protein reduction using 10 mM dithiotreitol (DTT), alkylation using 55 mM iodoacetamide (IAA), and tryptic or chymotryptic digestion. Peptides were extracted using a solution of 1% formic acid and 2% acetonitrile and lyophilized. Prior to mass spectrometric analysis, dried peptide samples were re-dissolved in a 10% acetonitrile and 0.1% TFA (trifluoroacetic acid) solution.

Mass Spectrometry data were obtained using an AB Sciex 5800 TOF/TOF System, MALDI TOF TOF (Framingham, MA, USA). Data acquisition and data processing were respectively done using a TOF TOF Series Explorer and Data Explorer (AB Sciex). The instrument is equipped with a 349 nm OptiBeam On-Axis laser. The laser pulse rate is 400 Hz. Reflectron positive mode was used. Reflectron mode was externally calibrated at 50 ppm mass tolerance and internally at 10 ppm. Each mass spectrum was collected as a sum of 400 shots. MALDI matrix, α–cyano–4–hydroxycinnamic acid (CHCA), was prepared as 5 mg/mL in 6mM ammonium phosphate monobasic, 50% acetonitrile, 0.1 % trifluoroacetic acid and mixed with the sample at 1:1 ratio (v/v). All procedures were performed at the London Regional Proteomics Centre (LRPC).

3.2.10 Statistical Analyses

Differences between multiple groups was determined an analysis of variance (ANOVA) and differences between two groups was determined by an unpaired two tail t-test. Results were considered significant when $P < 0.05$.

3.3 Results

3.3.1 Ku70 S155 is phosphorylated in response to DNA damage

We previously established a retroviral system using a murine stem cell virus construct (pMSCV) to stably re-express WT Ku70 and Ku70 mutants in immortalized Ku70-deficient mouse embryonic fibroblasts ($Ku70^{-/-}$ MEFs). Using this system, we determined that MEFs expressing Ku70 S155 amino acid substitutions exhibited altered survival following IR treatment (25). A mutant Ku bearing a Ku70 S155 substitution to alanine (Ku70 S155A) enhanced survival following IR treatment, causing a DNA damage signaling defect and compromising the activation of apoptosis in response to DNA damage. In contrast, substitution to a phosphomimetic residue (S155D) conferred hypersensitivity to IR treatment. These analyses suggested that S155 is a phosphorylation site that is targeted for phosphorylation in response to DNA damage. To determine whether this site is phosphorylated following DNA damage, we conducted Mass Spectrometry (MS) analyses on Ku70 immunoprecipitated from nuclear extracts obtained from WT Ku70-expressing MEFs either untreated, or 30 minutes following a 40 Gy IR treatment. Chymotryptic digestion of immunoprecipitated Ku peptides revealed a peak corresponding to a peptide doubly phosphorylated at positions S155 and S162 in the irradiated sample, but not in the unirradiated control samples (Supplementary Figure 3-1B). To confirm these results, we repeated the analysis with extracts obtained from Ku70 S155A-expressing MEFs. In this case, only a mono-phosphorylated peptide was observed, consistent with the mutation preventing phosphorylation at S155 and being solely phosphorylated at S162 (Supplementary Figure 3-1C). Thus, we repeated the procedure with MEFs expressing a Ku70 mutant bearing an alanine substitution at

position S162. Again, only one peak corresponding to the mono-phosphorylated peptide was observed, suggesting that this peptide was now only phosphorylated at the S155 position (Supplementary Figure 3-1D). Neither control samples obtained from Ku70 S155A or S162A expressing MEFs contained a peak corresponding to a peptide with phosphorylated S155. Overall these results suggest that Ku70 is phosphorylated at S155 after IR.

3.3.2 Ku70 S155D induces cell cycle arrest

While the expression of the Ku70 S155D mutant in $Ku70^{-/-}$ MEFs led to a strong hypersensitivity to IR (25), we also noted that Ku70 S155D-expressing MEFs proliferated abnormally under standard culturing conditions. Growth rate analysis in the absence of any DNA damaging agent showed that expression of Ku70 S155D conferred a marked defect in proliferation, as these cells exhibited a 5.7-fold decrease in percent growth compared to $Ku70^{-/-}$ MEFs re-expressing Ku WT by the fifth day of culture, and were even 3.6-fold slower than $Ku70^{-/-}$ MEFs, which have been previously reported to have proliferation defects (32) (Figure 3-1A). In contrast, the Ku70 S155A expressing MEFs proliferated faster than the WT counterparts, achieving a 1.8-fold increase over Ku70 WT MEFs by the fifth day of culture. In order to further analyze this proliferation defect, we compared the cell cycle profile of Ku70 WT, S155D, S155A cells and $Ku70^{-/-}$ MEFs (Figure 3-1B). Fluorescence activated cell sorting (FACS) analysis of Ku70 S155D-expressing MEFs showed that 46% of cells were in G1 phase, higher than the approximately 30% seen in the other three cell lines. Similarly, 27% of Ku70 S155D-expressing MEFs were in the G2 phase, higher than the approximately 8% seen in the WT, S155A and $Ku70^{-/-}$ cells (Figure 3-1B). Altogether this indicates that the Ku70

Figure 3-1 Expression of Ku70 S155D triggers cell cycle arrest

(A) Ku70 S155 mutants confer altered cell proliferation. Growth rates of Ku70-/- MEFs expressing Ku70 WT, S155A, S155D or empty vector were assessed for 5 days. Data represents percent growth relative to Day 1 of three independent experiments with error bars indicating SEM (*P<0.05, all cell lines compared to WT). (B) Ku70 S155D cells arrest in G1 and G2. FACS analysis of DNA content and EdU incorporation in asynchronous Ku70-/- MEFs expressing Ku70 WT, S155A, S155D or empty vector (Ku70-/-) stained with propidium iodide and Anti-Edu Alexa 647. Average percentage was determined by FlowJo cell cycle analysis in three separate experiments with error bars indicating SEM (*P<0.01 S155D compared to all other cell lines).

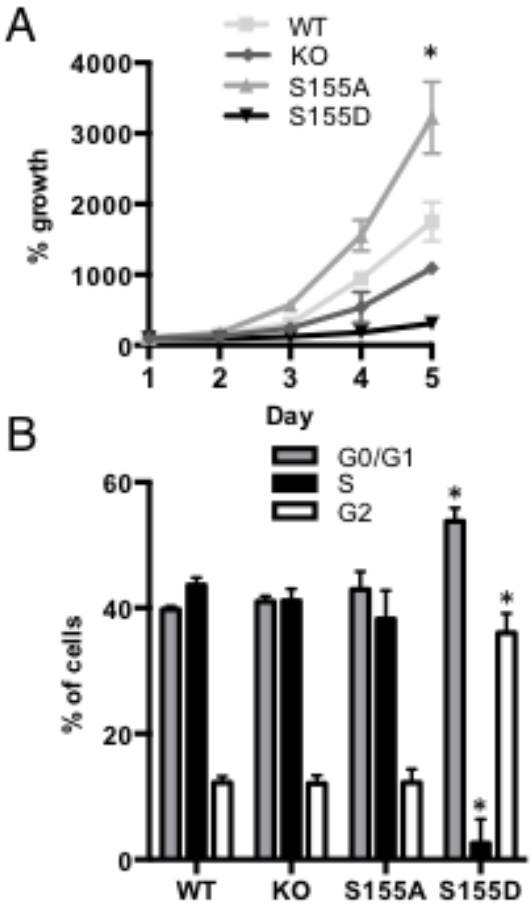
A
WT
KO
S155A
S155D
*
4000
3000
2000
1000
0
% growth
1
2
3
4
5
Day
B
G0/G1
S
G2
60
40
20
0
% of cells
*
*
*
WT
KO
S155A
S155D

serine 155 residue regulates cellular proliferation and the expression of the phosphomimetic S155D mutation induces cell cycle arrest at both the G1/S and G2/M checkpoints.

In order to analyze the global transcriptional changes that resulted in cell cycle arrest, an Affymetrix GeneChip was performed using RNA from Ku70$^{-/-}$MEFs expressing Ku70 WT and S155D. Several genes were either up- or downregulated in the Ku70 S155D-expressing MEFs relative to WT control (Supplementary Table 3-1), and subsequently, some were validated by RT-qPCR (Figure 3-2A). Cyclin D and CDK6, two proteins that form a complex to promote the progression through the G1/S checkpoint and Cyclin B, whose expression increases during the G2/M transition (33), were found 5.1-, 13.7-, and 7.2-fold downregulated, respectively, in Ku70 S155D-expressing MEFs. Similarly, expression of Protein phosphatase 1 (PP1), a serine/threonine phosphatase, involved in the dephosphorylation of several targets during the DDR to resolve DNA damage checkpoints (34), was 28.8-fold downregulated in Ku70 S155D-expressing MEFs. Finally, the X-linked inhibitor of apoptosis-associated factor 1 (XAF-1), which regulates apoptosis and G2/M arrest (35, 36), was upregulated by 5.1-fold in Ku70 S155D MEFs. We also assessed the protein levels of p21, an inhibitor of cyclin D and B-CDK complexes which is upregulated in a p53 dependent manner following DNA damage and activates the G1 and G2 cell cycle checkpoints (37, 38). Western blot analysis showed that while Ku70 WT MEFs required IR treatment to induce expression of p21, Ku70 S155D cells displayed a marked upregulation of p21 in the absence of any treatment (Figure 3-2B). Conversely, the Ku70 S155A MEFs failed to upregulate p21 levels, even after IR treatment (Figure 3-2C). Overall, consistent with the observation

Figure 3-2 Ku70 S155D-expressing MEFs display altered expression of cell cycle-related factors.

(A) RT-PCR analysis of Cyclin D, Cyclin B, CDK6, PP1 and XAF-1 gene expression. RNA samples from WT or S155D Ku70-expressing MEFs were analyzed by RT-qPCR using primer sets specific for the indicated genes. The fold change in gene expression of Ku70 S155D relative to Ku70 WT MEFs is shown, with error bars indicating SEM (**P<0.01, *P<0.05). (B) Comparison of p21 expression in Ku70 WT and mutant MEFs. Representative western blot analysis of p21 in Ku70 WT and S155D expressing MEFs without IR (above) and p21 induction at the time points indicated after 10 Gy of IR in Ku70 WT and S155A MEFs (below). Similar amount of extracts were loaded on both gels (30 μg). Due to the strong expression of p21 in the Ku70 S155D MEFs, the western blot on the left required only a 30-second exposure, compared to a 10-minute exposure for the western blot on the right required to obtain a similar intensity of p21 signal in response to DNA damage. Exposure time for the actin signal is similar for both western blots.

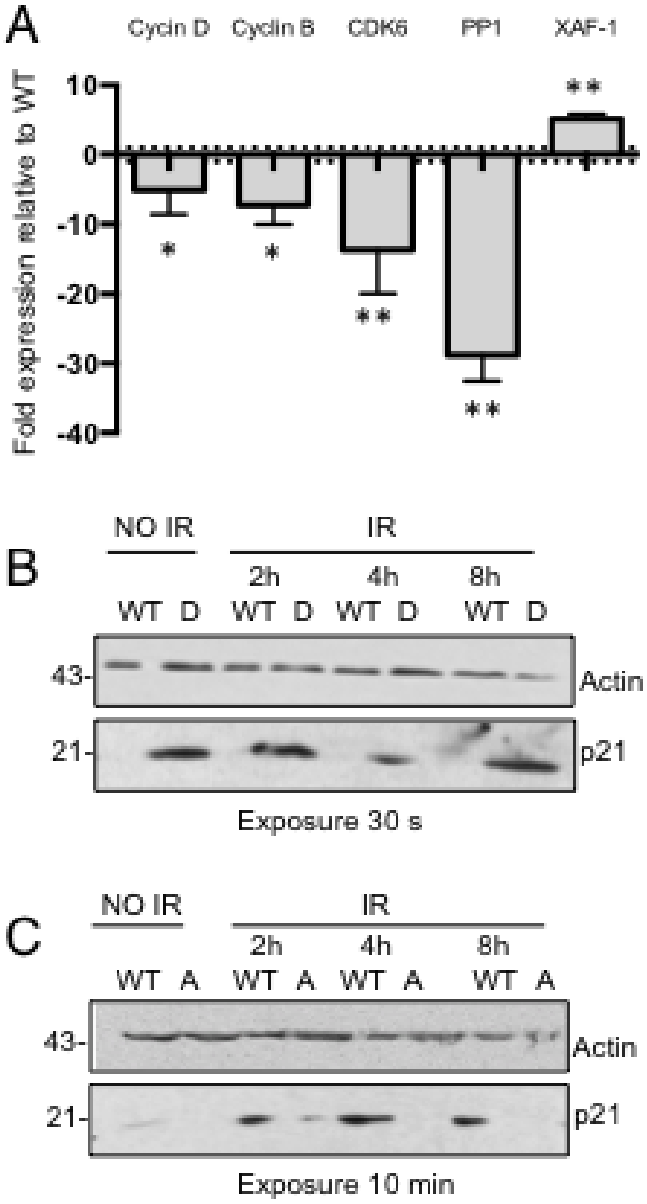
A
Cyclin D
Cyclin B
CDK6
PP1
XAF-1
Fold expression relative to WT
10
0
-10
-20
-30
-40
*
*
**
**
**
B
NO IR
IR
2h
4h
8h
WT D WT D WT D WT D
43-
Actin
21-
p21
Exposure 30 s
C
NO IR
IR
2h
4h
8h
WT A WT A WT A WT A
43-
Actin
21-
p21
Exposure 10 min

that the expression of Ku70 S155D results in the arrest of cells in the G1 and G2 phases, this mutant alters the expression of cyclins known to regulate the progression through both the G1/S and G2/M checkpoints, and markedly upregulates the cell cycle inhibitor p21.

3.3.3 Ku70 S155D induces a DNA damage response

We previously determined that an alanine substitution at Ku70 S155 decreased activation of apoptosis via an ATF2-dependent DDR pathway following IR treatment (25). The altered proliferation of Ku70 S155 mutant-expressing MEFs however, was occurring in the absence of any DNA damaging agent, and it was not clear whether this phenotype was related to the DDR defect observed previously, or if it was a direct effect of Ku on the cell cycle. To test this, we examined the presence of active DNA damage response markers following the expression of Ku70 S155 mutants. Surprisingly, immunofluorescence (IF) analysis of Ku70 S155D-expressing MEFs showed significantly increased ϒ-H2AX and 53BP1 foci formation compared to both Ku70 WT and S155A-expressing MEFs, in the absence of any DNA damage treatment (Figure 3-3A,B). Furthermore, western blot analysis for activated ATM, marked by an auto-phosphorylation at serine 1981, showed increased levels (relative to WT) in untreated S155D MEFs, while S155A MEFs had very little activation of ATM after even IR (Figure 3-3C). Interestingly, pre-treatment of cells with the ATM inhibitor KU-55933 prevented activation of ATM after IR in Ku70 WT and S155A MEFs, but had no impact on ATM activation in Ku70 S155D MEFs, suggesting that in these cells, ATM is constitutively phosphorylated at least to the same levels as those reached in response to 10 Gy of IR (Figure 3-3C) (39). Overall, these observations suggest that expression of the

Figure 3-3 Ku70 S155D expression induces a DNA damage response in the absence of DNA damage.

(A) Cells were analyzed by immunofluorescence with a ϒ-H2AX antibody with representative pictures shown (left). Foci-containing cells were quantified and shown as an average of three experiments with error bars indicating SEM (right) *(**P*<0.01, **P*<0.05*)*. Scale bars, 10 μm. Cells were scored positive when containing more than 5 foci. (B) Same procedure as in A, but the analysis was performed with a 53BP1 antibody. (C) Western blot analysis of p-S1981 ATM in Ku70 S155D, WT and S155A expressing MEFs. Samples were either left untreated (control), collected 30 minutes following 10 Gy of IR (IR), or collected 30 minutes after 10 Gy of IR following a 1 hour incubation with 10 μM ATM inhibitor (ATMi). Quantification of four separate experiments is shown (below) with error bars indicating SEM.

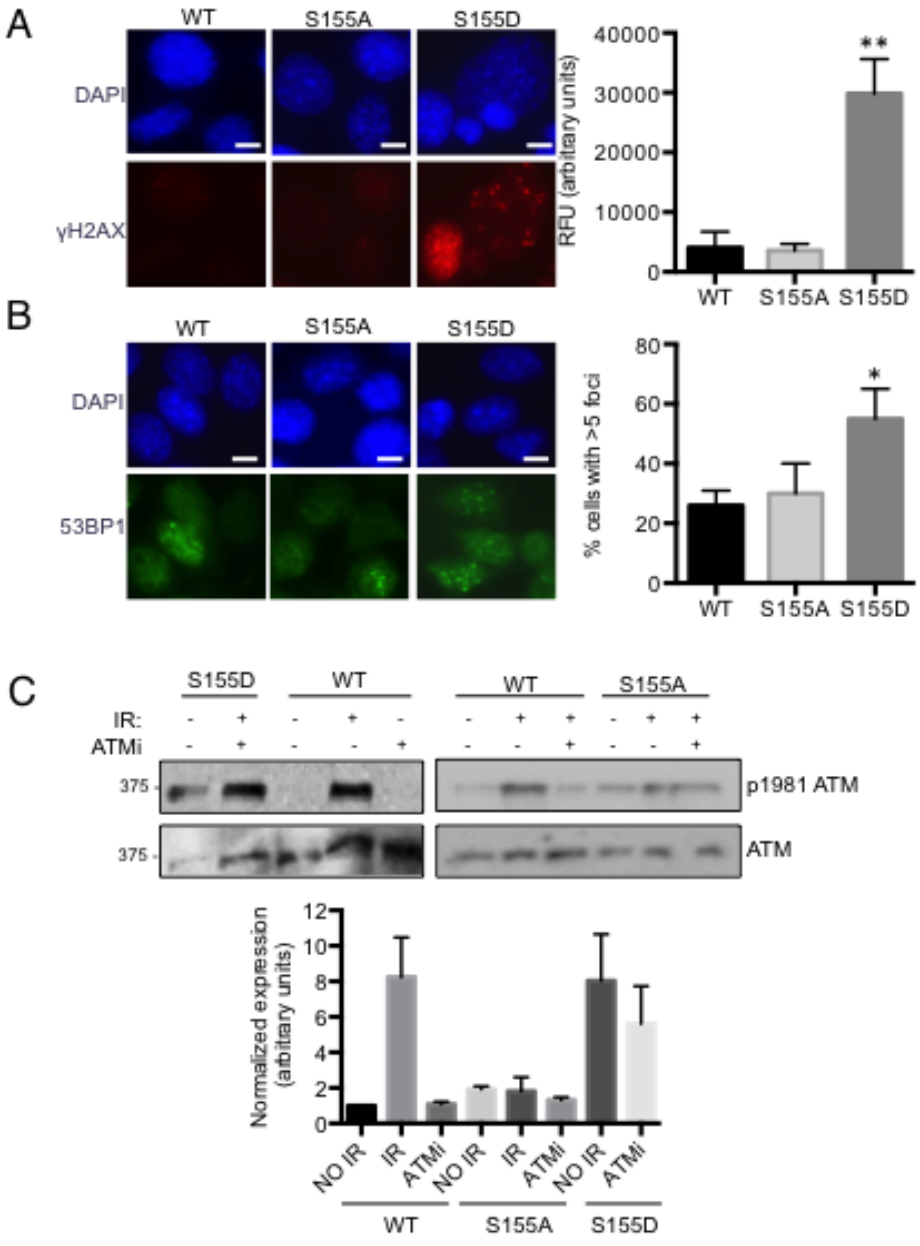
A
WT
S155A
S155D
DAPI
γH2AX
RFU (arbitary units)
40000
30000
20000
10000
0
**
WT
S155A
S155D
B
WT
S155A
S155D
DAPI
53BP1
% cells with >5 foci
80
60
40
20
0
*
WT
S155A
S155D
C
S155D
WT
WT
S155A
IR:
ATMi
375
375
p1981 ATM
ATM
Normalized expression (arbitary units)
12
10
8
6
4
2
0
NO IR
IR
ATMi
NO IR
IR
ATMi
NO IR
ATMi
WT
S155A
S155D

phosphomimetic Ku70 S155D constitutively activates an ATM-dependent DNA damage response pathway, in the absence of ectopically-induced DNA damage.

3.3.4 Ku70 S155D vWA domain is sufficient to induce cell cycle arrest

Ku is well characterized as a DNA binding protein functioning in both DNA repair via the NHEJ pathway and the protection of telomere ends (19). Although it appeared as though the Ku70 S155D mutation induced a constitutive signal for the DDR, the signaling mechanism was unclear. In order to test whether the DNA binding activity of Ku was needed to produce the DDR induced by Ku70 S155D, we generated truncated Ku70 Flag-tagged constructs containing only the vWA domain, either with the WT sequence or with the S155D substitution. The central ring domain is required for Ku70/Ku80 heterodimerization and DNA binding activity, so a truncated Ku70 construct containing only the vWA domain cannot fulfill either function (20). Similar to the full-length (FL) Ku70 S155D construct, the expression of the S155D vWA domain in $Ku70^{-/-}$ MEFs significantly decreased proliferation, as by the fifth day the Ku70 S155D vWA MEFs had a 16.4-fold lower proliferation rate as compared to the $Ku70^{-/-}$ MEFs expressing Ku70 WT vWA domain control (Figure 3-4A). Also, consistent with what was observed previously with Ku70 S155D, western blot analysis demonstrated a marked upregulation of p21 levels in Ku70 S155D vWA MEFs compared to Ku70 WT vWA control cells (Figure 3-4C). This suggests that recruitment of the Ku70 S155D mutant to DNA is not required to induce a DDR. These results were obtained in a Ku70 null background, so we sought to determine whether the Ku70 S155D mutation would have a dominant effect in a cell line that had normal Ku70 expression. Expression of the

Figure 3-4 N-terminal Ku70 S155D domain is sufficient to induce a DDR and cell cycle arrest.

(A) Growth rates of $Ku70^{-/-}$ MEFs expressing Ku70 WT or S155D vWA domain constructs were assessed for 5 days. Data represent percent growth relative to Day 1 of three independent experiments with error bars indicating SEM (*P<0.05 compared to WT). (B) Growth rates of IMR-90 cells were assayed as described above, for 10 days. (C) Western blot analysis of p21 levels in IMR90 and $Ku70^{-/-}$ MEFs expressing either Ku70 WT or S155D vWA domain. (D) IMR-90 cells expressing Ku70 WT or S155D vWA domain truncated constructs were stained with a solution containing X-gal (5-bromo-4-chloro-3-indolyl-β-D-galactopyranoside). Senescence induced over expression of the β-galactosidase enzyme cleaves X-gal to produce a blue dye observed in bright field microscopy. The percentage of cells stained blue were quantified and shown as an average of three experiments with error bars representing SEM (*P<0.05). Scale bars, 10 μm.

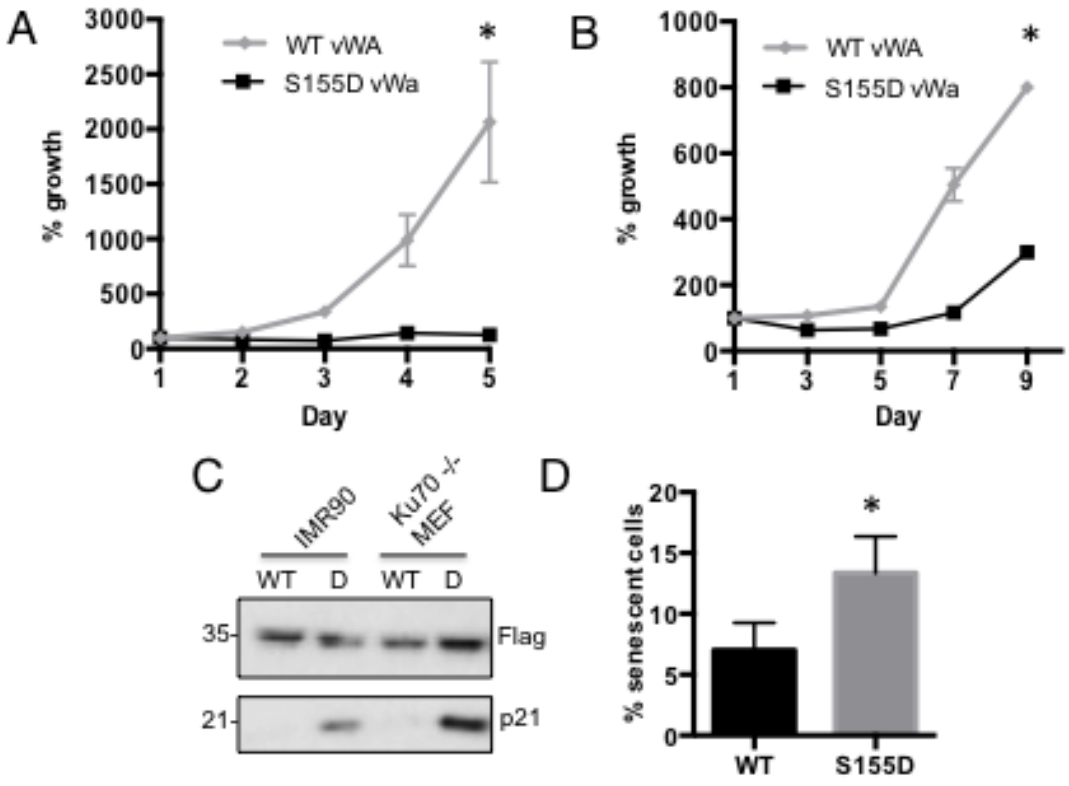
A
3000
2500
2000
1500
1000
500
0
% growth
WT vWA
S155D vWa
*
1
2
3
4
5
Day
B
1000
800
600
400
200
0
% growth
WT vWA
S155D vWa
*
1
3
5
7
9
Day
C
IMR90
Ku70 -/-
MEF
WT
D
WT
D
35
Flag
21
p21
D
20
15
10
5
0
% senescent cells
*
WT
S155D

retroviral Ku70 vWA-only constructs in the human cell line IMR-90 produced similar results, with the Ku70 S155D vWA domain significantly reducing proliferation by 3-fold compared to the Ku70 WT vWA domain at the tenth day of culture (Figure 3-4B). Again, a marked upregulation of the p21 protein levels in the S155D vWA-expressing IMR-90 cells was observed compared to WT vWA as measured by western blot (Figure 3-4C). Additionally, in this cell line, a senescence phenotype was observed (4), as a significantly increased level of beta-galactosidase activity was found in S155D expressing cells relative to WT (Figure 3-4D). Overall, the Ku70 S155D vWA domain does not require heterodimerization with Ku80 nor end-binding capabilities to induce cell cycle arrest and this phenotype is dominant to WT Ku.

3.3.5 Ku70 S155D interacts with and inhibits Aurora B

Given that the Ku70 S155D vWA domain lacking both its DNA binding domain and the ability to heterodimerize with Ku80 induced cell cycle arrest, we hypothesized that this domain was acting by binding to another factor(s) and either constitutively activating or inhibiting its activity. A general screen for interacting factors was performed using biotin-conjugated peptides of the loop region surrounding S155 (aa 145 to 163) and comparing factors that bound to peptides containing either an alanine or aspartic phosphomimetic mutant at the serine 155 position. S155A or S155D peptides were incubated with MEF nuclear extracts from cells that were either untreated or subjected to 10 Gy of IR. Interacting factors were pulled down with streptavidin beads and identified by mass spectrometry.

MS analysis identified Aurora B as a factor interacting with the S155D peptide in control and IR-treated extracts (Supplementary Figure 3-2). The interaction of Aurora

B with the S155D peptide was validated using pull-down of WT MEF extracts with S155 A/D peptides followed by western blot analysis (Figure 3-5A). We then verified the interaction between Aurora B and full length Ku70 S155D. Ku70 was immunoprecipitated from nuclear extracts from $Ku70^{-/-}$ MEFs (used as a control), and $Ku70^{-/-}$ MEFs re-expressing WT Ku70 or Ku70 S155D. Endogenous Aurora B was efficiently co-immunoprecipitated with Ku70 S155D, indicating that Aurora B interacts with the phosphomimetic form of Ku70 (Figure 3-5B). However, very little Aurora B was observed in the WT Ku70 immunoprecipitates, suggesting that phosphorylation of S155 is needed for interaction between the two proteins.

Aurora B, a member of the serine/threonine family of Aurora kinases, promotes the progression of the cell cycle through the G1/S, G2/M and mitotic checkpoints by the phosphorylation of several targets (5). Interestingly, studies examining the potential for Aurora B inhibitors in cancer therapy showed that chemical inhibition of Aurora B results in cell cycle arrest and the activation of several DDR markers, notably ϒ-H2AX and 53BP1, ATM S1981 phosphorylation and upregulation of p21 (15, 16). Thus, the effects of Ku70 S155D expression appeared to be similar to those reported in response to Aurora B inhibition, suggesting the possibility that interaction between Ku70 S155D and Aurora B could inhibit Aurora B.

First we investigated whether inhibition of Aurora B in Ku70 WT MEFs produced the same cellular response as that observed in MEFs expressing the Ku70 S155D mutant. Treatment of WT MEFs with 20 μM of the Aurora B selective inhibitor AZD-1152 (40) for 48 hours triggered a marked upregulation of the cell cycle inhibitor p21 relative to control (vehicle-treated) samples as measured by western blot analysis (Figure 3-6A).

Figure 3-5 Ku70 S155D interacts with Aurora B.

(A) Aurora B interacts with a Ku70 S155D peptide. Biotin-conjugated peptides of the 15 amino acids surrounding Ku70 S155 containing either a S155A or S155D substitution were used in a biotin-streptavidin pull-down with untreated WT Ku70 MEF extracts. Shown is a western blot analysis of Aurora B present in the samples pulled-down with the indicated peptides. (B) Interaction of Aurora B with Ku70 S155D. Extracts from $Ku70^{-/-}$ MEFs stably expressing Ku70 WT, Ku70 S155D or empty vector were immunoprecipitated with a Ku70 antibody. The immunoprecipitates were analyzed by western blot with antibodies against Ku70 and Aurora B.

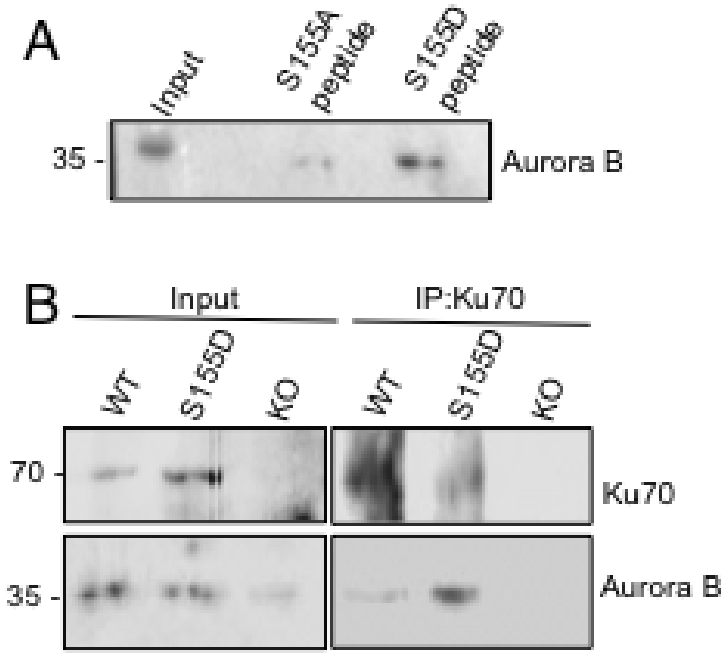
A
Input
S155A peptide
S155D peptide
35 -
Aurora B
B
Input
IP:Ku70
WT
S155D
KO
WT
S155D
KO
70 -
Ku70
35 -
Aurora B

Figure 3-6 Aurora B chemical inhibition induces a DNA damage response.

(A) Western blot analysis of p21 and p-S1981 ATM levels in WT Ku70 MEFs treated for 48h with either 20 μM of the Aurora B inhibitor AZD-1152 (+) or the DMSO vehicle control (-). (B) RT-PCR analysis of Cyclin B, CDK6, Cyclin D and XAF-1 in WT Ku70 MEFs treated with Aurora B inhibitor as described in A, normalized to the DMSO vehicle control (*P<0.05). (C) Immunofluorescence analysis of γ-H2AX and 53BP1 foci formation in MEFs treated with either AZD-1152 or the DMSO vehicle control as described above. Cells were scored positive when containing more than 5 foci and the results shown are averaged from three experiments with error bars indicating SEM (*P<0.05). Scale bars, 10 μm.

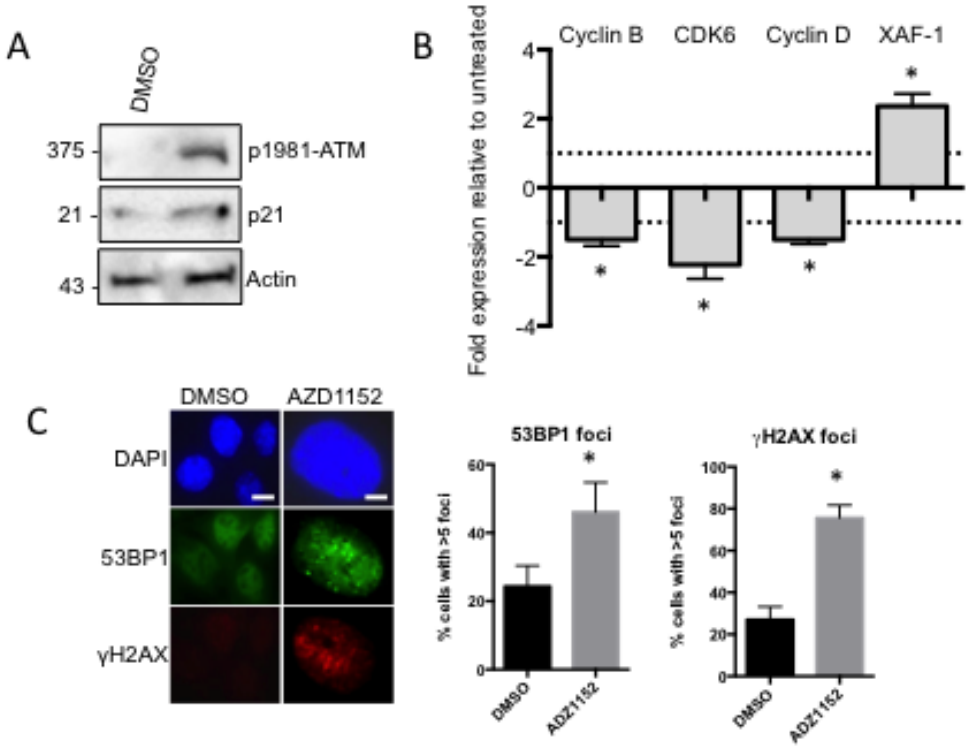
A
DMSO
375
p1981-ATM
21
p21
43
Actin
B
Cyclin B
CDK6
Cyclin D
XAF-1
Fold expression relative to untreated
4
2
0
-2
-4
*
C
DMSO
AZD1152
DAPI
53BP1
γH2AX
53BP1 foci
γH2AX foci
% cells with >5 foci
60
40
20
0
100
80
DMSO
ADZ1152

Next, we looked at the effect of Aurora B inhibition on the expression of the genes that we found deregulated in cells expressing Ku70 S155D. RT-PCR analysis of RNA extracted from Ku70 WT-expressing MEFs treated with AZD-1152 revealed, similar to what was observed in Ku70 S155D-expressing cells, Cyclin B, Cyclin D and CDK6 expression was significantly downregulated relative to the vehicle control-treated cells (Figure 3-6B). Lastly, we investigated the effect of Aurora B inhibition on the activation of the DDR. Immunofluorescence analysis of ϒ-H2AX and 53BP1 foci formation revealed that treatment of Ku70 WT MEFs with AZD-1152 significantly increased both 53BP1 and ϒ-H2AX foci (Figure 3-6C). Western blot analysis also showed an increase in ATM activation in the AZD-1152-treated samples, as determined by the pS1981-ATM levels (Figure 3-6A). Thus, Aurora B inhibition induced a DNA damage response and transcriptional changes that mirrored those induced by Ku S155D expression.

Since Ku70 S155D-expressing MEFs display cell cycle arrest and activation of a DNA damage response, a phenotype observed in Aurora B inhibitor-treated MEFs, we hypothesized that Ku70 S155D interaction with Aurora B could be inhibiting the activity of Aurora B. To explore the impact of Ku70 S155D expression on Aurora B kinase activity, we monitored phosphorylation of histone H3 on serine 10 (H3S10), which is catalyzed by Aurora B (9, 41, 42). Immunofluorescence analysis of phospho-H3S10 in MEFs expressing either WT or Ku70 S155D revealed that Ku70 S155D expression led to significantly decreased H3S10 phosphorylation compared to WT (11% of phospho-H3S10 foci-containing cells versus 43% in S155D) (Figure 3-7A). However, although this result showed that the Ku70 S155D expression led to the loss of a specific Aurora B

Figure 3-7 Ku70 S155D inhibits Aurora B kinase activity.

(A) Immunofluorescence analysis of phospho-H3S10 foci formation in Ku70 WT and S155D-expressing MEFs. Foci-positive cells were counted as a percentage of total cells and shown is the average of three experiments with error bars indicating SEM (*P<0.05). Scale bars, 10 μm. (B) Aurora B kinase activity assay. Ku70 WT or S155D-expressing MEF nuclear extracts were immunoprecipitated with an Aurora B antibody or IgG control. The immunoprecipitates were then incubated with 1 μg of purified Histone H3 and 10 μM of ATP and analyzed by western blot with antibodies to phospho-H3S10, Aurora B and Ku70. Phospho-H3S10 western blot signal was quantified and shown as an average of three separate experiments with error bars indicating SEM (*P<0.05)

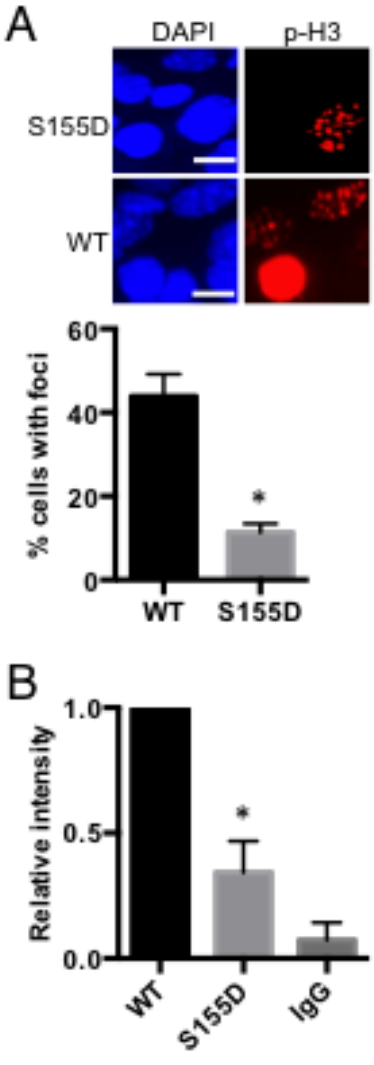
A
DAPI
p-H3
S155D
WT
% cells with foci
60
40
20
0
*
WT
S155D
B
Relative intensity
1.0
0.5
0.0
*
WT
S155D
IgG

phosphorylation event, the loss of H3S10 phosphorylation would be expected to happen in cells experiencing prolonged cell cycle arrest and no longer undergoing mitosis. To show that this was not the result of cell arrest, but a direct effect of Ku70 S155D on Aurora B kinase activity, we carried out an *in vitro* assay in which endogenous Aurora B was immunoprecipitated from either Ku70 WT or S155D-expressing MEFs and incubated with purified histone H3. Western blot analysis using an antibody directed against phosphorylated H3S10 detected phosphorylation with Aurora B immunoprecipitates from Ku70 WT-expressing MEFs in this assay (Figure 3-7B). However, phosphorylation of H3S10 was significantly lower (2.9-fold) in immunoprecipitates from Ku70 S155D-expressing MEFs, suggesting that complex formation of Aurora B and Ku S155D has an inhibitory effect on Aurora B kinase activity (Figure 3-7B).

3.3.6 Ku70 and Aurora B interact following DNA damage

Thus far, our results indicated that Ku70 S155 was phosphorylated in response to IR and that Ku70 comprising the phosphomimetic substitution S155D interacted with and inhibited the activity of Aurora B. These data led us to speculate that *in vivo*, Ku70 phosphorylation after IR could function to inhibit the activity of Aurora B and prevent cell cycle progression, potentially leading to the activation of cell cycle checkpoints and senescence. In order to test this model, we sought to determine if Ku70 and Aurora B interact following IR treatment. Since the localization of Ku to DSBs is difficult to observe directly by microscopy (43), we employed a proximity ligation assay (PLA), a method that was developed to monitor interactions of endogenous proteins directly in individual cells by immunofluorescence (44). Briefly, following incubation with primary

antibodies against the two proteins of interest, cells are incubated with secondary antibodies linked to short DNA oligonucleotides, called PLA probes. When two PLA probes come into close proximity, (within 40nm) they serve as a template for rolling-circle DNA synthesis, resulting in a PLA signal in the form of a dot by fluorescence microscopy analysis. Each protein-protein interaction is represented as a fluorescent dot which can be visualized by fluorescence microscopy. PLA was performed in $Ku70^{-/-}$ MEFs re-expressing either Ku70 WT or Ku70 S155A with antibodies directed against both Ku70 and Aurora B (Figure 3-8A). In untreated samples, few dots were detected in either the Ku70 WT or S155A-expressing cells. However, in cells treated with 10 Gy of IR, a significant increase in the number of dots was observed in the Ku70 WT-expressing MEFs, while no change was detected in the Ku70 S155A-expressing MEFs. These results suggest that while Ku70 and Aurora B do not associate in normally proliferating cells, a complex is formed following the introduction of DNA damage. This interaction is dependent upon the phosphorylation of Ku70 at S155, as it is not observed in the S155A samples, where the residue is not phosphorylated.

We next investigated the effect of Ku70 S155 mutations on Aurora B activity following IR, as measured by phospho-H3S10 foci formation. In Ku70 WT-expressing MEFs, a decrease in H3S10 phosphorylation was observed 2 hours following IR treatment (36% of foci-containing cells down to 21%) suggesting a decrease in Aurora B activity (Figure 3-8B). In Ku70 S155A-expressing MEFs, however, no significant difference in the phospho-H3S10 levels was not detected between control and irradiated (2h) samples suggesting that Aurora B activity was not reduced in these cells. This

suggests that Ku phosphorylation on Ku70 S155 in response to DNA damage functions to promote its interaction with Aurora B and inhibits its kinase activity.

Figure 3-8 Ku70 interacts with Aurora B after IR and Aurora B inhibition after IR is dependent on Ku70 S155 phosphorylation.

(A) Interaction of Aurora B and Ku after DNA damage using Proximity Ligation Assay (PLA). Ku70 WT and S155A expressing MEFs were left untreated or were treated with 10 Gy of IR and fixed after a 30-minute incubation. Cells were incubated with antibodies to Ku70 and Aurora B and processed for PLA analysis. Shown are representative immunofluorescent images. Green dots represent the PLA signal, the nuclei are stained with DAPI. Interactions were quantified by pixel density and shown as an average of three experiments with error bars indicating SEM. (*P<0.05). Scale bars, 10 μm. (B) Immunofluorescence analysis of phospho-H3S10 in Ku70 WT and S155A-expressing MEFs that were either left untreated, or were treated with 10 Gy of IR and incubated for 2 hours. Foci-positive cells were counted as a percentage of total cells and results are shown as an average of three experiments with error bars indicating SEM (*P<0.05). Scale bars, 10 μm.

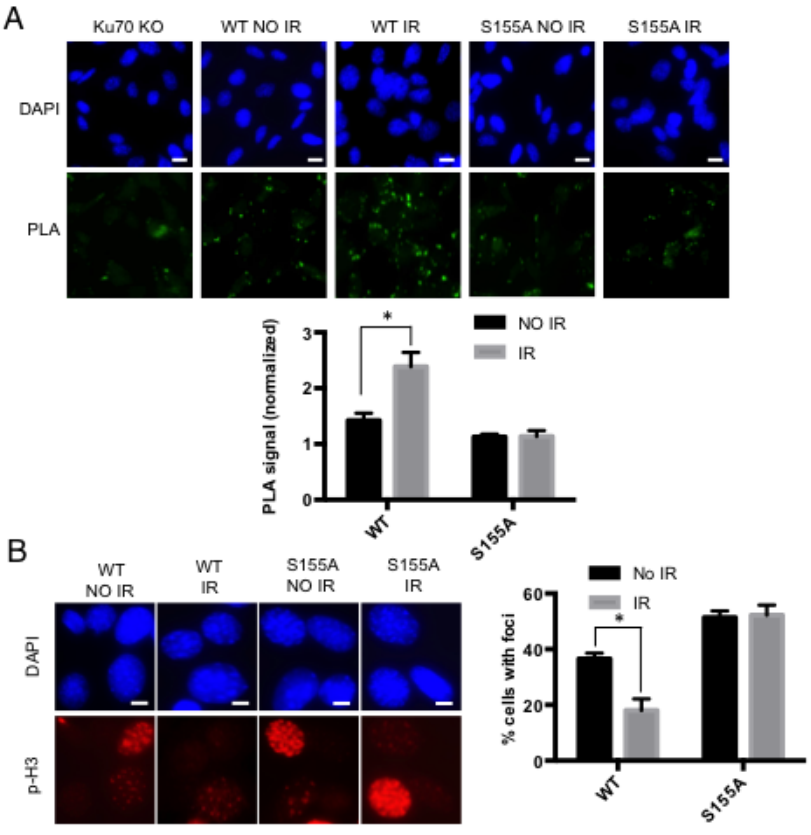
A
Ku70 KO
WT NO IR
WT IR
S155A NO IR
S155A IR
DAPI
PLA
PLA signal (normalized)
NO IR
IR
WT
S155A
B
WT NO IR
WT IR
S155A NO IR
S155A IR
DAPI
p-H3
No IR
IR
% cells with foci
WT
S155A

3.4 Discussion

This study identifies serine 155 of Ku70, as a novel phosphorylation site following DNA damage. Through expression of a phosphomimetic S155D mutant, we demonstrated that this phosphorylation event induces a DDR and cell cycle arrest. We found that Ku phosphorylated at Ku70 S155 interacts with the Aurora B kinase and inhibits its activity, suggesting that the DNA damage signaling events activated by Ku70 S155D occur through Ku's modulation of Aurora B kinase activity.

Expression of a phosphomimetic substitution at the serine 155 site into $Ku70^{-/-}$ MEFs induces a potent DDR leading to cell cycle arrest and senescence. This is in contrast to what is observed with cells expressing Ku70 with an alanine substitution at the S155 site, which exhibit increased growth rate, increased survival and decreased activation of DNA damage markers after IR. These opposing phenotypes led us to hypothesize that S155 is modified and that the alanine substitution prevents a phosphorylation event that dictates cell survival following DNA damage. Phosphorylated Ku has been observed in large scale and *in vitro* proteomic studies, in a number of different contexts and cell types. These include human Hela and K562 cancer cell lines, and upon mTOR-dependent signaling, stem cell differentiation and, interestingly, mitotic kinase inhibition (45-49). However in many cases functional significance of this phosphorylation could not be demonstrated. For example, alanine substitutions of several residues phosphorylated by DNA-PK *in vitro* had no impact on NHEJ efficiency (50, 51). Interestingly, some of these same residues, located in the Ku70 N-terminus, were deemed essential for apoptotic activation in neurons (52). Here, we demonstrate that phosphorylation of Ku70 on serine 155 is a DNA damage-induced event that modulates

cell fate decisions. The fact that S155 phosphorylation was not detected in previous proteomic studies could be due to low abundance of the pS155 peptide. We propose that S155 phosphorylation occurs on those Ku molecules actively involved in NHEJ at the break, and in the event of overwhelming damage that requires the activation of apoptosis or prolonged cell cycle arrest. This would result in very few phosphorylated Ku molecules relative to the total amount of this highly abundant protein, and would only occur under very specific conditions. We optimized detection of this residue by treating cells with a high dose of IR and immunoprecipitating Ku70, but still observed the phosphorylated peptide in low abundance. Furthermore, the previous proteomics studies employed proteolytic enzymes other than chymotrypsin and could have been producing pS155 peptides without a composition favorable for MS detection. It should be noted that our results also indicate a probable phosphorylation at the S162 position, a site that has not been reported in these large-scale studies.

It remains to be determined which kinase is responsible for phosphorylating S155 as it does not fall within any canonical kinase motif. Possible candidates include ATM and DNA-PK_{CS}, which have a loose consensus motif that includes S/TXXQ sequences, satisfied by the SDVQ sequence of Ku70 (53). Many other possibilities exist however, due to the abundance of serine/threonine kinases involved in the DDR. Indeed, proteomic data have implicated the kinases Chk1, CDK2 and Polo-like in Ku phosphorylation (47, 54, 55).

The expression of Ku70 S155D induced a DDR marked by H2AX phosphorylation, 53BP1 foci accumulation and activation of ATM. This phenotype correlates with the phenotypes observed in cells treated with Aurora B inhibitors and

suggests that the effects of Ku S155D are conferred, at least in part, through its inhibition of Aurora B activity. Studies using the broad Aurora kinase family inhibitors MLN8054, MK-0457, and VE-465, as well as our own study employing the specific Aurora B inhibitor AZD-1152, observed γ-H2AX and 53BP1 foci formation, and the activation of ATM signaling, as measured by ATM phosphorylation (15, 16). AZD-1552 treatment has been further shown to slow growth rate, induce cell cycle arrest and senescence, and increase sensitivity to IR, all phenotypes observed following Ku70 S155D expression (12-14, 56). We also observed some enlarged nuclei in Ku70 S155D-expressing MEFs (Figure 3-3A), a phenomenon indicative of failed cytokinesis and polyploidy, another common consequence of Aurora B inhibition (57).

Perhaps the most striking effect of Ku S155D expression is its ability to strongly activate p21. p21 gene (Cdkn1a) expression was increased in S155D cells (Supplemental Table 3-1) and p21 protein levels were markedly upregulated. In contrast, in cells expressing Ku70 S155A, p21 induction was severely attenuated in response to DNA damage. Aurora B has been suggested to repress p21 expression and Aurora B downregulation or inhibition was shown to result in p21 upregulation (58, 59). Again, this is consistent with an inhibitory role for Ku70 S155D on Aurora B activity leading to p21 activation, and with a lack of repression of Aurora B in Ku70 S155A cells, preventing p21 induction in response to DNA damage. Interestingly, Kumari et al. revealed that Aurora B inhibition activates p38 MAP kinase, which in turns promotes p21 induction by promoting transcriptional elongation of p21 transcripts (60). p38 is known to activate the transcription factor ATF2, which is also found strongly activated in Ku S155D MEFs (25). In addition, the expression of ATF3, a downstream target of ATF2

that is upregulated in the Ku70 S155D-expressing cells (Supplemental Table 3-1) is increased through Aurora B inhibition in a p38-dependent manner (61, 62). Altogether, the similarities between the effects caused by Aurora B inhibition and Ku70 S155D expression are consistent with the inhibition of Aurora B by Ku70 S155D.

Expression of a truncated Ku70 S155D comprising only the vWA domain triggered a similar growth defect in both $Ku70^{-/-}$ MEFs and in the cell line IMR90 which are non-transformed human lung cells that express normal levels of Ku. This demonstrates that the Ku70 S155D substitution exerts a dominant-negative effect, and that Ku70 S155 regulation is not specific to a particular cell line, although the amplitude of the response may vary depending on cell type. Moreover, it suggests that Ku70 S155D can exert its effects in absence of DNA binding. Indeed, the Ku70 vWA peptide lacks both heterodimerization and end-binding activities. However, we cannot exclude that it interacts with telomeres. How Ku binds to telomeres, whether it is through direct binding to telomeric DNA or through telomere protein interactions is still a matter of debate (19). Interestingly, residues in Ku70 vWA domain Helix 5 have been suggested to interact with the shelterin protein TRF2, however, whether this interaction is sufficient to recruit Ku to telomeres has not been investigated (26).

The interaction between Aurora B and Ku was dependent on phosphorylation at S155. We showed that while Ku70 and Aurora B do not interact in normally proliferating cells, Aurora B does associate with the phospho-form of Ku70, and they form a complex following DNA damage. Importantly, we found that Aurora B inhibition was dependent on Ku70 S155 phosphorylation, which suggests that the interaction of Ku pS155 with Aurora B is required for its inhibition. The full activation of Aurora B is achieved

through conformational changes induced by the binding of protein cofactors (63). There are a number of known activators of Aurora B, well characterized examples being the members of the chromosomal passenger complex (CPC), and this diversity allows for the specific targeting and local activation of Aurora B to different chromosomal structures (64). Similarly, inhibition of Aurora B is mediated through protein-protein interactions, including phosphatases PP1, PP2A and the checkpoint protein BubR1 (64). We propose that Ku, interacting with Aurora B through its Ku70 vWA domain, is an inhibitory cofactor following DNA damage. Thereby, the phosphomimetic S155D Ku70 mutant acts as a dominant negative, by constitutively binding and inhibiting Aurora B, either through direct hindrance of its catalytic activity or by precluding the interactions with other activating cofactors.

There is a body of evidence linking DNA repair proteins to the inhibition of Aurora B kinase activity. Similar to what we observed with Ku70 S155D, the alternative end-joining DSB repair protein PARP-1, was demonstrated to interact with and inhibit Aurora B kinase activity, in this case as a result of direct ribosylation of Aurora B (65). The HR proteins BRCA2/BARD1 were also shown to negatively regulate Aurora B by promoting its degradation (66). Together with our results, this suggests that several mechanisms involving factors from the three different DSB repair pathways converge to inhibit Aurora B activity in response to DNA damage.

Overall, our results suggest that upon the introduction of DNA damage, unphosphorylated Ku is recruited to DNA breaks where it promotes the assembly of the NHEJ DNA repair complex. We propose that Ku is phosphorylated at S155 under conditions of overwhelming damage or when the DNA break is too complex for proper

repair. This event ensures the sustained activation of the DDR and Aurora B inhibition to reinforce cell cycle arrest, providing time to complete DNA repair. If repair cannot be completed, the persistence of Ku70 S155 phosphorylation could contribute to senescence or activation of apoptotic pathways. Our model implies that Aurora B is recruited to DNA breaks, which remains to be confirmed. The role of Aurora B in the DDR is still poorly understood, however, it has previously been linked to prominent regulators of the DDR, such as the Repo-Man/PP1 complex and ATM (67-69). Our data provide additional evidence that Aurora B plays an important role in the response of cells to DNA damage. Our study also reinforces the notion that Ku's presence at the DNA break not only serves to recruit the NHEJ machinery, but also functions to relay signals to the DDR to modulate cellular responses, presumably as a function of DNA repair completion.

3.5 References

1. Goodarzi AA & Jeggo PA (2013) The repair and signaling responses to DNA double-strand breaks. *Advances in genetics* 82:1-45.
2. Surova O & Zhivotovsky B (2013) Various modes of cell death induced by DNA damage. *Oncogene* 32(33):3789-3797.
3. Marechal A & Zou L (2013) DNA damage sensing by the ATM and ATR kinases. *Cold Spring Harbor perspectives in biology* 5(9).
4. Munoz-Espin D & Serrano M (2014) Cellular senescence: from physiology to pathology. *Nature reviews. Molecular cell biology* 15(7):482-496.
5. Vader G & Lens SM (2008) The Aurora kinase family in cell division and cancer. *Biochimica et biophysica acta* 1786(1):60-72.
6. Song J, Salek-Ardakani S, So T, & Croft M (2007) The kinases aurora B and mTOR regulate the G1-S cell cycle progression of T lymphocytes. *Nature immunology* 8(1):64-73.
7. Terada Y (2006) Aurora-B/AIM-1 regulates the dynamic behavior of HP1alpha at the G2-M transition. *Molecular biology of the cell* 17(7):3232-3241.
8. Mountzios G, Terpos E, & Dimopoulos MA (2008) Aurora kinases as targets for cancer therapy. *Cancer treatment reviews* 34(2):175-182.
9. Ota T*, et al.* (2002) Increased mitotic phosphorylation of histone H3 attributable to AIM-1/Aurora-B overexpression contributes to chromosome number instability. *Cancer research* 62(18):5168-5177.
10. Nguyen HG*, et al.* (2009) Deregulated Aurora-B induced tetraploidy promotes tumorigenesis. *FASEB journal : official publication of the Federation of American Societies for Experimental Biology* 23(8):2741-2748.
11. Kitzen JJ, de Jonge MJ, & Verweij J (2010) Aurora kinase inhibitors. *Critical reviews in oncology/hematology* 73(2):99-110.
12. Walsby E, Walsh V, Pepper C, Burnett A, & Mills K (2008) Effects of the aurora kinase inhibitors AZD1152-HQPA and ZM447439 on growth arrest and polyploidy in acute myeloid leukemia cell lines and primary blasts. *Haematologica* 93(5):662-669.
13. Yang J*, et al.* (2007) AZD1152, a novel and selective aurora B kinase inhibitor, induces growth arrest, apoptosis, and sensitization for tubulin depolymerizing agent or topoisomerase II inhibitor in human acute leukemia cells in vitro and in vivo. *Blood* 110(6):2034-2040.
14. Wilkinson RW*, et al.* (2007) AZD1152, a selective inhibitor of Aurora B kinase, inhibits human tumor xenograft growth by inducing apoptosis. *Clinical cancer research : an official journal of the American Association for Cancer Research* 13(12):3682-3688.
15. Dreier MR, Grabovich AZ, Katusin JD, & Taylor WR (2009) Short and long-term tumor cell responses to Aurora kinase inhibitors. *Experimental cell research* 315(7):1085-1099.
16. Liu Y*, et al.* (2013) Targeting aurora kinases limits tumour growth through DNA damage-mediated senescence and blockade of NF-kappaB impairs this drug-induced senescence. *EMBO molecular medicine* 5(1):149-166.

17. Symington LS & Gautier J (2011) Double-strand break end resection and repair pathway choice. *Annual review of genetics* 45:247-271.
18. Chiruvella KK, Liang Z, & Wilson TE (2013) Repair of double-strand breaks by end joining. *Cold Spring Harbor perspectives in biology* 5(5):a012757.
19. Fell VL & Schild-Poulter C (2014) The Ku heterodimer: Function in DNA repair and beyond. *Mutation Resarch Reviews*.
20. Walker JR, Corpina RA, & Goldberg J (2001) Structure of the Ku heterodimer bound to DNA and its implications for double-strand break repair. *Nature* 412(6847):607-614.
21. Spagnolo L, Rivera-Calzada A, Pearl LH, & Llorca O (2006) Three-dimensional structure of the human DNA-PKcs/Ku70/Ku80 complex assembled on DNA and its implications for DNA DSB repair. *Molecular cell* 22(4):511-519.
22. Mahaney BL, Meek K, & Lees-Miller SP (2009) Repair of ionizing radiation-induced DNA double-strand breaks by non-homologous end-joining. *The Biochemical journal* 417(3):639-650.
23. Samper E, Goytisolo FA, Slijepcevic P, van Buul PP, & Blasco MA (2000) Mammalian Ku86 protein prevents telomeric fusions independently of the length of TTAGGG repeats and the G-strand overhang. *EMBO reports* 1(3):244-252.
24. Espejel S*, et al.* (2002) Mammalian Ku86 mediates chromosomal fusions and apoptosis caused by critically short telomeres. *The EMBO journal* 21(9):2207-2219.
25. Fell VL & Schild-Poulter C (2012) Ku regulates signaling to DNA damage response pathways through the Ku70 von Willebrand A domain. *Molecular and cellular biology* 32(1):76-87.
26. Ribes-Zamora A, Indiviglio SM, Mihalek I, Williams CL, & Bertuch AA (2013) TRF2 interaction with Ku heterotetramerization interface gives insight into c-NHEJ prevention at human telomeres. *Cell reports* 5(1):194-206.
27. Ribes-Zamora A, Mihalek I, Lichtarge O, & Bertuch AA (2007) Distinct faces of the Ku heterodimer mediate DNA repair and telomeric functions. *Nature structural & molecular biology* 14(4):301-307.
28. Strande N, Roberts SA, Oh S, Hendrickson EA, & Ramsden DA (2012) Specificity of the dRP/AP lyase of Ku promotes nonhomologous end joining (NHEJ) fidelity at damaged ends. *The Journal of biological chemistry* 287(17):13686-13693.
29. Roberts SA*, et al.* (2010) Ku is a 5'-dRP/AP lyase that excises nucleotide damage near broken ends. *Nature* 464(7292):1214-1217.
30. Whittaker CA & Hynes RO (2002) Distribution and evolution of von Willebrand/integrin A domains: widely dispersed domains with roles in cell adhesion and elsewhere. *Molecular biology of the cell* 13(10):3369-3387.
31. Grundy GJ*, et al.* (2013) APLF promotes the assembly and activity of non-homologous end joining protein complexes. *The EMBO journal* 32(1):112-125.
32. Gu Y, Jin S, Gao Y, Weaver DT, & Alt FW (1997) Ku70-deficient embryonic stem cells have increased ionizing radiosensitivity, defective DNA end-binding activity, and inability to support V(D)J recombination. *Proceedings of the National Academy of Sciences of the United States of America* 94(15):8076-8081.

33. Lukas J, Lukas C, & Bartek J (2004) Mammalian cell cycle checkpoints: signalling pathways and their organization in space and time. *DNA repair* 3(8-9):997-1007.
34. Kuntziger T, Landsverk HB, Collas P, & Syljuasen RG (2011) Protein phosphatase 1 regulators in DNA damage signaling. *Cell cycle* 10(9):1356-1362.
35. Wang J*, et al.* (2009) Identification of XAF1 as a novel cell cycle regulator through modulating G(2)/M checkpoint and interaction with checkpoint kinase 1 in gastrointestinal cancer. *Carcinogenesis* 30(9):1507-1516.
36. Liston P*, et al.* (2001) Identification of XAF1 as an antagonist of XIAP anti-Caspase activity. *Nature cell biology* 3(2):128-133.
37. Bunz F*, et al.* (1998) Requirement for p53 and p21 to sustain G2 arrest after DNA damage. *Science* 282(5393):1497-1501.
38. Brugarolas J*, et al.* (1995) Radiation-induced cell cycle arrest compromised by p21 deficiency. *Nature* 377(6549):552-557.
39. Hickson I*, et al.* (2004) Identification and characterization of a novel and specific inhibitor of the ataxia-telangiectasia mutated kinase ATM. *Cancer research* 64(24):9152-9159.
40. Mortlock AA*, et al.* (2007) Discovery, synthesis, and in vivo activity of a new class of pyrazoloquinazolines as selective inhibitors of aurora B kinase. *Journal of medicinal chemistry* 50(9):2213-2224.
41. Hsu JY*, et al.* (2000) Mitotic phosphorylation of histone H3 is governed by Ipl1/aurora kinase and Glc7/PP1 phosphatase in budding yeast and nematodes. *Cell* 102(3):279-291.
42. Adams RR, Maiato H, Earnshaw WC, & Carmena M (2001) Essential roles of Drosophila inner centromere protein (INCENP) and aurora B in histone H3 phosphorylation, metaphase chromosome alignment, kinetochore disjunction, and chromosome segregation. *The Journal of cell biology* 153(4):865-880.
43. Bekker-Jensen S*, et al.* (2006) Spatial organization of the mammalian genome surveillance machinery in response to DNA strand breaks. *The Journal of cell biology* 173(2):195-206.
44. Soderberg O*, et al.* (2006) Direct observation of individual endogenous protein complexes in situ by proximity ligation. *Nature methods* 3(12):995-1000.
45. Zhou H*, et al.* (2013) Toward a comprehensive characterization of a human cancer cell phosphoproteome. *Journal of proteome research* 12(1):260-271.
46. Hsu PP*, et al.* (2011) The mTOR-regulated phosphoproteome reveals a mechanism of mTORC1-mediated inhibition of growth factor signaling. *Science* 332(6035):1317-1322.
47. Kettenbach AN*, et al.* (2011) Quantitative phosphoproteomics identifies substrates and functional modules of Aurora and Polo-like kinase activities in mitotic cells. *Science signaling* 4(179):rs5.
48. Rigbolt KT*, et al.* (2011) System-wide temporal characterization of the proteome and phosphoproteome of human embryonic stem cell differentiation. *Science signaling* 4(164):rs3.
49. Olsen JV*, et al.* (2010) Quantitative phosphoproteomics reveals widespread full phosphorylation site occupancy during mitosis. *Science signaling* 3(104):ra3.

50. Chan DW, Ye R, Veillette CJ, & Lees-Miller SP (1999) DNA-dependent protein kinase phosphorylation sites in Ku 70/80 heterodimer. *Biochemistry* 38(6):1819-1828.
51. Douglas P, Gupta S, Morrice N, Meek K, & Lees-Miller SP (2005) DNA-PK-dependent phosphorylation of Ku70/80 is not required for non-homologous end joining. *DNA repair* 4(9):1006-1018.
52. Liu J, Naegele JR, & Lin SL (2009) The DNA-PK catalytic subunit regulates Bax-mediated excitotoxic cell death by Ku70 phosphorylation. *Brain research* 1296:164-175.
53. Bennetzen MV*, et al.* (2010) Site-specific phosphorylation dynamics of the nuclear proteome during the DNA damage response. *Molecular & cellular proteomics : MCP* 9(6):1314-1323.
54. Chi Y*, et al.* (2008) Identification of CDK2 substrates in human cell lysates. *Genome biology* 9(10):R149.
55. Blasius M*, et al.* (2011) A phospho-proteomic screen identifies substrates of the checkpoint kinase Chk1. *Genome biology* 12(8):R78.
56. Tao Y*, et al.* (2008) Enhancement of radiation response in p53-deficient cancer cells by the Aurora-B kinase inhibitor AZD1152. *Oncogene* 27(23):3244-3255.
57. Oke A*, et al.* (2009) AZD1152 rapidly and negatively affects the growth and survival of human acute myeloid leukemia cells in vitro and in vivo. *Cancer research* 69(10):4150-4158.
58. Trakala M, Fernandez-Miranda G, Perez de Castro I, Heeschen C, & Malumbres M (2013) Aurora B prevents delayed DNA replication and premature mitotic exit by repressing p21(Cip1). *Cell cycle* 12(7):1030-1041.
59. Gully CP*, et al.* (2012) Aurora B kinase phosphorylates and instigates degradation of p53. *Proceedings of the National Academy of Sciences of the United States of America* 109(24):E1513-1522.
60. Kumari G, Ulrich T, & Gaubatz S (2013) A role for p38 in transcriptional elongation of p21 (CIP1) in response to Aurora B inhibition. *Cell cycle* 12(13):2051-2060.
61. Kool J*, et al.* (2003) Induction of ATF3 by ionizing radiation is mediated via a signaling pathway that includes ATM, Nibrin1, stress-induced MAPkinases and ATF-2. *Oncogene* 22(27):4235-4242.
62. Kumari G, Ulrich T, Krause M, Finkernagel F, & Gaubatz S (2014) Induction of p21CIP1 Protein and Cell Cycle Arrest after Inhibition of Aurora B Kinase Is Attributed to Aneuploidy and Reactive Oxygen Species. *The Journal of biological chemistry* 289(23):16072-16084.
63. Carmena M, Ruchaud S, & Earnshaw WC (2009) Making the Auroras glow: regulation of Aurora A and B kinase function by interacting proteins. *Current opinion in cell biology* 21(6):796-805.
64. Carmena M, Wheelock M, Funabiki H, & Earnshaw WC (2012) The chromosomal passenger complex (CPC): from easy rider to the godfather of mitosis. *Nature reviews. Molecular cell biology* 13(12):789-803.
65. Monaco L*, et al.* (2005) Inhibition of Aurora-B kinase activity by poly(ADP-ribosyl)ation in response to DNA damage. *Proceedings of the National Academy of Sciences of the United States of America* 102(40):14244-14248.

66. Ryser S*, et al.* (2009) Distinct roles of BARD1 isoforms in mitosis: full-length BARD1 mediates Aurora B degradation, cancer-associated BARD1beta scaffolds Aurora B and BRCA2. *Cancer research* 69(3):1125-1134.
67. Qian J, Lesage B, Beullens M, Van Eynde A, & Bollen M (2011) PP1/Repo-man dephosphorylates mitotic histone H3 at T3 and regulates chromosomal aurora B targeting. *Current biology : CB* 21(9):766-773.
68. Peng A, Lewellyn AL, Schiemann WP, & Maller JL (2010) Repo-man controls a protein phosphatase 1-dependent threshold for DNA damage checkpoint activation. *Current biology : CB* 20(5):387-396.
69. Yang C*, et al.* (2011) Aurora-B mediated ATM serine 1403 phosphorylation is required for mitotic ATM activation and the spindle checkpoint. *Molecular cell* 44(4):597-608.
70. Andrews NC & Faller DV (1991) A rapid micropreparation technique for extraction of DNA-binding proteins from limiting numbers of mammalian cells. *Nucleic acids research* 19(9):2499.

3.6 Supplementary materials

Supplementary Figure 3-1 Identification of S155 phosphorylation.

(A) Theoretical chymotryptic digest of Ku70 amino acids 68-300 obtained from MS-Digest (UC San Francisco). Parameters allow 6 missed cleavages and consider oxidation and serine/threonine phosphorylation. (B) Experimental masses obtained from MALDI analysis of Ku70 immunoprecipitated from both unirradiated and 30 minutes following a 40 Gy IR treatment WT Ku70 MEF samples were matched to theoretical masses obtained from MS-Digest. Peptides including Serine 155 highlighted in yellow with amino acid modifications indicated. (C) Analysis as in B, with MEFs expressing Ku70 S155A. D. Analysis as in B, with MEFs expressing Ku70 S162A.

A

Theoretical digest:

Home | MS-Fit | MS-Tag | MS-Seq | MS-Pattern | MS-Bridge | MS-Digest | MS-Product | MS-Comp | DB-Stat | MS-Isotope | MS-Homology

MS-Digest Search Results

[–] Parameters

Database: User Protein

Considered modifications: | Oxidation (M) | Phospho (ST) |

Digest Used: ChymotrypsinFWYMEDLN

Max. # Missed Cleavages: 6

User AA Formula 1: C2 H3 N1 O1

Constant Modification: Carbamidomethyl (C)

Minimum Digest Fragment Mass: 500

Maximum Digest Fragment Mass: 3500

Minimum Digest Fragment Length: 4

Index Number: 1

pI of Protein: 8.7

Protein MW: 15902

Amino Acid Composition: A7 C1 D13 E5 F8 G11 H4 I7 K13 L14 M5 N8 P3 Q7 R7 S11 T4 V7 W1 Y4

1	YISKIISSDR	DLLAVVFYGT	EKDKNSVNFK	NIYVLQELDN	PGAKRILELD	QFKGQQGQKR	FQDMMGHGSD	
81	YSLSEVLWVC	ANLFSDVQFK	MSHKRIMLFT	NEDNPHGNDS	AKASRARTKA	GDLRDTGIFL	DLMHLKKPGG	

B

WT Ku70 IR sample

Experimental	Theoretical				
513.30072	513.2854		132	135	(D)LMHL(K)
524.16913	524.1843		62	65	(F)QDMM(G)
665.3548	665.3505		126	131	(D)TGIFLD(L)
668.36426	668.3436	1Oxidation	87	91	(D)VQFKM(S)
708.3714	708.3675		24	29	(D)KNSVNF(K)
708.3714	708.3675		26	31	(N)SVNFKN(I)
708.3714	708.3675		124	129	(L)RDTGIF(L)
723.36462	723.3494		79	84	(W)VC(Carbamidomethyl)ANLF(S)
741.39362	741.3964		130	135	(F)LDLMHL(K)
762.37238	762.3603		78	83	(L)WVC(Carbamidomethyl)ANL(F)
1077.5253	1077.5034		74	82	(L)SEVLWVC(Carbamidomethyl)AN(L)
1144.52	1144.4654		99	108	(L)FTNEDNPHGN(D)
1175.6154	1175.6129	1Oxidation	126	135	(D)TGIFLDLMHL(K)
1338.7152	1338.774		38	49	(E)LDNPGAKRILEL(D)
1353.7043	1353.7485		36	47	(L)QELDNPGAKRIL(E)
1401.6849	1401.6645		18	29	(F)YGTEKDKNSVNF(K)
1485.7487	1485.6831		78	89	(L)WVC(Carbamidomethyl)ANLFSDVQF(K)
1505.7894	1505.8079		90	101	(F)KMSHKRIMLFTN(E)
1520.6781	1520.6491	1Phospho	71	82	(D)YSLSEVLWVC(Carbamidomethyl)AN(L)
1522.7723	1522.8475	1Oxidation	90	101	(F)KMSHKRIMLFTN(E)
1580.8147	1580.705		65	78	(M)MGHGSDYSLSEVLW(V)
1594.8523	1594.8085		51	63	(D)QFKGQQGQKRFQD(M)
1597.8193	1597.7574	1Oxidation	53	65	(F)KGQQGQKRFQDMM(G)
1597.8193	1597.8107	1Phospho	87	98	(D)VQFKMSHKRIML(F)
1602.8799	1602.8139	1Phospho	1	13	(-)YISKIISSDRDLL(A)
1629.8309	1629.8005	2Oxidation 1Phospho	87	98	(D)VQFKMSHKRIML(F)
1769.9015	1769.8826	1Oxidation	84	97	(L)FSDVQFKMSHKRIM(L)
1895.8555	1895.8309	1Oxidation 2Phospho	85	98	(F)SDVQFKMSHKRIML(F)
1911.9117	1911.8258	2Oxidation 2Phospho	85	98	(F)SDVQFKMSHKRIML(F)
1962.988	1962.933	1Oxidation 1Phospho	84	98	(L)FSDVQFKMSHKRIML(F)
1962.988	1962.933	1Oxidation 1Phospho	85	99	(F)SDVQFKMSHKRIMLF(T)
1962.988	1962.933	1Oxidation 1Phospho	83	97	(N)LFSDVQFKMSHKRIM(L)

WT NO IR Sample

Experimental	Theoretical				
513.30206	513.2854		132	135	(D)LMHL(K)
516.33014	516.314		10	13	(D)RDLL(A)
524.17188	524.1843		62	65	(F)QDMM(G)
598.31818	598.3235		14	18	(L)AVVFY(G)
623.33002	623.3035		98	102	(M)LFTNE(D)
644.3501	644.3072	1Oxidation	131	135	(L)DLMHL(K)
723.38635	723.3494		79	84	(W)VC(Carbamidomethyl)ANLF(S)
792.27747	792.2811	1Phospho	18	23	(F)YGTEKD(K)
855.45392	855.4247		83	89	(N)LFSDVQF(K)
996.55414	996.5037		71	78	(D)YSLSEVLW(V)
996.55414	996.5659	1Oxidation	132	140	(D)LMHLKKPGG(-)
1014.5139	1014.502	1Phospho	123	130	(D)LRDTGIFL(D)
1076.5718	1076.596		53	61	(F)KGQQQGQKRF(Q)
1133.6256	1133.6161		2	11	(Y)ISKIISSDRD(L)
1142.5447	1142.521	2Oxidation 1Phospho	90	97	(F)KMSHKRIM(L)
1157.5491	1157.4697	1Phospho	74	82	(L)SEVLWVC(Carbamidomethyl)AN(L)
1175.6304	1175.6129	1Oxidation	126	135	(D)TGIFLDLMHL(K)
1193.5835	1193.6273		22	31	(E)KDKNSVNFKN(I)
1241.615	1241.6412	1Phospho	123	132	(D)LRDTGIFLDL(M)
1338.726	1338.774		38	49	(E)LDNPGAKRILEL(D)
1353.7074	1353.7485		36	47	(L)QELDNPGAKRIL(E)
1398.666	1398.6849	1Phospho	110	122	(D)SAKASRARTKAGD(L)
1401.681	1401.6645		18	29	(F)YGTEKDKNSVNF(K)
1431.7795	1431.8027		110	123	(D)SAKASRARTKAGDL(R)
1505.7802	1505.8079		90	101	(F)KMSHKRIMLFTN(E)
1520.6736	1520.6491	1Phospho	71	82	(D)YSLSEVLWVC(Carbamidomethyl)AN(L)
1522.7598	1522.8475	1Oxidation	90	101	(F)KMSHKRIMLFTN(E)
1594.8107	1594.8085		51	63	(D)QFKGQQQGQKRFQD(M)
1597.8033	1597.7574	1Oxidation	53	65	(F)KGQQQGQKRFQDMM(G)
1597.8033	1597.8107	1Phospho	87	98	(D)VQFKMSHKRIML(F)
1769.9053	1769.8826	1Oxidation	84	97	(L)FSDVQFKMSHKRIM(L)
1962.9733	1962.933	1Oxidation 1Phospho	84	98	(L)FSDVQFKMSHKRIML(F)
1962.9733	1962.933	1Oxidation 1Phospho	85	99	(F)SDVQFKMSHKRIMLF(T)
1962.9733	1962.933	1Oxidation 1Phospho	83	97	(N)LFSDVQFKMSHKRIM(L)

C

Ku70 S155A IR sample

Experimental	Theoretical				
513.31018	513.2854		132	135	(D)LMHL(K)
524.20166	524.1843		62	65	(F)QDMM(G)
537.31311	537.3031		30	33	(F)KNIY(V)
712.35645	712.3148		18	23	(F)YGTEKD(K)
723.36591	723.3494		79	84	(W)VC(Carbamidomethyl)ANLF(S)
855.44745	855.4247		83	89	(N)LFSDVQF(K)
1025.6068	1025.5514		1	9	(-)YISKIISSD(R)
1046.5553	1046.5598	1Oxidation	90	97	(F)KMSHKRIM(L)
1076.5413	1076.47	1Phospho	71	78	(D)YSLSEVLW(V)
1076.5413	1076.596		53	61	(F)KGQQGQKRF(Q)
1175.6117	1175.6129	1Oxidation	126	135	(D)TGIFLDLMHL(K)
1338.7183	1338.774		38	49	(E)LDNPGAKRILEL(D)
1353.6865	1353.7485		36	47	(L)QELDNPGAKRIL(E)
1401.6742	1401.6645		18	29	(F)YGTEKDKNSVNF(K)
1505.7886	1505.8079		90	101	(F)KMSHKRIMLFTN(E)
1522.7894	1522.8475		1	13	(-)YISKIISSDRDLL(A)
1580.8094	1580.705		65	78	(M)MGHGSDYSLSEVLW(V)
1602.8657	1602.8139	1Phospho	1	13	(-)YISKIISSDRDLL(A)
1769.9117	1769.8826	1Oxidation	84	97	(L)FSDVQFKMSHKRIM(L)
1783.8479	1783.9225		13	28	(L)LAVVFYGTEKDKNSVN(F)
1895.8875	1895.8309	1Oxidation	87	101	(D)VQFKMSHKRIMLFTN(E)
1895.8875	1895.9983	1Oxidation	49	64	(E)LDQFKGQQGQKRFQDM(M)
1969.9022	1969.9549				

Ku70 S155A NO IR sample

Experimental	Theoretical				
507.32974	507.3177				
524.20233	524.1843		32	35	(N)IYVL(Q)
550.34277	550.3235		62	65	(F)QDMM(G)
712.28613	712.3148		126	130	(D)TGIFL(D)
723.35962	723.3494		18	23	(F)YGTEKD(K)
745.33362	745.3168		79	84	(W)VC(Carbamidomethyl)ANLF(S)
1025.6021	1025.5514	1Phospho	126	131	(D)TGIFLD(L)
1175.6068	1175.6129		1	9	(-)YISKIISSD(R)
1338.7156	1338.774	1Oxidation	126	135	(D)TGIFLDLMHL(K)
1505.7819	1505.8079		38	49	(E)LDNPGAKRILEL(D)
1522.765	1522.8475		90	101	(F)KMSHKRIMLFTN(E)
1602.8645	1602.8139		1	13	(-)YISKIISSDRDLL(A)
1646.8513	1646.819	1Phospho	1	13	(-)YISKIISSDRDLL(A)
1769.9143	1769.8826	1Phospho	26	38	(N)SVNFKNIYVLQEL(D)
1783.8447	1783.9225	1Oxidation	84	97	(L)FSDVQFKMSHKRIM(L)
1969.9006	1969.9549		13	28	(L)LAVVFYGTEKDKNSVN(F)
2035.0427	2034.9233	1Oxidation	49	64	(E)LDQFKGQQGQKRFQDM(M)
504.289	504.2776		53	70	(F)KGQQGQKRFQDMMGHGSD(Y)
513.27612	513.2854		36	39	(L)QELD(N)
524.20337	524.1843		132	135	(D)LMHL(K)
529.28955	529.2803		62	65	(F)QDMM(G)
712.29852	712.3148	1Oxidation	132	135	(D)LMHL(K)
713.33014	713.2906		18	23	(F)YGTEKD(K)
723.36377	723.3494	1Phospho	74	78	(L)SEVLW(V)
738.34955	738.3305		79	84	(W)VC(Carbamidomethyl)ANLF(S)
745.31989	745.3168		98	103	(M)LFTNED(N)
1025.6003	1025.5514	1Phospho	126	131	(D)TGIFLD(L)
1175.6093	1175.6129		1	9	(-)YISKIISSD(R)
1338.7006	1338.774	1Oxidation	126	135	(D)TGIFLDLMHL(K)
1354.671	1354.7253		38	49	(E)LDNPGAKRILEL(D)
1401.6584	1401.6645		12	23	(D)LLAVVFYGTEKD(K)
1505.7809	1505.8079		18	29	(F)YGTEKDKNSVNF(K)
1580.8036	1580.705		90	101	(F)KMSHKRIMLFTN(E)
1602.86	1602.8139		65	78	(M)MGHGSDYSLSEVLW(V)
1613.8459	1613.7523	1Phospho	1	13	(-)YISKIISSDRDLL(A)
1613.8459	1613.8056	2Oxidation	53	65	(F)KGQQGQKRFQDMM(G)
1646.8459	1646.819	1Oxidation 1Phospho	87	98	(D)VQFKMSHKRIML(F)
1769.9038	1769.8826	1Phospho	26	38	(N)SVNFKNIYVLQEL(D)
1783.8328	1783.9225	1Oxidation	84	97	(L)FSDVQFKMSHKRIM(L)
2035.0067	2034.9233		13	28	(L)LAVVFYGTEKDKNSVN(F)
			53	70	(F)KGQQGQKRFQDMMGHGSD(Y)

D

Ku70 162A IR sample

Experimental	Theoretical				
504.26657	504.2776		22	25	(E)KDKN(S)
513.25793	513.2854		132	135	(D)LMHL(K)
524.17059	524.1843		62	65	(F)QDMM(G)
529.26031	529.2803	1Oxidation	132	135	(D)LMHL(K)
623.32245	623.3035		98	102	(M)LFTNE(D)
668.33911	668.3436	1Oxidation	87	91	(D)VQFKM(S)
711.4118	711.4076		13	18	(L)LAVVFY(G)
723.3623	723.3494		79	84	(W)VC(Carbamidomethyl)ANLF(S)
738.32159	738.3305		98	103	(M)LFTNED(N)
745.35406	745.3168	1Phospho	126	131	(D)TGIFLD(L)
855.46509	855.4247		83	89	(N)LFSDVQF(K)
1014.5145	1014.502	1Phospho	123	130	(D)LRDTGIFL(D)
1025.6133	1025.5514		1	9	(-)YISKIISSD(R)
1064.5375	1064.4812	1Phospho	26	33	(N)SVNFKNIY(V)
1144.5438	1144.4654		99	108	(L)FTNEDNPHGN(D)
1175.6173	1175.6129	1Oxidation	126	135	(D)TGIFLDLMHL(K)
1338.7003	1338.774		38	49	(E)LDNPGAKRILEL(D)
1353.7028	1353.7485		36	47	(L)QELDNPGAKRIL(E)
1401.6826	1401.6645		18	29	(F)YGTEKDKNSVNF(K)
1406.6698	1406.6328	2Phospho	2	12	(Y)ISKIISSDRDL(L)
1505.7958	1505.8079	2Oxidation 2Phospho	64	75	(D)MMGHGSDYSLSE(V)
1522.7721	1522.8475		1	13	(-)YISKIISSDRDLL(A)
1580.8107	1580.705		65	78	(M)MGHGSDYSLSEVLW(V)
1597.8069	1597.7574	1Oxidation	53	65	(F)KGQQGQKRFQDMM(G)
1602.8734	1602.8139	1Phospho	1	13	(-)YISKIISSDRDLL(A)
1646.8423	1646.819	1Phospho	26	38	(N)SVNFKNIYVLQEL(D)
1769.9078	1769.8826	1Oxidation	84	97	(L)FSDVQFKMSHKRIM(L)
1783.8558	1783.9225		13	28	(L)LAVVFYGTEKDKNSVN(F)
1833.9534	1833.854	1Phospho	84	97	(L)FSDVQFKMSHKRIM(L)
1895.8716	1895.9983	1Oxidation	87	101	(D)VQFKMSHKRIMLFTN(E)
1962.9751	1962.933	1Oxidation 1Phospho	84	98	(L)FSDVQFKMSHKRIML(F)
1962.9751	1962.933	1Oxidation 1Phospho	85	99	(F)SDVQFKMSHKRIMLF(T)
1962.9751	1962.933	1Oxidation 1Phospho	83	97	(N)LFSDVQFKMSHKRIM(L)
2035.0055	2034.9233		53	70	(F)KGQQGQKRFQDMMGHGSD(Y)

Ku70 162A No IR sample

Experimental	Theoretical				
524.17334	524.1843		62	65	(F)QDMM(G)
537.31348	537.3031		30	33	(F)KNIY(V)
723.36835	723.3494		79	84	(W)VC(Carbamidomethyl)ANLF(S)
738.32764	738.3305		98	103	(M)LFTNED(N)
792.26416	792.2811	1Phospho	18	23	(F)YGTEKD(K)
1025.6025	1025.5514		1	9	(-)YISKIISSD(R)
1077.531	1077.5034		74	82	(L)SEVLWVC(Carbamidomethyl)AN(L)
1402.642	1402.6735	2Oxidation 1Phospho	90	99	(F)KMSHKRIMLF(T)
1466.7736	1466.7169	1Oxidation	53	64	(F)KGQQGQKRFQDM(M)
1466.7736	1466.7499		50	61	(L)DQFKGQQGQKRF(Q)
1505.7833	1505.8079		90	101	(F)KMSHKRIMLFTN(E)
1518.8159	1518.7716	1Phospho	24	35	(D)KNSVNFKNIYVL(Q)
1522.759	1522.8475		1	13	(-)YISKIISSDRDLL(A)
1580.8105	1580.705		65	78	(M)MGHGSDYSLSEVLW(V)
1597.8372	1597.7574	1Oxidation	53	65	(F)KGQQGQKRFQDMM(G)
1602.8577	1602.8139	1Phospho	1	13	(-)YISKIISSDRDLL(A)
1749.8984	1749.8775		90	103	(F)KMSHKRIMLFTNED(N)

Supplementary Table 3-1 S155D Ku70 induces expression changes in genes regulating cell cycle and apoptosis.

Samples from WT and S155D Ku70 expressing MEFs were subjected to microarray analysis using a GeneChip Mouse Gene 1.0 ST Array (Affymetrics, Santa Clara, CA). GeneChips were processed at the London Regional Genomics Centre (Robarts Research Institute, London, ON; http://www.lrgc.ca). Shown is the list of genes, organized by cellular process, identified as differentially expressed in S155D Ku70 MEFs compared to the WT Ku70 control, with the fold expression change indicated for two separate experiments.

	Gene	Fold S155D/WT expression Microarray 1	Microarray 2
Cell cycle	CDK1	-1.13272	-1.5631
	CDK11B	1.1717	-1.35505
	CDK12	-1.23528	-1.54936
	CDK14	-1.52117	-1.39001
	CDK17	-1.23738	-1.65717
	CDK2	-1.10442	-2.29363
	CDK20	1.30282	-1.34152
	CDK4	-1.21157	-1.62155
	CDK6	-1.71747	-1.62557
	CDK7	-1.12377	-1.94373
	CDK8	-1.04368	-1.64662
	CDK9	-1.06108	-1.41405
	Cdkn1a	1.78469	1.8669
	Cyclin B1	-1.02889	-1.73742
	Cyclin D1	/	-1.85051
	Cyclin D3	-1.08789	-1.19947
	Cyclin E1	/	-1.66409
	Cyclin F	-1.29918	-1.74507
	Cyclin J	-1.5685	-1.54095
	Cyclin Y	-1.5685	-2.47138
	Id1	-1.71293	-3.30425
	Id2	-1.54394	-2.97433
	Id3	-1.55826	-3.07059
	Inca1	2.08792	1.09476
Apoptosis	Atf3	2.29076	1.11201
	Ddit3	3.86476	2.64323
	Trp53inp1	3.92893	2.38246
	Xaf1	10.0812	9.14192
Phosphatases	Dusp6	-1.78878	-2.23834
	Ppp1ca	-1.04564	-1.51597
	Ppp1cb	-1.7477	-3.1441
	Ppp1cb	-1.7477	-3.1441
	Ppp1cc	-1.03787	-1.31621
	Ppp2ca	-1.28673	-2.18602
	Ppp4r1	-1.27836	-1.30361
	Ppp4r1	-1.27836	-1.30361
	Ppp4r4	-1.45548	-1.07197
	Ppp4r4	-1.45548	-1.07197
	Ppp6r3	-1.27171	-1.20221
Other	Gadd45a	1.82471	4.08577
	Gadd45g	-1.30705	-1.70421
	Parp9	2.63466	1.53339
	Parp14	3.6658	3.17908
	Parp10	4.87628	4.04058

Supplementary Figure 3-2 Pulldown of proteins interacting with biotin-conjugated Ku70 peptides.

(A) Silver stained gel of streptavidin-biotin pulldown of proteins interacting with Ku70 peptide containing either an alanine or aspartic acid substitution at the S155 position. Pull down was performed in MEF extracts that were either untreated or treated with 10 Gy of IR and incubated for 30 minutes. Band boxed in red was identified by MS/MS as being Aurora B. (B) Proteins were subjected to trypsin digestion and peptide masses obtained from MS/MS analysis. MASCOT (Matrix Science) database results for boxed band with parameters indicated.

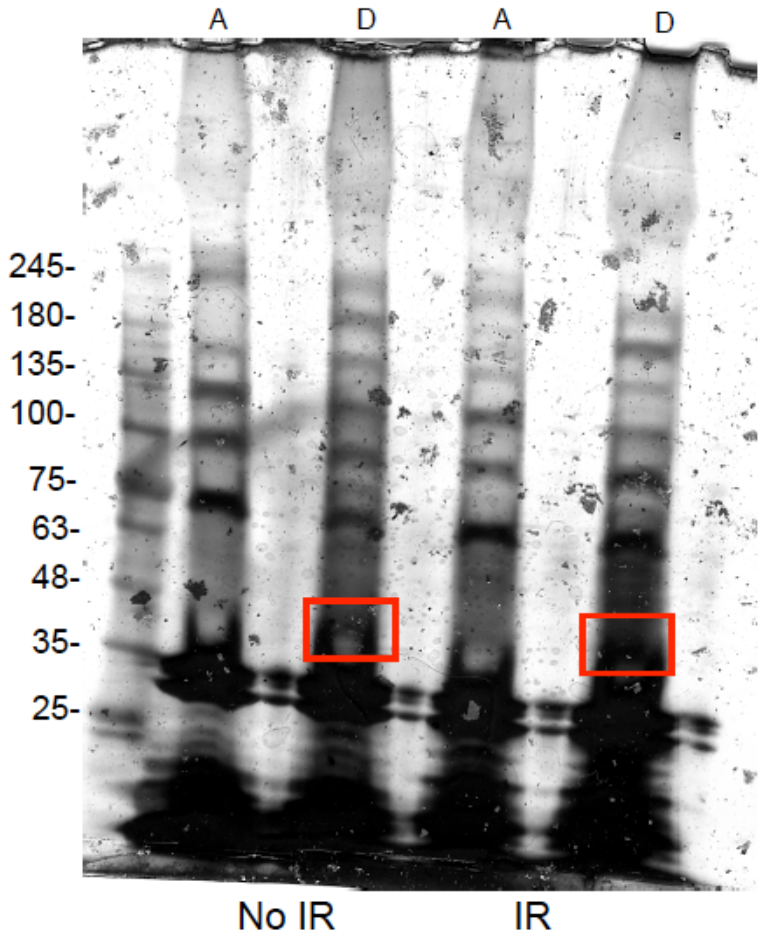
A
D
A
D
245-
180-
135-
100-
75-
63-
48-
35-
25-
No IR
IR

MASCOT Search Results

Protein View: gi|51317394

aurora kinase B [Mus musculus]

Database:	NCBInr
Score:	24
Expect:	5.1e+02
Nominal mass (M_r):	39588
Calculated pI:	9.47
Taxonomy:	Mus musculus

This protein sequence matches the following other entries:

- gi|341940262 from Mus musculus
- gi|26344858 from Mus musculus
- gi|74204872 from Mus musculus
- gi|148678525 from Mus musculus

Sequence similarity is available as an NCBI BLAST search of gi|51317394 against nr.

Search parameters

Enzyme:	
Fixed modifications:	Carbamidomethyl (C)
Variable modifications:	Oxidation (M)
Mass values searched:	76
Mass values matched:	4

Protein sequence coverage: 11%

Matched peptides shown in ***bold red***.

```
  1 MAQKENAYPW  PYGSKTSQSG LNTLSQRVLR KEPATTSALA  LVNRFNSQST
 51 AAPGQKLAEN KSQGSTASQG SQNKQPFTID NFEIGRPLGK  GKFGNVYLAR
101 EKKSRFIVAL  KILFKSQIEK EGVEHQLRRE IEIQAHLKHP NILQLYNYFY
151 DQQRIYLILE  YAPRGELYKE LQKSRTFDEQ RTATIMEELS  DALTYCHKKK
201 VIHRDIKPEN  LLLGLQGELK IADFGWSVHA PSLRRKTMCG  TLDYLPPEMI
251 EGRMHNEMVD  LWCIGVLCYE LMVGNPPFES PSHSETYRRI  VKVDLKFPSS
301 VPSGAQDLIS  KLLKHNPWQR LPLAEVAAHP WVRANSRRVL  PPSAL
```

Unformatted sequence string: 345 residues (for pasting into other applications).

Sort peptides by (•) Residue Number ( ) Increasing Mass ( ) Decreasing Mass

Show predicted peptides also

Start – End	Observed	Mr(expt)	Mr(calc)	ppm	M	Peptide
45 – 61	1790.8965	1789.8892	1789.8958	-3.70	1	R.FNSQSTAAPGQKLAENK.S
93 – 102	1196.6475	1195.6402	1195.6349	4.43	1	K.FGNVYLAREK.K
129 – 138	1236.7520	1235.7447	1235.6986	37.3	1	R.REIEIQAHLK.H
289 – 292	515.3500	514.3427	514.3591	-31.9	1	R.RIVK.V

No match to: 522.1439, 524.1525, 526.1677, 527.3412, 532.1259, 544.2593, 546.1281, 550.1316, 552.1475, 562.2569, 568.1403, 570.1439, 571.3336, 574.6748, 590.1094, 590.2841, 591.3544, 592.0972, 603.2925, 606.3408, 612.0964, 614.1000, 617.0551, 618.0634, 621.3695, 634.0793, 636.0825, 637.3045, 644.3737, 650.0524, 652.0555, 659.2951, 691.0883, 693.0884, 705.3827, 780.4994, 801.1160, 823.1085, 825.1118, 830.4670, 835.5049, 839.0843, 841.0833, 842.5198, 845.1009, 847.0994, 854.5222, 856.5255, 861.0728, 867.4332, 870.5452, 943.5807, 945.5692, 956.3621, 959.0843, 969.5425, 976.4651, 1027.5116, 1034.1311, 1036.1300, 1045.5720, 1050.1051, 1052.1104, 1057.5663, 1132.5400, 1154.5925, 1155.6062, 1176.5413, 1179.6077, 1252.6168, 1493.7444, 1726.7675

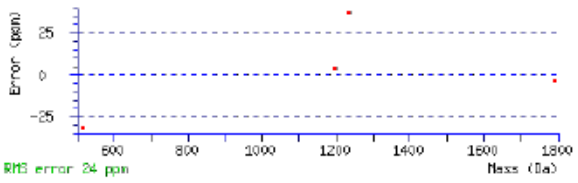

Cyclin B1	Forward	ATCGGGGAACCTCTGATTTT
	Reverse	TCACACACAGGCACCTTCTC
Cyclin D1	Forward	GCGTACCCTGACACCAATCTC
	Reverse	CTCCTCTTCGCACTTCTGCTC
PP1c	Forward	GATGTCGTCCAGGAAAGATTGT
	Reverse	TCAGTGGTGCTTCCAATTCCA
Xaf1	Forward	AGCCATGTGTCTGAGTGCAAA
	Reverse	GCAAAGATCACAACGGGTTTTTC
CDK6	Forward	GGCGTACCCACAGAAACCATA
	Reverse	AGGTAAGGGCCATCTGAAAACT

Supplementary Table 3-2 Primers used in this study.

RT-PCR primer sequences.

Chapter 4

4 General Discussion

4.1 Summary of findings

Prior to the start of this investigation, there was little known about the contribution of Ku's vWA domain to the execution of NHEJ. This domain, named after the prototypic member, the von Willebrand factor A, frequently functions to mediate protein-protein interactions. We aimed to identify a possible role for this domain in response to IR by producing a series of alanine mutants at different positions throughout the vWA domain. Our hypothesis was that this domain could be mediating interactions with Ku and other NHEJ factors, so we chose residues that were more likely to participate in interactions, such as those that were present on the solvent exposed surface and showed some degree of conservation amongst Ku homologs.

Through this investigation, we identified two important regions of the Ku70 vWA domain in response to IR (Chapter 2). Firstly, helix 5, particularly residues D192/D195, is required for efficient completion of NHEJ. Mutation of these residues to alanine results in severely compromised survival in response to IR. The analysis of DNA repair efficiency demonstrated that this mutation greatly decreases DNA repair capacity relative to WT, indicating that the survival defect was due to a loss of NHEJ capability. Next, the mutation of S155 to alanine produced a surprising phenotype. Unlike what would be expected of a mutation impairing DNA repair, alanine substitution of this residue resulted in increased survival in response to IR. There was decreased activation of the ATF2 dependent DDR cascade that resulted in decreased activation of apoptosis. Given the

prevalence of serine phosphorylation in the DDR, we hypothesized that this alanine substitution was preventing a phosphorylation event at this residue that is required for the DDR activation of apoptosis in the event of unsuccessful repair. We went on to confirm this phosphorylation (Chapter 3) event and utilized a phosphomimetic mutant (S155D) to demonstrate that this modification after IR is required for the interaction and inhibition of the kinase Aurora B. Expression of the phosphomimetic mutant induces a profound phenotype, marked by constitutive activation of DDR and cell cycle arrest in the absence of damage. These results suggested that phosphorylation of S155 occurred after IR, perhaps in the case of overwhelming damage, in order to mediate the inhibition of Aurora B and induce cell cycle arrest or activation of apoptosis.

4.2 Ku70 vWA domain in DNA repair

Our work has identified helix 5 of the Ku70 vWA domain has being essential for DNA repair in MEFs (1). The requirement for these residues appears to be conserved amongst eukaryotes as it has also been shown to be required for DNA repair in yeast. A previous study by Ribes-Zamora et al., using *S. cerevisiae* as an experimental system, investigated the requirement for certain residues in DNA repair by performing random mutagenesis across the entire Ku heterodimer followed by *in vitro* plasmid repair assay (2). They identified the mutation of residues R189A/D192A/D195R in helix 5 the Ku70 vWA domain as conferring a DNA repair defect. They later confirmed our results in a mammalian system, demonstrating that the transfection of a Ku70 D192A/D195R mutant into human cell lines resulted in significantly decreased survival in response to IR compared to the WT control (3).

Despite the evidence that the Ku70 vWA helix 5 is required for efficient NHEJ in response to IR, we have yet to elucidate the exact role of these residues. As a protein-protein interaction domain, we hypothesize that this region mediates the recruitment of NHEJ factors to the break and the mutation is preventing this recruitment and therefore hindering completion of break repair. There are numerous possibilities given number of proteins involved in processing and ligation of a DSB, however making some assumptions based on the data available can reasonably narrow the pool of candidates. Firstly, this mutation inhibits the repair of relatively simple DSBs generated from endonucleases in a plasmid repair assay (2, 4) as well as confers a dramatic survival defect after IR, which produces a variety of complex DSBs (5-7). Thus, it seems unlikely that it would be recruiting an accessory processing factor but instead a member of the core NHEJ machinery required to ligate even basic DSBs (8). Secondly, although the mechanism of NHEJ is a fairly conserved process amongst eukaryotes, there are several participants in mammalian NHEJ that are not present in yeast. For example, there is no obvious yeast homolog for DNA-PK_{CS}, so it is unlikely that this helix is required for recruitment and formation of the DNA-PK complex. Instead the focus should be placed on proteins that have homologs across eukaryotic organisms, such as ligase IV and XRCC4, which have direct homologs in yeast (9).

This question would be best addressed using a system to monitor DSBs in an *in vivo* setting, such as laser microirradiation (micro-IR). This technique utilizes high-powered lasers from confocal microscopy to generate a dense cluster of DNA damage in discrete locations in the nucleus (10, 11). This method allows for the visualization of NHEJ proteins at the site of damage due to their concentration at a specific location,

unlike conventional DNA damaging agents that produce uniform damage throughout the nucleus, and therefore a diffuse localization of proteins (10, 11). Through this system, one can monitor the accumulation of NHEJ factors at the break and determine if the mutation of D192A/D195R is preventing the recruitment of a factor essential for the completion of NHEJ.

Interestingly, Ribes-Zamora et al. propose that this helix 5 is required to mediate heterotetramerization of two Ku dimers (3). They suggest that after Ku molecules load onto the ends, this region mediates the bridging of the DNA. Their results did indeed demonstrate that mutation of helix 5 decreased co-immunoprecipitation between transfected Ku molecules relative to their WT counterparts. However, these experiments were performed in the absence of DNA and in DNA-PK_{CS} deficient cells and therefore do not accurately represent the conditions of *in vivo* NHEJ, and does not definitively prove that this helix is required for DNA end bridging. Previously, an *in vitro* DNA end bridging assay demonstrated that the presence of Ku promoted the association of two DNA molecules (12). Instead of testing the ability of Ku70 D192A/D195R mutants to associate with each other, a DNA end-bridging assay may be more informative regarding whether this mutation impairs the ability of Ku to bring two DNA molecules together.

4.3 Ku70 vWA in DNA damage signaling

The coordination between DNA repair and the cell cycle and apoptotic machinery is an essential part of the DDR. This is required to relay the signal of completed repair to terminate cell cycle checkpoints, or perhaps in the case of complicated or unsuccessful repair, to induce prolonged cell cycle arrest and the activation of apoptosis. We propose

that the phosphorylation of S155 on Ku70 acts as one of these coordinating signals between NHEJ and the DDR.

Our initial observations suggested a role for S155 distinct from DNA repair. S155A expressing MEFs demonstrated increased survival and decreased activation of apoptosis in response to IR treatment. This mutant also displays decreased activation of several DDR markers after IR, including ATM and the ATF2-dependent signaling pathway. Interestingly, we confirmed that this residue does not appear to play a role in NHEJ, as the mutation had no impact on DNA repair efficiency, and was even able to rescue survival when introduced in conjunction with our established DNA repair mutant (D192A/D195R). Therefore, we hypothesize that this residue is required for the activation of cell cycle checkpoints and apoptosis in response to IR, likely in the event of unsuccessful repair and persistent DSBs. Indeed, we observed the prolonged presence of ϒ-H2AX foci in S155A MEFs after IR, a phenotype previously observed in cells surviving with unrepaired breaks (13), indicative of the cells not properly activating apoptosis in response to irreparable damage. This notion is further supported by the phenotype of our phosphomimetic mutant (S155D), which we hypothesize would act as constitutive signal for unrepaired breaks. This mutation confers extremely low survival in response to IR, and the constitutive activation of DDR markers and cell cycle checkpoints in the absence of any ectopic DNA damage. In contrast, the alanine substitution mimics a constitutively unphosphorylated residue and is able to bypass cell cycle arrest and apoptosis despite persistent DNA damage.

An important consequence of S155 phosphorylation that we have uncovered is the modulation of Aurora B activity. We observed an interaction between the Ku70 S155D

mutant and an inhibition of Aurora B activity in S155D expressing MEFs. Furthermore, the phenotype of cells treated with an Aurora B chemical inhibitor closely mimics that of our S155D mutant. We hypothesize that following Ku recruitment to the DSB, Ku70 S155 is phosphorylated, and this promotes interaction with Aurora B to inhibit its kinase activity. We postulate that this event occurs in response to overwhelming or complicated damage in order to induce cell cycle arrest. Indeed, we observed an interaction between endogenous WT Ku70 and Aurora B after the introduction of DNA damage but not in control (untreated) cells. Aurora B activity was also inhibited following IR treatment in WT Ku70 cells, but this inhibition was blocked by the S155A mutation, confirming that the phosphorylation is required for Aurora B inhibition.

In order to fully understand the mechanism of inhibition of pS155 Ku70 on Aurora B, it is important to elucidate the spatio-temporal control of both Ku70 phosphorylation and the inhibition of Aurora B activity. If Ku70 phosphorylation is used as a signal of delayed or unsuccessful repair, then this would be an event that occurs at a small subset of breaks, and would likely not appear until after the first 30 minutes, when the vast majority of simple breaks are resolved and NHEJ complexes dissociated (8). It remains to be determined which kinase is responsible for the phosphorylation of S155 as there is a large array of serine/threonine kinases involved in the DDR. The use of bioinformatics tools designed to predict phosphorylation based on the known consensus motifs of various kinases did not pinpoint any in particular with a strong likelihood (14, 15). While there are many possibilities, a strong candidate is ATM. ATM activity is often dispensable for simple NHEJ repair, but it is required for the completion of lengthy repair, reactions that would often induce prolonged cell cycle arrest as observed in the

S155D MEFs (8, 16). Furthermore, ATM is involved in promoting its own positive feedback loop that amplifies its signal and maintains the prolonged signaling cascade required to sustain cell cycle arrest (17, 18). Since S155 phosphorylation controls the activation of ATM after IR, it could be yet another mechanism by which ATM propagates its own signaling cascade.

Unfortunately, addressing these questions has proved challenging thus far. We were able to observe S155 phosphorylation after IR by utilizing MALDI-TOF MS/MS, however this technique is not conducive to the finite monitoring of the phosphorylation and dephosphorylation of S155 due to the method's insensitivity and large abundance of material required. The kinetics of Ku phosphorylation after IR *in* vivo would be best analyzed by western blot or immunofluorescence. We attempted to generate a phospho-specific antibody directed against this site, but this antibody cross-reacted with other proteins and could not be utilized for further studies. The successful generation of a phospho-S155 antibody would be an invaluable tool for understanding the timing and necessary kinase activity for Ku phosphorylation.

While we have established that an interaction between Aurora B and pS155-Ku70 mediates the inhibition of Aurora following DNA, we now need to establish the nature of this interaction. The regulation of Aurora B is achieved through the binding of a variety of different cofactors. Aurora B, for example, is most well known for its participation in the chromosomal passenger complex, where it interacts with subunits INCENP, Survivin and Borealin that stimulate its kinase activity towards several substrates in mitosis (19). Aurora B only makes direct contact with INCENP, with its N-terminal regulatory and catalytic domains of Aurora B interacting with the IN box motif of INCENP, a

requirement for basal kinase activity at the kinetochore (20, 21). The other subunits do not interact directly but are involved in the correct localization and clustering of Aurora B molecules that are essential for full activity (22). Therefore, it is possible that Ku is directly modulating kinase by binding and hindrance of the catalytic domain, binding the regulatory region to induce unfavorable conformational changes or precluding the interactions with activator subunits. It is also possible that Ku and Aurora B do not interact directly and their association is mediated by another factor.

The role of Aurora B following DNA damage is not well understood. Aurora B kinase activity has been shown by us and others to be inhibited following DNA damage (23), but whether Aurora B is recruited to DSBs has never been demonstrated. This is not entirely surprising if its recruitment is dependent upon an interaction with Ku however, since Ku does not assemble at a break in large enough numbers to be visible by conventional microscopy. Similar to what is utilized to visualize NHEJ factors at the break, micro-IR would be an excellent tool for observing the localization of Aurora B to DSBs and determine the time course of its interaction with Ku. Another unknown is the link between inhibition of Aurora B and the activation of ATM signaling. Aurora B has actually been shown to activate ATM by phosphorylating serine 1403, but this event was shown to specifically mediate the spindle assembly checkpoint in mitosis (24). Our results point to DNA damage specific role for Aurora B regulation of ATM, not dependent upon any particular cell cycle phase, and this remains to be clarified. There are some indirect connections between Aurora B and ATM, with an interesting one involving the protein Repo-man. During mitosis, Repo-man is required for correct Aurora B localization but also counteracts Aurora B activity by dephosphorylating several of its

substrates (25, 26). Repo-man has also been shown to localize with inhibit ATM activity, only to be released from chromatin after DNA damage to allow ATM activation (27). It is possible that following DNA damage, Repo-man is released from ATM and complexes with Ku70 and Aurora B to inhibit its activity, but this remains to be investigated.

It is currently unclear whether the effects of the S155 mutants can all be attributed to Aurora B activity, or whether there are additional signaling events occurring following Ku70 S155 phosphorylation. In Chapter 2, we describe the expression of S155A repressing the activation of an ATF2 dependent DDR, resulting in the deregulation of several ATF2 transcriptional targets such as ATF3 and CHOP (28). While this could be a distinct signaling pathway regulated by S155 phosphorylation, there have been studies demonstrating that many of the effects of Aurora B inhibition are dependent upon the activation of the p38 kinase pathway, a kinase that is the main regulator of ATF2 (29-31). The repression of ATF2 signaling after IR in S155A cells could be explained by a loss of Aurora B inhibition and subsequent lack of p38 pathway activation. If the gene expression changes observed after S155D expression are due to the Aurora B dependent activation of the p38 pathway, it would be interesting to test whether the use of a p38 inhibitor could rescue its dramatic phenotype. However, there are other gene expression changes that cannot be explained by Aurora B inhibition. In an examination of the microarray data obtained from S155D expressing MEFs relative to WT (Supplementary Table 3-1), it is interesting to note that a large number of phosphatases are found downregulated following S155D expression. This is consistent with a constitutively active DDR and cell cycle arrest, as phosphatases are required to resolve checkpoints and resume normal cycling after the repair of damage (32, 33). Yet, the downregulation and

inhibition of phosphatases has been demonstrated to increase Aurora kinase activity, which is in clear opposition of our findings (34, 35). This apparent contradiction could be due to additional factors or pathways being modulated by S155 phosphorylation that are independent of Aurora B activity.

4.4 Conclusion

In summary, this work has contributed to the broader understanding of the Ku70 vWA domain function in response to DSBs on two fronts: demonstrating the requirement for helix 5 for proper DSB repair in mammalian cells, and identifying a novel phosphorylation site that signals to the DDR to modulate cell fate decisions. We propose a model for the function of the Ku70 vWA domain in NHEJ (Figure 4-1) where Ku is rapidly recruited to a DSB, and helix 5 participates in the completion of NHEJ by either mediating the recruitment of another essential NHEJ factor, or the interaction with another Ku heterodimer at the break. If repair cannot be completed, S155 is phosphorylated, and this results in the inhibition of Aurora B activity, thereby inducing prolonged cell cycle arrest or the activation of apoptosis.

A thorough understanding of DNA repair and the DDR has broad implications for human health as genome instability is a hallmark of cancer (36). We now understand that Ku not only is involved in the repair of breaks, but also through the phosphorylation of S155, is essential for the elimination of cells damaged beyond repair. The loss of this regulation would lead to the proliferation of unstable cells, potentially resulting in genomic instability and cancer. It would be interesting to investigate the consequences of a S155 alanine substitution at the organismal level, and whether the loss of this phosphorylation has oncogenic potential. On the contrary, we have observed that the

Figure 4-1 Model for the function of the Ku70 vWA domain in response to DSBs.

(A) Following recruitment of the Ku heterodimer to the break, the Ku70 α-helix 5 is positioned inwards towards the DNA end. This helix is required for NHEJ and cell survival in response to DSBs, and there are currently two hypotheses to explain its role: (i) protein-protein interaction surface utilized in the recruitment of an essential NHEJ factor, (ii) interaction surface between two Ku70 molecules to mediate heterotetramerization of Ku in order to bridge DNA ends at the break. (B) (i) Ku attempts repair by NHEJ (ii) Following unsuccessful or prolonged repair, an unknown kinase phosphorylates Ku70 on residue serine 155. (iii) Ku70 pS155 interacts with Aurora B kinase, either directly or indirectly, in order to inhibit Aurora B kinase activity. (iv) Inhibition of Aurora B kinase results in increased activity of ATM and ATF2 and upregulation of p21, leading to the activitation of cell cycle checkpoints, senescence and apoptosis.

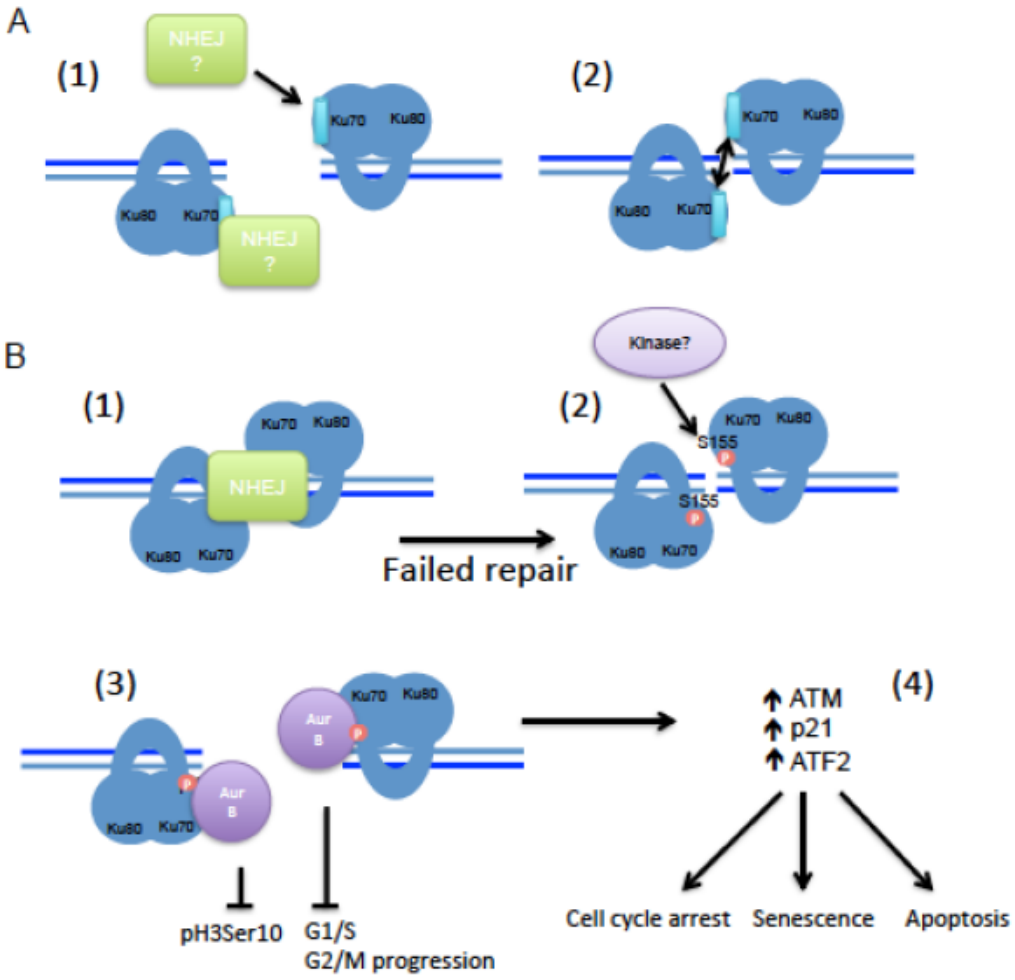
A
(1)
NHEJ ?
Ku70
Ku80
Ku80
Ku70
NHEJ ?
(2)
Ku70
Ku80
Ku80
Ku70
B
(1)
Ku70
Ku80
NHEJ
Ku80
Ku70
Failed repair
(2)
Kinase?
Ku70
Ku80
S155
S155
Ku80
Ku70
(3)
Aur B
Ku70
Ku80
Aur B
Ku80
Ku70
pH3Ser10
G1/S
G2/M progression
(4)
ATM
p21
ATF2
Cell cycle arrest
Senescence
Apoptosis

transfection of the S155D vWA had a profound effect on both mouse and human cell lines, inducing cell cycle arrest and senescence, through a modulation of Aurora B activity. Given the prevalence of small molecules being generated against the Aurora kinases for the treatment of cancer, it raises the possibility of whether this phosphomimetic peptide of Ku has therapeutic potential.

4.5 References

1. Fell VL & Schild-Poulter C (2012) Ku regulates signaling to DNA damage response pathways through the Ku70 von Willebrand A domain. *Mol Cell Biol* 32(1):76-87.
2. Ribes-Zamora A, Mihalek I, Lichtarge O, & Bertuch AA (2007) Distinct faces of the Ku heterodimer mediate DNA repair and telomeric functions. *Nat Struct Mol Biol* 14(4):301-307.
3. Ribes-Zamora A, Indiviglio SM, Mihalek I, Williams CL, & Bertuch AA (2013) TRF2 interaction with Ku heterotetramerization interface gives insight into c-NHEJ prevention at human telomeres. *Cell reports* 5(1):194-206.
4. Boulton SJ & Jackson SP (1996) Saccharomyces cerevisiae Ku70 potentiates illegitimate DNA double-strand break repair and serves as a barrier to error-prone DNA repair pathways. *The EMBO journal* 15(18):5093-5103.
5. Lindahl T & Barnes DE (2000) Repair of endogenous DNA damage. *Cold Spring Harbor symposia on quantitative biology* 65:127-133.
6. Cadet J*, et al.* (1999) Hydroxyl radicals and DNA base damage. *Mutation research* 424(1-2):9-21.
7. Goodhead DT (1994) Initial events in the cellular effects of ionizing radiations: clustered damage in DNA. *International journal of radiation biology* 65(1):7-17.
8. Reynolds P*, et al.* (2012) The dynamics of Ku70/80 and DNA-PKcs at DSBs induced by ionizing radiation is dependent on the complexity of damage. *Nucleic Acids Res* 40(21):10821-10831.
9. Daley JM, Palmbos PL, Wu D, & Wilson TE (2005) Nonhomologous end joining in yeast. *Annual review of genetics* 39:431-451.
10. Kong X*, et al.* (2009) Comparative analysis of different laser systems to study cellular responses to DNA damage in mammalian cells. *Nucleic Acids Res* 37(9):e68.
11. Botchway SW, Reynolds P, Parker AW, & O'Neill P (2010) Use of near infrared femtosecond lasers as sub-micron radiation microbeam for cell DNA damage and repair studies. *Mutation research* 704(1-3):38-44.
12. Ramsden DA & Gellert M (1998) Ku protein stimulates DNA end joining by mammalian DNA ligases: a direct role for Ku in repair of DNA double-strand breaks. *EMBO J* 17(2):609-614.
13. Olive PL (2011) Retention of gammaH2AX foci as an indication of lethal DNA damage. *Radiotherapy and oncology : journal of the European Society for Therapeutic Radiology and Oncology* 101(1):18-23.
14. Horn H*, et al.* (2014) KinomeXplorer: an integrated platform for kinome biology studies. *Nature methods* 11(6):603-604.
15. Blom N, Sicheritz-Ponten T, Gupta R, Gammeltoft S, & Brunak S (2004) Prediction of post-translational glycosylation and phosphorylation of proteins from the amino acid sequence. *Proteomics* 4(6):1633-1649.
16. Goodarzi AA*, et al.* (2008) ATM signaling facilitates repair of DNA double-strand breaks associated with heterochromatin. *Mol Cell* 31(2):167-177.

17. Marechal A & Zou L (2013) DNA damage sensing by the ATM and ATR kinases. *Cold Spring Harbor perspectives in biology* 5(9).
18. Shiloh Y & Ziv Y (2013) The ATM protein kinase: regulating the cellular response to genotoxic stress, and more. *Nature reviews. Molecular cell biology* 14(4):197-210.
19. Carmena M, Wheelock M, Funabiki H, & Earnshaw WC (2012) The chromosomal passenger complex (CPC): from easy rider to the godfather of mitosis. *Nature reviews. Molecular cell biology* 13(12):789-803.
20. Honda R, Korner R, & Nigg EA (2003) Exploring the functional interactions between Aurora B, INCENP, and survivin in mitosis. *Molecular biology of the cell* 14(8):3325-3341.
21. Bishop JD & Schumacher JM (2002) Phosphorylation of the carboxyl terminus of inner centromere protein (INCENP) by the Aurora B Kinase stimulates Aurora B kinase activity. *J Biol Chem* 277(31):27577-27580.
22. Jeyaprakash AA*, et al.* (2007) Structure of a Survivin-Borealin-INCENP core complex reveals how chromosomal passengers travel together. *Cell* 131(2):271-285.
23. Monaco L*, et al.* (2005) Inhibition of Aurora-B kinase activity by poly(ADP-ribosyl)ation in response to DNA damage. *Proc Natl Acad Sci U S A* 102(40):14244-14248.
24. Yang C*, et al.* (2011) Aurora-B mediated ATM serine 1403 phosphorylation is required for mitotic ATM activation and the spindle checkpoint. *Mol Cell* 44(4):597-608.
25. Qian J, Lesage B, Beullens M, Van Eynde A, & Bollen M (2011) PP1/Repo-man dephosphorylates mitotic histone H3 at T3 and regulates chromosomal aurora B targeting. *Curr Biol* 21(9):766-773.
26. Wurzenberger C*, et al.* (2012) Sds22 and Repo-Man stabilize chromosome segregation by counteracting Aurora B on anaphase kinetochores. *J Cell Biol* 198(2):173-183.
27. Peng A, Lewellyn AL, Schiemann WP, & Maller JL (2010) Repo-man controls a protein phosphatase 1-dependent threshold for DNA damage checkpoint activation. *Curr Biol* 20(5):387-396.
28. Gozdecka M & Breitwieser W (2012) The roles of ATF2 (activating transcription factor 2) in tumorigenesis. *Biochem Soc Trans* 40(1):230-234.
29. Kumari G, Ulrich T, Krause M, Finkernagel F, & Gaubatz S (2014) Induction of p21CIP1 protein and cell cycle arrest after inhibition of Aurora B kinase is attributed to aneuploidy and reactive oxygen species. *J Biol Chem* 289(23):16072-16084.
30. Kumari G, Ulrich T, & Gaubatz S (2013) A role for p38 in transcriptional elongation of p21 (CIP1) in response to Aurora B inhibition. *Cell Cycle* 12(13):2051-2060.
31. Cuadrado A & Nebreda AR (2010) Mechanisms and functions of p38 MAPK signalling. *The Biochemical journal* 429(3):403-417.
32. Lee DH & Chowdhury D (2011) What goes on must come off: phosphatases gate-crash the DNA damage response. *Trends Biochem Sci* 36(11):569-577.

33. Heideker J, Lis ET, & Romesberg FE (2007) Phosphatases, DNA damage checkpoints and checkpoint deactivation. *Cell Cycle* 6(24):3058-3064.
34. Ajiro K, Yoda K, Utsumi K, & Nishikawa Y (1996) Alteration of cell cycle-dependent histone phosphorylations by okadaic acid. Induction of mitosis-specific H3 phosphorylation and chromatin condensation in mammalian interphase cells. *J Biol Chem* 271(22):13197-13201.
35. Guo XW*, et al.* (1995) Chromosome condensation induced by fostriecin does not require p34cdc2 kinase activity and histone H1 hyperphosphorylation, but is associated with enhanced histone H2A and H3 phosphorylation. *EMBO J* 14(5):976-985.
36. Hanahan D & Weinberg RA (2011) Hallmarks of cancer: the next generation. *Cell* 144(5):646-674.

Appendices

Appendix 1 Permissions

LAST UPDATED: November 5, 2009

ASM Journals Statement of Authors' Rights

Authors may post their articles to their institutional repositories

ASM grants authors the right to post their accepted manuscripts in publicly accessible electronic repositories maintained by funding agencies, as well as appropriate institutional or subject-based open repositories established by a government or non-commercial entity. Since ASM makes the final, typeset articles from its primary-research journals available free of charge on the ASM Journals and PMC websites 6 months after final publication, ASM recommends that when submitting the accepted manuscript to PMC or institutional repositories, the author specify that the posting release date for the manuscript be no earlier than 6 months after the final publication of the typeset article by ASM.

Authors may post their articles in full on personal or employer websites

ASM grants the author the right to post his/her article (after publication by ASM) on the author's personal or university-hosted website, but not on any corporate, government, or similar website, without ASM's prior permission, provided that proper credit is given to the original ASM publication.

Authors may make copies of their articles in full

Corresponding authors are entitled to 10 free downloads of their papers. Additionally, all authors may make up to 99 copies of his/her own work for personal or professional use (including teaching packs that are distributed free of charge within your own institution). For orders of 100 or more copies, you should seek ASM's permission or purchase access through Highwire's Pay-Per-View option, available on the ASM online journal sites.

Authors may republish/adapt portions of their articles

ASM also grants the authors the right to republish discrete portions of his/her article in any other publication (including print, CD-ROM, and other electronic formats) of which he or she is author or editor, provided that proper credit is given to the original ASM publication. "Proper credit" means either the copyright lines shown on the top of the first page of the PDF version, or "Copyright © American Society for Microbiology, [insert journal name, volume number, year, page numbers and DOI]" of the HTML version. For

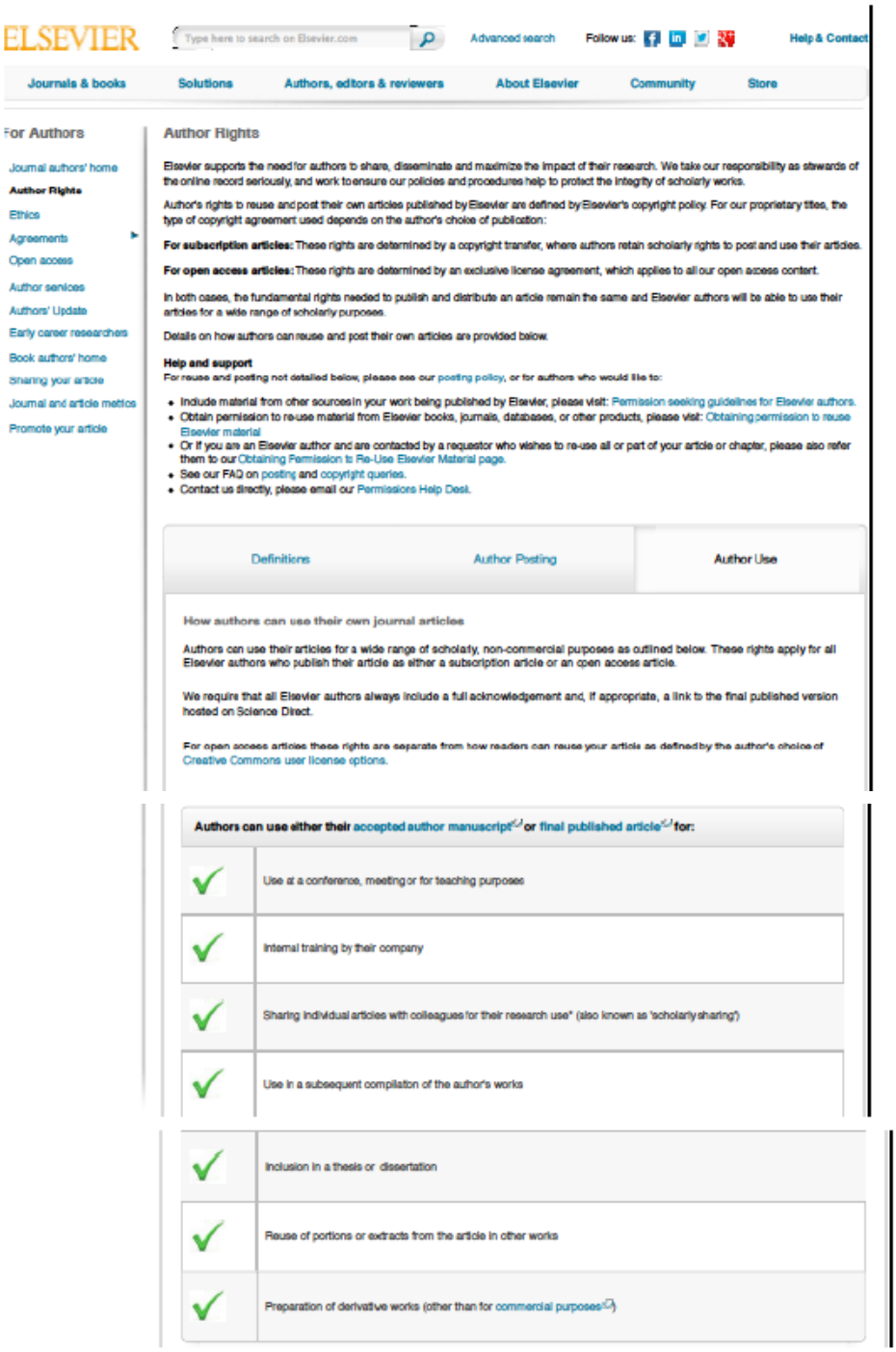

ELSEVIER

Type here to search on Elsevier.com

Advanced search Follow us: Help & Contact

Journals & books | Solutions | Authors, editors & reviewers | About Elsevier | Community | Store

For Authors

- Journal authors' home
- **Author Rights**
- Ethics
- Agreements
- Open access
- Author services
- Authors' Update
- Early career researchers
- Book authors' home
- Sharing your article
- Journal and article metrics
- Promote your article

Author Rights

Elsevier supports the need for authors to share, disseminate and maximize the impact of their research. We take our responsibility as stewards of the online record seriously, and work to ensure our policies and procedures help to protect the integrity of scholarly works.

Author's rights to reuse and post their own articles published by Elsevier are defined by Elsevier's copyright policy. For our proprietary titles, the type of copyright agreement used depends on the author's choice of publication:

For subscription articles: These rights are determined by a copyright transfer, where authors retain scholarly rights to post and use their articles.

For open access articles: These rights are determined by an exclusive license agreement, which applies to all our open access content.

In both cases, the fundamental rights needed to publish and distribute an article remain the same and Elsevier authors will be able to use their articles for a wide range of scholarly purposes.

Details on how authors can reuse and post their own articles are provided below.

Help and support

For reuse and posting not detailed below, please see our posting policy, or for authors who would like to:

- Include material from other sources in your work being published by Elsevier, please visit: Permission seeking guidelines for Elsevier authors.
- Obtain permission to re-use material from Elsevier books, journals, databases, or other products, please visit: Obtaining permission to reuse Elsevier material
- Or if you are an Elsevier author and are contacted by a requestor who wishes to re-use all or part of your article or chapter, please also refer them to our Obtaining Permission to Re-Use Elsevier Material page.
- See our FAQ on posting and copyright queries.
- Contact us directly, please email our Permissions Help Desk.

Definitions | Author Posting | **Author Use**

How authors can use their own journal articles

Authors can use their articles for a wide range of scholarly, non-commercial purposes as outlined below. These rights apply for all Elsevier authors who publish their article as either a subscription article or an open access article.

We require that all Elsevier authors always include a full acknowledgement and, if appropriate, a link to the final published version hosted on Science Direct.

For open access articles these rights are separate from how readers can reuse your article as defined by the author's choice of Creative Commons user license options.

Authors can use either their accepted author manuscript or final published article for:	
✓	Use at a conference, meeting or for teaching purposes
✓	Internal training by their company
✓	Sharing individual articles with colleagues for their research use* (also known as 'scholarly sharing')
✓	Use in a subsequent compilation of the author's works
✓	Inclusion in a thesis or dissertation
✓	Reuse of portions or extracts from the article in other works
✓	Preparation of derivative works (other than for commercial purposes)

Curriculum Vitae

Victoria Fell

Education

2014 Ph.D., Biochemistry
- University of Western Ontario, London, Ontario Canada

2008 B.Sc., Molecular Biology and Genetics
- University of Guelph, Guelph, Ontario, Canada

Research Experience

2008-14 PhD Candidate, Department of Biochemistry, University of Western Ontario
- Supervised by Dr. Caroline Schild-Poulter, Robarts Research Institute
- Thesis: The role of the Ku70 vWA domain in the response to DNA double strand breaks

2007-08 Honours Thesis Project, Department of Molecular and Cellular Biology, University of Guelph
- Supervised by Dr. Andrew Bendall, University of Guelph
- Thesis: Regulation of the Collagen type II promoter by the Dlx transcription factor family in chondrocytes

2007 Summer Student, Mammalian Virology Lab, Ontario Veterinary Clinic, University of Guelph
- Supervised by Dr. Susy Carman
- Catalogued and genotyped veterinary clinic samples for influenza virus

Publications

- V.L. Fell, S. Rogers, A. Aiken and C. Schild-Poulter. Regulation DNA damage signaling and inhibition of Aurora B through a phosphorylation site on Ku70. In revision, EMBO Rep. Dec 2014.
- V.L. Fell and C. Schild-Poulter. The Ku Heterodimer: Function in DNA repair and beyond. Mut Res Rev. In Press. 2014.

- V.L. Fell and C. Schild-Poulter. Ku regulates signaling to DNA damage response pathways through the Ku70 von Willebrand A domain. Mol Cell Biol. 2012 Jan;32(1):76-87.

Selected Conference Presentations

- V. Fell*, S. Rogers, and C. Schild-Poulter. Ku70 S155 regulates cell cycle checkpoints and DNA damage signaling. **Canadian Student Health Research Forum. Winnipeg, MB, June 2014.** *Poster presentation.*
- V. Fell*, S. Rogers and C. Schild-Poulter. Ku70 S155 regulates cell cycle checkpoints and DNA damage signaling. **2nd Canadian Symposium on Telomeres and Genome Integrity. Lac de lage, QC, May 2014**. *Oral presentation.*
- V. Fell* and C. Schild-Poulter. Ku70 S155 phosphorylation regulates DNA damage signaling. **Experimental Biology 2013. Boston, MA, April 2013.** *Poster presentation.*
- V. Fell* and C. Schild Poulter. Ku70 vWa domain in the DNA damage response. 1st Canadian **Symposium on Telomeres and Genome Integrity. London, ON, May 2012.** *Poster presentation.*
- V. Fell* and C. Schild Poulter. Ku70 vWa domain in the DNA damage response. **Abcam Maintenance of Genome Stability 2012. Nassau, Bahamas, March 2012.** *Poster presentation.*
- V. Fell* and C. Schild Poulter. Ku70 vWa domain in the DNA damage response. **Gordon Research Conference: Mammalian DNA Repair. Ventura, CA, February 2011.** *Poster presentation.*

Awards

- Selected to attend CIHR Canadian Student Health Research Forum national poster competition and received CIHR travel award. 2014
- 2nd Canadian Symposium on Telomeres and Genome Integrity Best Trainee Oral presentation. 2014
- London Health Research Day Poster award. 2014
- UWO Oncology Research and Education Day Poster award. 2013
- Schulich Graduate Scholarship. 2008-13.
- Schulich Graduate Thesis Research Award. 2011-12.
- UWO Department of Biochemistry Publication Award. 2012.